

**STUDIES ON CONDUCTING POLYMERS  
SYNTHESIS AND CHARACTERIZATION OF  
CONDUCTING POLYMER BLENDS**

A THESIS  
SUBMITTED TO THE  
**BHARATI VIDYAPEETH PUNE**  
(DEEMED UNIVERSITY)  
FOR THE DEGREE OF

**DOCTOR OF PHILOSOPHY**  
**IN**  
**CHEMISTRY**

**BY**

**SHIVKALYAN. A. KANHEGAOKAR**

**DIVISION OF POLYMER SCIENCE & ENGINEERING  
NATIONAL CHEMICAL LABORATORY  
PUNE - 411008  
January 2004**

**DEDICATED TO  
MY PARENTS  
AND  
LATE GRAND PARENTS**

For their continued support and valuable feedback to me over the years that has encouraged me to grow in a healthy way.

## CERTIFICATE

Certified that the work incorporated in the Thesis entitled “ **Studies on Conducting Polymer Blends; Synthesis and Characterization of Conducting Polymer Blends**” submitted by **Mr.Shivkalyan A. Kanhegaokar**, was carried out by him under my supervision at the Polymer Science and Engineering Group, Chemical Engineering Division, National Chemical Laboratory, Pune-8. Such material as has been obtained from other sources has been duly acknowledged in the thesis.

January 2004

**Dr.S. Radhakrishnan**  
Research Guide

## ACKNOWLEDGEMENTS

I would like to thank my guide Dr.S.Radhakrishnan for his constant support, strong motivation and constant encouragement throughout my work. His continued involvement added greatly to my educational experience.

I would like to thank the Director of NCL for permitting me to submit this work in the form of Ph.D thesis, which I carried out in this research paradise.

I likewise acknowledge the help of Dr.Hegde and Ms.Agashe in IR characterization.

I greatly appreciate the personal involvement of Arindam Adhikari in this work.

This work would never have been finished timely without the endless efforts of my colleagues Francis, Santhosh Paul, Sreejit, Subramaniam, S.B.Kar and Y. Bhole. Their tireless efforts deserve a lot of credit. This work carried out with their unstinted support, I am sure will be beneficial to both industrial and academic communities.

It is a pleasure to acknowledge the benefit of valuable comments and suggestions from friends and colleagues who have read the parts of this manuscript.

Ultimately, I would like to acknowledge the loving support of my parents and brother Kalidas, who always stood by me & encouraged to strive for the best in whatever I do. I will always remember their sacrifice.

## CONTENTS

List of symbols	i
List of acronyms	iii

### CHAPTER-I: Introduction

1.1	Types of Inherently Conducting Polymers (ICP)-----
1.2	Why Polyaniline is important among all the conducting polymers? i) Chemical synthesis----- ii) Electrochemical synthesis-----
1.3	Synthesis Techniques for Conducting Polymers----- a) Doping of polymers----- b) Effect of doping on conducting polymers----- c) Low and Intermediate Doping-----
1.4	Electrical conductivity in polymers----- A. The Charge Carriers----- i) Intrinsic charge carrier generation----- ii) Impurity Conduction----- B. Localized states ----- C. Injection Process-----
1.5	Advantages and Disadvantages of Conducting Polymers-----
1.6	Why Blending is Necessary? -----
1.7	Preparation methods of the Conducting Polymer Blends----- a) Blends prepared by electrochemical methods----- b) Electrode coating method----- c) Co deposition method----- d) Blends prepared by chemical synthesis----- e) Mixture of Blend components----- f) Polymerization of the conductive polymer in the insulating matrix.
1.8	Physical Blending-----

1.8.1	Effect of interaction between filler particles-----
1.8.2	No contact between the conducting particles-----
1.8.3	Conductive particles in close proximity to each other-----
1.8.4	Physical contact between the conducting particles-----
1.8.5	Network formation between filler particles-----
1.8.6	Conducting Polymer Composite Materials (CPC)-----
1.8.7	Structure and Conductivity of CPC-----
1.8.8	Processing conditions and conductivity of composite materials-----
1.8.9	Distribution of filler in conducting polymer composites based on polymer Blends-----
1.9	Polymerization filling— a novel technique for manufacturing-----
1.10	Conducting composite materials-----
1.11	Application of Conducting Polymer-----
1.12	Factors, affecting Electrical Conductivity and Electrical Measurement
1.13	Aim and scope-----

## **CHAPTER-II: Experimental**

2.1	<b>Introduction</b> -----
2.2	Chemicals used-----
2.3	Methods of synthesis-----
2.3.1	Synthesis of conducting polymer-----
	(a) Chemical synthesis-----
2.3.2.	Synthesis of Blends-----
	(a) Insitu blends-----
	(b) Ex-situ blends-----
2.4	Sample preparation-----
2.5	Doing with HCL solution-----
2.6	Sample preparation for property measurement-----
	a) Electrode configuration-----
	b) Surface cell-----
	c) Moisture sensitivity Measurement-----

2.7	Characterization-----
2.7.1	FTIR Spectroscopy-----
2.7.2.	UV-VIS Spectroscopy-----
2.8	Structural and compositional characterization-----
2.8.1	X-ray diffraction studies-----
2.8.2	Thermo Gravimetric Analysis (TGA)-----
2.9	Measurement of properties-----
2.9.1	Conductivity measurements-----
2.9.2	I-V characterization-----
2.9.3	Temperature dependence of Conductivity-----

### **CHAPTER-III: Polyaniline-Poly vinyl acetate Blend**

3.1	<b>Introduction-----</b>
3.2	Experimental-----
	1) Preparation of insitu Blend-----
	2) Preparation of Ex-situ Blend-----
3.3	Results and discussion-----
3.4	Characterization-----
3.4	FTIR Spectroscopy-----
3.5	UV-VIS Spectroscopy-----
3.6	Measurement of properties-----
	1) R.T. Electrical Conductivity Measurement-----
	2) Temperature dependent Conductivity Measurement-----
	3) Activation energy ( $\Delta E$ )-----
	4) I-V Characteristics-----
3.7	TGA/DTA-----
3.8	Moisture sensitivity-----

3.9 Conclusions-----

## **CHAPTER -IV: Polyaniline / Poly acryl amide Blend**

4.1 **Introduction**-----

4.2 Experimental-----

a) Polymerization of acrylamide-----

b) Preparation of insitu Blends-----

c) Preparation of ex-situ Blends -----

4.3 Results and disscusion-----

4.3A Pani-Pam blend-----

4.4 Characterization-----

4.4 FTIR Spectroscopy-----

4.5 UV-VIS Spectroscopy-----

4.6 Measurement of properties-----

1) R.T. Electrical Conductivity of the blends-----

2) Temperature Dependent Conductivity of the blends-----

3) Activation Energy studies for the blends ( $\Delta E$ )-----

4) Charge Transport studies in the blends-----

4.7 T.G.A./D.T.A.-----

4.8 Moisture sensitivity-----

4.9 Conclusions-----



## **CHAPTER-V: Polyaniline-Nylon-6 Blend**

<b>5</b>	<b>Introduction-----</b>
5.1	Experimental-----
	1) Preparation of insitu blend-----
	2) Preparation of exsitu blend-----
5.2	Results and disscusion-----
5.2	Characterization
5.3	FTIR Spectroscopy-----
5.4	UV-VIS Spectroscopy-----
5.5	X-ray Diffraction Technique-----
5.6	Optical Microscopy-----
5.7	Electrical Conductivity Measurement-----
	1) R.T. Electrical Conductivity Measurement-----
	2) Temperature Dependent Conductivity-----
	3) Activation Energy ( $\Delta E$ )-----
	4) I-V Characteristics-----
5.8	TGA/DTA-----
5.9	Moisture sensitivity-----
6	Conclusions-----
6.1	References-----
	<b>CHAPTER-VI: Summary and conclusions-----</b>

## List of symbols

$\sigma_0$	Initial conductivity
$\sigma$	Conductivity
$k$	Boltzman's constant
$T$	Temperature
$E_v$	Fermi energy
$E_g$	forbidden energy gap
$F$	Fermi Dirac distribution function
$E$	Energy
$\exp$	exponential
$\phi$	Work function
$EA$	Electron affinity
$S$	spin quantum no.
$2\theta$	X-ray diffraction angle
$\lambda$	mean free path
$d$	depth
$\gamma$	Fall-off in wave function with distance
$P$	Average separation of sites
$E_{act}$	energy required to cross the potential barrier
$q$	charge

$m^*$	effective mass
$\epsilon$	dielectric constant
$y$	shear speed
$I$	current
$V$	volume
$R$	Resistance
$A$	Area
$l$	thickness
$\rho$	resistivity
$\Delta E$	Activation energy
$T_g$	glass transition temperature
$\Phi_f$	volume fraction of filler material
$V_p$	voltage present across the interparticle gap
$I_p$	current flowing across the polymer layer
$S$	Siemens
$W$	Gap width
$V_o$	Potential barrier
$H$	Humidity
$Cu$	Copper
$s$	sensitivity
$E_g$	Electronic gap
$\eta$	Viscosity

## List of acronyms

<b>ICP</b>	Inherently Conducting Polymer
<b>SCE</b>	Saturated Calomel Electrode
<b>NMP</b>	N-methyl pyrrolidone
<b>NaCl</b>	Sodium chloride
<b>EPR</b>	Electron Paramagnetic Resonance
<b>THF</b>	Tetra hydro furan
<b>Pani</b>	Polyaniline
<b>Pt</b>	Platinum
<b>AC</b>	Alternating Current
<b>DC</b>	Direct Current
<b>CPC</b>	Conducting Polymer Composite
<b>TCR</b>	Temperature Coefficient of Resistance
<b>PTC</b>	Positive Temperature of Coefficient
<b>PVAc</b>	Poly vinyl acetate
<b>Pam</b>	Poly acryl amide
<b>EMI</b>	Electro Magnetic Induction
<b>RF</b>	Radiation Frequency
<b>FTIR</b>	Fourier Transform Infrared Spectroscopy
<b>UV-VIS</b>	Ultra-Violet Spectroscopy
<b>TGA</b>	Thermo Gravimetric Analysis

<b>DTA</b>	Differential Thermal Analysis
<b>XRD</b>	X-ray diffraction
<b>WAXD</b>	Wide angle x-ray diffraction
<b>IPN</b>	Inter Penetrating Network
<b>EDAX</b>	Energy dispersive x-ray analysis
<b>APIMS</b>	Expensive atmospheric ionization mass spectroscopy
<b>VRH</b>	Variable range hopping
<b>MW</b>	Molecular Weight
<b>HFMO</b>	Highest Filled Molecular Orbital
<b>LEMO</b>	Lowest empty Molecular Orbital
<b>M-I-M</b>	Metal-Insulator-Metal

# CONTENTS

List of symbols	i
List of acronyms	iii

## CHAPTER-I: Introduction

1.1	Types of Inherently Conducting Polymers (ICP)-----
1.2	Why Polyaniline is important among all the conducting polymers? i) Chemical synthesis----- ii) Electrochemical synthesis-----
1.3	Synthesis Techniques for Conducting Polymers----- a) Doping of polymers----- b) Effect of doping on conducting polymers----- c) Low and Intermediate Doping-----
1.4	Electrical conductivity in polymers----- A. The Charge Carriers----- i) Intrinsic charge carrier generation----- ii) Impurity Conduction----- B. Localized states ----- C. Injection Process-----
1.5	Advantages and Disadvantages of Conducting Polymers-----
1.6	Why Blending is Necessary? -----
1.7	Preparation methods of the Conducting Polymer Blends----- a) Blends prepared by electrochemical methods----- b) Electrode coating method----- c) Co deposition method----- d) Blends prepared by chemical synthesis----- e) Mixture of Blend components----- f) Polymerization of the conductive polymer in the insulating matrix.
1.8	Physical Blending-----
1.8.1	Effect of interaction between filler particles-----
1.8.2	No contact between the conducting particles-----

1.8.3	Conductive particles in close proximity to each other-----
1.8.4	Physical contact between the conducting particles-----
1.8.5	Network formation between filler particles-----
1.8.6	Conducting Polymer Composite Materials (CPC)-----
1.8.7	Structure and Conductivity of CPC-----
1.8.8	Processing conditions and conductivity of composite materials-----
1.8.9	Distribution of filler in conducting polymer composites based on polymer Blends-----
1.9	Polymerization filling— a novel technique for manufacturing-----
1.10	Conducting composite materials-----
1.11	Application of Conducting Polymer-----
1.12	Factors, affecting Electrical Conductivity and Electrical Measurement
1.13	Aim and scope-----

## **CHAPTER-II: Experimental**

2.1	<b>Introduction</b> -----
2.2	Chemicals used-----
2.3	Methods of synthesis-----
2.3.1	Synthesis of conducting polymer-----
	(a) Chemical synthesis-----
2.3.2.	Synthesis of Blends-----
	(a) Insitu blends-----
	(b) Ex-situ blends-----
2.4	Sample preparation-----
2.5	Doing with HCL solution-----
2.6	Sample preparation for property measurement-----
	a) Electrode configuration-----
	b) Surface cell-----
	c) Moisture sensitivity Measurement-----
2.7	Characterization-----
2.7.1	FTIR Spectroscopy-----

2.7.2.	UV-VIS Spectroscopy-----
2.8	Structural and compositional characterization-----
2.8.1	X-ray diffraction studies-----
2.8.2	Thermo Gravimetric Analysis (TGA)-----
2.9	Measurement of properties-----
2.9.1	Conductivity measurements-----
2.9.2	I-V characterization-----
2.9.3	Temperature dependence of Conductivity-----

### **CHAPTER-III: Polyaniline-Poly vinyl acetate Blend**

3.1	<b>Introduction</b> -----
3.2	Experimental-----
	1) Preparation of insitu Blend-----
	2) Preparation of Ex-situ Blend-----
3.3	Results and Discussion-----
3.4	Characterization-----
3.4	FTIR Spectroscopy-----
3.5	UV-VIS Spectroscopy-----
3.6	Measurement of properties-----
	1) R.T. Electrical Conductivity Measurement-----
	2) Temperature dependent Conductivity Measurement-----
	3) Activation energy ( $\Delta E$ )-----
	4) I-V Characteristics-----
3.7	TGA/DTA-----
3.8	Moisture sensitivity-----
3.9	Conclusions-----



## CHAPTER -IV: Polyaniline / Poly acryl amide Blend

4.1	<b>INTRODUCTION</b> -----
4.2	Experimental-----
	a) Polymerization of acryl amide-----
	b) Preparation of insitu Blends-----
	c) Preparation of ex-situ Blends -----
4.3	Results and Discussions-----
4.3A	Pani-Pam blend-----
4.4	Characterization-----
4.4	FTIR Spectroscopy-----
4.5	UV-VIS Spectroscopy-----
4.6	Measurement of properties-----
	1) R.T. Electrical Conductivity of the blends-----
	2) Temperature Dependent Conductivity of the blends-----
	3) Activation Energy studies for the blends ( $\Delta E$ )-----
	4) Charge Transport studies in the blends-----
4.7	T.G.A./D.T.A.-----
4.8	Moisture sensitivity-----
4.9	Conclusions-----

## CHAPTER-V: Polyaniline-Nylon-6 Blend

5	INTRODUCTION-----
5.1	Experimental-----
	1) Preparation of insitu blend-----
	2) Preparation of exsitu blend-----
5.2	Results and disscusion-----
5.2	Characterization
5.3	FTIR Spectroscopy-----
5.4	UV-VIS Spectroscopy-----
5.5	X-ray Diffraction Technique-----
5.6	Optical Microscopy-----
5.7	Electrical Conductivity Measurement-----
	1) R.T. Electrical Conductivity Measurement-----
	2) Temperature Dependent Conductivity-----
	3) Activation Energy ( $\Delta E$ )-----
	4) I-V Characteristics-----
5.8	TGA/DTA-----
5.9	Moisture sensitivity-----
6	Conclusions-----
6.1	References-----
	CHAPTER-VI: Summary and conclusions-----

## List of symbols

$\sigma_0$	Initial conductivity
$\sigma$	Conductivity
$k$	Boltzman's constant
$T$	Temperature
$E_v$	Fermi energy
$E_g$	forbidden energy gap
$F$	Fermi Dirac distribution function
$E$	Energy
$\exp$	exponential
$\phi$	Work function
$EA$	Electron affinity
$S$	spin quantum no.
$2\theta$	X-ray diffraction angle
$\lambda$	mean free path
$d$	depth
$\gamma$	Fall-off in wave function with distance
$P$	Average separation of sites
$E_{act}$	energy required to cross the potential barrier
$q$	charge
$m^*$	effective mass
$\epsilon$	dielectric constant

$\dot{\gamma}$	shear speed
$I$	current
$V$	volume
$R$	Resistance
$A$	Area
$l$	thickness
$\rho$	resistivity
$\Delta E$	Activation energy
$T_g$	glass transition temperature
$\Phi_f$	volume fraction of filler material
$V_p$	voltage present across the interparticle gap
$I_p$	current flowing across the polymer layer
$S$	Siemens
$W$	Gap width
$V_O$	Potential barrier
$H$	Humidity
$Cu$	Copper
$s$	sensitivity
$E_g$	Electronic gap
$\eta$	Viscosity

## List of acronyms

<b>ICP</b>	Inherently Conducting Polymer
<b>SCE</b>	Saturated Calomel Electrode
<b>NMP</b>	N-methyl pyrrolidone
<b>NaCl</b>	Sodium chloride
<b>EPR</b>	Electron Paramagnetic Resonance
<b>THF</b>	Tetra hydro furan
<b>Pani</b>	Polyaniline
<b>Pt</b>	Platinum
<b>AC</b>	Alternating Current
<b>DC</b>	Direct Current
<b>CPC</b>	Conducting Polymer Composite
<b>TCR</b>	Temperature Coefficient of Resistance
<b>PTC</b>	Positive Temperature of Coefficient
<b>PVAc</b>	Poly vinyl acetate
<b>Pam</b>	Poly acryl amide
<b>EMI</b>	Electro Magnetic Induction
<b>RF</b>	Radiation Frequency
<b>FTIR</b>	Fourier Transform Infrared Spectroscopy
<b>UV-VIS</b>	Ultra-Violet Spectroscopy
<b>TGA</b>	Thermo Gravimetric Analysis
<b>DTA</b>	Differential Thermal Analysis

<b>XRD</b>	X-ray diffraction
<b>WAXD</b>	Wide angle x-ray diffraction
<b>IPN</b>	Inter Penetrating Network
<b>EDAX</b>	Energy dispersive x-ray analysis
<b>APIMS</b>	Expensive atmospheric ionization mass spectroscopy
<b>VRH</b>	Variable range hopping
<b>MW</b>	Molecular Weight
<b>HFMO</b>	Highest Filled Molecular Orbital
<b>LEMO</b>	Lowest empty Molecular Orbital
<b>M-I-M</b>	Metal-Insulator-Metal

## 1 Introduction

Polymers are known as insulators. But some of the conjugated polymers show unique electronic properties derived from the presence of  $\pi$ -electrons which are delocalized over the long portion of the polymer chain. The essential properties of delocalized  $\pi$ -electron system, which differentiate a typical conjugated polymer from conventional polymers, are as follows.

The electronic  $\pi$ -band gap ( $E_g$ ) is relatively small ( $\sim 1$  to  $3.5$  eV) with corresponding low excitation energy leading to semi conductive behavior. The polymer molecules easily oxidized or reduced usually through charge transfer with atomic or molecular dopant species to produce conducting polymer. Net charge carrier mobilities in the conducting state are large enough so that high electrical conductivities are realized. Quasiparticles (polarons, bipolarons and solitons), which under certain conditions may move relatively freely through the materials. These properties are found in Polyacetylene, Polyaniline, Polypyrrole, Polythiophene, and Polyphenylene etc. used in the semiconductor devices<sup>1</sup>

### 1.1 Types of Inherently Conducting Polymers (ICP)

- 1) Inherently Conducting polymers
- 2) Conducting Polymer Composites
- 3) Ionically Conducting Polymers

The research on conducting polymers began nearly a quarter century ago, when films of acetylene were found to exhibit dramatic increase in electrical conductivity when exposed to iodine vapors. The procedure for synthesizing polyacetylene was based on a route discovered in 1974 by Shirakawa and coworkers through addition of 1000 times the normal amount of catalyst during the polymerization of acetylene<sup>3</sup> these films were also semi conductive and had an energy band gap of  $1.4$  eV. Leading on from this breakthrough, many other small conjugated molecules were found to polymerize producing conjugated polymers which were either insulating or semi conductive but becoming conductive upon oxidation or reduction **fig.1** shows some conjugated polymers, which have been studied as ICPs.

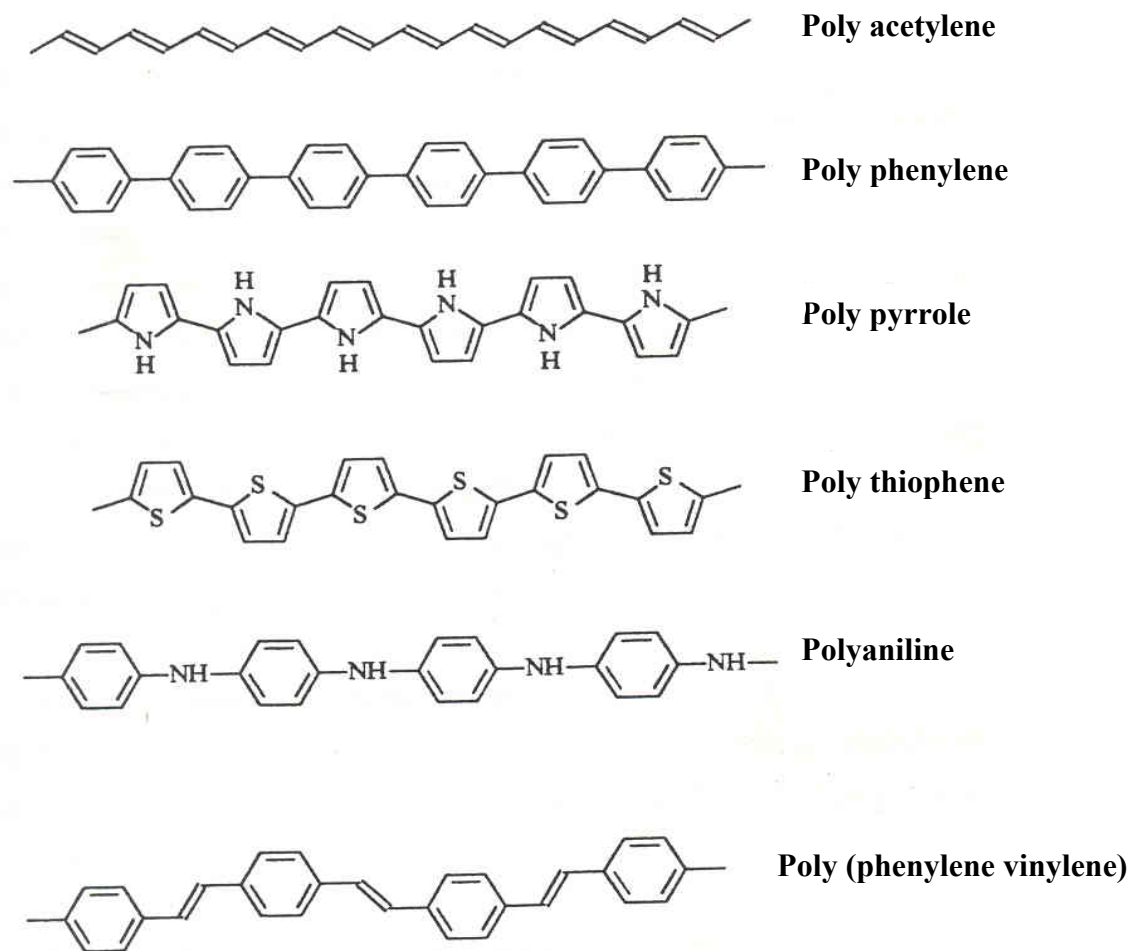


**Fig.1 Geometrical structure of conducting polymers**

The unique electronic properties of the conjugated polymers are derived from the presence of  $\pi$ - electrons, the wave functions of which are delocalised over long portion of polymeric chain, when the molecular structure of backbone is planar. It is therefore necessary that there are no large torsion angles at the bonds, which could decrease the delocalization of the pi electron system<sup>4,5</sup>.

The essential properties of the delocalized  $\pi$ -electron system, which differentiate typical conjugated polymers from conventional polymers with  $\sigma$ -bonds are as follows (a) The electronic  $\pi$ - band gap ( $E_g$ ) is relatively small ( $\sim 1$  to  $3.5$  eV)



with corresponding low excitations and semi conducting behavior (b) The polymer molecules are easily oxidized or reduced usually through charge transfer with atomic or molecular dopant species to produce conducting polymers (c) net charge carrier mobilities in the conducting state are large enough so that high electrical conductivities are realized and (d) quasiparticles which under certain conditions may move relatively freely through the materials<sup>6,7</sup> the electrical and optical properties of these materials depend on the electronic structure and basically on the chemical nature of the repeat unit. The general requirements of the electronic structure in these polymers were recognized and described many years ago.

The electronic conductivity is proportional to both the density and the drift mobility of the carriers. The carrier drift mobility is defined as the ratio of drift velocity to the electronic field and reflects the ease with which carriers are propagated. Enhancing the electrical conductivity of a polymer then requires an increase in the carrier mobility and the density of charge carriers.

## **1.2 Why Polyaniline is important among all the conducting Polymers?**

Polyaniline is a typical phenylene based polymer having a chemically flexible -NH- group in the polymer chain flanked either side by phenylene ring. The protonation, deprotonation and various other physico-chemical properties of polyaniline are due to the presence of this -NH- group. Polyaniline is the oxidative polymeric product of aniline under acidic conditions and has been known since 1862 as aniline black<sup>8</sup>. Wills tatter and co-workers<sup>9-10</sup> in 1907 and 1909 regarded aniline black as an eight-nucleus chain compound having an indamines structure. However, in 1910 Green and Woodhead<sup>11</sup> were able to report various constitutional aspects of aniline polymerization. The authors carried out oxidative polymerization studies using mineral acids and oxidants such as per sulfate, dichromate and chlorate and determined the oxidation states of each constituent by red ox titration using  $TiCl_3$ . Polyaniline has a special representation due to (1) monomer is inexpensive (2) Easy synthesis (3) environmental stability (4) simple doping by protonic acids (5) The conversion of monomer to polymer is straightforward (6) The polymerization proceeds with high yields (7) the resulting salt is quite stable and shows relatively

high level of conductivity (8) when treated with base the conducting pani salt converts to the base form. (9) It is the only conducting polymer whose electronic structure and electrical properties can reversibly be controlled by both oxidation and protonation (10) it has interesting electrochemical behavior and very high stability (11) It is the only known conducting polymer with nitrogen atoms occupying the bridging to the benzenoid and quinoid rings in its backbone structure and playing an important role to the  $\pi$ -bond formation and the electrical intrachain conduction. (12) Many non-degenerate ground state polymers such as Polythiophene and Polypyrrole have been studied. Polyaniline is different from these polymers in three important aspects; firstly charge conjugation in polyaniline is not symmetric that is fermilevel and band gap are not formed in the center of the band so that valence band and conjugation bands are quite asymmetric, secondly both carbon rings and nitrogen atoms are with in the conjugation path, this conjugation differs for e.g. From polypyrrole, whose hetero atoms do not contribute significantly to the  $\pi$ -bond formation. Thirdly, the electronic state of the polymer can be changed through vibration of either the number of electrons or the number of protons.

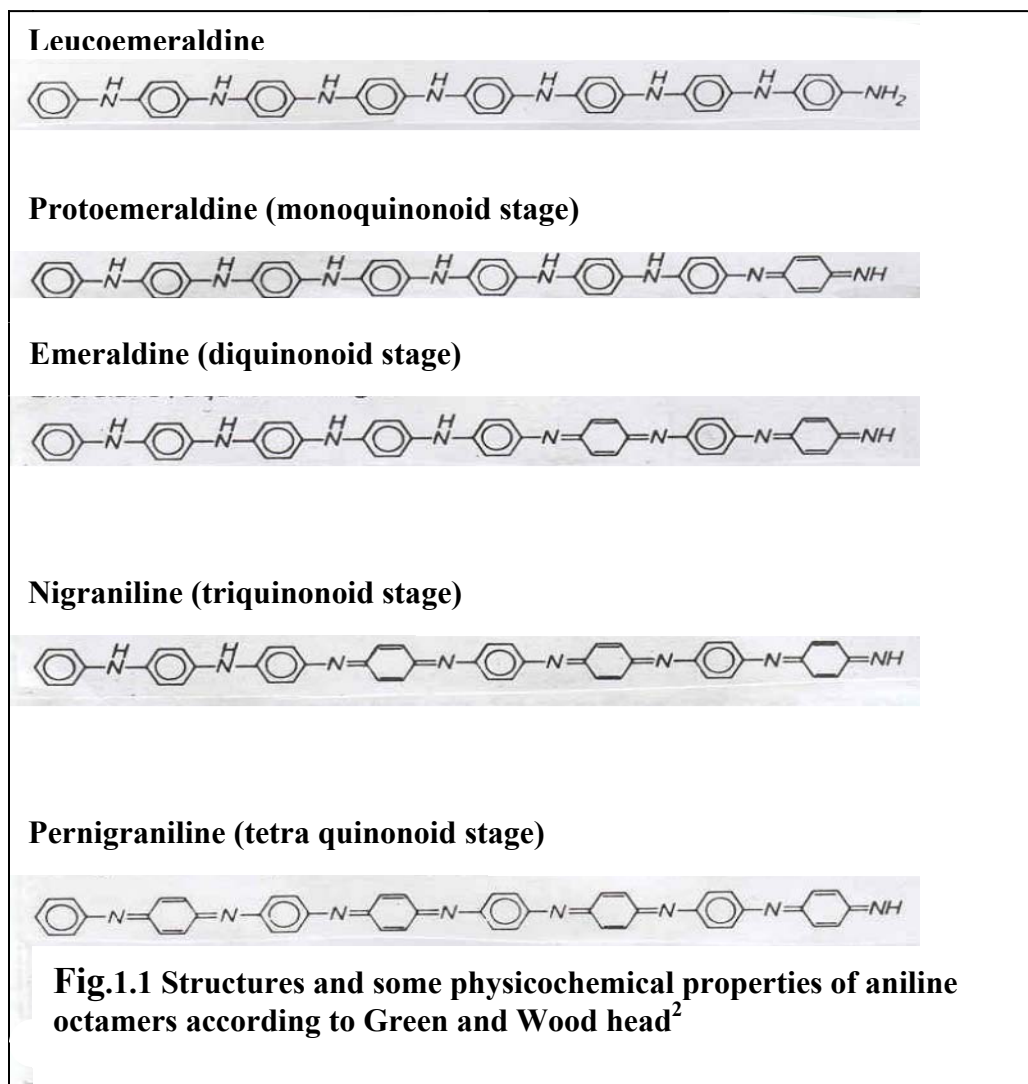
### **i) Chemical Synthesis**

The most preferred method for synthesis of polyaniline by chemical oxidative route involves the use of either hydrochloric or sulfuric acid with ammonium per sulfate as an oxidant in aqueous solution<sup>12-13</sup>. Oxidative polymerization is a two-electron change reaction and hence, the per sulfate requirement is one mole per mole of a monomer. However, the small quantity of oxidant is used to avoid oxidative degradation of the polymer formed. The synthesized polyaniline exists in various oxidation states; they are termed as (1) Lucoemeraldine (2) Emeraldinebase (3) Emeraldine salt and (4) Pernigraniline.

Pron et.al<sup>14</sup>. Compared the electrical conductivity and the reaction yield of polyaniline, polymerized with four different oxidizing agents and at different aniline/oxidant ratios. These authors concluded that the redox potential of the oxidizing agent is not a dominant parameter in the chemical polymerization of

aniline; most oxidizing agents gave similar results. Armes et.al.<sup>15</sup> studied the polymerization of polyaniline at 200°C using ammonium per sulfate as an oxidant.

The various forms of polyaniline are schematically shown in **Figure 1.1**<sup>2</sup>



In their study of the effect of the oxidant\monomer initial mole ratio, they concluded that the conductivity, yield, elemental composition and degree of oxidation of the resulting polyaniline are essentially independent of this ratio when its value was below 1.15. On the basis of elemental analysis, the authors concluded that over oxidation of polyaniline occurs at higher oxidant/monomer mole ratios. Asturias et.al.<sup>16</sup> investigated the influence of the polymerization atmosphere (air or argon) on the degree of oxidation of chemically prepared polyaniline, using  $(\text{NH}_4)_2\text{S}_2\text{O}_8$  as an

initiator. Cao<sup>17</sup> et.al. Established optimum synthesis conditions for the polymerization of aniline by ammonium per sulfate with respect to viscosity, electrical conductivity and reaction yield. They found that the reaction yield was not strongly sensitive to most synthesis variables, while the viscosity or molecular weight and electrical conductivity were found to be markedly affected. In addition they reported that the commonly employed procedure for protonation of polyemeraldine salt (long time stirring of as-polymerized polyaniline powder with conc.aq.HCl solution) leads to significant degradation of polyaniline.

## **(2) Electrochemical Synthesis**

Electrochemical polymerization of aniline is generally carried out in protonic acid in distilled water at platinum electrode. This electrochemical synthesis is achieved by using any one of the following methods (1) Galvanostatic: constant current in the range 1-10 mA. (2) Potentiostatic: at constant potentials – 0.7 to 1.1 V versus SCE and (3) Sweeping the potential: between –0.2 to + 1.0 V versus SCE.

Mohilner et.al.<sup>18</sup> have reported mechanistic reports of aniline oxidation. Major interest in the electrochemistry of polyaniline was generated only after the discoveries that aromatic amine, pyrrole, thiophene furan, indole and benzene can be polymerized anodic ally to a conducting film<sup>19-20</sup>. The anodic oxidative polymerization of aniline is the preferable method to obtain a clean and better –ordered polymer as a thin film. Diaz et.al<sup>21</sup> and others<sup>22-23</sup> reported the preparation of polyaniline in an aqueous acid solution using platinum electrode at potentials between -0.2 to –0.8 V versus SCE. Toshima et.al<sup>24</sup> have reported the formation of polyaniline film by decarboxylation of poly (anthranilic acid). The physicochemical properties of polyaniline films cast from organic solvent like NMP are reported by Kang et.al<sup>25</sup>. Chinese group Shaolin et.al.<sup>26</sup> reported the effect of salts on the electrochemical polymerization. These workers reported that the conductivity of PANI films prepared in the presence of NaCl is about 30 times higher than that of PANI films without NaCl. Chen and Lee<sup>27</sup> investigated the structure and doping behavior of PANI freestanding film plastic zed with NMP. The preparation of PANI films by using FeCl<sub>3</sub> was reported by Yasuda and Shimidzu<sup>28</sup>. They also reported the spectroscopic analysis of these films. Genies

et.al<sup>29</sup>.have carried out aniline oxidation in  $\text{NH}_4\text{F} + 2.3 \text{ HF}$  at 1.0 V. They proposed an intermediate nitrenium cation as an intermediate in the polymerization reaction. Further from EPR studies they showed that there are two polaron-bipolaron states in the polyaniline.

Various authors<sup>30-35</sup> have reported that an X-ray diffraction pattern for acid doped polyaniline. Baughman et.al.<sup>36</sup> investigated crystals of  $\text{ClO}_4^-$  and  $\text{BF}_4^-$  salts of “tetramers” and “dimers” of aniline. Pouget et. al.<sup>37</sup> have thoroughly carried out x-ray studies of the various oxidation states of polyaniline. They reported that starting from amorphous bases, the crystallinity of polyaniline increases with the doping level. They found the orthorhombic crystal structure with parameters such as:  $a = 7.80 \text{ \AA}$ ,  $b = 5.75 \text{ \AA}$  and  $c = 10.5 \text{ \AA}$  for the NMP cast stretched film;  $a = 7.65 \text{ \AA}$ ,  $b = 5.75 \text{ \AA}$  and  $c = 10.2 \text{ \AA}$  for the THF/ NMP extracted powder. These authors showed the regardless of the type of preparation, almost 50% of the polyaniline base could not be transformed by more doping in to “ crystalline” salt.

The electrical conductivity of undoped polyaniline is reported to be in the range of  $10^{-10}$  to  $10^{-7} \text{ S/cm}$ . Upon acid doping it attains higher values in the range  $10^2$  to  $100 \text{ S/cm}$ . The temperature dependence of the conductivity of PANI shows that most of the currently synthesized PANI grades are somewhat away from the metal-to-insulator transition, i.e. the conduction process is dominated by some sort of hopping conduction. Undoubtedly, the hopping process involves a mechanism having  $T^{-1/2}$  temperature dependence. However, the assignment of this temperature dependence of conductivity to the responsible hopping mechanism is not straightforward. The mechanisms, i.e. the one-dimensional variable range hopping, the three dimensional variable range hopping and Sheng’s charge energy limited tunneling effect, could account for the observed temperature behavior.

### **1.3 Synthesis techniques for conducting polymers**

There is no singular method for synthesizing polymers<sup>38</sup> that can be transformed in to conductive polymers; the incorporation of extended  $\pi$ -electron conjugation is of foremost importance. Conductive polymers except ionomeric polymers may be synthesized using standard methods of polymerization including

conventional as well as specific routes, which include Witting, Horner and Grignard reactions, polycondensation processes and metal catalyzed Polymerisation techniques. Oxidative coupling with oxidizing Lewis acid catalysts generally leads to polymers with aromatic or heterocyclic building blocks.

Conductive polymers may be synthesized by any one of the following techniques:

1. Chemical Polymerization
2. Electrochemical Polymerization
3. Photochemical Polymerization
4. Metathesis Polymerization
5. Concentrated emulsion Polymerization
6. Inclusion Polymerization
7. Solid state Polymerization
8. Plasma Polymerization
9. Pyrolysis
10. Soluble precursor polymer Polymerization

Among all the above categories, chemical polymerization <sup>(39-42)</sup> is the most useful method for preparing large amounts of conductive polymers, since it is performed without electrodes. Chemical Polymerisation (oxidative coupling) is followed by the oxidation of monomers to a cat ion radical and their coupling to form dictations and repetition of this process generates a polymer. All the classes of conjugated polymers may be synthesized by this technique.

Electrochemical polymerization is normally carried out in a single or dual compartment cell by adopting a standard three-electrode configuration in a supporting electrolyte, both dissolved in an appropriate solvent. Electrochemical Polymerisation <sup>(43-46)</sup> can be carried out potentiometrically by using a suitable power supply (pototential, galvanostat) generally, Potentiostatic conditions are recommended to obtain thin films, while galvanostatic conditions are recommended to obtain thick films. The electrochemical technique has received wider attention both because of the simplicity and the added advantage of obtaining a conductive polymer being simultaneously doped. Besides this, a wider choice of cat ions and anions for use as “dopant ions” is available in the electrochemical Polymerisation process.

Freestanding as well as self-supporting conductive polymer films of desired thickness or geometry can be obtained. Using this novel technique a variety of conductive polymers like polypyrrole, polythiophene, polyaniline, polyphenylene oxide pyrrole and polyaniline /polymeric acid composite have been generated. Pyrrole in aqueous acetonitrile solvent containing tetraethyl ammonium<sup>47</sup>

This method has also been used to polymerise acetylene. In an electrochemical cell, consisting of Pt as cathode, acetylene gas is and a Ni strip as anode, acetyleneTetrafluoro the  $\text{BF}_4^-$  ion (do pant) was obtained as a film deposited on the Platinum electrode surface gas is passed over a solution comprising  $\text{NiBr}_2$  dissolved in  $\text{CH}_3\text{CN}$ . On application of voltage varying from 5 to 40 V for about 50 min, polyacetylene films can be easily grown on a Pt borate was electropolymerised in two-electrode electro chemical cell. Polypyrrole containing electrode. The degree of doping depends on the do pant concentrations, voltage applied and amount of charge passed.

Photochemical Polymerisation<sup>48</sup> takes place in the presence of sunlight. This Technique utilizes photons to initiate a Polymerisation reaction in the presence of photo sanitizers. Recently, pyrrole has been photopolymerised using a ruthenium (II) complex as photosensitizer. Under photoirradiation, Ru (II) is oxidized to Ru (III) and the Polymerisation is initiated by a one-electron transfer oxidation process Polypyrrole films may be obtained by photosensitized Polymerisation of pyrrole using a copper complex as the photo sensitizes. Photo Polymerization of benzo (c) thiophene in acetonitrile using  $\text{CCl}_4$  and tetra butyl ammonium bromide.

Plasma Polymerization is a technique for is technique for preparing ultra thin uniform layers (50-100 Å) that strongly adhere to an appropriate substrate. Electric glow discharge is used to create low-temperature “cold” plasma. The advantage of this technique is that it eliminates various steps needed for the conventional coating process. Metathesis Polymerization is unique, differing from all other polymerizations in that Ziegler-Natta Polymerization in that the catalysts used are similar, and often identical i.e. a transition metal compounds plus usually an organ metallic alkyl ting agent. Meta thesis Polymerization is further divided in to three classes: ring opening metathesis of cycloolefins all the double bonds in the monomer

remain in the polymer. It was a natural outgrowth of (ROMP); metathesis of alkynes, a cyclic or a cyclic; and metathesis of diolefins. By far the greatest amount of work has been done on ROMP. Most of these techniques are time consuming and involve the use of costly chemical pyrolysis is one of the oldest approaches utilized to synthesize conductive polymers by eliminating form and nature of the standing polymer including the pyrolysis condition. Nevertheless, conductive polymers have been also synthesized by other techniques such as chain Polymerization, step growth Polymerization, chemical vapor deposition, Solid-state Polymerization, soluble precursor polymer preparation concentrated emulsion Polymerization, etc. However, most of these techniques are time consuming and involve the use of costly chemicals.

#### **(a) Doping of Polymers**

May be as high as 50%<sup>51</sup> Also incorporation of the do pant molecules in the quasi one dimensional polymer systems considerably disturbs the chain order leading to reorganization of the doping of polymeric semiconductors is different from that in inorganic or traditional semiconductors<sup>49</sup>. Inorganic semiconductors, have a three-dimensional crystal lattice and on incorporation of specific do pant, n-type or p-type in ppm levels; the lattice is only slightly distorted. The dopant is distributed along specific crystal orientations in specific sites on a repetitive basis.

Doping of conducting polymers involves random dispersion or aggregation of dopants in molar concentrations in the disordered structure of entangled chains and fibrils The dopant concentration polymer doping of the inorganic semiconductors generates either holes in the valence band or electrons in the conduction band. On the other hand, doping polymer leads to the formation of conjugation defects, viz. solitons, polarons or bipolarons in the polymer chain<sup>50</sup>. Thus the ultimate conductivity in polymeric semiconductors depends on many factors, viz. nature and concentrations of do pants, homogeneity of doping, carrier mobility crystallinity and morphology of polymers.



### **Effect of doping on Conducting Polymer**

An x-ray diffraction study on iodine doped poly acetylene shows that the C-C bond length of the polyacetylene chain increases with donor doping but decreases on acceptor doping. In 1,4 -Poly (butadiene) polymers having a non-conjugated backbone have been doped with halogen to form semiconductors<sup>51</sup> effective doping of polymer ions during chemical Polymerization of pyrrole using Fe<sup>3+</sup> based oxidants and electrolyte increases the conductivity even demonstrated that certain dopants could give rise to magnetic ordering in these polymers along with the electron acceptor (e.g. iodine, FeCl<sub>3</sub>, AsF<sub>5</sub>, etc.) or electron donor (e.g. Na, Li etc.) to the polymer which is considered to generate positive carriers (holes) or negative carriers (electrons) in the  $\pi$ -conjugated system. High concentration of doping degrades the polymer backbone.

#### **(c) Low and intermediate doping**

Doping with acceptor and donor molecules causes a particle oxidation or reduction of the polymer molecule. Positively or negatively charged quasi particles are created, presumably polarons in the first steps of doping. When doping proceeds, reactions among polarons take place, leading to energetically more favorable quasiparticles, i.e. a pair of charged solitons in materials with a degenerate ground state and a bipolaron with polymers with single ground state. Applying statistical mechanics allows calculation of the density of polarons, bipolarons and solitons, and the density of electrons and holes in band states at any temperature. The basis of this calculation is the neutrality condition and the fermi distribution function. Furthermore it has to be assumed that the lifetime of the electrons (holes) and polarons are sufficiently long to treat them as quasiparticles. On this basis Conwell has given an estimate of the density of free electrons at a doping level of 5 % and found a value for free charge density of about  $3 \times 10^{24} \text{ m}^{-3}$  or less at 300 K. this is about a fraction of 1/1000 to the total dopant concentration. If the charge carriers in the band states have mobility comparable to that in inorganic semiconductors, the contribution alone would already be the measured conductivity values. The quasiparticles (polarons, bipolarons and solitons) exist in a much higher concentration, but have presumably a

significantly lower mobility. In view of this, the contributions of various particles to the conductivity are unclear. Recent theoretical treatments of three-dimensional interactions in trans (CH)<sub>n</sub> have suggested soliton order in an adjacent chains solitons confinement and the absence of polarons and bipolarons. These findings shed additional light upon these questions and might explain the importance of free carriers in conduction band. Although only outlined for (CH)<sub>n</sub>, these considerations are relevant for other conducting polymers with only polarons, electrons and holes in the bands as carriers for the electrical transport.

#### **1.4 Electrical Conductivity in Polymers**

Frequently it is found that electrical conductivity varies exponentially with temperature, is a function of time<sup>52</sup>, and may vary with the electrical field: i.e.,

$$\sigma = \sigma_0 \exp - E_\sigma / kT = f(\text{time}) = Af(E).$$

Changes in  $E_\sigma$ , the activation energy of conduction, are often observed in the neighborhood of glass-transition temperatures. Since conductivity is made of terms relating to both the number and the mobility of the charge carriers, any prediction regarding the conduction process that does not recognize these dependences is meaningless. As more mobility measurements have been carried out, it has become recognized that the motion of the charge carriers is an activated process. Thus, the simple assumption that polymer can be described in terms similar to those used for crystalline covalent semiconductors.

#### **The Charge Carriers**

The electrical conductivity of polymers increases exponentially with increasing temperature. This has been explained in terms of classical semiconductor theory to indicate that intrinsic charge carrier creation occurs as described by conventional solid-state physics. The implication is that the charge carriers and the generation step are intrinsic to the polymer. Particularly in insulating materials. Frequently nonlinear current-voltage characteristics are observed; electrode effects are noted, irreversible irreversible changes with time are observed. The nonohmic behavior has often been attributed to ionic conductivity; seldom have mass- transport

measurements been carried out to determine if mass transport, the best criterion for ionic conduction, takes place. There are number of mechanisms in addition to ionic conduction by which nonlinear current-voltage characteristics can arise.

### **1 Intrinsic charge-carrier generation**

Materials are classified as metals, semiconductors or insulators depending upon the way in which their electrical resistivity changes with temperature. With metals, the resistivity increases with temperature: with semiconductors and insulators, the resistivity decreases exponentially with temperature. The difference between semiconductors and insulators is one of degree rather than kind.

The motion of an electron, detached from its parent atom or molecule but free to move in a periodically varying potential field such as that existing between atoms on a covalent lattice, can be described in terms of a modulated, traveling wave function. Such a wave function has real solutions for certain ranges of energy, termed energy bands. The ranges of energy for which there are no real roots are called forbidden energies. In a real solid, the highest filled band called the valence band, the lowest empty band called the conduction band, and the difference in energy between them, called the forbidden energy gap. The conduction properties are controlled by the width of the forbidden energy gap and the range of the allowed energies in the conduction and valence bands. The width of the band at a given interatomic distance depends upon the interatomic interaction or, in the case of molecules, the intermolecular interaction. In a strongly interacting system, the allowed bands are wide; in a weakly interacting system, such as a molecular crystal, the bands are narrow. Within the band, the energy levels remain discrete but are closely spaced.

Another important parameter resulting from the band approach is the effective mass of the charge carrier, which is related to the width of the energy band. The effective mass is important because it relates the response of the charge carrier to the accelerating effect of an external electric field and is also related to the width of the band, for example, in a narrow band, the effective mass is high and the charge carrier responds slowly to an applied electric field. Consequently the mobility is low. This is of particular significance in molecular materials where the intermolecular overlap

integral is small and the bands are narrow. In polymers, it has been calculated that the bandwidth for a single linear polyethylene chain should be large (McCubbin and Manne, 1968). However, disorder and the relatively large distances between polymer chains suggest that the limiting step will be transfer of charge carriers between adjacent polymer segments or between specific sites which may be on the same or on a different polymer chain. If the energy band is partially filled with electrons, the material is metallic and there is no forbidden energy gap, the material is a semiconductor. If the energy gap is large, it is an insulator. Sodium, with one 3s electron per atom, is a metal, since the lowest energy band is only half filled and the electrons are free to move. On the other hand, a covalent material, such as silicon, contains two electrons in each bond and all the available orbitals are completely filled. An ionic material has no easily available electrons, since each shell is completely filled. Similarly, polymers based on carbon, Oxygen and nitrogen contain two electrons for each available state. Such materials with all available energy levels completely filled are insulators. The removal or addition of electrons from filled energy bands will lead to a situation in which there are more available states than electrons; a material with more available states than electrons to fill them will conduct charge. Therefore for materials with completely filled states, no electrical conduction should occur until an electron is excited from a filled orbital in to the lowest empty orbital. Consequently, such materials should be insulators. However, in reality, covalent and ionic materials do conduct but at a low level. This low level of conductivity arises because in any material there will always be a small fraction of electrons with energy in excess of the forbidden energy gap. Statically, the number of charge carriers is controlled by the Boltzman distribution law. If the forbidden energy gap is  $E_g$ , then the number of electrons with energy above  $E_g$  depends upon the temperature  $T$ . If  $n$  electrons excite from the ground state to the conducting state (conduction band) leave behind an equivalent number of vacancies  $p$  in the ground state (valence band), which also contribute to the conductivity; i.e.,

$$n = p \quad \text{and} \quad n^2 = n_0 \exp [- (E_g / kT)].$$

This is the origin of intrinsic semi conduction.

Another useful concept is that of the Fermi level. At 0 K, all the electrons fall into the lowest allowed energy level. As the temperature is increased, the probability of higher-energy electronic states being occupied is given by the Fermi-Dirac distribution function  $f = 1 / (1 + \exp. (E - E_f) / kT)$ , where  $E_f$  is the Fermi energy. In a metal, it represents a real state: it is the energy level that corresponds to the highest filled states at 0 K and can be obtained directly by measuring the energy required to remove the electron from metal to the infinity. This parameter is called the work function  $\phi$ . It is also equivalent to the chemical potential of the electrons and, as such, is a useful thermodynamic concept to bear in mind. In a semiconductor, the Fermi energy lies within the forbidden energy gap and cannot be measured directly; but it is equal to half the sum of the ionization potential  $I$  and electron affinity  $E_a$ , i.e.

$$E_f = (I + E_a) / 2$$

There is no clear distinction between insulators and semiconductors. The main difference lies in the width of the forbidden energy gap, hence in the number of charge carriers. It is calculated that, for a material with  $10^{22}$  atoms/cm<sup>3</sup> and a forbidden energy gap of 14 kcal (0.6 eV), there are  $10^{12}$  charge carriers/cm<sup>3</sup> at 25 deg. Celsius. This is not an unreasonable number, which combined with a mobility of  $10^2$  cm<sup>2</sup>/V sec, only corresponds to a conductivity of  $10^{-5}$  /cm-ohm. An energy gap of 42 kcal (1.8 eV) would correspond to  $10^{-8}$  carriers/cm<sup>3</sup> and a conductivity of  $10^{-5}$  ohm-cm<sup>-1</sup>, which is ridiculously low.

In summary, band theory suggests that conductors have more energy states available than there are electrons to fill these states. Semiconductors and insulators have the same number of electrons as energy states (allowing for the spin quantum number  $S$  of 2). Intrinsic conduction in a semiconductor arises by the excitation of an electron across the forbidden energy gap either by thermal, photolytic, or other means, a process that creates an equal number of excited electrons and vacancies (positive holes) in the highest field states. For ordered arrays of atoms, the terminology is that of band theory - the conduction band being the next band at higher unoccupied states and the valence band (ground state). For molecular material, the equivalent terms are the highest field molecular orbital (HFMO) and the lowest empty molecular orbital (LEMO). The intermolecular orbital overlap is small.

Consequently the energy bands are narrow; charge-carrier mobility is low and, and important from a photoconduction viewpoint, the spectroscopic properties of molecular crystal resemble those of an array of an isolated molecules rather than those of a strongly Interacting array.

If charge transport involves the charge carrier spending the greater part of its time on specific molecules, than on a time scale equivalent to the vibrational relaxation times ( $10^{-12}$  sec), the localized states involved are, in fact, radical anions and radical cations. Charge transfer may then be thought of as a localized oxidation or reduction reaction, e.g.,



The energies of the oxidation-reduction couple due to the applied field can then play critical roles in determining the electrical properties.

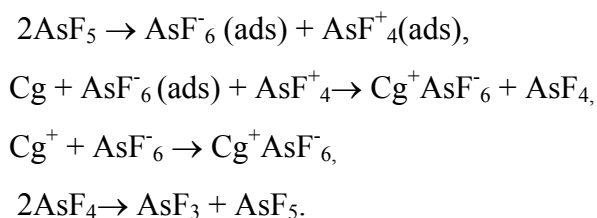
## 2. Impurity Conduction

In semiconductors and insulators, it is assumed that, for each electron that is excited to the conduction band from the ground state, a vacancy is created in the valance band. This vacancy is called a positive hole. Conduction can occur by means of electrons moving in the conduction band or by means of electrons in the valence band moving to vacancies in the ground state, the result is the movement of a positive hole in the direction of the field.

If an electron donor or an electron acceptor is introduced in to the host matrix, the electrical properties can be controlled in a way similar to that in which doping of inorganic crystals by altermvalent ions is used to create n- or p- type conduction.

Another way in which conduction is increased is to produce materials that are mixtures of easily ionized electron donors and electron acceptors. These materials, in which the charge is shared between the donor and acceptor, are called charge- transfer complexes. A number of these compounds have been shown to be conductive. The conductivity depends upon the ionic character of the complex. Fully ionic compounds are more conductive in the ground state than weakly ionic compounds.

For example, the extremely high conductivity of graphite-arsenic penta fluoride materials is thought to involve the sequence of reactions;



Three  $\text{AsF}_5$  molecules create one  $\text{AsF}_3$  molecule (detected) and two conducting states (Forsman, 1977; Bartlett et al., 1978).

Similarly, doping of polyacetylene by sodium or arsenic penta fluoride creates n- or p-type conductivity. The key to the behavior of these donor-acceptor materials lies in the ionization potential and electron affinity. There are well-known methods for deciding which elements and structures will be useful for lowering ionization potentials and increasing the electron affinity of the donor and acceptor (Turner, 1966; Brigleb, 1964). At one time it was also suggested that stable free radicals would provide a means of doping molecular materials and polymers (Eley and Parfitt, 1955). Certainly rapid motion of the unpaired electron along a carbon chain is suggested by the ESR hyperfine structure of many free radicals. However, little intermolecular transfer is observed, since the energy required to detach the unpaired electron from its parent free radical is comparable to the energy required to ionize a molecule (Eley and Willis, 1961).

## **B Localized states:**

In discussing electrical conduction in the context of band theory, the need for regular arrays of similar atoms is clear as the interaction between atoms decreases, the width of the allowed energy band decreases and the effective mass of the charge carrier (this related to the response of the charge carrier to an to an external field) increases. A molecular material, such as anthracene is calculated to be about the limit to which band theory applies (LeBlanc, 1961; Friedman 1964). In the case of a polymer, the condition of a regular spacing of like atoms applies only to the case of simplest Carbon – hydrogen polymers. Such as Polymethylene  $(-\text{CH}_2-)_n$ , polyenes, polyacetylenes, etc. and only along the chain axis.

Breakdowns in local structure, e.g. cis-trans forms in polyacetylene or dipoles in the chain, will all impact the system energetics (Duke and Fabish, 1976; Fabish, 1979). Thus it is not to be expected that even the most highly crystalline nonpolar polymers will have high mobilities and that the mobilities will be isotropic (Baughman and Chance, 1978). This indeed appears to be the situation in polyacetylenes in which mobilities are  $\sim 1 \text{ cm}^2 / \text{V}\cdot\text{sec}$  in the chain direction and the anisotropy is  $>10^2 (\mu_{\text{chain}} / \mu_{\text{n}})$  (Reimer and Bassier, 1975, 1976; Siddiqui, 1980). Thus, for such materials, the existence of narrow bands similar to those of molecular crystals would be expected. Many polymers contain polar groups; each dipole can act as an electron or hole trap. Fox and Turner (1966) have calculated that a dipole of 1.65 D is capable of binding an electron (with the additional effect of dielectric relaxation around the trapped charge carrier). As far as electrical properties are concerned, the effect of the crystallinity is to lower the conductivity. The precise mechanism by which this occurs depends on the precise conduction mechanism; if conduction is ionic, ion mobility through the crystalline regions will be low; if electronic, it will perhaps be faster, but the crystalline-amorphous interface may act as a trapping region—a phenomenon akin to Maxwell-Wagner interfacial polarization.

As far as electrical properties are concerned, the relevance of rubbery and glassy states is still open to speculation. Evidence is accumulating that changes in conductivity can be related to the onset of certain molecular motions. For example, thermal discharge of electrets can be related to the onset of molecular motions in poly(vinylidene fluoride), polyethylene, and other polymers.

The localized energy states, i.e., states not forming extended band-like states, can be envisioned associated with at least the following on a molecular level:

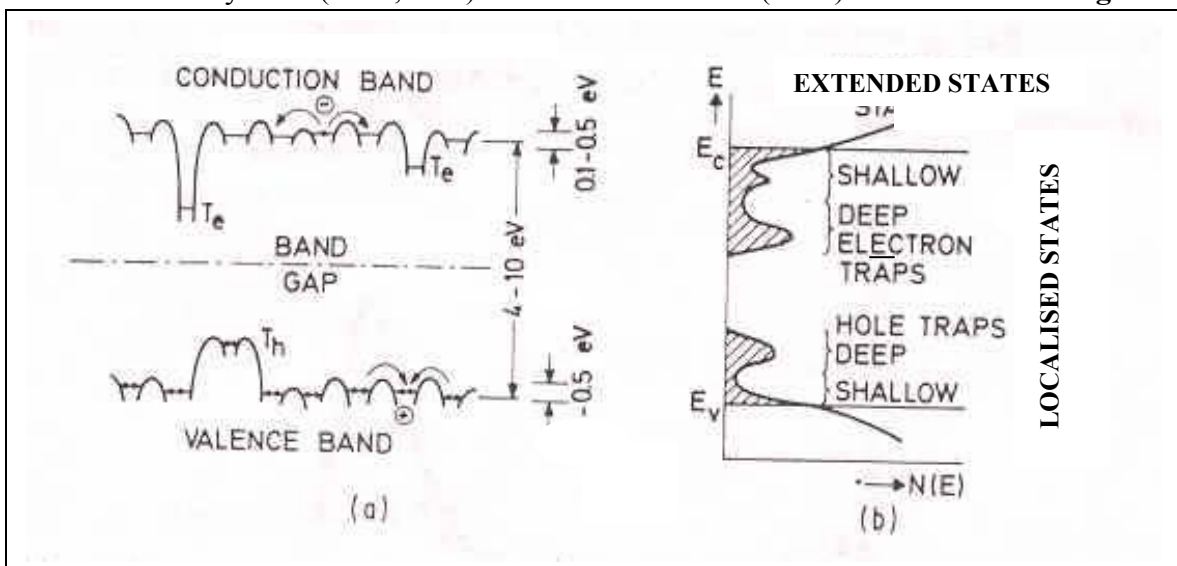
- 1) Surface states induced by strain or chemical reactions,
- 2) Surface dipole states
- 3) Bulk dipole states
- 4) Bulk molecular ion states
- 5) Impurities (different chemical groups, polar groups, ionic groups)
- 6) Chain ends
- 7) Chain branches



- 8) Chain folds
- 9) Changes in tacticity or stereochemistry
- 10) Crystalline- amorphous boundaries
- 11) Broken bonds
- 12) Polar on states (trapped charge and region of surrounding polarized dielectric), and
- 13) Localized fluctuations

Escape from these localized states may be purely thermal; it may depend on the local environments and specific molecular motions. The local field may assist in detrapping. Thus the energy diagram appropriate for a polymer might be represented by a figure. This indicates regular crystallites surrounded by amorphous regions. These crystallites contain some defects, but by and large, has a regular array of atoms. There are interfacial states at the crystalline-amorphous boundary, with in the amorphous region; the localized states are of neither uniform depth for description.

The localized states may act in trapping carriers from the extended states of the crystalline region. According to semiconductor theory, a neutral acceptor state or an ionized donor state will trap electrons and a neutral donor state or an ionized acceptor state will trap holes. A trapped charge can also act as a recombination center. Lattice polarization around charge in localized state can lead to an increase time in depth trap and tend to make transport more difficult (polarons). In the amorphous region, the density fluctuations will create localized states and possibly a mobility band as described by Mott (1967,1969) and Mott and Davies (1971). As shown in the **fig.1.2**



motions. The local field may assist in detrapping. Thus the energy diagram appropriate for a polymer might be represented by figure. The figure indicates a uniform crystallite surrounded by amorphous regions. This crystallite contains some defects, but, by and large, has a regular array of atoms. There are interfacial states at the crystalline-amorphous boundary, with in the amorphous region; the localized states are of neither uniform depth for description. (Seanor 1967).

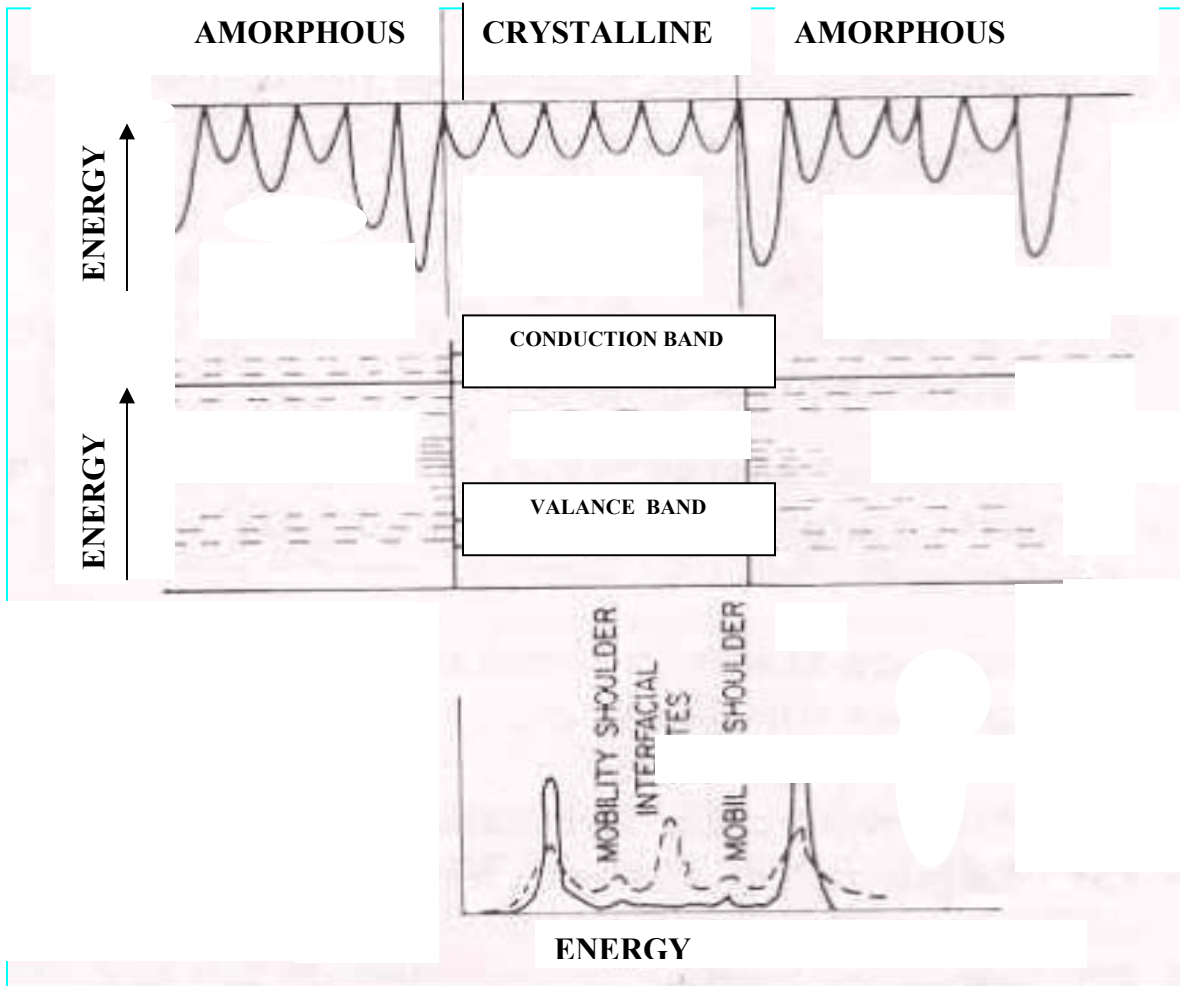


**Fig. 1.3) the energy diagram of a polymer with crystalline and amorphous regions. Crystalline region density of states; -----, amorphous region density of states. It is not known whether the mobility shoulder is real or not.**

because of the differences in local environment could have energy level variations of as much as 1eV. Consequently, the hopping probability is much reduced an important outcome of their hypothesis is that localized states deep within the energy gap are an important property of the polymer and are related directly to its chemical structure it

is not necessary to invoke impurities or disorder to explain traps, although lack of long-range orders will contribute to the range of energy associated with a particular chemical group. Because the energy of closely adjacent sites is unlikely to be the same, both the distance and energy terms in the equation describing hopping probability.

$$P_n \propto \exp(-\Delta E) \exp(-\gamma P),$$

will be small. Here  $\Delta E$  represents the energy difference between the initial and final states,  $\gamma$  describes the fall-off in wave function with distance, and  $p$  is the average separation of the sites.

Another way of stating the Duke-Fabish concepts is to suggest that disorder leads to a range of energetically different environments for each chemically different group in the polymer. Once a charge carrier is trapped, the polarons states created are also spread over a broad range of energy (Duke, 1978).

In addition to bulk states, there can also be surface states and interfacial states, the crystalline and amorphous regions are distributed in three dimensions. The two dimensional representation.

### **C. Injection Processes**

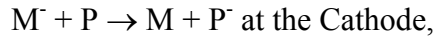
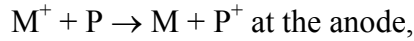
It is considered only that thermal generation of the charge carrier within the materials itself. Other methods of charge-carrier generation involve emission from electrodes or generation under the influence of light (photoconduction). Direct emission from electrodes is particularly important at high fields, and only recently has the extent to which this type of process affects conduction been realized.

It is assumed that, once the charge carrier is inside the solid, it does not know its origin. It recognizes only the influence of temperature, the local electric field (which may be affected by the way in which the charge carrier enters the solid), and the molecular nature of the material.

Electrons in a metal are free to move throughout the bulk of the solid. However when they reach the surface, they are subjected to a constant imposed by the

non-continuity of the solid. In order to move beyond the surface, they are subjected to a constraint imposed by the noncontinuity of the solid. In order to move beyond the surface, they require excess energy. The work done to remove an electron to infinity is called the work function  $\Phi_m$ . If, instead of a vacuum being adjacent to the metal, a dielectric is placed there, the potential barrier will be modified, and both electrons and holes can be injected, depending upon the energy levels in the dielectric.

Such processes can be represented by the equations.



Where M represents the electrode and P the polymer.

In the absence of the surface states, the energetic of such processes can be represented by the conditions that for hole injection

$$\phi_P - (\phi_P + E_{act}) \leq 0,$$

and for electron injection

$$\phi_M - (E_A + E_{act}) \leq 0,$$

Where  $\phi_p$  is the work function of the polymer,  $E_A$  is its electron affinity, and  $E_{act}$  is the energy required to cross the potential barrier at the electrode polymer interface. However, the surface of the polymer is complex and the surface states extends some distance in to the polymer .On making contact between the electrode and polymer; electron transfer will take place until thermodynamic equilibrium is attained .The contact charge will cause some lowering of the polymer to injection.

There are three ways in which the energy required to escape from the metal may be supplied:

1. by thermal methods in a process known as thermonic emission,
2. by the application of high electric fields in field emission, and
3. by photon absorption at sufficiently short wave lengths in the photoemission process.

Mechanisms 1 &3 may be modified by the Schottky effect, which arises from the field dependent lowering of the potential barrier to injection.

A number of experimental observations on polymeric systems have been explained in terms of emission processes. Miyoshi and Chino (1967) have documented Schottky emission in to polyethylene. Lily and McDowell (1968) have studied the Schottky effect in Polyester films and have suggested that injection into surface states takes place followed by a field-dependent detrapping process. To allow for surface states, trapped charge, and local polarization effects, Taylor and Lewis (1971) have argued in favor of a more generalized barrier- lowering term of the form

$$E(x) = \phi q K / (ax)^n.$$

The equivalent form of the equation for barrier lowering becomes

$$i = i_0 \exp\{-(\phi - q\beta E^{n/n+1}) / kT\},$$

where  $\beta = (n+1) (K / ax)^{n/n+1}$ . Data for polyethylene and polyester yield  $n=0.45$  and  $n=0.15$ , respectively, and the values for the energy barriers compatible with the polymer work functions of Davies (1969).

The exponential dependence of current on  $E^{1/2}$  is not characteristic of just Schottky barrier lowering. If the charge carrier becomes trapped in a coulombic potential well, then the field induced lowering of the barrier to detrapping has the same functional dependence. The difference arises because in the coulombic well the force between the charge carrier and the charged site varies as  $q^2 / x^2$ , where as the force between the injected charge and its image charge in the electrode varies as  $q^2/(2x)^2$ . Consequently, the formalism of the Poole-Frenkel trap barrier lowering exhibits the same  $E^{1/2}$  dependence. If the local dielectric constant is known, it is possible to distinguish between the two effects. Alternatively, electrodes of different workfunction should allow injection currents to be distinguished from detrapping phenomena.

At high fields, the width of the potential barrier decreases. As a result, the probability of finding an electron on the other side of the potential barrier by quantum mechanical tunneling increases. The tunneling process is independent of temperature, and the tunneling current is characterized by the equation

$$T = (q^2 V / h^2 d) (2m^* \phi)^{1/2} \exp [-4\pi d(2m^* \phi)^{1/2} / h]$$

(If  $T \rightarrow 0$  and  $qV \ll \phi$ ), where  $m^*$  is the effective mass of the charge carrier and  $h$  is Planck's constant. Charge-carrier tunneling predominated at low temperatures and low voltages, whereas Schottky barrier lowering was observed at high temperatures and voltages.

### **1.5 Advantages and Disadvantages of the Conducting Polymers**

The conducting polymers show many advantages over the other polymers, form of films, which can be directly used in chemical gas sensors and microelectronic devices. The functionalization of the conducting polymers with various alkyl chains or other cyclic chains gives better process ability to these polymers. The copolymerization of these polymers reported to give better optical properties by lowering its band gap. Conducting polymers exhibit better electrical conductivity and hence, they are better semiconductor alternatives to the conventional inorganic such as silicon and bismuth arsenate etc. The conducting polymer batteries show better efficiency than the normal lead-sulfuric acid batteries. The other advantage is lying in the fact that former is lightweight and handy as compared to latter. The conducting polymeric films are directly obtained in its doped state, which offers them good scope in electrical coating technology. The disadvantages with conducting polymers arise from the fact that they are not highly stable compounds even at moderate temperatures ( $>150^\circ\text{C}$ ), The most of the conducting polymers exhibit dark color due to their highly oxidized states. These polymers are insoluble in most of the common organic solvents; hence they become practically nonprocessable though these are often termed as 'Synthetic meals' they have not achieved the higher conductivity as metal possesses to make them processable through many methods are being used, these are adding to the cost of material, which are not economically viable.

### **1.6 Why Blending is necessary?**

In order to overcome the above-mentioned drawbacks, it is essential to blend conducting polymers with the conventional polymers. Mixtures of polymers, which

are homogeneous or heterogeneous depending upon morphology, are called blends, properties such as tensile strength, high impact strength, thermal resistance and chemical resistance; easy processing and dimensional stability etc. will be enhanced by blending the polymer.

There are various types of blending the conducting polymer with other polymers. These are; dry blending, solution blending and insitu blending.

### **1.7 Preparation methods of the Conducting Polymer Blends**

It is divided in to two subsections: blends prepared by electrochemical methods and those prepared by chemical synthesis of the conductive polymer<sup>53</sup>. Electrochemical methods are generally used for small-scale preparation or for the production of different kinds of devices. Chemical preparation allows large-scale production of the conductive polymer and, consequently, of blends or composites.

#### **a) Blends prepared by electrochemical methods**

Conductive polymer films can be electrochemically deposited on the surface of metallic or semi-conducting electrodes .The area of the films depends on the dimension of the electrodes, while the thickness depends on the charge density used .A rotating drum electrode was developed by Naarman which permits continuous production of polypyrrole films by the electrochemical method <sup>(54)</sup>, however, this alternative process has not been used to produce blends.

#### **b) Electrode coating method**

A one compartment-cell with three-electrodes (reference, working and counter) is usually used. The conductive polymer is obtained by the anodic deposition on to a suitable working electrode using a solution containing an electrolyte and the monomer .In the case of polyaniline and its derivatives it is necessary to lower the pH of the electrolyte solution to 1.0 using a suitable acid. To obtain blends, the working electrode is coated with a film of the insulating polymer, prior to the anodic deposition of the conducting film. The coated electrode is

immersed in the electrolyte solution containing the desired monomer and swells over a period of time.

When the swelling process is complete, the current can flow between the coated working electrode and the counter electrode. By applying the potential necessary to oxidize the monomer, polymerization starts at the electrode/film interface and proceeds to fill the bulk of the insulating film until reaching the film/electrolyte interface. Depending on the miscibility of the conductive and the insulating polymers, the formation of a blend (good miscibility) or formation of a conductive polymer film between the electrode and the insulating polymer film (very poor miscibility) results. In intermediate cases a composite may form.

Three conditions must be fulfilled by the insulating polymer film: 1) swelling of the solution containing the monomer and the electrolyte, 2) a certain degree of miscibility with the conducting polymer and 3) stability in the potential range and in the medium used for the polymerization.

### **C) Co deposition method**

This uses the same chemical setup, but dissolves the insulating polymer host in the electrolyte solution, which also contains the monomer of the conductive polymer. As the conductive polymer film is anodically deposited on the surface of the electrode, it becomes soaked with the insulating polymer solution. After accumulating the required charge density, the film formed on the electrode is dried, thus removing the solvent and leaving the insulating polymer combined with the conductive polymer.

Soluble polyelectrolytes can be used in this method, eliminating the need to use an electrolyte salt. In this case, the polyelectrolyte acts also as counter ion or dopant. Membranes and self-supported films were prepared by this method.

### **d) Blends prepared by chemical synthesis of the conductive polymer**

The advantage of chemical synthesis is that large-scale preparation of the conductive polymer can be achieved. Blend preparation can be carried out in two different ways.



#### **e) Mixture of Blend components**

This can be achieved by two methods. One is the mechanical mixture of conductive and insulating polymer using a counter-rotating mixer or a double screw-extruder. In this case the resulting conductivity will strongly depend on the miscibility and the rheological properties of the components of the blend. For example, the percolation threshold is strongly affected by the miscibility of the blend components. The conductive polymer used for the blending is normally synthesized by chemical methods.

Blends of polyaniline and poly (vinyl chloride) has been prepared using this procedure<sup>55</sup>Mixing temperature, design of the screw and rotating speed are variables which must adjusted according to the polymers to be blended. The temperature must be sufficiently high to permit a good flow of the molten polymers yet sufficiently low to avoid thermal degradation. The design of the screw should provide a sufficiently long mixing zone with the shortest residence time possible. Rotation of the mixer blades or the extruder screw must be adjusted to permit good mixing and to avoid degradation by shearing. The optimization of these parameters will decrease thermal and shear-degradation and increase the productivity. The second method is the co dissolution of the blend components in a common solvent followed by the evaporation of the solvent. Here, phase segregation may occur during solvent evaporation because of the different solubility of the polymers in the common solvent. In this case, the miscibility is also an important factor. In polyaniline; the polymer can be reduced in a basic solution (dedoped) in order to increase its solubility in common organic solvents. After preparation of the blend it can be doped again

#### **e) Polymerization of the conductive polymer in the insulating matrix**

Several methods have been used following this method, leading to blends, composites and semi interpenetrating polymer networks. Polymerization can be achieved by addition of the heterocyclic monomer to a solution of the insulating polymer containing oxidizing agent films of the blend are obtained by evaporation of

the solvent. Using this method is also possible to obtain an aqueous suspension of the latex covered by polypyrrole<sup>56</sup> or a colloidal dispersion of polypyrrole/poly (2-vinyl pyridine)<sup>57</sup>. Films can be obtained by casting, spin coating or spraying. Interfacial polymerization of a conductive polymer producing a material with different superficial properties is also an alternative method. With this method a two-phase system is necessary: One solution containing an insulating polymer and a heterocyclic monomer (organic phase) and another containing an oxidizing agent aqueous phase. The monomer diffuses to the interface, where oxidative polymerization occurs. Blends were obtained by this method combining polypyrrole with nafion<sup>58</sup> or with poly methyl methacrylate<sup>59</sup>.

Polymers can also be swollen with the solution of an oxidant, blotted with tissue or filter paper and dried, retaining the oxidant as filler in its bulk. The blend is obtained by exposing the polymer containing the oxidant to vapors of the heterocyclic monomer in a closed chamber. Blends were prepared using this method and combining polypyrrole with cellulose<sup>60</sup> with poly (ethylene terephthalate)<sup>61</sup> or with nylon<sup>62</sup>.

The solid inorganic oxidant can be introduced in to the insulating polymer as filler. In this case, blends can be also prepared by exposure of such solid polymer matrices, containing the oxidant; to vapors of the heterocyclic monomer. The polymerization kinetics for the conductive polymer will depend on the diffusion coefficient of the monomer in to the insulating polymer host. Also, formation of the conductive polymer near the surface of the insulating host may preclude further diffusion of the monomer to its bulk, impeding the formation of a homogeneous blend. In this case it must also consider the possibility of the polymer oxidant solid solution being homogeneous or heterogeneous as the properties of the resulting blend depend on the phase behavior of this solution. For heterogeneous solution we obtain only heterogeneous blends; the monomer diffuses in to the polymer matrix, polymerizes around the oxidant particles and no percolation path is formed. For homogeneous solid solid solution the properties of the blends are again determined by the miscibility between the different polymers. Phase segregation may occur after polymerization, precluding percolation.

The mechanical mixture of oxidant and polymer is also an interesting method to incorporate the oxidant in the polymer matrix. Blends of polypyrrole and EPDM rubber (a terpolymer of ethylene, propylene and ethylidene norbornene) was obtained using an EPDM matrix impregnated with  $\text{CuCl}_2$  by calendaring<sup>63</sup>

The oxidant can also be incorporated in to the polymer matrix by dissolution with the insulating polymer in a common solvent, followed by solvent evaporation. This procedure was used to prepare blends of polypyrrole with poly (vinyl chloride)<sup>64,65</sup> and with poly (vinyl alcohol)<sup>66</sup>

Reactive extrusion is also to obtain the blends .In this technique the oxidant and the insulating polymer are fed in to the extruder and melt mixed. In an intermediate section of the screw the monomer is introduced under pressure and mixed with the molten phases. Polymerization occurs in the second mixing region of the screw .The equipment must be fitted with an injection port of the monomer and a degassing port to liberate the gaseous products .In this case, the oxidant would be introduced as a filler at the feeding port of the extruder, together with the other components of the formulation. This method has not yet been used to obtain conductive polymer blends.

## **1.8 Physical Blending**

Conductive polymer composites<sup>67</sup> can be defined as insulating polymer matrices, which has been blended with filler particles such as carbon black, metal flakes or powders, or other conductive materials to render them conductive. Composites consisting of a conducting polymer filler (in the powder form) and an insulating polymer matrix provide a convenient solution to these processing problems. The conductive composites have an advantage in that the mechanical and the physical properties of the composite can be influenced by the choice of the host-insulating matrix.

### **1.8.1 Effect Of Interaction Between Filler Particles And Host Matrix.**

The addition of a conductor or a semiconductor to an insulator affects the electrical properties of the composite according to the filler loading and the proximity

of the conductive particles to other conductive particles. Three conditions are possible: no contact between the particles, close proximity, and physical contact between the particles.

### **1.8.2 No contact between the conductive particles**

When the conducting particles are isolated, the conductivity of the composite changes only slightly or not at all. The composite remains an insulator, although its dielectric properties may change significantly.

### **1.8.3 Conductive particles in close proximity to each other**

When the conductive particles are in close proximity to each other, electron can cross the gap between particles, creating a current flow. The ability of an electron to cross a gap under a given voltage field increases exponentially with decreasing gap size. Gaps as large as 10 nm can be jumped.

Electron transport across an insulator gap can occur by one of two methods: hopping or tunneling. Tunneling is a special case of hopping where electrons can tunnel from the valence band of molecules or ions on one side of the gap to the conduction band of molecules or ions on one side of the gap to the conduction band of molecules or ions on the other side of the gap without any energy exchange. Hopping consists of the same type of electron flow between conductors across an insulating gap. However in this case an electron must have its energy level increased to that of an appropriate level from which it can jump across the gap. Hopping therefore required activation energy.

### **1.8.4 Physical contact between conductive particles**

Under the condition the composite conducts through the particle network by the conduction mechanism of the conductive particles. Composite using metal particles as the conductor would exhibit band-type conduction. Band conduction and hopping conduction can be differentiated by the A.C and D.C. behavior of the composite. A composite, which conducts by a hopping mechanism, will exhibit a higher A.C. conductivity than D.C. conductivity. It will also show an increase in conductivity than D.C. conductivity with an increase in frequency. Highly loaded

composites, which show linear current-voltage characteristics (i.e. show Ohmic behavior) contain filler particles that are in actual physical contact with each other, where as those composites with lower filler loadings exhibit non-Ohmic behavior because they rely upon the hopping mechanism for electron transport. The total non-Ohmic behavior of composites is claimed to be due to extended space charge distributions near the electrodes. Space charge distributions are claimed to be generated by local polarization of the matrix material. It is probable that metal particles and fibrous conductive fillers conduct by hopping, although actual physical contact between the particles is also possible. Their much large size makes them less likely to be isolated from other conductive particles and more likely to penetrate a thin film.

### **1.8.5 Network formation between filler particles**

Composites consisting of an insulating matrix and a conductive filler will show a transition from insulator to conductor over a very narrow range of filler concentration. A typical curve of resistivity versus filler concentration (**figure1.4**) will show that the composite remains an insulator at low concentrations.

At a critical volume fraction, the resistivity of the composite falls sharply to a level at which the composite can readily conduct electricity. Increases in filler concentrations above the critical loading do not appreciably reduce the resistivity.

The sharp change from insulator to conductor is due to the formation of a network among the filler particles. Network formation has most frequently been treated as a percolation process.

The percolation models refers to a means of continuous network formation through a lattice, taking in to accounts the relative amounts of the two materials comprising the network. It is a stastical representation and is most frequently analyzed by Monte Carlo techniques.

The probability of a continuous network being formed by filler particles in a matrix is related to the stastical average number of contact each particle makes with neighboring particles and the average number of contacts per particle that are satirically possible.

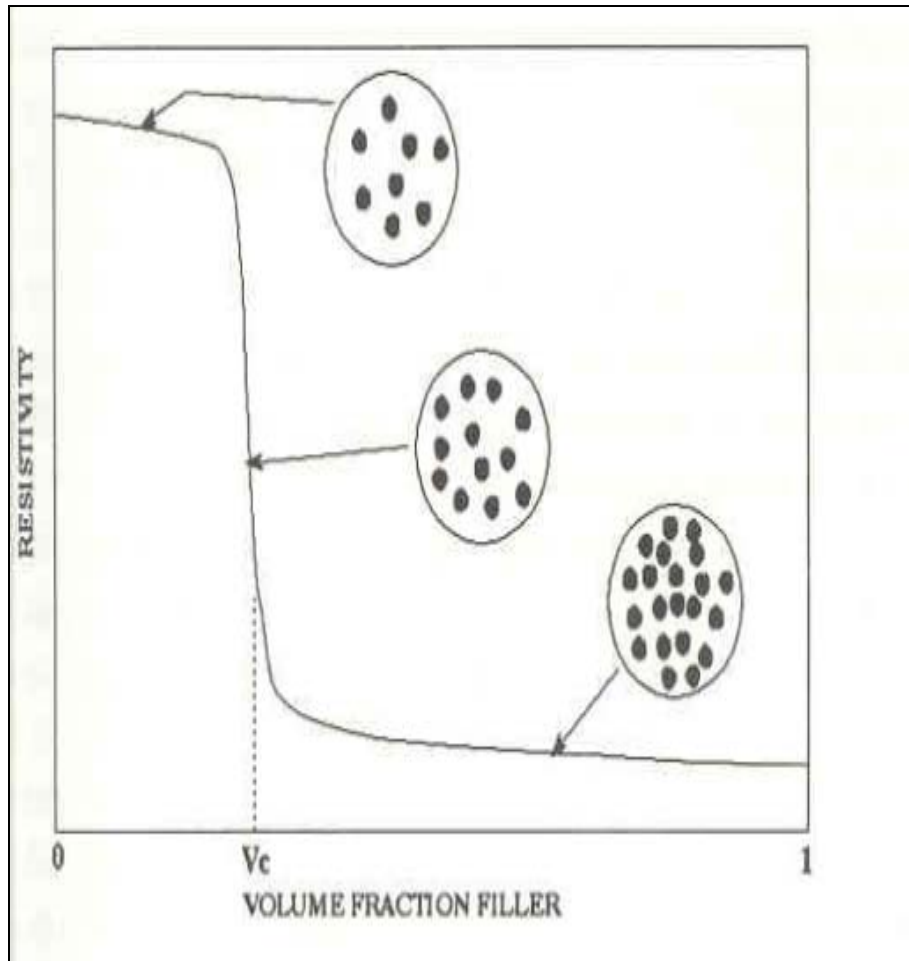


**Fig. 1.4 A schematic graph of Resistivity vs. filler cocentration**

### 1.8.6 Conducting Polymer Composite Materials (CPC)

The CPC constituents are conducting filler and polymer matrix where this filler is dispersed randomly. It has usually been considered from their constituents and properties. Direct current can flow along such materials only through continuous chains of filler particles<sup>68</sup>. The probability of finding such a structure depends on a variety of factors, namely: quantity of filler, shape of filler particles and their capability of becoming combined with a polymer, method of mixing etc. A choice of matrix is determined mainly by the operating conditions of a material and the desired physical-mechanical properties of composite. The value of the CPC conductivity does not depend on a choice of polymer matrix.

Conducting fillers are classified in accordance with the following parameters

- 1 - material (organic, metallic)
- 2- aspect ratio  $l/d$  ( $l/d \sim 1$  – disperse;  $1 < l/d < 1000$ - flakes; short fibers;  $l/d > 1000$ - long fibers);
- 3- distribution of filler particles according to the size –  $F(l, d, l/d)$ ;
- 4- filler Conductivity

The shape of the filler particles varies widely, but only the particle aspect ratio, the main parameters which determines the probability of neighboring particle contact of a given degree of filling, is important from the view point of using them in the CPC. The aspect ratio  $l/d$  is a ratio of maximum and minimum ( $d$ ) dimensions of a geometrical body and from this point of view, a sphere, cube, ellipsoid are approximately similar bodies having  $l/d \sim 1$ .

At present the most promising filler are those with  $l/d > 1$  i.e. fibers and flaky fillers that makes it possible to reduce filler concentration in a composite and thus, facilitate the processing and improve physical-mechanical properties. Besides cut carbon fibers that have higher conductivity has been developed.

### **1.8.7 Structure and Conductivity of CPC**

Conducting polymer composite materials are typical disordered structures consisting of randomly (or according to a certain law) arranged particles of conducting filler that are submerged in to a polymer medium. In this case the filler particles have macroscopic (as compared with a free path of electrons in the particles) dimensions, which facilitates the study of such structures allowing one to neglect quantum effects. However, the role of such effects in the CPC is practically unstudied, though in some cases, at the filler-polymer boundary it may prove to be significant (e.g. the fluctuation tunneling model allowing for quantum modulation of carrier transfer between conducting particles at low temperatures<sup>69-70</sup>). One more simplification, which is not stated but in most cases is tacitly assumed, relates to the role of a polymer matrix which is considered as a certain continuous medium with dielectric constant  $\epsilon'$  that serves only to fix filler particles in space. Such an approach is useful for the consideration of CPC general properties and true, with a sufficient

degree of accuracy, for amorphous polymers. However it is not satisfactory in the case of, say, crystallizing polymers as the filler where particles are pushed out of crystal regions because of their large size and become concentrated in amorphous zones. This means inhomogeneous spatial distribution of the particles, or, in other words, their segregation<sup>71</sup>.

The percolation theory<sup>72-75</sup> is the most adequate for the description of an abstract model of the CPC. As the majority of a polymers are typical insulators, the probability of transfer of current carriers between two conductive points isolated from each other by an interlayer of the polymer decreases exponentially with the growth of a gap  $l_g$  (the tunneling effect) and is other than zero only for  $l_g < 100A^\circ$ . For this reason, the transfer of current through macroscopic (compared to the sample size) distances can be effected via the contacting-particles chains. Calculation of the probability of the formation of such chains is the subject of the percolation theory. It should be noted that the concept of contact is not just for the particles in direct contact with each other but, apparently, implies, convergence of the particles to distances at which the probability of transfer of current carriers between them becomes other than zero.

Experimental dependences of conductivity  $\sigma$  of the CPC on the conducting filler concentration have, as a rule, the form predicted by the percolation theory with small values of  $C$ ,  $\sigma$  of the composite is close to the conductivity of a pure polymer. In the threshold concentration region when a macroscopic conducting chain appears for the first time, the conductivity of the composite material (CM) drastically rises (resistivity  $Q_v$  drops sharply) and then slowly increases practically according to the linear law due to an increase in the number of conducting chains.

Calculation of dependence of  $\sigma$  on the conducting filler concentration is a very complicated multifactor problem, as the results depend primarily on the shape of the filler particles and their distribution in a polymer matrix. According to the nature of the distribution of the constituents, the composites can be divided in to matrix, stastical and structarized systems. In matrix systems, one of the phases is continuous for any filler concentration. In stastical systems, constituents are spread at random



and do not form regular structures. In structured systems, constituents form chain-like, flat or three-dimensional structures.

The maximum values of the percolation threshold are characteristic of matrix systems in which the filler does not form the chain-like structures till large concentrations are obtained. In practice, stastical or structured systems are apparently preferable because they become conductive at considerably smaller concentrations of the filler. The deviation of the percolation threshold from the values of  $C_p$  to either side for a stastical system ( $\sim 0.15$ ) can be used to judge the nature of filler distribution.

An example of the structured system is a composite obtained by pressing a mixture of the polymer powders and metal with radii of  $R_p$  and  $R_m$ , respectively ( $R_p > R_m$ ) granules. When the powders are being mixed, metal particles stick around polymer granules and, if the pressing temperature is lower than the polymer melting temperature, do not penetrate inside the granules. As the material volume accessible for the filler is thus artificially reduced, conducting chains are formed at lesser concentration and the larger the ratio  $R_p/R_m$  the more reduced is the percolation threshold.

The composites with the conducting fibers may also be considered as the structured systems in their way. The fiber with diameter  $d$  and length  $l$  may be imagined as a chain of conducting spheres with diameter  $d$  and chain length  $l$ . Thus, comparing the composites with dispersed and fiber fillers, we may say that  $N = l/d$  particles of the dispersed filler are as if combined in a chain. From this qualitative analysis it follows that the lower the percolation threshold for the fiber composites the larger must be the value of  $l/d$ . This conclusion is confirmed both by the calculations for model systems and by the experimental data<sup>76-77</sup> so, for  $l/d \sim 10^3$  the value of the threshold concentration can be reduced to between 0.1 and 0.3 percent of the volume.

As was noted above, when the conducting filler particles converge to a distance of  $l_g < 100\text{\AA}$ , the current transfer among them is possible by tunneling the electron through a quantum mechanical barrier. However, the equivalent resistance of such a junction is rather high, in any case it is higher than that with direct contact with the particle. These places may be considered as defects in the chain like structure of

composites. The defects of other kind may be associated with the high contact resistance in the places where the particles touch due to oxide layers or other admixtures present on their surfaces. Whatever nature of the defect may be, the presence of the defects makes the introduction of an extra amount of the filler necessary to compensate for the defect. This is not always desirable for various reasons. But such defects may be cured by the application of a high dc voltage, which results in the electrical breakdown of the insulating interlayer. As was proved, for  $C < C_p$  600v pulses with a duration of 1 ms is absent in the compositions made up of polytetra fluoro ethylene and carbon fibers. With the initial value of  $Q_v^\circ$  of the composition being  $1.8 \times 10^4 \text{ Ohm} \times \text{cm}$ , after the effect of the pulse action  $Q_v$  decreases 37 times, while with  $Q_v^\circ = 0.92 \text{ Ohm.cm}$ , it decreases only 1.4 times. Thus, the smaller the difference in  $C - C_p$ , the higher is the effectivity of curing the defects by the action of the voltages.

The defects caused by the high contact resistance especially manifest themselves in the metal filled composites where the value of the percolation threshold may reach 0.5 to 0.6. This is caused by the oxidation of the metal particles in the process of CPC manufacture. For this reason only noble metals Ag and Au, and, to a lesser extent, Ni are suitable for the use as fillers for highly conductive cements used in the production of radio electronic equipment.

The CPC structure also determines the following properties important in practice: the temperature coefficient of resistance, dependence of conductivity on frequency, etc.

In conclusion the preparation of the samples of the polymer composites with the corresponding electrical properties in the form, say, of the plates, bars, pellets etc. that are usually used for the purpose of research in the laboratories, and of real articles should be considered as two inter related problems. As the values of the conductivity and other parameters obtained for the simple forms might prove different for the forms that may be used as constructional elements. Therefore, these circumstances should be taken in to account at the design stage of a conducting composite as well as the optimum technological techniques of molding of practically important articles.

### 1.8.8 Processing Conditions and Conductivity of Composite Materials

The wide use of articles made of conducting composite materials depends on reproducibility of their physical-mechanical and electrical properties. Constituent mechanical properties (strength, modulus of elasticity) are comparatively easy to obtain, however the task of obtaining stability of electrical properties is rather complicated. It is bound up with the fact that mechanical properties of composite materials are mainly determined by average filler concentration, whereas electrical properties depend on whether a continuous net of contacting filler particles is formed in the material, i.e. on their distribution and local concentration. In other words, the technological chain “constituents → mixing → CCM → processing to article → article” each step makes its own, frequently unpredictable, contribution to a change of local concentration of the filler.

The above may be illustrated by the following suitable example <sup>(78)</sup>. **Figure 1.5**

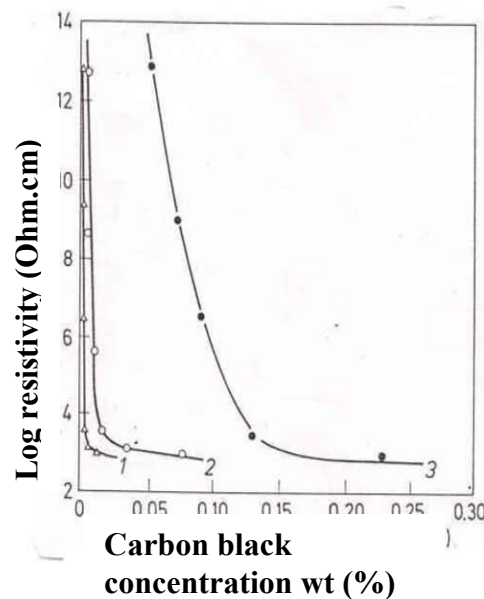


**Fig.1.5 Conductivity-concentration relationship of composite depending manufactures technique.**

**Fig.1.5** shows the relationship of conductivity of polystyrene- based composite materials and the filler concentration (carbon black Ketjen-black EC). The materials are fabricated by the different methods: (1) pressing of a mixture of carbon black and polymer powder; (2) mixing of carbon black with toluene dissolved polymer in a ball-mill, moulding of film by slow evaporation of the solvent, grinding of the film and pressing ;(3) Calendaring of a mixture of a carbon black and polymer between heated rollers, grinding of the product and pressing.

In pressing the threshold concentration of the filler amounts to about 0.5% of volume. The resulting distribution of the filler corresponds, apparently, to the model of mixing of spherical particles of the polymer (with radius  $R_p$ ) and filler (with radius  $R_m$ ) for  $R_p \gg R_m$  as the size of the carbon black particles is usually about  $1000 \text{ \AA}$ . During this mixing, the filler, because of electrostatical interaction, is distributed mainly on the surface of polymer particles, which facilitates the forming of conducting chains, and entails low values of the percolation threshold. For the second method the threshold concentration of the filler in a composite material amounts to about 5 volume % i.e. below the percolation threshold for stastical mixtures .It is bound up with the fact that carbon black particles are capable (in terms of energy) of being used to form conducting chain structures, because of the availability of Functional groups on their surfaces. The relatively “sparing” method of composite material manufacture like film molding by solvent evaporation facilitates the forming of chain structures.

During calendaring, the value of threshold concentration of the filler rises to about 25% by volume, i.e. above the threshold for stastical mixtures. Obviously, in this case mechanical forces, especially shearing stresses, destroy the forming chain structures of black particles. The data on the effect of the prolonged mixing in an extruder on the composite material conductivity are indicative of the same fact. In the case of thorough mixing, the value of conductivity drops sharply due to the break up of soot aggregates and uniform distribution of the carbon black in the composite material. These data were obtained in researching the mixtures of carbon black and copolymer of polypropylene and vinyl chloride, and the mixture of high-density polyethylene copolymers of ethylene

with ethylacrylate and vinyl acetate <sup>(79)</sup>. The above data provide the proof of the crucial effect of a method of constituents mixing and composite material processing on the distribution of the filler an, thus, on electrical properties of conducting composite materials. These issues are considered hereinafter.

### **1.8.9 Distribution of Filler in Conducting Polymer Composites Based on Polymer Blends**

As was noted earlier, with the uniform distribution of the conducting filler in a matrix, it is necessary to introduce large amounts of the filler so as to reach the desired level of composite conductivity, which entails aggravation of mixture processing and mechanical properties of the conducting polymer composite. To reduce the filler concentration, it should be segregated, localized in the limited volumes so that the filler concentration in these regions becomes higher than the average one, accordingly, the probability of forming of the conducting channels and conductivity itself are higher in these regions, and this entails the rise of the composite conductivity as a whole. To achieve this goal different methods can be used, for instance, introduction of neutral filler such as kaolin, talc, etc. Such fillers decrease, in a composite, the volume of a region accessible for the conducting filler. Nevertheless, general concentration of the fillers remains high and this does not improve mechanical properties of the conducting polymer composite.

But there is another method – the use of the heterogeneous blends of polymers. To this end electrical properties and distribution of the filler (carbon black) in the mixtures of polyethylene and thermodynamically incompatible polymers were investigated.

Compositions were prepared by mixing in the molten state on micro rolls using four methods: (1) — the filler is preliminarily introduced in to polyethylene and then is mixed with another polymer; (2) — the filler is preliminary introduced in to a polymer and then is mixed with polyethylene; (3) — the filler is introduced in to the polymer mixture; (4) — a part of the filler is introduced in to polyethylene, another in to the polymer in the proportion equal to the contents of the polymers in the mixture, and then all the components are mixed together. Polypropylene, copolymer of

ethylene with vinyl acetate and others were used as polymers that are thermodynamically incompatible with polyethylene.

The study of filler distribution by the methods of optical and electronic microscopy has shown that in all compositions obtained by method 4 the filler is distributed rather uniformly as in an individual polymer. In the mixtures of incompatible polymers, obtained by methods 1 and 2, the filler is distributed nonuniformly and there are zones of high concentration of the filler and almost empty ones. The size of such zones is close to the size of polymer regions known for mixtures of thermodynamically incompatible polymers — 1 to 10  $\mu$ .

In the case of filler localization in one of the polymer components of the polymer mixture, an increase of the proportion of the second unfilled polymer components in it entails sharp (by a factor of  $10^{10}$ ) rise of  $\sigma$  in the conducting polymer composite. In this case the filled phase should be continuous, i.e. its concentration should be higher than the percolation threshold.

One more fact, important in practice, lies in that  $\sigma$  of the compositions based on heterogeneous blends of polymers obtained by the method 3, depends considerably on mixing temperature  $T_m$ . This is bound up with a variation of the polymer viscosity with the temperature: on being introduced in to the polymer mixtures, a fillers becomes distributed mostly in the less viscous polymer and, if the viscosity of polymers is almost the same, it is distributed comparatively uniformly and  $\sigma$  of the composition decreases. Therefore, the dependence of  $\sigma$  of the conducting polymer composite on  $T_m$  has a minimum (by a factor of  $10^2$  to  $10^4$ ) in the  $T_m$  region when the viscosities of the polymer components are close.

It is well known, that under industrial conditions a method of introducing filler in to the polymer mixture is used. In this case, the filler is introduced in the form of paste containing up to 60% water in order to reduce the viscosity. As heating is affected by viscous friction, the temperature conditions are not stable on mixing and, therefore, the conductivity of the conducting polymer composites becomes unreproducible.

On mixing by method 1,  $\sigma$  of the composition does not depend on  $T_m$  and, thus, is more stable in relation to the variations of mixing process parameters.

The above-described laws of filler distribution in heterogeneous mixtures of polymers are true when the particle is significantly less than the size of the polymer zones in such mixtures (1 to 10  $\mu$ ). So, powders of graphite and molybdenum ( $S_s = 2 \text{ m}^2/\text{g}$ ) are distributed equally uniformly in all the studied mixtures of polymers irrespective of the mixing conditions for in this case the particle size is comparable with the size of the polymer zones.

Thus the size of the heterogeneous blends of polymer  $s$  is a successful example of creating the ordered structure of the filler distribution: conductance occurs when the filler concentration exceeds the threshold  $\phi_f$  in the polymer phase the concentration of which in its turn is higher than the threshold  $\phi_p$ . In other words, the percolation threshold in such a system equals  $\phi_f \cdot \phi_p$ , which is considerably less than the threshold  $\phi_f$  for the case of the homogeneous matrix. The industrial techniques of processing of filled polymer compositions are based on the effect of significant shearing deformations that destroy the current- conducting chains of filler particles. With an increase of shear speed  $\gamma$ ,  $\sigma$  of the compositions drops to a definite limit ( $\sigma_{\min}$ ) minimal for a given composition, which is reached for  $\gamma = 10$  to  $30 \text{ s}^{-1}$  for the most conducting polymer composites. For some types of carbon filler, carbon black in particular, a chain (secondary) structure has thixotropic properties and, when the action of shearing deformation stops, it gradually becomes restored by the action of van der Waals forces, the lower the polymer viscosity, the greater the speed of restoration.

However, the relaxation process is rather slow where as thermoplastic processing calls for almost instantaneous cooling of the melt after molding and due to this fact the chain structure is not restored. From this it follows that in molding a conducting polymer composite the cooling of the melt should have a speed comparable to the speed of restoration of the filler secondary structure, otherwise the conductivity of the polymer composite will be reduced.

### **1.9 Polymerization filling — A Novel Technique for Manufacturing Conducting Composite Materials**

Quite naturally, novel techniques for manufacturing composite materials are in principle rare. The polymerisation filling worked out at the Chemical Physics

Institute of the USSR Academy of sciences is an example of such techniques<sup>80-82</sup>. The essence of the technique lies in that monomer polymerization takes place directly on the filler surface, i.e. a composite material is formed in the polymer forming stage, which excludes the necessity of mixing constituents of a composite material.

Practically, any material may be used as filler; the use of conducting fillers makes it possible to obtain a composite material having electrical conductance. The material thus obtained in the form of a powder can be processed in the form of powder can be processed by traditional methods, with polymers of many types (polyolefins, polyvinyl chloride, elastomers etc) used as matrix. Natural graphite and synthetic graphite were used as fillers for the manufacture of conducting composite materials by the polymerization filling technique the manufacture of conducting polymer composite materials by this technique on the basis of some kind of carbon black is well known. To obtain a graphite- and a polypropylene based composite material the Ziegler and Natta catalysts are used.<sup>83</sup> To this end, first  $(C_2H_5)_2AlCl$  and then  $TiCl_4$  are applied from the gas phase on to the graphite preevacuated at about  $200^\circ C$  (the investigations have shown that another sequence of application of catalyst components entails the decrease of composite material conductivity by several orders of magnitude). Therefore, activated filler is introduced into liquid propylene or propylene solution where polymerization occurs. As a result, a powder-like product is obtained, with the polypropylene applied on to the graphite being noted for high stereoregular properties and having an fraction 3 to 4% of the mass. This is a specific feature of graphite as support material on which the polymerisation catalyst is secured.

The degree of filling depends on polymerisation time: the greater the time, the thicker the layer of polymer on the surface of the filler particles, and the smaller the filling degree which, thus, can be regulated in a wide range from less than 1 to 90% by weight. And the composite material obtained by the polymerization filling technique and containing up to 85 % by weight of graphite retains admissible mechanical properties, while the composite material containing the same amount of graphite but obtained by ordinary mixing methods (blade mixer and laboratory extruder) has no mechanical stability, i.e. falls apart.



The comparison of conductivity of polypropylene–and natural graphite-based composite materials obtained by polymerisation filling and mechanical mixing has shown in **fig. 1.6**.

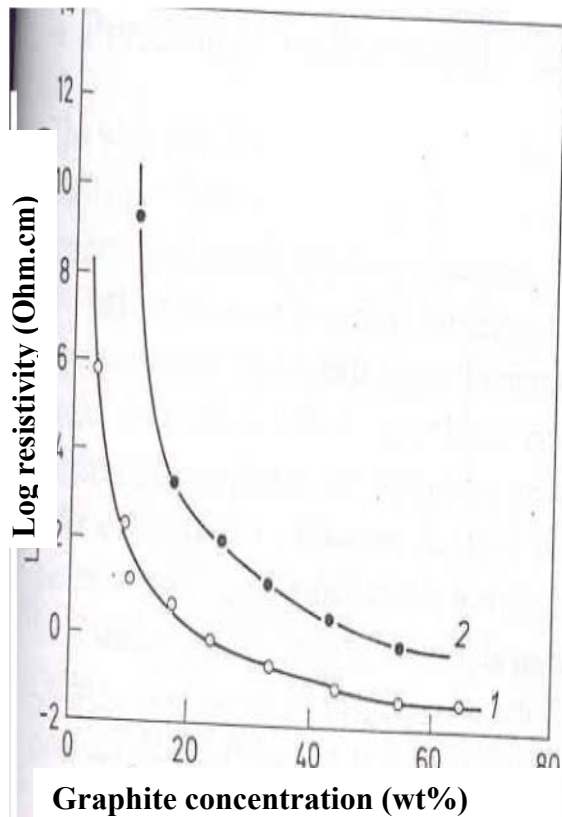


**Fig.1.6 Relationship of conductivity of polypropylene based polymer composites and filler concentration (natural graphite): 1 — polymerization filling; 2 —mechanical mixtures**

Given an equal concentration of graphite, the latter have a much lower conductivity (samples for conductivity measurements were prepared by processing). With graphite concentration of about 10 % by volume the difference reaches a factor of  $10^8$  and this difference drops with filler concentration increase to reach a factor of  $10^2$  at a concentration of about 50 % by volume. It should be noted, that at a given concentration  $\sigma$  of the composite material obtained by polymerisation filling amounts to about  $10^2 \text{ ohm}^{-1} \text{ cm}^{-1}$  which can not be achieved if the traditional ways of mixing carbon fillers are used.

The important parameter, both from the viewpoint of conductance mechanism and practical utilization of composite materials are the temperature dependence of  $\sigma$ , which may be characterized by the energy of activation of the conductivity or the temperature coefficient of a resistance (TCR). It turned out that, for composite materials obtained by polymerization filling, the value of TCR in the temperature range from 4.2 to 300 K is not higher than  $1 \times 10^{-4} \text{ K}^{-1}$  (activation energy is about 0.5eV), which is considerably lower than for compositions obtained by mechanical mixing or for the known conducting composites. In this case the material withstands multiple thermal cycles from liquid helium temperature to room temperature and vice versa, which is indicative of high mechanical stability of the composite. Pronounced decrease of occurs only at temperatures higher than 353 K but even this region the smaller the concentration of graphite in a composite material the larger the value of TCR.

Among other properties, distinguishing natural graphite-based CPC obtained by polymerization filling from composite materials obtained by mechanical mixing, the following should be noted: (1) a linearity of current-voltage characteristic up to current density of about  $1 \text{ A} / \text{cm}^2$ ; (2) a high degree of homogeneity of electrical properties within the material volume; (3) higher thermal conductivity (up to  $1 \text{ W}/(\text{m} \cdot \text{K})$ ) with graphite concentration being 30 % of mass; (4) high physical-mechanical properties; (5) unusual mechanical properties.

The nature of change of mechanical properties is somewhat unusual for polymerizations-filled composite materials with the increase of natural graphite concentration. The modulus of elasticity of the composite material increases fivefold

with graphite concentration 'C' changing from 0 to 60 % of mass (for mechanically obtained mixtures the value of modulus is 1.6 times lower). In this case, elongation at rupture drops naturally, reaching 5 % for C = 10 %, and at an increase of C the materials becomes short brittle. The tensile strength and compressive yield point are practically constant up to graphite concentration of 70 % and the polymerised composite materials do not collapse even up to C=70% (a sample becomes barrel shaped) whereas mechanically obtained mixtures are short-brittle even at C = 10 % of mass. The usual physical-mechanical properties of composite materials obtained by Polymerization filling may be obviously explained by stronger adhesive interaction of the filler and the polymer matrix owing to the essences of the technique – chemical grafting of polymer to filler. The most probable reason for improvement of the properties of composite materials obtained by the Polymerization filling, as compared with mechanical mixtures, lies in the peculiarities of a structure of natural graphite and the Polymerization process. It is known that natural graphite represents sufficiently large crystals of a laminated structure; the individual lamellas are weakly interlinked owing to a large distance between them. During Polymerization a catalyst can penetrate between the separate lamellas, and the forming polymer pushes away the lamellas thus weakening their bonds to a greater extent .So during Polymerization filling a spill ting of natural graphite particles to separate flakes, that have large aspect ratio, occurs. The data from X-ray examination and measurements of anisotropy coefficients of the electrical and thermal conductivity of these materials, that reaches 20 (where as for mechanical mixtures its value is not in excess of 4) point of this fact.

The data obtained during the use of graphite of another structure confirm the proposed explanation. Thus, the properties of a composite material do not depend on the manufacture technique if in the capacity of filler synthetic graphite was used, the particles of which consisted of micro crystallites about 200 Å leads to the same conclusion.

Alternative explanation of the high conductivity of composite materials obtained by Polymerizations filling are given in works where conductivity higher than that of the graphite proper is attributed to a polymer interlayer between graphite

particles, are, in our opinion, insufficiently convincing and can not explain the whole of the experimental data.

## 2. Applications of conducting Polymers

Conducting polymers are now being produced on a commercial scale by several Industries<sup>84-87</sup>. Besides their intrinsic electrical conductivity, they also present electro activity, electrochromism and semi conductor behavior which qualify them for several applications, such as Loudspeakers (electrostatic), memory devices (electrical, optical), molecular electronics, Nonlinear optics, packaging materials, Actuators, pH modulator, ant radiation coating-Polymer /Solid electrolytes, Antistatic carpets, coatings, fibers, films, paints, Artificial Muscles, Batteries<sup>88</sup> (lightweight, high energy density, rechargeable, flexible, odd shaped) Capacitors<sup>89</sup> and super capacitors, Catalysts, Coating for metal plating on plastics, Conductors (lightweight), Controlled release medicine delivery systems, Corrosion preventive paints, Electro chromic displays<sup>90-92</sup>, Smartwindows, Electrodes(catalysts, fuelcells) .  
electromagnetic shielding<sup>100</sup>, Electromechanical Actuators for biomedical devices, micropositioners, micro tweezers, micro valves, etc., electron beam resists, fuses(reversible)-Gas separation membranes, Heating elements (e.g. clothing), Infrared reflectors, Lithographic resists.

**Semiconductor Devices:** p-n Junctions, Photovoltaic<sup>96</sup>, Schottky diodes, light-emitting diodes<sup>95</sup>, field effect transistors<sup>93-94</sup>, transparent conductors and Photo electrochemical cells<sup>97-99</sup>

### 2.1 Factors affecting on Electrical Conductivity and Electrical measurement

Phenomena that affect parameters such as lattice spacings, adsorption equilibrium, potential distribution, dipole orientation and molecular species can impact electrical conductivity. Typically processes such as first-order and second-order phase transitions, chemical degradation, dipole alignment and molecular motion, charge carrier trapping and detrapping, impurities and electrodes have been shown to affect electrical measurements in polymers.

Powders present a number of problems, among these can be listed effects of particle size, contacts, interfacial effects, mixing and compacting. Certainly in the case of polymers the presence of residual solvent, changes in the

crystalline/amorphous ratio, the sample cooling rate (by its influence on the glass transition temperature or crystallite size) and the ambient atmosphere, all affect the electrical behavior.

The properties of the filler play a significant role in determining the conductivity of the composite. Filler (Pani powder) properties, such as particle size, can also have an effect on the electrical conductivity. It has been shown that for spherical particles, smaller particle size will lower the percolation threshold. It has also been shown that an aspect ratio (ratio of length to diameter,  $l/d$ ) greater than one, as well as a broader range of aspect ratios will lower the percolation threshold. In this case, other properties of the filler should be taken in to consideration when choosing the right filler for the application.

Another important item for consideration is the method by which the composites are made. There are several studies that show the effects that filler orientation has on the electrical conductivity of blends and composites and how this can be quantified.

The surface properties of the filler and polymer also have a significant effect on the conductivity and the percolation threshold of the composite. The surface free energies of the filler and matrix will influence the interaction between two materials, and how well the polymer wets the surface of the filler can be quantified by the difference between the surface energies of the two materials. Smaller differences between the two energies lead to better wetting of the filler by the polymer. Therefore, better wetting of the filler can improve its dispersion within the matrix material. While this can increase the percolation threshold of the composite, it can also improve the overall conductivity of the composite.

In general, a smaller difference between the surface energy of the filler and polymer is desirable to obtain high composite electrical conductivity.

## **2.2 Aim and Scope**

The synthesis work on blend is carried out systematically. The blends will be synthesized by insitu blending method. The dry blends also can be prepared by using powder of conducting polymer and insulating polymer. These studies were mainly focused on the comparative study of insitu blending and exsitu (powder or dry)

blends in respect of their, electrical properties such as, charge transport and temperature dependent conductivity.

Further we are looking for their structural changes, morphology, and phase separation, phase segregation, agglomeration and wetting using techniques such as X-ray, IR, UV-VIS, TGA/DTA and Optical microscopy.

It is planned to synthesize the blends of conventional polymers, such as nylon-6, polyvinyl acetate and polyacrylamide with conducting polyaniline. This goal can be achieved by two methods, namely 1) insitu blending and 2) powder blending. The blends to be studied by insitu synthesis give higher conductivity because aniline polymerizes to polyaniline in a conventional polymer solution. By this procedure, more intimate mixing of the two components is possible; consequently the outcome is reflected as an interpenetrating network of the conducting polymer in the matrix than is obtained by mechanical blending because of the incompatibility of most polymers. Thus blending may be achieved at a sub-micron level and ensure a better mixing of the polymers and hence lower percolation threshold. The effect of various parameters such as the method of synthesis of the blend, viscosity of the conventional polymer solution in which monomer (aniline) may trap and thus hinders the polymerization process, doping level and composition of the conducting polymer on the barrier formation are studied.

Percolation threshold is expected in the range of 5-20 % w/w and conductivity reached a maximum value of 5-7 S/cm. In the exsitu blends, the relation between the substrate material, polymer loading and electrical performance have been considered. The temperature dependence of conductivity of the composite in the range 77-450 K depends upon the insulating polymer and the polyaniline; a positive temperature coefficient (PTC) phenomena may be expected by the interruption of the percolation path. In this direction to enhance conductivity by the addition of low quantity of the blend powder, these blends will be subjected for electrical conductivity measurements. Some cursory experiment also carried out, in the insitu synthesis of nylon-6-polyaniline blends. 33 % PANI in the blend shows conductivity  $2.94 \times 10^5$  S/cm. The ex-situ blends show conductivity  $2.94 \times 10^5$  S/cm after addition of 60% PANI in the blend. In the PVAc blends at 27% PANI gives conductivity

$36.496 \times 10^5$  S/cm., where as in the ex-situ blends,  $1.592 \times 10^3$  S/cm conductivity is found, when 60% of polyaniline is added in the blend. These blends have applications such as EMI/RF shielding, antistatic coating and as a humidity sensor. The literature survey indicates that the work on blend is reported and patented earlier, but this technique has not been studied in detail before

Morphology of the composite film was dependent upon the polymerization time, conc. of HCl and the matrix used. The blend exhibit good environmental stability and mechanical properties. These conducting polymer composite materials are found applications such as electrodes, conductive coatings and adhesives.

## **2.1: Introduction:**

The various ways of synthesis of blends and composites, which have been discussed earlier, polymerization of a monomer in conventional polymer solutions is a useful approach for the in situ preparation of new materials and in the ex-situ technique, conducting Pani powder and conventional polymer powder is mixed to obtain a powder blend. The present chapter elaborates the methods of synthesis, characterization and measurement of properties of conducting polymer blends. Polyaniline was chosen for the purpose owing to their better stability in ambient conditions than other ICPs. The various methods of sample preparation along with characterization by techniques viz., FT-IR, UV-VIS, spectroscopy, X-ray diffraction studies, Optical microscopy, TGA/DTA studies are described herein. The measurement of properties by various techniques such as moisture sensitivity and electrical properties. The techniques for investigating charge transport mechanisms like I-V characterization, conductivity-temperature studies are also presented.

## **2.2: Chemicals Used**

The aniline monomer was A.R. grade reagent obtained from M/S S.D. Fine Chem. (India), The chemical ammonium persulfate [  $(\text{NH}_4)_2\text{S}_2\text{O}_8$  ] was received from M/S Loba Chemie India and was used as such. The acid namely, hydrochloric acid was concentrated solution obtained from M/S S.D. Fine Chem. (India). The solvents distilled water and methanol were used after purification.

## **2.3: Methods of synthesis:**

### **2.3.1 Synthesis of conducting polymer:**

#### **(a) Chemical synthesis:**

Aniline was polymerized separately in a clean and dry conical flask containing 150 ml distilled water, 9 ml aniline; 10ml HCl .The initiator ammonium per sulfate was taken 11 gm in separate beaker containing 100 ml distilled water and this solution was then added drop wise with stirring. Pani was formed after 8 hrs. and this was precipitated in the distilled water, filtered, washed, dried and crushed to fine powder.



### **2.3.2. Synthesis of Blends:**

Blends were prepared by two methods: insitu technique and ex-situ technique

#### **(a) insitu blends:**

Aniline was polymerized in a conventional polymer solution. Precipitated in non solvent, filtered, washed the precipitate using non solvent and dried the powder by this procedure, more intimate mixing of the two components is possible than is obtained by mechanical blending because of the incompatibility of most polymers. Polyaniline blends with PVAc, Pam and Nylon-6.

#### **(b) Ex-situ blends:**

The ex-situ blends were prepared by external addition of Pani powder with PVAc, Pam and Nylon-6 powder. Compositional variation was carried out in case of all the blends.

### **2.4 Sample preparation:**

The blends prepared by insitu technique and ex-situ techniques were obtained in the powder form. In order to prepare to test samples, 300 mg blend powder was pressed in a single ended compaction die held at 3-ton pressure for sixty seconds so as to form pellets (0.2 cm thick). These were used for characterization and conductivity measurement

### **2.5 Doing with HCL solution**

Two molar HCL solution was made, in that 0.3 gm powder of each insitu blend compositions was added and stirred slightly and left over night. The doped blend compositions was then filtered and washed with distilled water to remove excess HCL present in it. Same procedure was repeated for the entire insitu blend.

### **2.6 Sample preparation for property measurement**

#### **a) Electrode configuration:**

The electrodes were prepared by vacuum deposition of copper on Epoxy sheet, later the sheet was cut in 2x2 cm chip. Configuration was made.

### **b) Surface cell:**

Surface cell was made using copper coated epoxy sheet an interdigitated electrode pattern was made as presented in the **fig.2.2 (a)** and **(b)**. The electrode gap was 1mm. The copper wire leads were attached to these portions with the help of air-drying silver paste. Electrical connections were made to the two electrodes. These cells are further used in the measurements sensitivity for moisture vapors.

### **c) Moisture sensitivity Measurement:**

Surface cells are essential for measurement of moisture sensitivity of the polymers for sensor application. In order to study the moisture sensitivity of Pani-PVAc insitu blend. These were first dispersed in film forming matrix and then coated on the electrode. This approach was needed since the conducting polymer powders have no known solvent at room temperature. PVAc was chosen for dispersing the Pani-PVAc blend compositions; it forms films easily and allows moisture vapors to diffuse through. Earlier studies from this laboratory indicated that PVAc is most appropriate for testing moisture sensitivity of Pani-blends for applications in sensors and PVAc is moisture sensitive.

In order to make blend films, typically 0.2 gms. of Pani-PVAc blend powder was added in 10 ml methanol. Mixture appeared green in color, masticated thoroughly so as to form a paste. The fine smooth paste was then applied on the interdigitated electrodes and dried at room temperature for 24 hrs (**fig.2.2a**) same procedure is repeated for remaining blend compositions with rising Pani in the blend as well as Pani-Pam blend compositions, in Pani-Pam blends, Pam was chosen for dispersing the Pani-Pam blend compositions. It is difficult to form a film of Pani-nylon-6 blend compositions, pellets were made and gold was deposited on the surface of the pellet, an interdigitated electrode pattern was made. The copper wire leads were attached to these portions with the help of air-drying silver paste as shown in the (**fig.2.2b**). The electrical conductivity of the sensor was monitored by continuously recording resistivity or currents at constant potential using a stabilized DC power supply a Keithley electrometer and a fast X-Y-T recorder [Lienses, Germany].

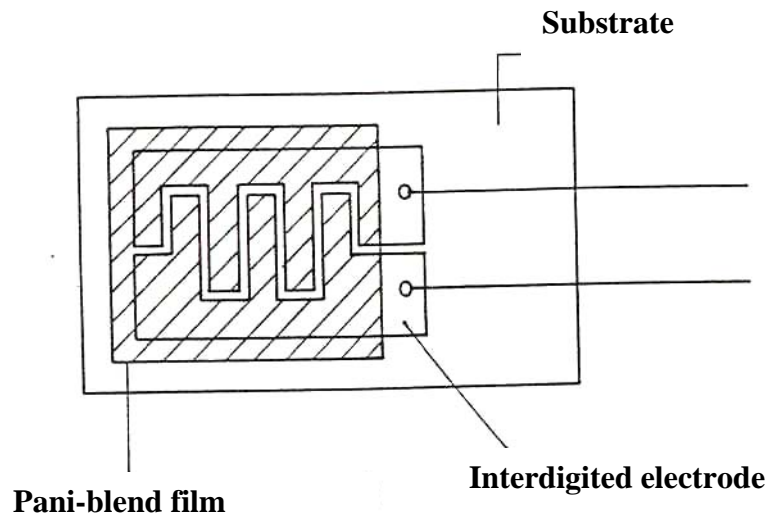


**Fig. 2.2 a**

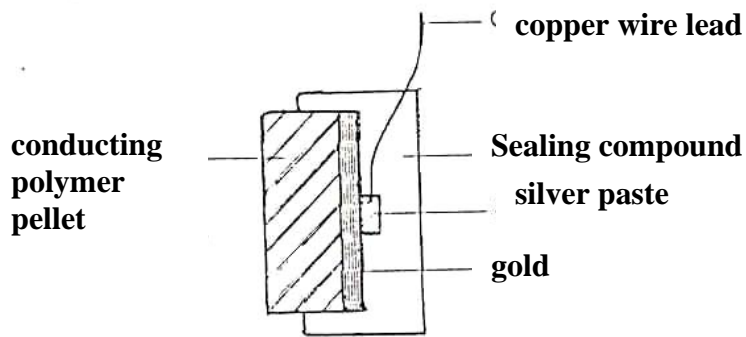


**Fig.2.2 b: Pellet configuration for moisture measurement**

**Fig.22b**

The moisture sensitivity of these surface cells to moisture vapors was tested using specially designed chamber with facilities for injecting and evacuating vapors, (fig.2.3) which is described in the following section.

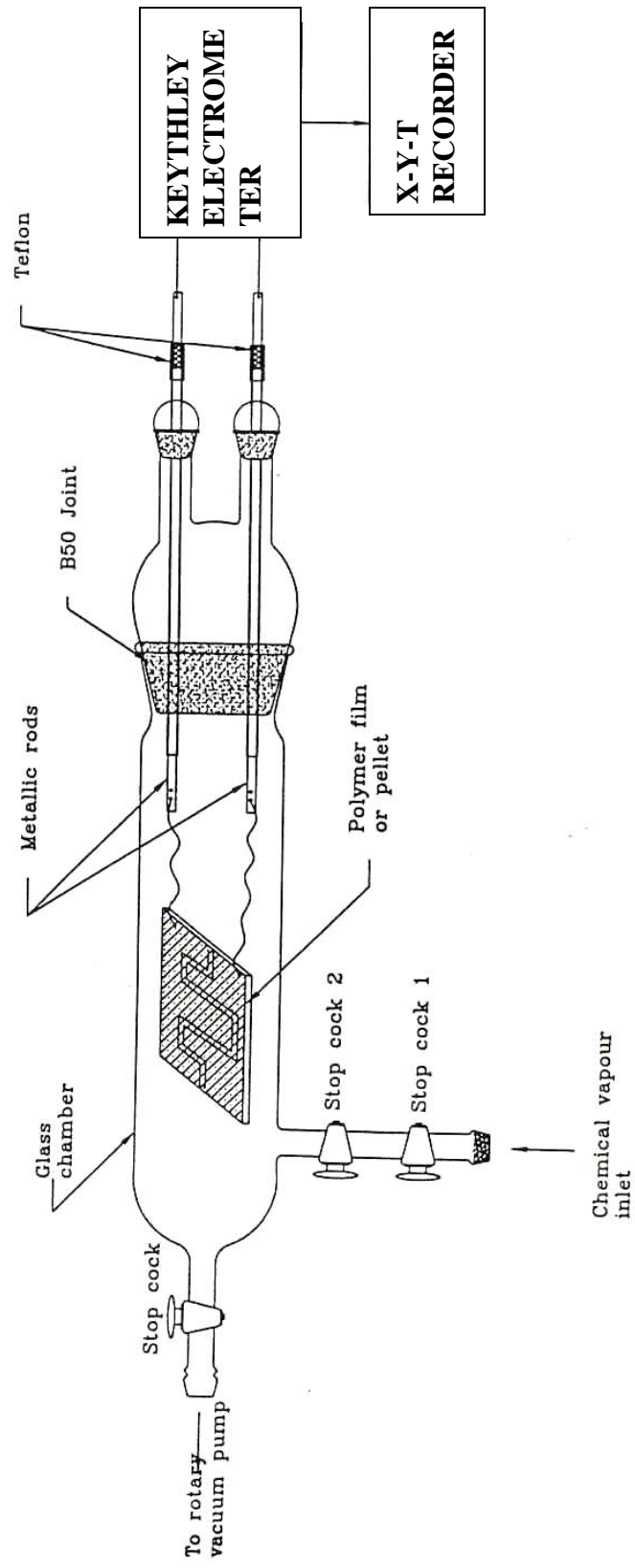


**Fig.2.3** † Apparatus for studying the sensitivity of polymer films towards various gases. Various parameters such as the response time, decay time and the sensitivity factor were determined as a function of resistivity.

The apparatus consists of thick glass wall chamber fitted with an arrangement of evacuation the system. On one side there is a stopcock system, through which, controlled doses of moisture vapors can be injected in to the system. The upper portion of the glass chamber has two electrodes which are directly connected to a Keithley electrometer .The samples were connected to these two electrodes inside the chamber and their resistance was recorded before and after moisture vapour. The sensitivity factor was calculated using the formula,

$$S=R_v / R_o$$

where  $R_v / R_o$  are the resistance after the exposure to moisture vapors and initial resistance respectively.

## **2.7 CHARACTERIZATION**

### **2.7.1: FTIR Spectroscopy:**

IR spectroscopy has provided valuable information regarding the formation of Pani blends. FTIR studies have confirmed the presence of Pani and analyze the effect of doping on the conductivity. The Pani-blend samples were mulled with dry potassium bromide crystals and these were mounted in IR cell in the conventional way to record the IR spectra using Perkin Elmer model 1600.The spectrum was recorded in the wavelength region of  $500\text{-}2000\text{ cm}^{-1}$ . The characteristic absorption bands obtained were tabulated and compared with known literature data.

### **2.7.2. UV-VIS Spectroscopy:**

UV-VIS spectroscopy has been widely used to characterize Pani blends. The UV-VIS spectra of Pani resemble the characteristic spectrum of the emeraldine salt of Pani.and additional mid-gap states formed owing to doping can be studied by UV-VIS spectroscopy .The blend powder samples were dissolved in formic acid and placing the dilute solution in the cuvetts. The spectrum was recorded in the wavelength region of  $300\text{-}900\text{ nm}$ . These measurements were carried out on Shimadzu Spectrometer with UV-240 model.

## **2.8 Structural and compositional characterization:**

### **2.8.1 X-ray diffraction studies:**

The Pani blend synthesized by chemical route offered an amorphous structure. The dopant size often played an important role in arrangement of the polymer chains. Hence it is blended with conventional polymer is expected to show some structural changes and crystallinity of modified polymer.

Pani-polyamide-6 blends have characteristic of an ordered structure. No ordering was observed for the Pani at any cure temperature. This implies that the two polymers, which were miscible or in a single phase prior to amidation continue to be so after amidation. The presence of a Pani chain in the vicinity of a polyamide chain restricts polyamide-6 ordering, which would be expected if phase separation were to occur. As a result of the initial Pani-polyamide-6 interaction, it forms 'IPN'.

These changes are studied using a well-known technique of wide angle X-ray diffraction (WAXD). The crystalline structure of various blend compositions was investigated by WAXD; using a pellet X-ray diffractometer (Philips PW 1730 model) using  $\text{CuK}\alpha$  source and  $\beta$  Ni filter. All the scans were recorded in the  $2\theta$  regions of  $5-50^\circ$  at a scan rate of  $5^\circ / \text{min}$ . From the  $2\theta$  values for the reflections, 'd' values were calculated using well-known Bragg's equation,

$$2d \sin \theta = n \lambda.$$

These values were compared with those estimated for known/assigned structure. Energy Dispersive X-ray Analysis [EDAX] was carried out to estimate the doping levels for various polymers. From these studies various atomic ratios such as Cu /S, Cu /Cl etc. can be determined.

### **2.8.2 Thermo Gravimetric Analysis (TGA):**

Thermo gravimetric analysis (TGA) is a useful technique for characterizing the thermal stability of conducting Pani-blend. The relative mass composition of these materials is easily determined from the mass loss owing to the volatilization of the

conducting polymer component. Thermo gravimetric analysis was carried out for various polymers to determine the weight loss at different temperatures. All the measurements were carried out using TG/DTA (Seiko II SSC 5100 Japan model). The samples used were in the form of powder and tested under nitrogen atmosphere at the rate of 10° /min from room temperature to 500° C. The thermal analysis of pure conducting polymer was recorded for comparison as original standard in any given system. The weight loss recorded for the blends was then compared with that of the pure one in order to estimate the fractional component of the polymer that was vapor phase deposited at a fixed temperature and composition.

## **2.9 Measurement of properties:**

### **2.9.1 Conductivity measurements:**

The conductivity measurements were carried out by a two-probe technique recorded by a Keithley electrometer 614 model. Samples were tested in a surface cell as well as in a sandwich cell form. Pellets were also used in the case of pure conducting polymers. The specific resistivity was calculated as,

$$\rho = RA/l$$

Hence

$$\sigma = 1/\rho$$

where  $\rho$  is its resistivity, A the cross sectional area, l is the thickness, R is the sample resistance and  $\sigma$  is the conductivity.

### **2.9.2 I-V characterization:**

The I-V characteristics were recorded for the polymer blends using a constant DC power supply and Keithley electrometer. The current was recorded as a function of the changing applied potential across the two terminals.

### **2.9.3 Temperature dependence of Conductivity:**

The temperature dependence of conductivity was determined by placing the pellet in a suitably designed apparatus as shown in the **fig.2.4**. The pellet used in this

measurement is a sandwich type cell where in the polymer blend pellet is placed in between two platinum electrodes, which were connected to the two terminal of the Keithley electrometer. The apparatus consists of a sample holder, which was enclosed in an electromagnetic shielded cell, which in turn was mounted inside a glass jacket, which could be sealed and connected to a rotary vacuum pump. A small heater was mounted close to the pellet and using a suitable control device controlled its temperature (rate of rise) .A digital temperature indicator connected to a thermocouple placed near the sample measured the temperature inside the cell. The temperature was varied from room temperature to about 100°C at a rate of 3° C per minute.

The change in the resistivity with temperature were noted using an electrometer (Keithley 614 model) and its conductivity was estimated using the formula:

$$\rho = RA / l \text{ ----- (2.1)}$$

$$\sigma = 1/\rho \text{ ---- (2.2)}$$

$$\sigma = \sigma_0 \exp. (\Delta E / kT) \text{ or ----- (2.3)}$$

$$\text{Log } \sigma = \Delta E / kT + \log \sigma_0 \text{ ----- (2.4)}$$

Where k is the Boltzman constant. The slope of the plot of  $\sigma$  versus  $1/ T$  can be calculated as follows:

$$\text{Slope} = \frac{\log \sigma_2 - \log \sigma_1}{1/T_1 - 1/T_2} = \Delta E / k \text{ ----- (2.5)}$$

above equation can be rewritten in a convenient form by substituting the proper values for the constants and converting from natural logarithms to base 10 as:

$$\Delta E = \text{Slope} \times k \text{----- (2.6)}$$

where  $k = 1.96 \times 10^{-4} \text{ eV}$ .



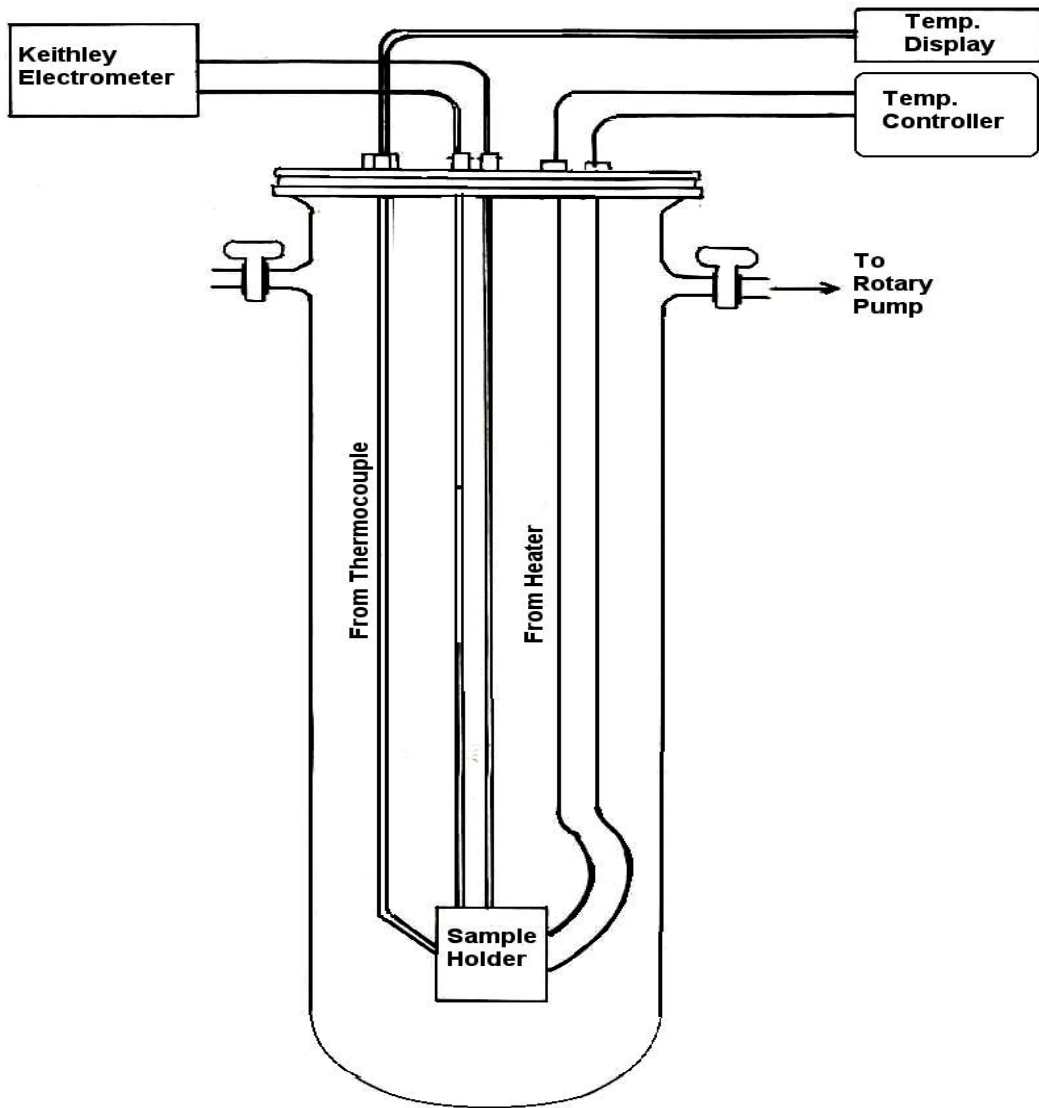


**Fig.2.4: Conductivity Measurement Apparatus**



## CHAPTER-III: Polyaniline-Poly vinyl acetate Blend

3.1	<b>INTRODUCTION</b> -----
3.2	Experimental-----
	1) Preparation of insitu Blend-----
	2) Preparation of Ex-situ Blend-----
3.3	Results and Discussion-----
3.4	Characterization-----
3.4	FTIR Spectroscopy-----
3.5	UV-VIS Spectroscopy-----
3.6	Measurement of properties-----
	1) R.T. Electrical Conductivity Measurement-----
	2) Temperature dependent Conductivity Measurement-----
	3) Activation energy ( $\Delta E$ )-----
	4) I-V Characteristics-----
3.7	TGA/DTA-----
3.8	Moisture sensitivity-----
3.9	Conclusions-----

### **3.1 Introduction:**

Polyvinyl acetate (PVAc) is used extensively in coatings, adhesives<sup>101</sup> and films. The carbonyl group (C=O) in the structure of PVAc forms hydrogen bonding (like polyamide) with amine and hydroxyl groups and this may also enhance miscibility with polyaniline. Hence, PVAc has been chosen for blending with Pani. Further, PVAc can be used in moisture sensor and after blending with Pani its conductivity would be in semiconducting range having the moisture response, which will be suitable for easy measurement. It was expected that, the given blend may give higher conductivity than Nylon-6/Pani blend, because 1) PVAc and Pani solubility parameter values match closely: the Hildebrand solubility parameter ( $\delta$ ) of aniline is  $21.1 \text{ Mpa}^{1/2}$  and PVAc is found to be  $20 \text{ Mpa}^{1/2}$ , 2) Its miscibility also increases due to H-bonding forces of attraction was observed in amine group of Pani and 'CO' group of PVAc. 3) PVAc has excellent sticking properties to different substrates which makes it useful as an adhesive and 4) Work function values of Pani as well as PVAc match closely. It is interesting to mention that PVAc has a low Tg ( $28^\circ \text{C}$ ) and thus may serve as a polymeric plasticizer for Pani, which would help to improve processability and/or film formation.

There are many methods of blending polymers but only limited techniques can be applicable for conducting polymers. PVAc is soluble in high dielectric constant solvent such as methanol. However, Pani is not soluble in this solvent even after modification with suitable dopants. Hence, a new method has been adopted for blending these two components; i.e. the in situ blending method, which has been described in chapter 2. This chapter describes in situ blend formation of PVAc and Pani and explains electrical properties and charge transport processes in the blend.

### **3.2 Experimental**

#### **1) Preparation of insitu blend**

Synthesis of polyaniline-polyvinyl acetate blend was carried out by insitu technique and compared with the blends prepared by ex-situ technique.

In the insitu synthesis, polyvinyl acetate obtained (M.W.40000), 2 gram dissolved in 100ml methanol was taken in a beaker. To that, 0.51 grams of monomer aniline (0.005 M) and 5 ml of 1N HCl solution were added. About 25 ml of 0.1M initiator ammonium per sulfate was added slowly to the above reaction mixture under constant stirring. Similar reactions were carried out with aniline concentration of 0.01M, 0.02 M and 0.05 M and 10 ml of 1N HCl, 20 ml of 1N HCl, 50ml of 1N HCl solution. The aniline to ammonium per sulfate molar ratio in all the above reactions was 1:1, so as to reproduce same conditions in all cases.

The polymerization of aniline was carried out simultaneously in each vessel. The reaction was carried out at ambient temperature for 10 hr. The blend was precipitated in distilled water, filtered, washed with distilled water several times and dried in a vacuum till moisture was removed. The green mass of, each composition of the blend was crushed in mortar and pestle to a fine powder. Yield is given in the **table-3.1**

Samples for characterization and measurement of conductivity were made as described in the chapter II.

## **2) Preparation of Ex-situ Blend**

In the ex-situ technique, PVAc powder was made by cryogenic grinding process. In this technique, the lump of PVAc was cut in pieces, which were then exposed to liquid nitrogen for five to ten minutes in order to make the PVAc flakes brittle (temperature much below T<sub>g</sub>) for making fine powder. These were immediately transferred in a high-speed mixer and crushed.

Polyaniline was synthesized separately in aqueous medium by standard route described in chapter II using HCl dopant. This polyaniline powder was then mixed physically in polyvinyl acetate powder, from 0% to 100% in the composition of the blend. Samples were made for measuring electrical conductivity as before. Blend formation is shown in the **fig.3.2**.

**TABLE 3.1****Chemical Synthesis data of PANI-PVAc blends**

<b>Serial No</b>	<b>Aniline Grams</b>	<b>Ammonium Per sulfate Grams</b>	<b>Hydrochloric Acid ml</b>	<b>PVAc Grams</b>	<b>% Yield</b>
1	0.51	1.2	0.5	2	76.11
2	1.02	2.3	1	2	75.35
3	2.04	4.6	2.5	2	72.75
4	5.1	11.4	6	2	97.3

**Solvent: Methanol 100ml for each experiment,**

**Reaction temperature: Room temperature; Reaction time: 10 hrs.**

**3.3 Results and Discussion:****3.4 Characterization:****3.4 FTIR spectroscopy**

**Fig.3.3** shows i.r.spectra of insitu blends (powder in KBr pellet) where, the curve 'a' corresponds to pristine PVAc and the curves b, c, d, e are the increasing concentration of Pani in the blend while 'f' corresponds to Pani itself. There are large number of absorption bands noted for which the assignment data is given in the**Table3.5**.Although there is an overall increase or decrease of the intensities of the major bands corresponding to increase / decrease of the particular component, which would be expected for blend, other changes are also seen in these spectra.

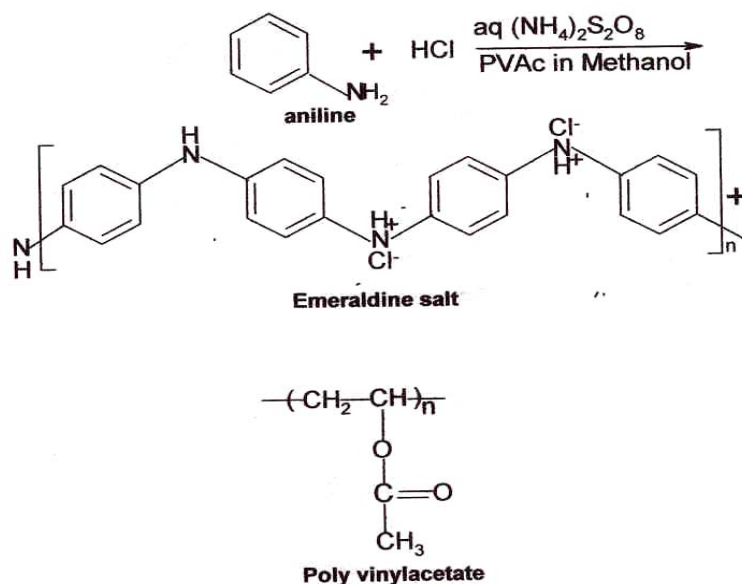


**Fig.3.2: Pani-PVAc insitu blend.**

In the carbonyl absorption region, the carbonyl stretching vibration of PVAc occurs at  $1732\text{ cm}^{-1}$ . Upon blending with Pani-HCl, the band position of the blend shifts to higher frequencies indicating that the carbonyl groups are interacting with the functional moieties of Pani. There is corresponding change in the NH-phenyl mode frequency which is prominent in Pani. This could arise from H-bonding interaction between CO and amine group of Pani as indicated in the **fig.3.4**

The extent of frequency shift to the carbonyl band is small observed in Polycaprolactone/Phenoxy blends<sup>102</sup>

The blend was being doped as such during synthesis. The Peak at  $1512\text{ cm}^{-1}$  further confirmed this and  $1591\text{ cm}^{-1}$  are observed. These changes resulting from protonation were the signatures of the conversion of the quinoid rings to benzenoid rings by the proton induced spin unpairing mechanism and the characteristic of the stretching vibrations of

nitrogen atoms in aromatic and diamine units respectively. It had already been published in many papers that these bands were of equal strength in the emeraldine oxidation state of Pani. The absorption band observed at  $1375\text{ cm}^{-1}$  in a fig. Was a halogen sensitive band, which confirms the salt formation between chlorine anions and protonated Nitrogen atoms next to the quinoid rings and was consistent with the higher conductivity of the protonated blend.

The peak observed at  $1140\text{ cm}^{-1}$  has been associated with electron delocalization and electrical conductivity in Pani<sup>103-104</sup>. The above band can be assigned to vibrational mode of a  $\text{B-NH}^+=\text{Q}$  structure (B=benzenoid ring; Q= quinonoid ring), which was formed during protonation. It indicates the existence of positive charge in the chain and the distribution of the dihedral angle between the quinone and benzenoid ring.

However the peak at  $820\text{ cm}^{-1}$ , assigned to the out-of-plane vibration of p-disubstituted benzene ring, which means the formation of Pani increases as the Pani concentration increases in the blend.

From the above results, it was clear that insitu blend was formed successfully. It was confirmed that the blend was being doped as such during polymerization and thus conducting blend was formed.



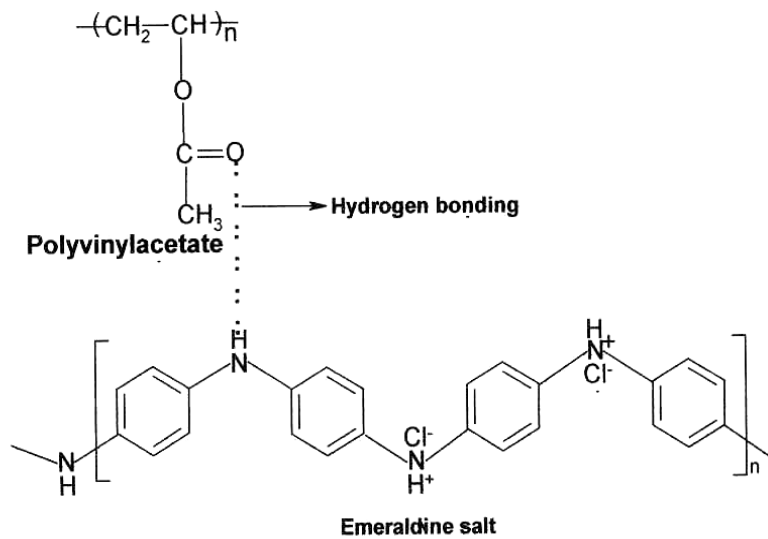


**Fig.3.4: Proposed scheme of the Hydrogen bonding between Pani and PVAc**

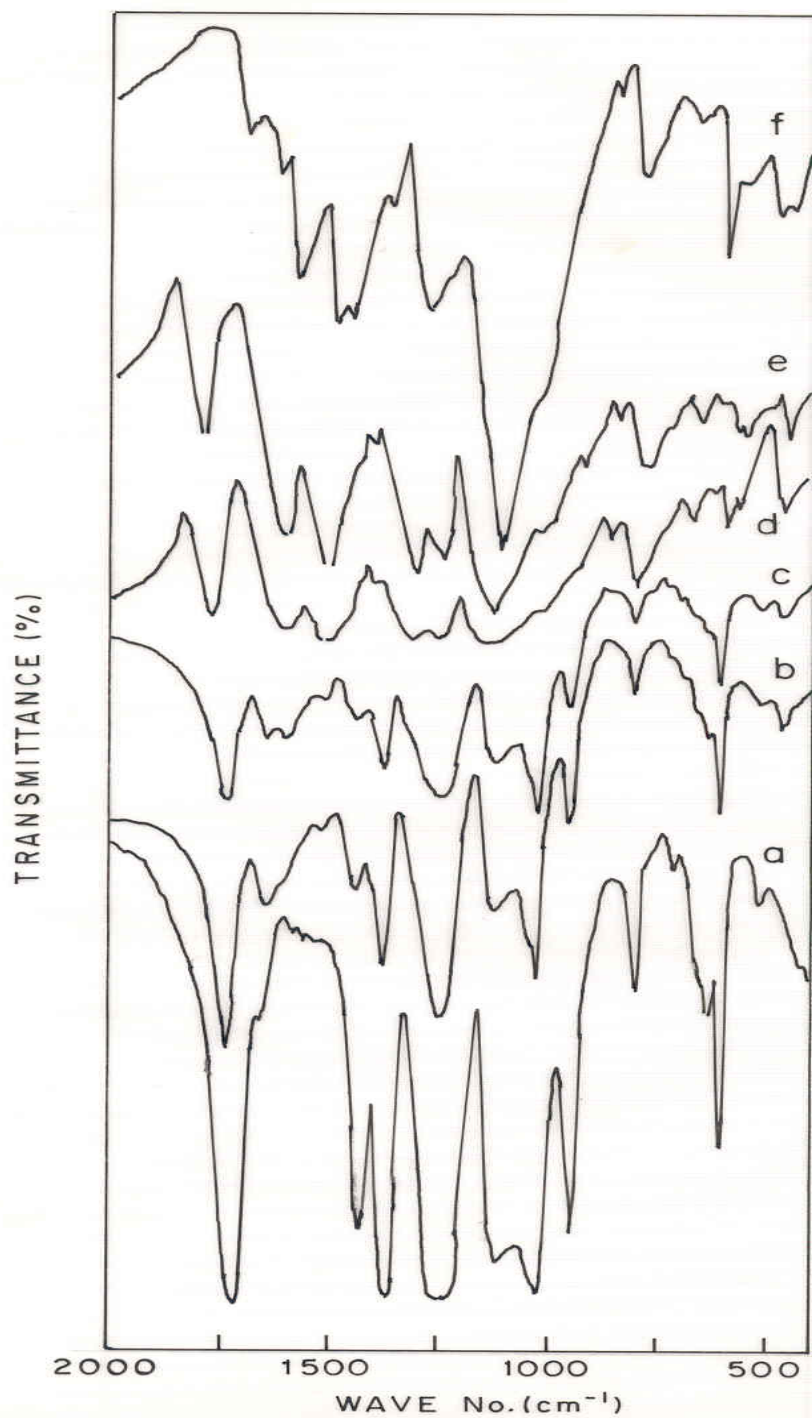


**Fig.3.3 FTIR absorption spectrum of Pani-PVAc insitu blends**

**a) PVAc, b) 3% Pani, c) 7% Pani, d) 13% Pani, e) 68% Pani, f) Pani**

**Table 3.5: FTIR data of Pani-PVAc Insitu Blends**

<b>PVAc</b>	<b>Pani (3%)</b>	<b>Pani (7%)</b>	<b>Pani (13%)</b>	<b>Pani (68%)</b>	<b>Pani (100%)</b>	<b>Assignment</b>
1732 s	1738 s	1735 s	1740 s	1740 s	—	-CO group
—	—	1591 vw	1591 w	1591 m	1589 w	Str. Of N=Q=N
—	1512 vw	1512 vw	1512 w	1512 s	1500 s	Str. Of N-B-N
1434 m	1436 w	1436	—	—	—	Alicyclic (CH <sub>2</sub> ) Scissor
—	—	—	—	—	1469 s	Str. of Benzene ring
1373 s	—	—	—	—	—	-O-CO-CH <sub>3</sub> Symmetrical bending of acetoxy methyl
—	1375 s	1375 m	1375 vw	1375 vw	—	C-N Str. In QB <sub>t</sub> Q
—	—	—	—	—	1286 w	C-C, C-N
1226 s	—	—	—	—	—	Alkane groups;
—	1244 s	1244 s	1244 w	1244 w	—	C-N Str. in BBB
—	1120 w	1120 w	1120 s	1120 s	1129vs	A mode of Q=N <sup>+</sup> H-B or B-NH-B
1024 s	1020 m	1020 m	—	—	—	C-C
—	—	—	—	—	910	Stretching in benzene ring
947 m	947 m	947 m	—	—	—	Out of plane bending of terminal vinyl
—	—	—	—	—	806 w	C-H deformation vibration in 1,4
796 m	796 m	796 m	796 m	796 m	—	CH out-of-plane
—	—	—	—	—	617 w	Aromatic ring deformation

Abbreviations: str, stretching; B, benzenoid unit; q, quinoid unit; t, trans; c, cis

### 3.5 UV-VIS Spectroscopy

Given **fig.3.6**, shows UV-VIS spectra for insitu blends, 'a' corresponds to pristine Pani and 'b' and 'c' shows, increasing Pani concentration in the blend. The samples were prepared in the HCOOH solution. Color of the solution was found to be green.

The main special feature of interest in the case of  $H^+$  doped blend concentration is the band near 820 nm, which represents the strong absorption even for small content of Pani in the blend beginning in the infrared, is the signature of protonated Pani. Band at  $\approx 420\text{nm}$  gives a shoulder on the 320nm band are assigned to the polaron modes, by analogy to those of  $H^+$  doped Pani<sup>105</sup> 590 nm, shows  $\pi-\pi^*$  transition and the excitation band of the quinonoid ring respectively from this band position, it is again clear that the blend doped during synthesis and was conductive. These peaks were found in pristine Pani. As shown. A typical UV-VIS spectrum of protonated Pani, (polyemeraldine form) has three distinct absorption bands in the regions 300-330 nm, 400-430nm, and 780-826nm<sup>106-107</sup>

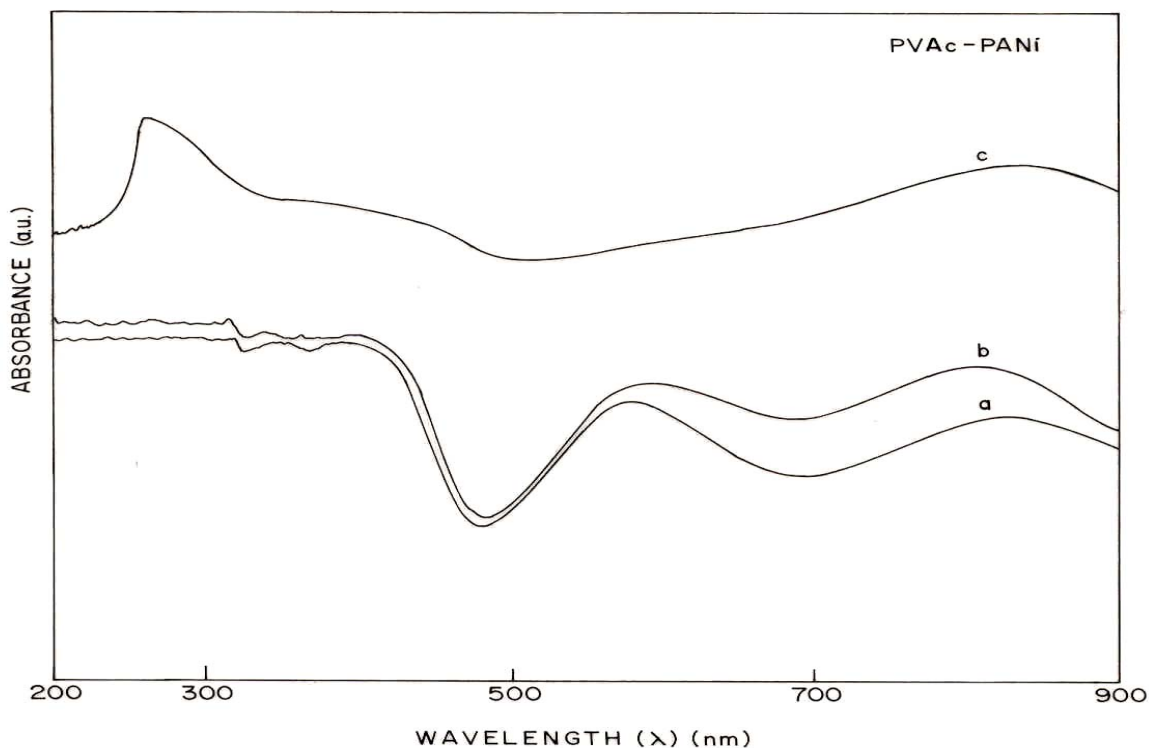


**Fig.3.6: UV-VIS spectra of Pani-PVAc insitu blend compositions in HCOOH. a) Pani, b) 3% Pani, c) 7% Pani**

### 3.6 Electrical Conductivity Measurements

#### 1) Compositional variation of Conductivity at ambient condition:

**Fig.3.7** shows the graph of conductivity of insitu blends at room temperature with Pani content in the blend. The curve 'a' corresponds to blend compositions after additional doping while 'b' corresponds to blends as obtained from reactor. It was observed that, initially 3% Pani in the blend gives conductivity  $5.46 \times 10^{-12}$  S / cm, and as the concentration of Pani increases in the blend conductivity rises again. Further increase in concentration shows conductivity at 68% Pani in the insitu blend  $3.7 \times 10^{-4}$  S / cm, and thereafter it remains constant. <sup>(108,110,11-112)</sup> It was noticed that the same blend composition after additional doping i.e. 3% Pani gives, conductivity  $0.5 \times 10^{-11}$  S / cm. As the concentration of Pani increases in the blend conductivity rises again and it gets saturated at 68% Pani and conductivity was found to be  $7 \times 10^{-2}$  S/cm and thereafter it remains constant. After redoping, the conductivity rises compare to the lower doping blends and percolation threshold was found to be 7%. <sup>114</sup>

R.T. log conductivity was explained on the basis of model, it is shown in the **fig.3.7a**. <sup>113</sup>

A polymer which has the conducting filler material uniformly dispersed in it may be considered to be a matrix of particles with average dimension  $D$  displaced at an average distance  $d$  from each other, as shown in the **fig 3.7a**. (for cubic approximation). Its electrical equivalence will be a network of resistors  $R_p$  and  $R_f$  (where  $R_p$  and  $R_f$  are effective resistances of the antiparticle junction and the filler particle itself respectively). Since the charge is transported via the least resistive path, it can safely be assumed that this network consists of a linear array of a number  $N_s$  of  $R_p$  and  $R_f$  alternatively placed in series and  $N_p$  such arrays placed in parallel as far as the external circuit is concerned (see fig.) These number of series elements ( $N_s$ ) and parallel arrays ( $N_p$ ) depend on the filler concentration through the interparticle distance as

$$N_s = (L-d) / (D+d)$$

$$N_p = (B-d)^2 / (D+d)^2$$

(1)

Where  $L$  is the length and  $B^2$  is the cross section of the filled polymer sample. Simple geometrical considerations show that the interparticle distance and the filler concentration  $\phi$  (volume fraction) are related as

$$\phi^{1/3} = D \cdot (L-d) / (D+d) \cdot L \quad (2)$$

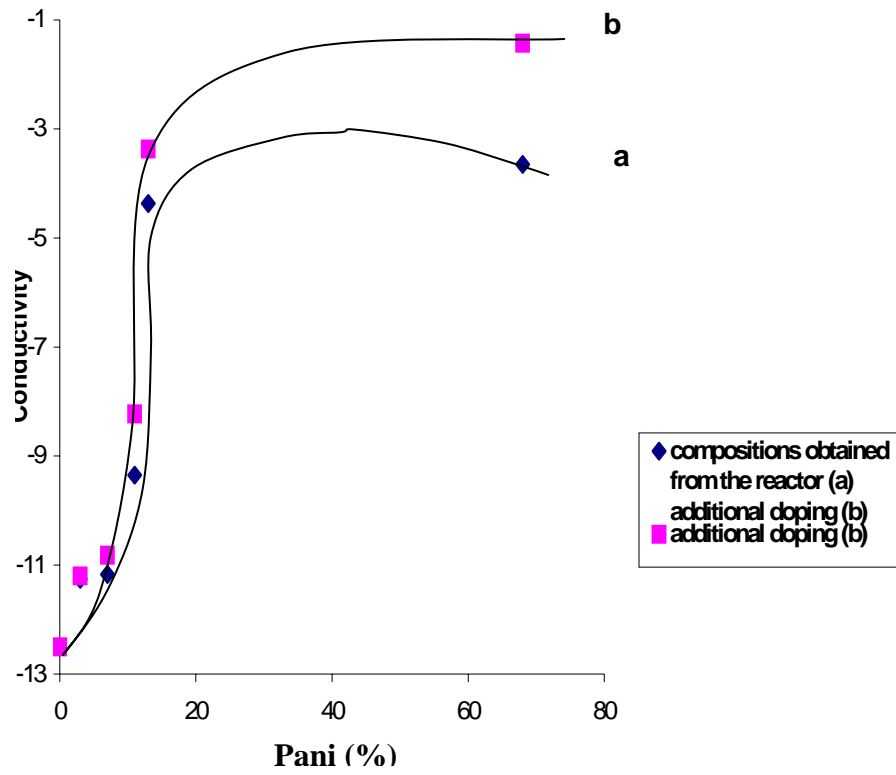
The externally measured resistance ( $R_x$ ) is given by

$$R_x = \left[ \frac{(B-d^2)}{(D+d^2)} \right]^{-1} \frac{(L-d)}{(D+d)} (R_p + R_f) \quad (3)$$

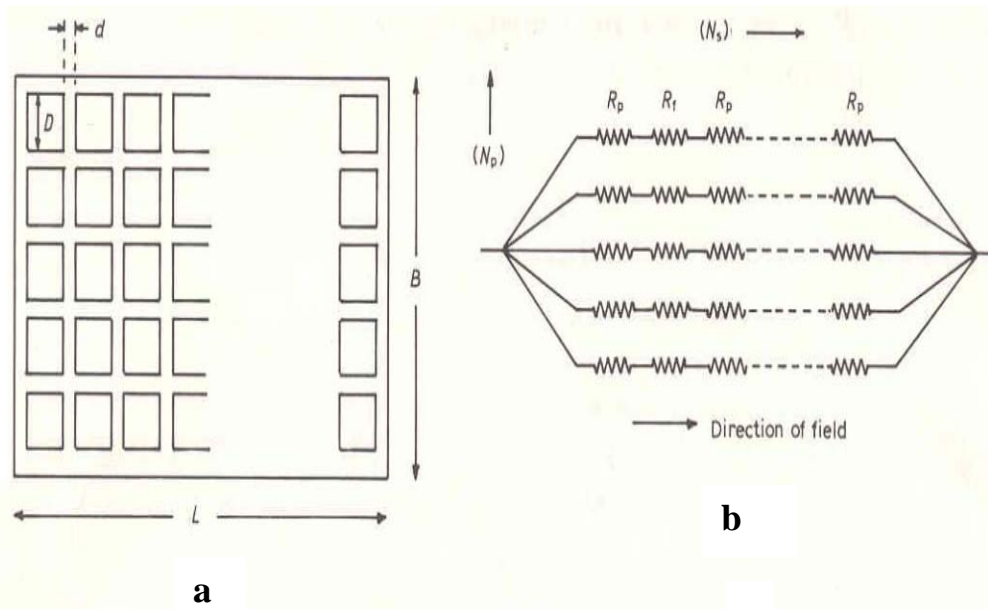
Now the resistance  $R_p$  depends upon the type of conduction process taking place in the polymeric material as well as the type of contact (ohmic or barrier type) that is formed between the particle and the polymer. In a simple case of ohmic conduction  $R_p$  is given by  $\rho_p d / D^2$  and  $R_f$  as  $\rho_f / D$  where  $\rho_p$  and  $\rho_f$  are bulk resistivities of polymer and filler particle respectively. Thus  $R_x$  is related to  $\phi$  as (in a unit cube  $L=B$ ),

$$R_x (\text{OH}) = \frac{1}{2} \rho_p \frac{(1-\theta^{1/3})}{\theta^{1/3} \left( 1 + \frac{L}{D} \theta^{1/3} \right)} + \frac{1}{L} \rho_f \theta^{1/3} \quad (4)$$

However, it is well known that the charge transport characteristic in polymers is mostly non-ohmic, especially at high fields. In Poly (vinyl fluoride), for example, space charge limited conduction mechanism with the current varying as square of the voltage is the main process while in poly (vinylidene fluoride) it is trap assisted tunneling which governs the conduction process. In the filled system, there are number of particles in series across which the external field is applied. The voltage thus gets divided between the particles and the voltage present across the interparticle gap is  $V_p$  equal to  $V/N_s$ , assuming the filler resistance to be much smaller than the polymeric one. Further, the interparticle distance is quite small and thus there is a large build up of internal field across the polymeric layer.



**Fig.3.7: Compositional dependence of conductivity with respect to the Pani concentration For the Pani-PVAc insitu blend.**



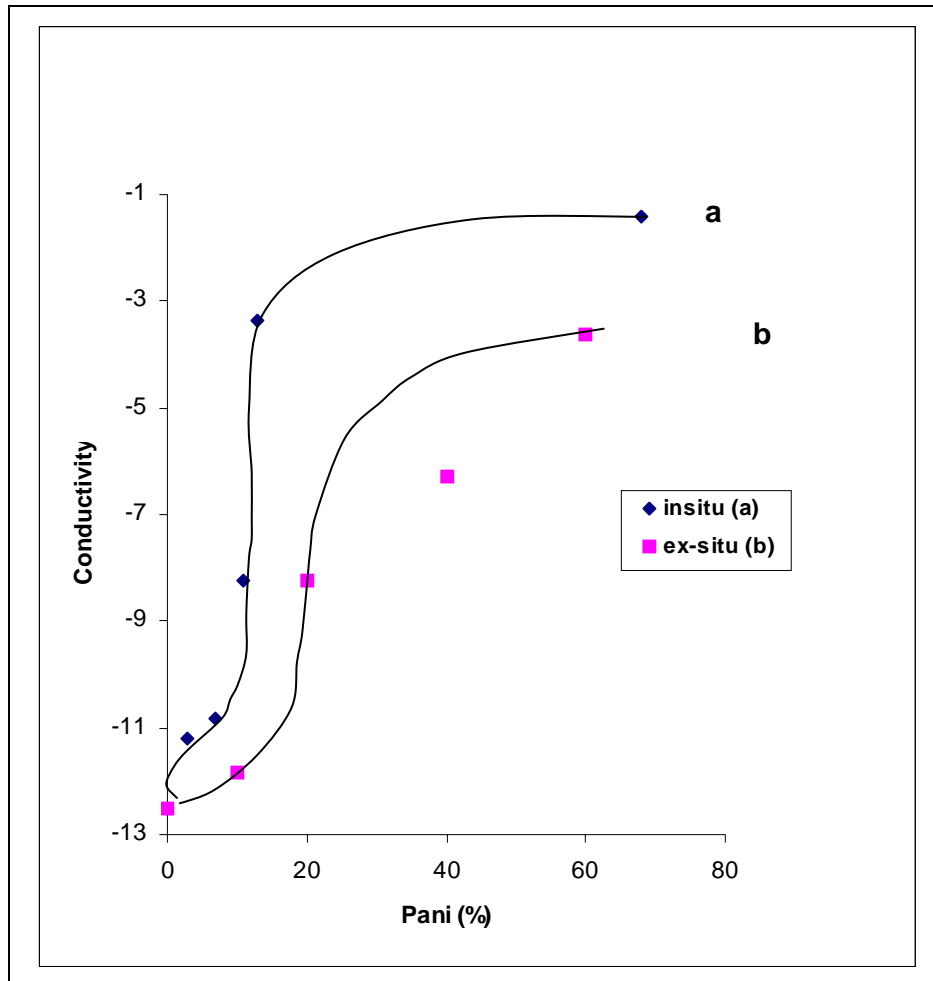


**Fig.3.8: Compositional dependence of conductivity with respect to Pani concentration for the Pani-PVAc blend.**

This field can be quite high even at moderate filler concentrations. For example, if there are seventy particles of 10  $\mu\text{m}$  size in series (i.e.34% filler loading) in a 1.0 mm thick sample and the applied voltage is around 100V, this, field can be of the order of  $10^4 \text{ Vcm}^{-1}$ . Thus it becomes essential to take in to consideration the non-ohmic (high field) processes while looking in to the resistivity behavior of filled polymers. (It is explained with the help of fig. in 1<sup>st</sup> chapter) One can derive expressions for  $R_p$  by taking in to account the exact current-



voltage relationship in the individual non-Ohmic process, as  $R_p = V_p / I_p$  where  $I_p$  is the current flowing across the polymer layer. Thus  $R_p$  will depend on the field and thickness at the interparticle gap, which in turn depend on the filler concentration, giving rise to a complex relationship between  $R_x$  and  $\phi$ . **Fig.3.8.** shows that in the graph, 'a' corresponds to 'insitu' and 'b' corresponds to 'exsitu' blend. In the insitu blend, 3% PANI gives conductivity  $0.5 \times 10^{-11}$  S / cm. In the ex-situ blend, 10% Pani gives conductivity  $2.97 \times 10^{-11}$  S / cm. and as the concentration of Pani increases in the blend, conductivity rises further and reaches to saturation and there after it remains constant. It was found that in the insitu blend at 68% Pani gives conductivity  $7 \times 10^{-2}$  S / cm. and ex-situ blend shows conductivity at 60% Pani,  $1.59 \times 10^{-3}$  S / cm. in the exsitu blend the percolation threshold value was found to be 20%.

The large difference between the electrical resistivities of the insulating matrix (PVAc matrix) and conducting Pani filler results in a mixed compound whose conductivity increases as the amount of Pani is increased. There is a volume fraction of Pani known as the percolation threshold at which it can be assumed that a continuous interconnecting Pani network exists in the blend and above this volume fraction the electrical resistivity is relatively low. Below this threshold, the compound behaves essentially like an insulator and the resistivity is more difficult to monitor. In the region of the percolation threshold, it has been suggested that changes to the relative locations and the orientation of the filler (Pani) particles.

From the above results it was clear that conductivity rises after redoping the pellets. Thus insitu blend shows higher conductivity compare to ex-situ blends. The conducting elements of these paths are either making physical contact between themselves or separated by very small distances across which electron can tunnel.

### **Percolation threshold**

With the help of theory based on scaling law, percolation threshold can be studied in more detail. Typically, the conductivity depends on concentration of additive follows the relation<sup>87</sup>

$$\sigma = A (\phi - \phi_c)^f \quad (1)$$

The **Fig.3.9** shows plot of Log conductivity vs.  $\log (\phi - \phi_c)$ . In the graph, the curve ‘a’ corresponds to ‘insitu’ and ‘b’ corresponds to ex-situ respectively. The nature of the graph was to found to be linear which thus follows the percolation model of conduction. It is further seen that the percolation threshold for the in situ blend is much lower than that made by ex situ method. This can be explained with the help of conduction processes

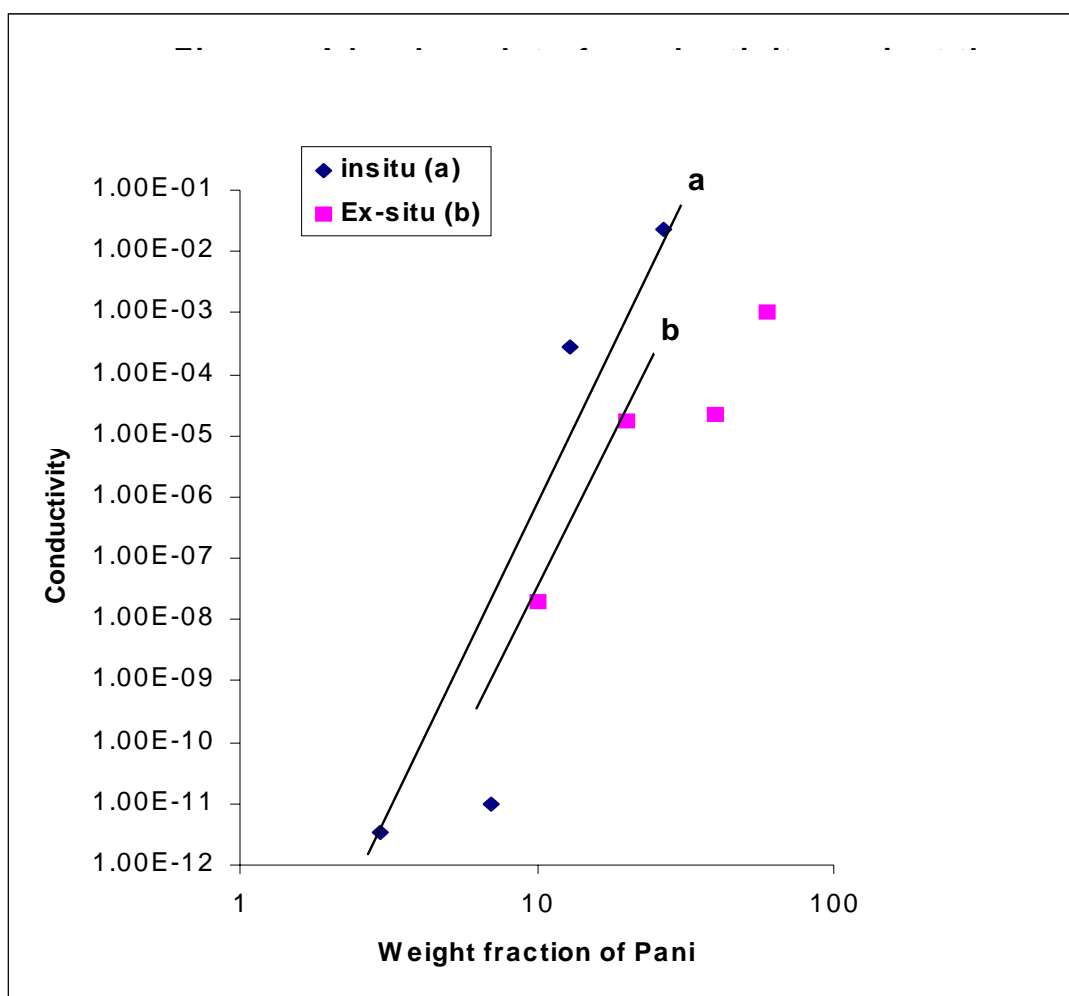


**Fig.3.9, A log-log plot of conductivity against the weight fraction of Pani-PVAc blends**

studied for the blends. In the insitu blend, when the Pani coated PVAc particles increases in the number, barrier of the PVAc get reduced and forms a close contact, conductivity was found to be increased  $10^{-2}$  S/cm and reaches to saturation. In the ex-situ blend, when Pani

concentration increases in the blend, conductivity rises but PVAc particles affects on conductivity ( $10^{-11}$  S/cm). It may considered as forming an M-I-M<sup>115</sup> contact, i.e. conducting path gets affected by the barrier of insulator region as seen in earlier system (Pani-Nylon-6 blend). This insulator region (barrier) was reduced as the concentration of Pani increases in the blend. There is no such barrier formed between Pani particles at higher concentrations of Pani in the blend as observed insitu blend i.e. network of conducting particles were observed in the insitu blend. The exponent 'f' in the equation (1) was found to be 0.26 in insitu blend and in the ex-situ blend, 'f' was found to be 0.28

## 2) Temperature Dependence of Conductivity:

**Fig.3.10 (A)** shows the temperature dependence of conductivity as plot of Log conductivity vs.  $1/T$  Temperature, for insitu blend and **fig. (B)** for ex-situ blend. In the 'insitu blend', a, b, c, d and e are the blend compositions obtained from the reactor and A, B, C, D and E are the blend compositions after additional doping. It was observed that initially at lower concentration of Pani in the blend, the nature of the graph was nonlinear. The conductivity was slightly enhanced here (1 order of magnitude) after additional doping. This was because as the temperature increases mobility of the charge carrier increases and it hops among the conducting particles, barrier of PVAc affects the mobility, and it requires higher activation energy (excitation energy) to hop, so the resistance rises and conductivity decreases and the nature was found to be nonlinear.

It was further observed that as the concentration of Pani increases in the blend, conductivity rises again and rises after additional doping at this point, pani coated PVAc particles forms a network and decreases the intergranular barriers. Hence, conduction occurs via interchain and intrachain hopping, it is based on Mott's variable range hopping (VRH) model<sup>116</sup>

$$\sigma = \sigma_0 \exp(-T/T)^{1/4} \quad \text{Eq. 2.3}$$

Wherein  $\log \sigma$  is dependent on  $(-T/T)^{1/4}$ . Hence plot of  $\sigma - T$  were represented as  $\log \sigma$  against  $T^{-1/4}$  as shown in the fig. It is said that conduction occurs by VRH model in the case of blend containing Pani.

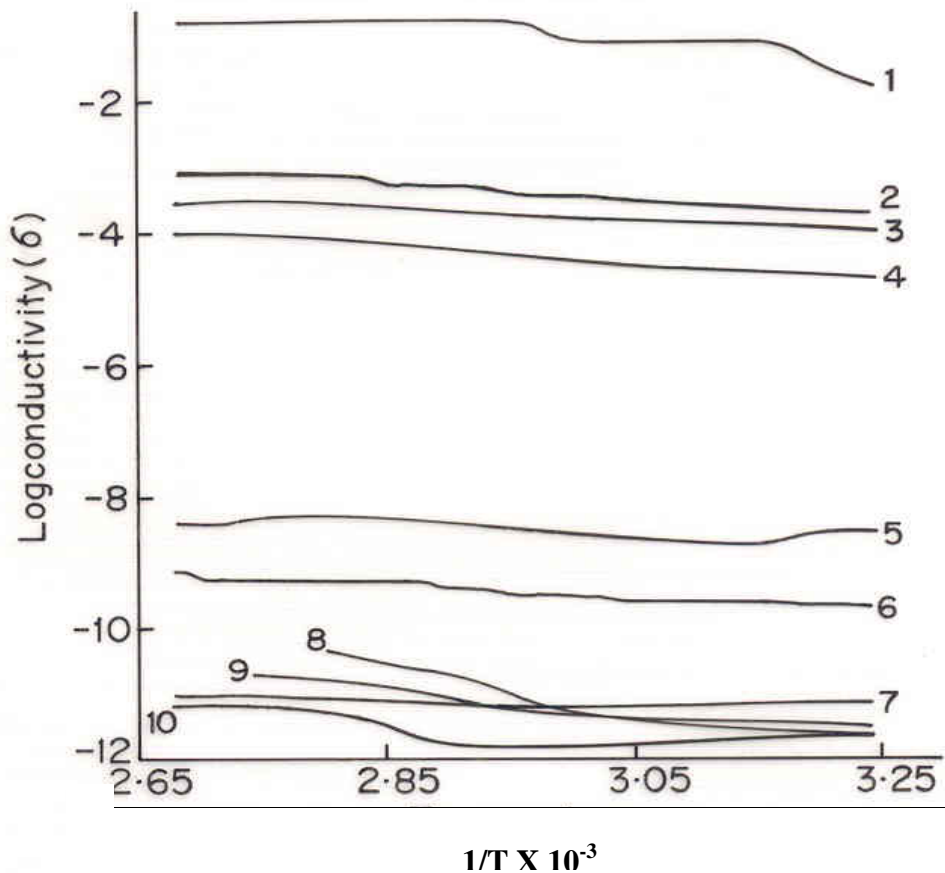


**Fig.3.10A: Plots of log conductivity versus reciprocal of temperature for Pani-PVAc insitu blend**

**Blend compositions obtained as such from the reactor**  
**10) 3% Pani, 9) 7% Pani, 6) 11% Pani, 4) 13% Pani, 3) 68% Pani**

**Blend compositions after additional doping**  
**7) 3%Pani, 8) 7% Pani, 5) 11% Pani, 2) 13% Pani, 1) 68% Pani**

In the ex-situ blend, the temperature dependence of  $\sigma$  shows initially nonlinear nature for lower concentration of Pani and as the concentration of Pani is increased, the conductivity rises. Barriers of PVAc are reduced and linearity is observed. Nature of the graph follows the Arrhenius law. i.e. at this concentration the graph is more or less linear. The slope of the Arrhenius curve decreases suggesting that the activation energy for

conduction decreases as the Pani content increases in the blend. i.e. at this concentration electrons require very less activation energy to transport from one conducting particle to another. **Fig.3.11** shows the ex-situ blend graph.

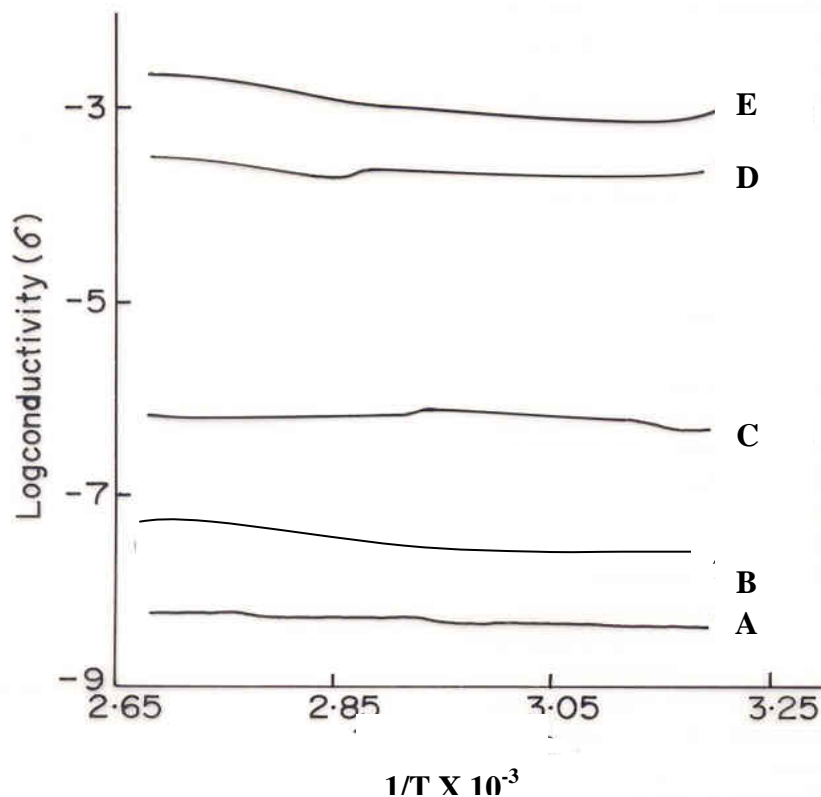


**Fig.3.10B: Plots of log conductivity versus reciprocal of temperature for Pani-PVAc ex-situ blend.**

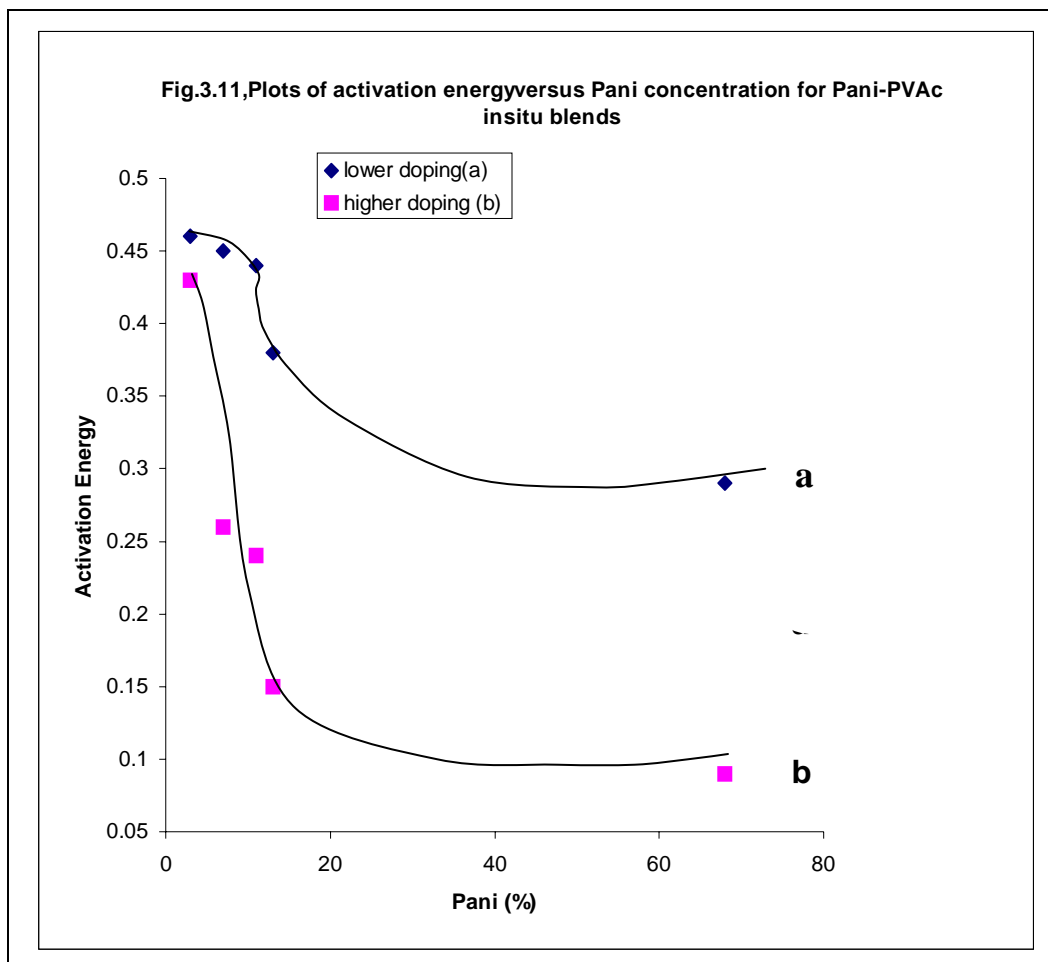
**Blend compositions of ex-situ blend**

A) 10% Pani, B) 20% Pani, C) 40% Pani, D) 60% Pani, E) 80% Pani

### 3) Activation Energy ( $\Delta E$ ) For the Blends:

The activation energy for conduction was calculated from the graph of log conductivity vs. Pani. **Fig.3.11** shows the variation of ( $\Delta E$ ) with composition for the insitu blends before (curve 'b') and after (curve 'a') additional doping. It was observed that blends with 3% Pani have ( $\Delta E$ ) value 0.46 eV but as the concentration of Pani increases in the blend, the activation energy decreases and it was found to be 0.29eV for blends

containing 68%Pani. The same concentrations after additional doping exhibit lower ( $\Delta E$ ) values i.e. 3% Pani shows activation energy 0.43 eV and 0.09 eV at 68% Pani. After additional doping the conducting phase becomes more conducting and also due to the additional energy levels created by doping, the barrier between the particles gets reduced and giving lower  $\Delta E$  value.



In the ex-situ Blend, (**Fig.3.13**), it was observed that 10% Pani shows activation energy 0.49eV and as the concentration increases to 40 % Pani the activation energy 0.35eV is obtained. It was noticed that ‘in situ’ blend gives lower  $\Delta E$  compared to ex-situ blends.

**Table 3.12: Activation Energy Data of Pani Blends**

<b>Lower Doping in Pani (%)</b>	<b>Activation Energy (<math>\Delta E</math>)</b>	<b>Higher Doping in Pani (%)</b>	<b>Activation Energy (<math>\Delta E</math>)</b>
3	0.46	3	0.43
7	0.45	7	0.26
13	0.38	13	0.15
68	0.29	68	0.09

This is because, in the ‘insitu blend as aniline polymerizes in the PVAc solution, simultaneously PVAc particles gets coated during polymerization and when ‘Pani’ coated PVAc particles increases in the number, the contact between them (barrier of PVAc) decreases, conducting network was formed and conducting particles require very less activation energy (excitation energy) to hop from one conducting particle to another and the resistance was found to be decreased.

In the ex-situ blend, PVAc particle acts as a barrier, it inhibits electron-hopping process hence resistance increases so the activation energy also increases even though conducting network is formed. In the ex-situ blend the gradual decrease in activation energy was found when 60% Pani is added in the blend and in the insitu blend the gradual decrease in activation energy was found to be at 68% Pani. The  $\Delta E$  data for ‘insitu’ blend and for ‘ex-situ’ blend composition was given in the **table 3.12 and 3.14**

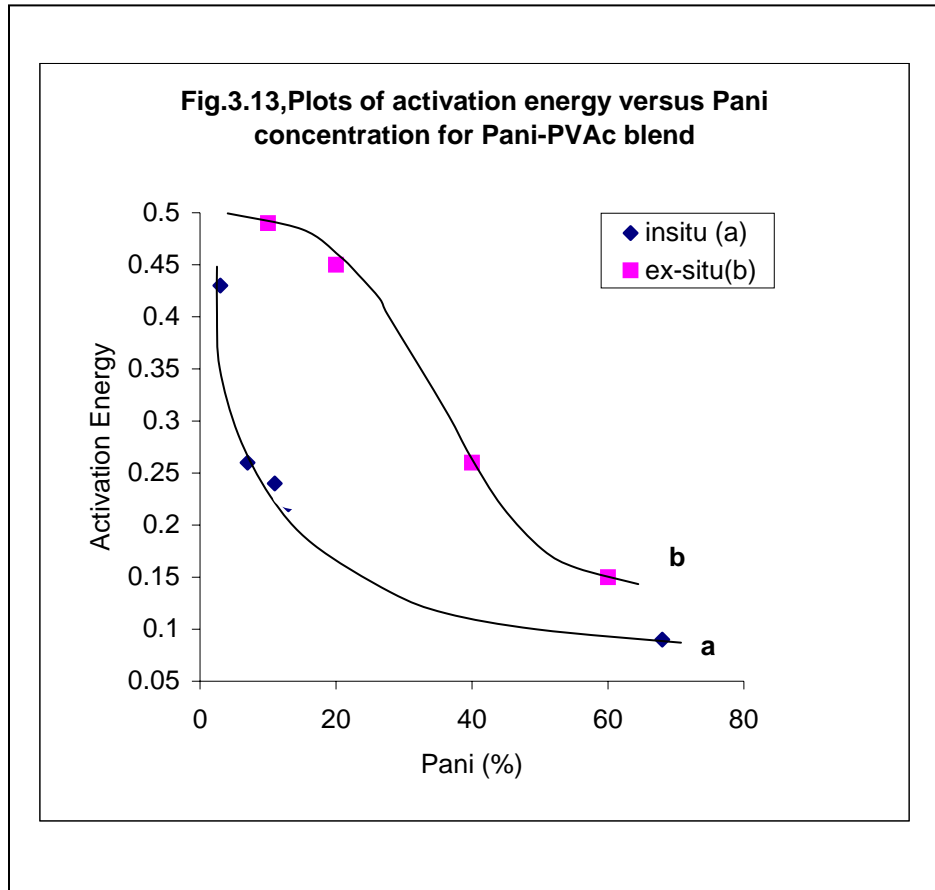


**Table3.14: Activation Energy Data of Exsitu Blends**

<b>Pani (%)</b>	<b>Activation Energy (<math>\Delta E</math>)</b>
10	0.49
20	0.45
40	0.26
~	~

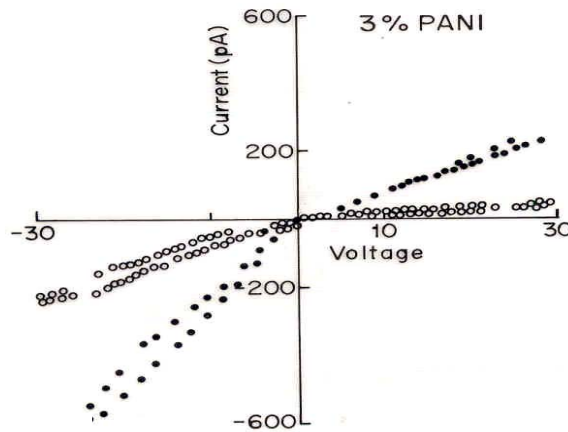


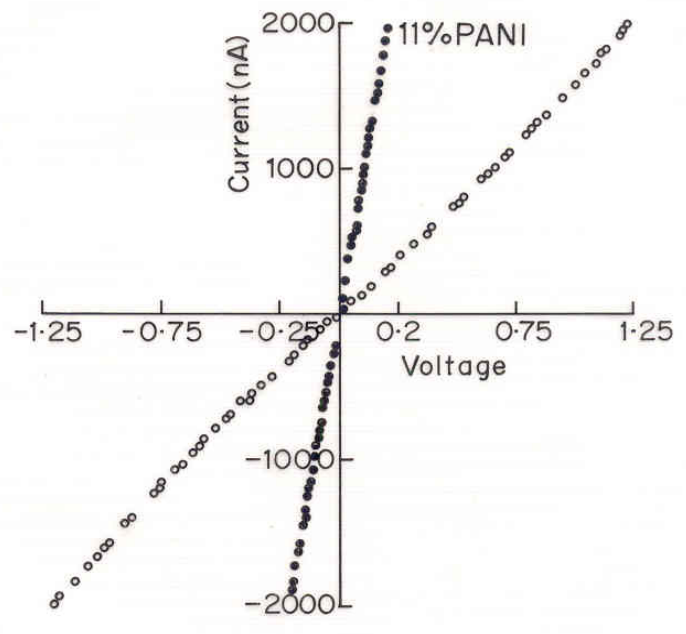
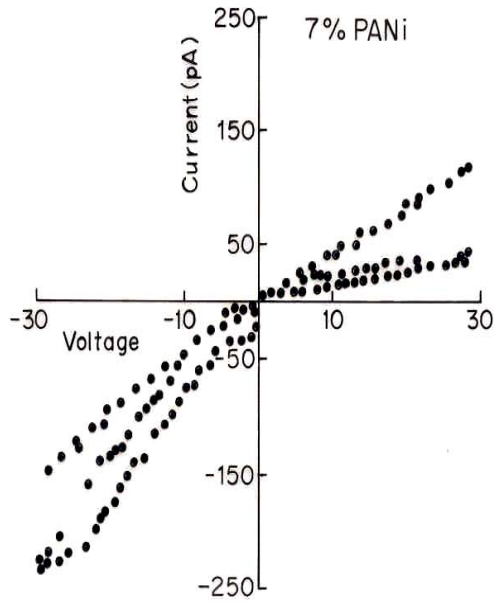
#### 4) Current vs. Voltage (I-V) Characteristics:

**Fig.3.15** shows the hysteresis as curve for insitu blends. In a fig.3% Pani shows non ohmic (nonlinear) nature even after additional doping the same composition. It requires low voltage to reach the 2000pA current, it was found that, the graph shows ohmic nature as the concentration of Pani increases in the blend and current value was reached in  $\mu\text{A}$ . It requires very less voltage to reach the 2000 $\mu\text{A}$ . current. This was observed at 27% Pani in the insitu blend compositions obtained from the reactor. It was noticed that, when the compositions of the insitu blend were additional doped, the nature of the graph shows ohmic (linear) and voltage was still reduced again to reach the 2000 $\mu\text{A}$ . given fig. shows the IV-curves of the blend.

The same charge transport process was observed in the 'ex-situ' blend, as shown in the **fig.3.16**, It was noticed that 10 % Pani, in the ex-situ blend shows nonohmic nature, and

**Fig.3.15:Insitu blend compositions**





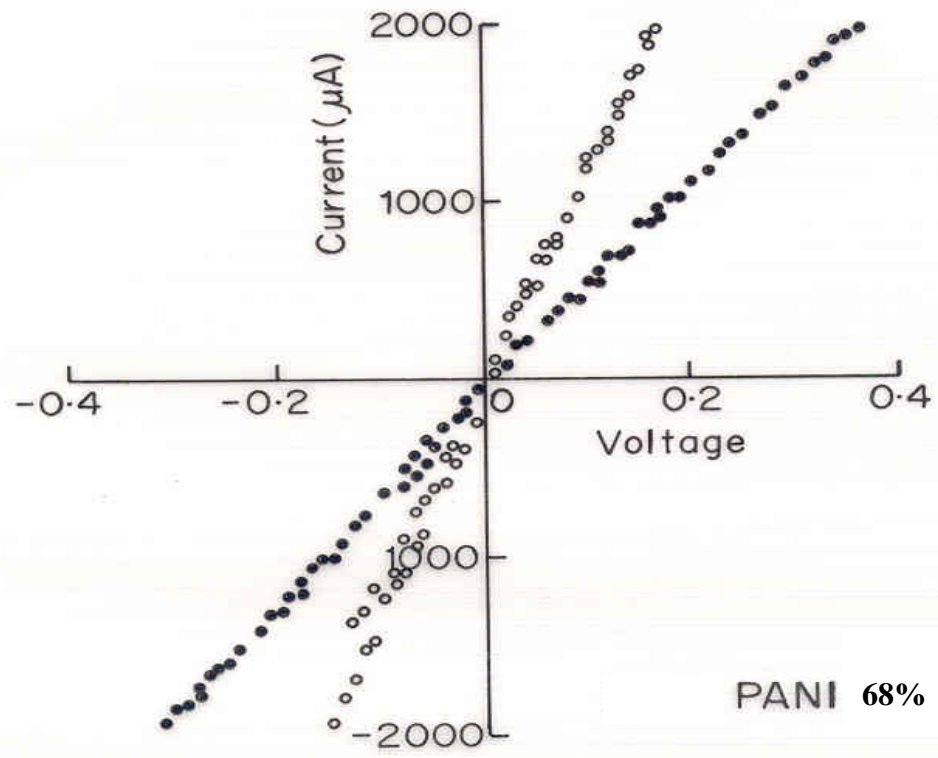
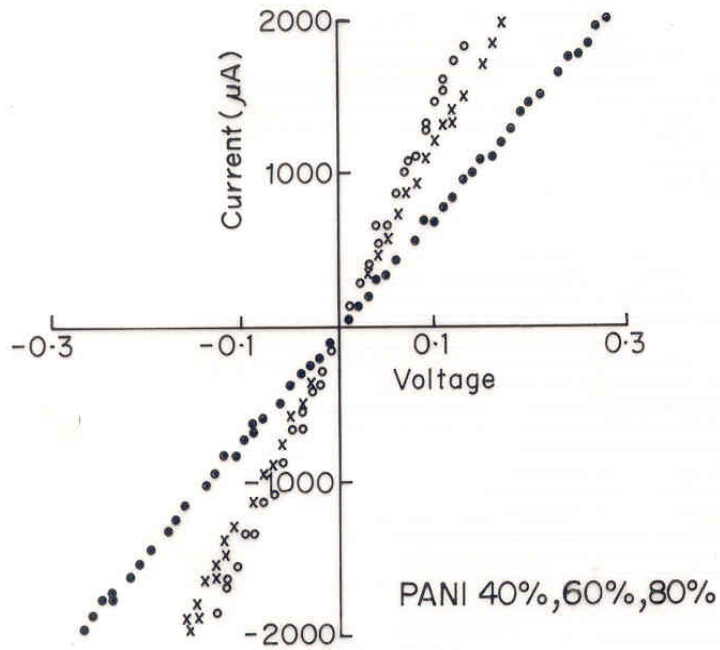
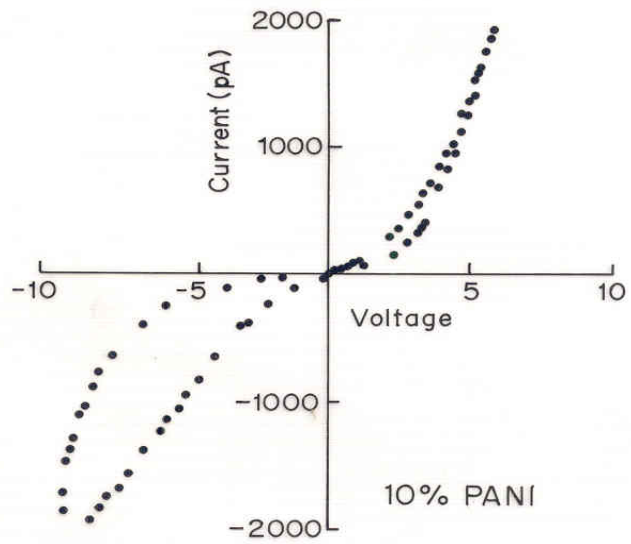


**Fig.3.16: Ex-situ blend compositions**



as the concentration of Pani increases in the blend i.e. at 60% Pani shows ohmic nature, and it requires low voltage to reach the 2000  $\mu$ A.

In the ex-situ blend, (3.14) the charge transport process was affected by the barrier of PVAc particles and even at higher concentration of Pani; there was no close contact found, barrier still affects the charge transport process and the voltage value was found to be more in ex-situ blend comparing to insitu blend. It was observed that even low concentration of Pani in the insitu blend shows ohmic nature compare to ex-situ Blend. This was because the barrier of PVAc gets reduced as the 'Pani' concentration increases in the blend and conducting network is formed. The charge carriers are created and their intramolecular as well as intermolecular charge transport takes place in the blend because of miscibility formed by the hydrogen-bonding between the two polymers (Pani and PVAc). The junction of PVAc do not affect the charge transport because the work function value of PVAc was found to be 4.38 eV and that of Pani was found to be 5.1 eV, which match closely with one another.

The DC conduction phenomena was studied by Chutia and Barua<sup>117</sup>PVAc-Films .He studied the phenomena by plotting the current (I) as a function of applied voltage (V) on a log, log scale at five different temperatures for a typical film 1.2 $\mu$ m thick .It was seen that at low voltages conduction was ohmic ( $I \propto V$ ) indicate that the current was controlled by thermally generated carriers .In the voltage range approximately. 50-160 V. He too found the ohmic nature, this may be because of thermally generated carriers reduces the junction of PVAc.

### 3.7 T.G.A./D.T.A.

The interaction between the polymers can also be noted from the degradation curves through T.G.A. studies. given **fig.3.17**, shows the wt.loss and thermal stability in the blend. Thermogram was scanned under the nitrogen atmosphere at the rate of 10<sup>o</sup> / min. (heating) and the temp.range were 25<sup>o</sup> c to 500<sup>o</sup> c. Thermal data is given in the **table 3.18**The T.G.A. curve of Pani and PVAc shows three steps wt.loss .The first wt.loss in both the pristine polymers at 150<sup>o</sup> c to 300<sup>o</sup> c was owing to the loss of absorbed moisture and solvent from room temperature to around 300<sup>o</sup> c. The second stage occurring at 350<sup>o</sup> c, decreased from 68.75<sup>o</sup> c to 52<sup>o</sup> c and the broad DTA peak of PVAc shows that the melting

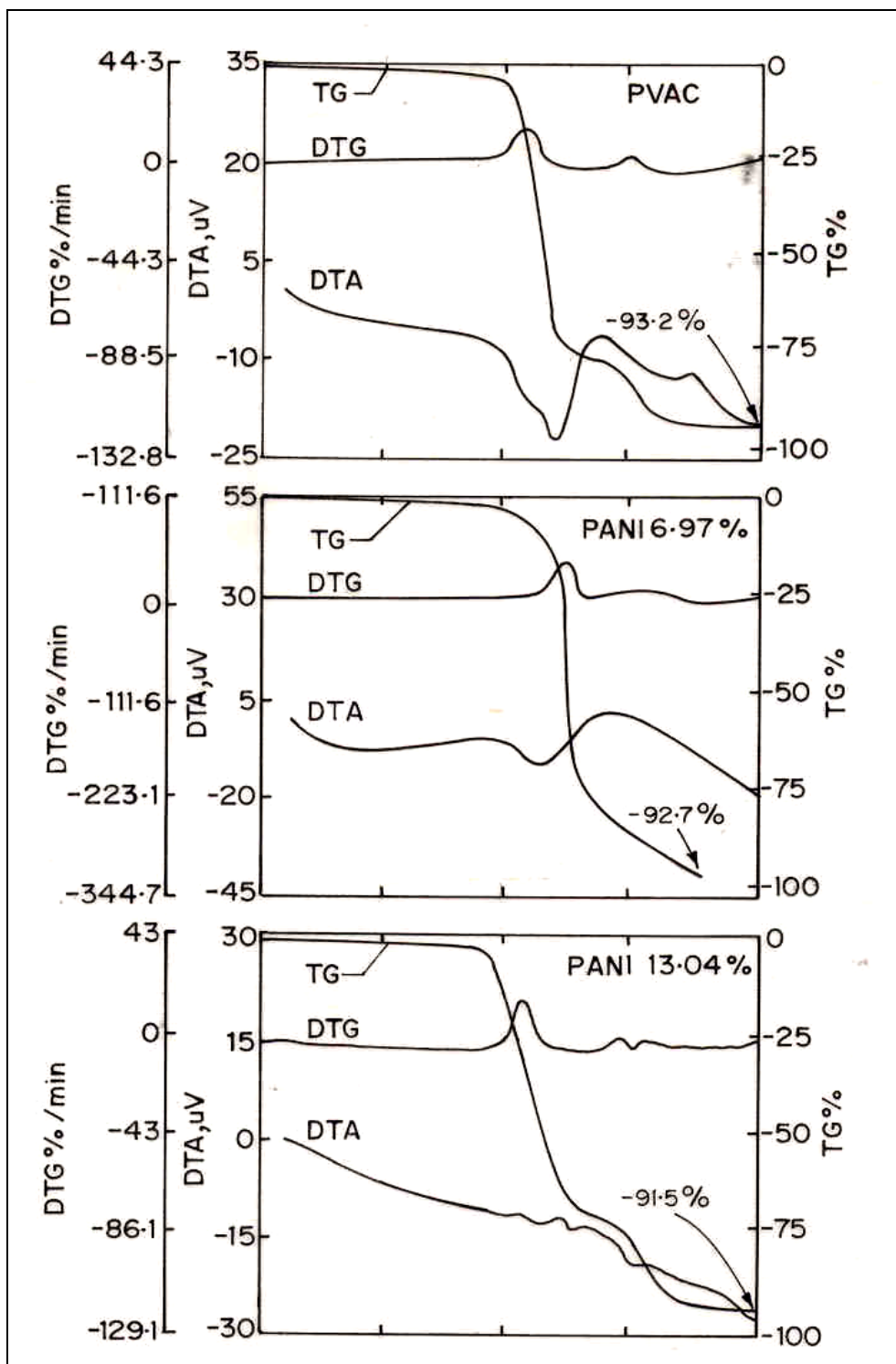
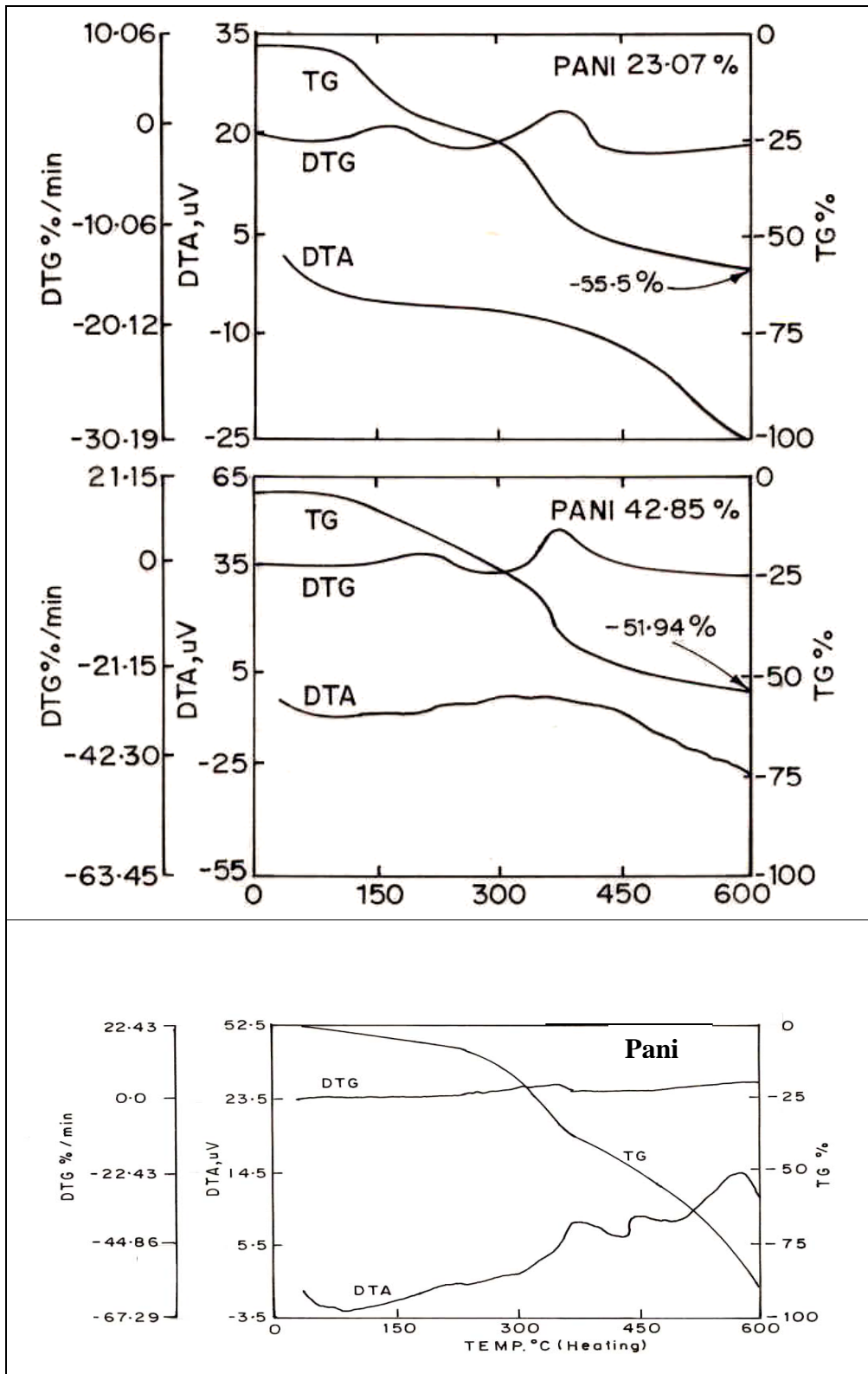


**Fig.3.17: Thermogram of Pani-PVAc insitu blends**



owing to the loss of acid dopant in Pani salt, as there is very less interaction between N atom and Cl atom and degradation of PVAc chain. The final degradation of the polymers occurs from 350° c to 500° c. S.H. Goh et.al<sup>109</sup> has studied the T.G.A. of the same blend film. It was observed that the nature of the degradation pattern matches very closely to our data.

It was noticed that as the concentration of Pani in the blend is increased the wt.loss decreased from 68.75° c to 52° c and the broad DTA peak of PVAc shows that the melting temperature was reduced on modification. From the thermogram it was observed that the blend shows the improvement in thermal stability.

**Table: 3.18, Thermal Data of Insitu Blend**

Sr.No.	Temp (° C)	PVAc wt.loss in %	Pani (3%) wt.loss in %	Pani (7%) wt.loss in %	Pani (13%) wt.loss in %	Pani (68%) wt.loss in %	Pani wt.loss in %
1	100	1	1	1	3	2	3
2	200	4	2	6.25	14	13.50	6
3	300	10.50	36.50	29	26	30	18
4	400	37	44	48	43.75	43.50	40
5	500	68.75	63	72	56.25	52	60

As the PVAc concentration increases in the blend, and blend concentration follows the same nature (trend) of degradation pattern as observed in PVAc.

The wt.loss found in the blend concentration is not observed in pristine polymers, suggesting the presence of interaction between the polymers, which alters the degradation pattern.



### 3.8 Moisture sensitivity

Sensor<sup>118</sup> can be defined as a transducer that converts the measurand into a signal. The conventional polymers, such as nylon-6, PVAc and Pam are sensitive towards moisture and Pam is water-soluble polymer. These polymers are blended with Polyaniline for measuring moisture response. Films of insitu blends were casted (coated) over electrode; the base of the electrode is made up of epoxy polymer chip (2x2) inch. Development of an electrolytic sensor that can quickly detect trace levels of moisture. This new moisture sensor uses a novel insitu blend film as an electrolyte, which is coated over an integrated array of electrodes made up of copper films. A Keithley Electrometer connections applied to electrode during the sensing process, moisture diffuses through the solid insitu blend film. The produced current was measured and was used to determine the concentration of moisture. The response time of the moisture was found to be 30 minutes. Presence of moisture may result in electrical property defect in the polymer processing industry detection of moisture content in the monomer is very important to keep the reactors running at their maximum efficiency and control the desired mol.wt. of the polymer. In corrosive and reactive gases, moisture contamination can severely damage gas lines, valves, and pressure regulators and mass flow controllers. The moisture content and its measurement depend on the type and the nature of the process involved.

Several techniques are available for detecting moisture such as, Chilled mirror Hygrometers, Quartz crystal oscillators, Capacitive sensors and the highly accurate and Expensive atmospheric ionization mass Spectroscopy (APIMS) techniques. The application of technique varies depending upon the process. This new moisture analyzer has a fast response time; Response time can be defined as the length of time required for the output to rise to a specified percentage of its final value (as a result of step change in measured) is expensive and small but can't tolerate high levels of moisture owing to its limited lifetime. This electrolytic moisture sensor rely on the absorption of H<sub>2</sub>O molecules by a highly hygroscopic material such as Pani-ny-6 blend films, Pani-PVAc-Pani blend films and Pani-

Pam blend film produces current directly proportional to the moisture content in the sample (blend film). These moisture sensors are being widely used in detecting trace levels of moisture. The moisture sensor device contains a pair of thin copper wires (metal electrodes) and is packed in a water-containing cell.

A sample stream is introduced into the body and the moisture is retained by the hygroscopic blend (insitu) film. The retained moisture is then electrolyzed at the electrodes and the current required electrolyzing the moisture is measured. Additional work in this area wasn't observed. They are convenient to use, these are inexpensive and offer very low levels of detection. However, the electrolytic moisture sensor has some major flaw. It is incapable of detecting moisture at very high levels owing to non-electrolytic current between the electrodes.

This work describes an improved electrolytic moisture sensor that is capable of sensing and signaling the moisture content in a few parts-per-billion levels. Its stability, response and recovery times and performance towards moisture have been studied.

**Humidity sensitive behavior:**

Humidity is defined (H) as the mass of vapor carried by a unit mass of vapor-free gas. The partial pressure of each species in the mixture is in direct proportion to its molar fraction. Thus

$$H = (M_A \cdot P_A) / [M_B \cdot (1 - P_A)] \text{----- I}$$

Where, M = mol.wt.

P = partial pressure of the constituents

A = water vapor

B = air

Relative humidity is defined as the ratio of the partial pressure of water vapor to the saturated vapor pressure (P<sub>s</sub>) of the water at the gas temperature.

$$RH = P/P_s$$

The dew point can also be used as a characteristic parameter for the water vapor content in the air. It is defined as the temperature (T<sub>d</sub>) at which the gas becomes saturated during cooling.

$$P(T_d) = P_s(T)$$

The connections between the measured parameters are given by the laws of psychrometry.

A lot of polymer types are known to absorb moisture. It is well known that water molecules undergo chemisorption and physisorption on the solid surfaces. The

chemisorption, which is the stronger process, causes dissociation of water molecules to form surface hydroxyls. Physisorption then takes place on top of this. The water molecules in the first physisorbed layer are double hydrogen bonded to two surface hydroxyls. Physisorption then takes place on top of this. The water molecules in the first physisorbed layer are double H-bonded to two surface hydroxyls, which they are singly H-bonded in the second and succeeding layers. If there are pores, capillary condensation of water takes place in addition to the adsorption. Capillary condensation causes the presence of water liquid in all pores with radii up to the critical value, given by the Kelvin's law.

Generally a porous humidity sensitive polymer is considered to be composed of two phases, i.e. solid polymer material and water absorbed and condensed in it (called quasi-liquid water). The relative permittivities of polymers used in humidity sensors are ranges from 3 to 10. Whereas pure water has a far larger value of about 78 at 25° C. Thus the capacitance of polymer layers changes sensitively with the absorption of water. The humidity sensitive characteristics can be derived according to the phase law of two mixed phases using one of the versions of the effective medium theory. There are several mixture formulas for the mentioned problem. Because the volume fraction of absorbed water in polymers is quite small.

### **Humidity Sensors**

As humidity is continuously changing component of our environment. Measurement, and/or control of humidity are important not only for human comfort, but also for a broad spectrum of application fields, such as domestic appliances, automotive electronics, medical service, industry, agriculture and metrology. There are three major groups of humidity sensors: those that measure mechanical property changes; physicomeric measurements that compare the latent heat of evaporation of a saturated environment to the environment in question; and those that respond to electrical or optical property change such as resistance, capacitance and color. Polymer films are well suited to standard IC processing techniques to fabricate small low cost sensors. Owing to the research efforts of the last few years a lot of different types have been developed, which can be categorized as follows.

- Capacitance types
- Resistance types, including ionic and electronic conduction versions

- Transistor structures (FET; CFT)
- Resonators (mainly BAW and SAW types)
- Electrochemical types
- Fiber optic types

**Resistance type humidity sensors:**

Resistance type (or impedance) type humidity sensors are made of conductive polymers, which can be categorized in to ionically conductive polymers and electrically conductive polymers.

The sensing mechanism of humidity sensors of porous polymer over coating film covers the top of the humidity-sensitive film .The resistance value of the coated electrode varies according to the change in relative humidity as an exponential function. These investigations have proven that the response time is determined by the film thickness and porosity.

The swelling of the polymer owing to water absorption counteracts ohmic contacts between dispersed conductive particles and thus the electronic resistance of the film will be increased .the switching effect of the polymer composites results in a sharp increase in the resistance as the relative humidity approaches 100%.

Electro conductive conjugated polymers were also investigated as sensitive layers in relative humidity sensors. Conducting polymers with a conjugated backbone are known for their interaction with small gaseous molecules giving rise to change in electrical conductivity, Pani for instance shows an increase in conductivity, when exposed to H<sub>2</sub>O vapors owing to the possibility of proton exchange between the water molecules and the protonated and the unprotonated forms of this polymer.

**Humidity-Sensitive behavior:** The swelling of the polymer owing to water absorption causes the breakdown of ohmic contacts between dispersed conductive particles and thus the resistance of the film increases sharply as the relative humidity approaches 100%. These films belong to the group of the electronic conduction type humidity sensitive layers. Humidity also depends upon the size of the pores of the polymer.

**Experimental:**

The sensor substrate with a dimension of (2x2) inches is made up of Epoxy polymer as a base. An interdigitated array of copper electrodes was deposited on one side of the Epoxy polymer chip. The two ends of this chip are soldered to thin copper wire, which is rubbed already to remove dust adsorbed on the Cu wire surfaces. The sensor chip electrode was cleaned with acetone.

**Polymer Film:** Pani- PVAc blend (insitu) was dissolved in methanol, the solution is stirred finely. A thin film of blend from solution was casted on the substrate. The fine thin film is observed when it is dried. The sensor assembly cell was then connected to Keithley Electrometer through the two terminals of the cell. The film exposed to moisture vapors. (By keeping the blend film coated electrode to the known height from the water-containing cell). Sensitivity of this film is noted. Moisture sensitivity of Pani-nylon-6 blend film and Pani-Pam blend film is also noted. A glass sheet packed the moisture cell by pasting grease to both the surfaces (Sensor cell and glass sheet) to prevent from external leaks.

**Results and Discussions:**

Moisture sensitivity of the blend films was noted by varying pani concentrations in the films. In Pani-PVAc blends, at lower concentration of pani (3%); charge transport takes place ionically, intergranular distance between PVAc molecules is found to be more and it is difficult to transport the charge, that affects the 'R' value as observed initially. As the pani concentration increases in the blend, two phenomena will be observed, the barrier in PVAc molecules get reduced i.e. intergranular distance is reduced and charge transport takes place by ions very easily. Moisture absorption also depends upon the pores of the conventional polymers.

At 13% pani in the blend, it is observed that, the 'R' value shoots to 156.71 i.e. at this point the barrier is still reduced and intergranular distance decreases further and charge transport takes place very easily. It is noticed that at higher concentrations of pani there was no gap in between pani molecules i.e. intergranular distance between two pani molecules is very less and pani is hydrophobic, which affect the charge carrier mobility and acts as a barrier in between least number of PVAc molecules

The same procedure is repeated and the same nature of graph is observed in Pani - Nylon-6, blend and Pani--Pam blend.

**Table: 3.19, Moisture sensitivity of Pani-PVAc insitu blend**

<b>Sr.No.</b>	<b>Pani (%)</b>	<b>Sensitivity Factor Moisture vapors</b>
1	0	7.04
2	3	6.72
3	7	16.5
4	13	156.71
5	68	2.44
6	100	22.90

Sensitivity factor is calculated by the following formula

$$S = R_0 / R$$

Where,

S = Sensitivity

R<sub>0</sub> = Resistance before moisture absorption

R = Resistance after moisture absorption.

Data of moisture sensitivity is given in the **table 3.20** and **graph (fig.3.19)** is shown below

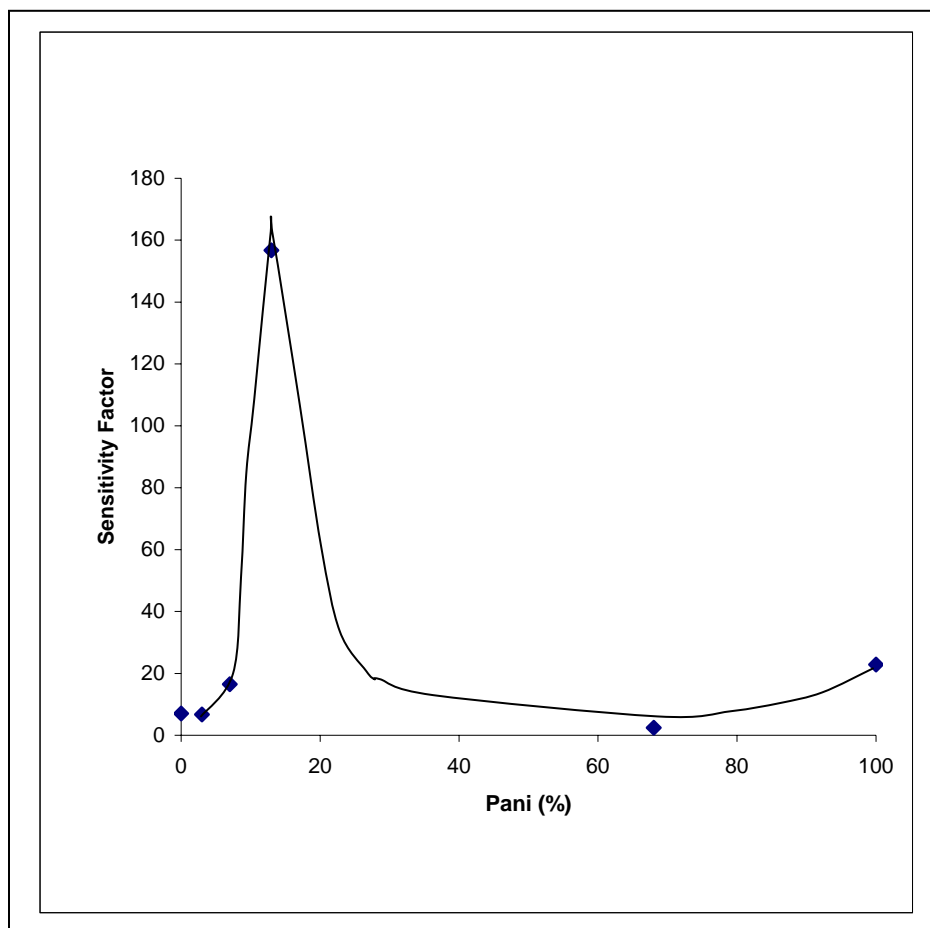


**Fig. 3.20, Plots of sensitivity factor versus Pani concentration for water vapors with Pani-PVAc integrated electrode.**

### 3.9 Conclusion:

The blend was studied with the help of characterization, electrical conductivity and comparative study of insitu blend and ex-situ blend. It was found that in the 'insitu' synthesis, the polymerization of aniline didn't affect by the PVAc solution, but it required more induction period, Following conclusions were observed with the help of results obtained.

From the i.r. Spectroscopy, it was noticed that, conductive insitu blend was formed, aniline polymerization in PVAc solution wasn't affected and pani was doped as such during synthesis. The peaks observed confirmed this  $1600\text{ cm}^{-1}$ ,  $1500\text{ cm}^{-1}$  and  $1120\text{ cm}^{-1}$ . The peak found at  $1714\text{ cm}^{-1}$ , slightly shifted to lower frequencies when the concentration of Pani was increased in the blend composition, it was the indication of H-bonding

interaction between amine group of Pani and Carbonyl group of PVAc, this confirmed the blend miscibility i.e. intermolecular interaction between the polymers.

The UV-VIS spectroscopy, shows the peaks at 820nm, 420nm, 320nm and 590nm. From this peaks, it was again clear that conducting Pani (i.e. emeraldine salt) was formed and plarons-bipolarons were created in the blend.

TGA/DTA data shows that, interaction between the polymers, altered the rate of degradation and wt.loss decreases as the PVAc concentration increases in the blend i.e. thermal stability increases and the decrease in wt.loss. was observed from 68.75% to 52%.

Conductivity at ambient temperature of the insitu blends shows that, the blend after additional doping shows rise in conductivity than the blends doped as such during synthesis (i.e. lowers doping). Here percolation threshold value was observed at 7% Pani. And 27% Pani after additional doping log conductivity was found in the range of  $10^{-2}$  to  $10^{-1}$  S/cm. The conductivity at ambient temperature was observed, it gave higher conductivity in the range of 40% to 60% Pani and percolation threshold observed at 20% Pani in the Ex-situ blend.

Temperature dependent conductivity showed that, insitu blend as well as ex-situ blend follows Arrhenius law. It was noticed that the higher concentration of Pani in the blend showed more linearity compare to ex-situ blend. The linear nature was observed because of charge carriers were created and the mobility was increased, the barrier of PVAc was found to be decreased and it required very less Activation energy (excitation energy) compare to ex-situ blends i.e. in other words, electrons hop from one conducting particle to another without inhibition of PVAc barrier.

Activation energy ( $\Delta E$ ), calculated from Temp.dependent conductivity for both the blends, was found to be decreased, as the Pani concentration was increased in both the blends (insitu blend and e-situ blend). The  $\Delta E$  value of the insitu blend was decreased from 0.43eV to 0.21eV and in the ex-situ blend the value was found to be in the range of 0.19 eV to 0.11eV.

The percolation threshold temperature, corresponds to volume fraction of Pani of about 0.26 in the insitu blend and that in the ex-situ blend it was 0.28



The charge transport process was found to ohmic (linear) as the concentration of Pani increases in both the blends i.e. the intermolecular and intermolecular charge transport process was not affected by PVAc barrier.

Characterization studies and Electrical measurements show that insitu blending technique was effective than ex-situ blending technique. This can arise from the fact that, as the concentration of Pani increases in the blend, the contact points between the Pani coated PVAc particles increases in the number giving higher conductivity than the physical mixtures.

This blend gives higher conductivity even at lower concentration of Pani; this was because solubility parameter values matches closely in PVAc and PANi. Moreover the work function values ( $\phi$ ) of both the polymers matches closely, from this physical properties data, it was again confirmed that PANi-PVAc was higher conductive and PVAc adsorbs Pani strongly and is used in adhesives and acts as a binder.

## CHAPTER -IV: Polyaniline / Poly acryl amide Blend

4.1	INTRODUCTION-----
4.2	Experimental-----
	a) Polymerization of acryl amide-----
	b) Preparation of insitu Blends-----
	c) Preparation of ex-situ Blends -----
4.3	Results and Discussions-----
4.3A	Pani-Pam blend-----
4.4	Characterization-----
4.4	FTIR Spectroscopy-----
4.5	UV-VIS Spectroscopy-----
4.6	Measurement of properties-----
	1) R. T. Electrical Conductivity of the blends-----
	2) Temperature Dependent Conductivity of the blends-----
	3) Activation Energy studies for the blends ( $\Delta E$ )-----
	4) Charge Transport studies in the blends-----
4.7	T.G.A./D.T.A.-----
4.8	Moisture sensitivity-----
4.9	Conclusions-----

#### **4.1 Introduction:**

Pam is an ionic structured polymer. In aqueous solution, it displays more anionic structure. polyacrylamide is closest in chemical nature with Pani. Due to the presence of the amide groups one can expect hydrogen bonding between the two polymers, which may lead to better miscibility. Pam is also used in the moisture sensors and measures moisture response. It is also used as a gel actuator. In the insitu technique, Pam acts as a good compatibiliser, when aniline is polymerized in the same solution. So the Pam is chosen for the blend preparation. This blend is also prepared by ex-situ technique.

Polyacrylamide has sticking properties and it is being used as an adhesive<sup>119</sup>. In the insitu preparation, Pani may coat (adhere) strongly on the Pam particles, so the conductivity was expected to be high.

Present chapter explains comparative studies of the insitu and exsitu blends with the respect to their electrical conductivity, moisture sensitivity and thermal stability.

#### **4.2 Experimental:**

##### **a) Polymerization of acrylamide:**

Acrylamide was polymerized to Polyacrylamide by bulk polymerization technique. In this experiment, known quantity of acrylamide was taken in the flask, which contains known quantity of distilled water, 0.2gm ammonium per sulfate (initiator) dissolved in 10 ml distilled water was added drop by drop in to a beaker containing acrylamide solution. The above mixture was heated in the heating mantle for one hour at 70°C. It was observed that the solution became transparent and viscous. Beaker was removed from the heating mantle, and kept for cooling. After cooling, it was precipitated in a non-solvent (distilled Methanol). White lumps of Pam obtained was filtered and dried in the vacuum for 4 hrs and this dried mass was chopped to pieces and these were used for insitu synthesis of Pani-Pam blend.

##### **b) Preparation of insitu blend:**

In the insitu synthesis, 1gram Pam was dissolved in 100 ml distilled water and same measured quantity has taken in four separate beakers. To that, 0.51 grams of aniline (0.005 M) and 5 ml of 1N HCl solution were added. About 25 ml of 0.1M ammonium per

sulfate was added slowly to the above reaction mixture under constant stirring. Similar reactions were carried out with aniline concentration of 0.01M, 0.02 M and 0.05 M and 10 ml of 1N HCl, 20 ml of 1N HCl, 50ml of 1N HCl solution. The aniline to ammonium per sulfate molar ratio in all the above reactions was 1:1. Polymerization of aniline was carried out simultaneously in each beaker. It was observed that reaction became exothermic which accelerated the rate of propagation.

The reaction was carried out at ambient temperature for 10 hr. The blend was precipitated in distilled methanol, filtered, washed with distilled methanol several times and dried in vacuum till moisture was removed. The green mass of each composition of the blend was crushed in mortar and pestle to fine powder.

Samples for characterization and measurement of conductivity were made as described in chapter II.

**Redoping of Pellets:** Pellets of each composition of 'insitu blend' were redoped in 2M HCl; the pellets were doped for 12 hrs. Later it was removed from HCl solution and kept for drying in vacuum.

### c) Preparation of Ex-situ Blend

Pam synthesized by the above method was taken for ex-situ blending. Aniline was polymerised separately in aqueous medium by standard route described in chapter II using dopant. This polyaniline powder was then mixed physically with Pam powder. From 0% to 100 % in the composition of the blend. Samples were made for measuring electrical conductivity as before.

## 4.3 Results and Discussions:

### 4.3 A: Pani / Pam blend

Pam obtained by bulk polymerization technique has mol.wt.41000.measured by viscometry technique and mol.wt. is calculated by the following equation<sup>120-121</sup>,

$$[\eta] = \bar{K} \cdot M^a \quad 4.1a$$

Where,  $[\eta]$  has been related to the intrinsic viscosity of a solution,  $\bar{K}$  and  $a$ , are constants for a given polymer/solvent/temperature system and  $M$  =molecular mass of dissolved Polymer. Its characteristic peaks were observed in the FTIR spectra, which are given in

the assignment data. Thermogram and thermal data shows that, it is thermally stable at higher temperature. Pani was synthesized in Pam solution, viscosity of the Pam solution was found to be 0.530 poise, which may affect aniline polymerization. Pani-Pam viscous solution didn't develop turbidity. Solubility parameter of the Pam is found to be 0.48  $\text{Mp}^{1/2}$  and that of the aniline is found to be 21.1  $\text{Mpa}^{1/2}$ , which doesn't match. The pH of the medium was found to be 1.0. The storage stability of aq. Pani-Pam system remained undiminished with increase in Pani loading. The Pani-Pam system lost their redispersibility in methanol like Pam precipitated in it. The reaction scheme by which chemical synthesis proceeds for Pani / Pam blend is represented in the table 4.1 and blend formation is shown in the fig.4.2

**TABLE-4.1**

**Chemical Synthesis data of Pani - Pam blends**

<b>Serial No</b>	<b>Aniline (Grams)</b>	<b>Hydrochloric Acid (ml)</b>	<b>Ammonium Per sulfate (Grams)</b>	<b>Pam (Grams)</b>	<b>%Yield</b>
1	0.51	0.5	1.2	1	75.26
2	1.02	1	2.3	1	71.85
3	2.04	2.5	4.6	1	88.38
4	5.1	6	11.4	1	94.36

**Solvent: Distilled water 50 ml for each experiment**

**Reaction temperature: Room temperature (25° C)**

**Reaction time: 12 hours**

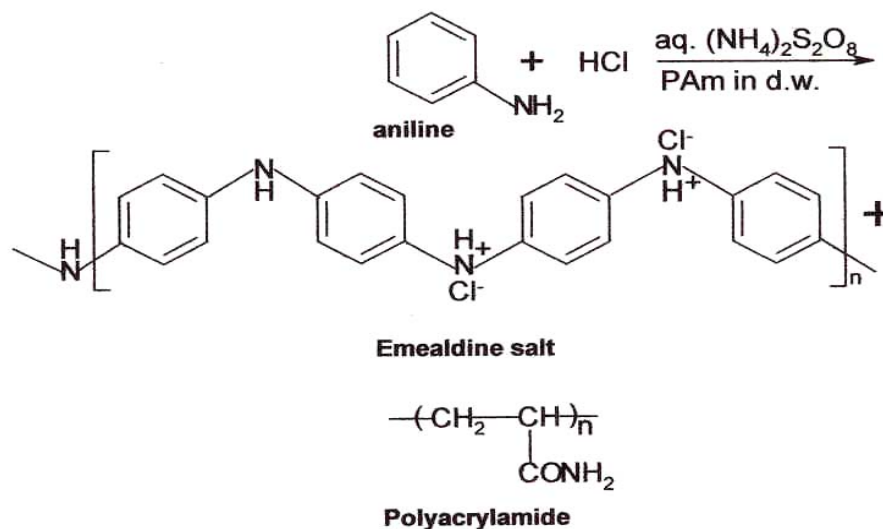


**Fig.4.2: Pani-Pam insitu blend.**

#### 4.4 Characterizations:

##### 4.4 FTIR Spectroscopy:

Given fig.4.3 shows spectra for insitu blends. In that fig. 'a' corresponds to pristine 'Pam' and 'b', 'c', 'd', and 'e' shows the increased concentration of Pani in the blend and 'f' corresponds to Pristine 'Pani',

There are large number of absorption bands noted for which the assignment data is given in the Table 4.5, Although there is an overall increase or decrease of the intensities of the major bands corresponding to increase / decrease of the particular component, which would be expected for blend, other changes are also seen in these spectra.

Pristine Pam shows a band for the amide C=O stretching, appears at  $1665\text{ cm}^{-1}$ , shifted in peak position was found in the blend compositions. This shifting was owing to hydrogen-bonding interaction between amino group of Pani and carbonyl group of Pam.

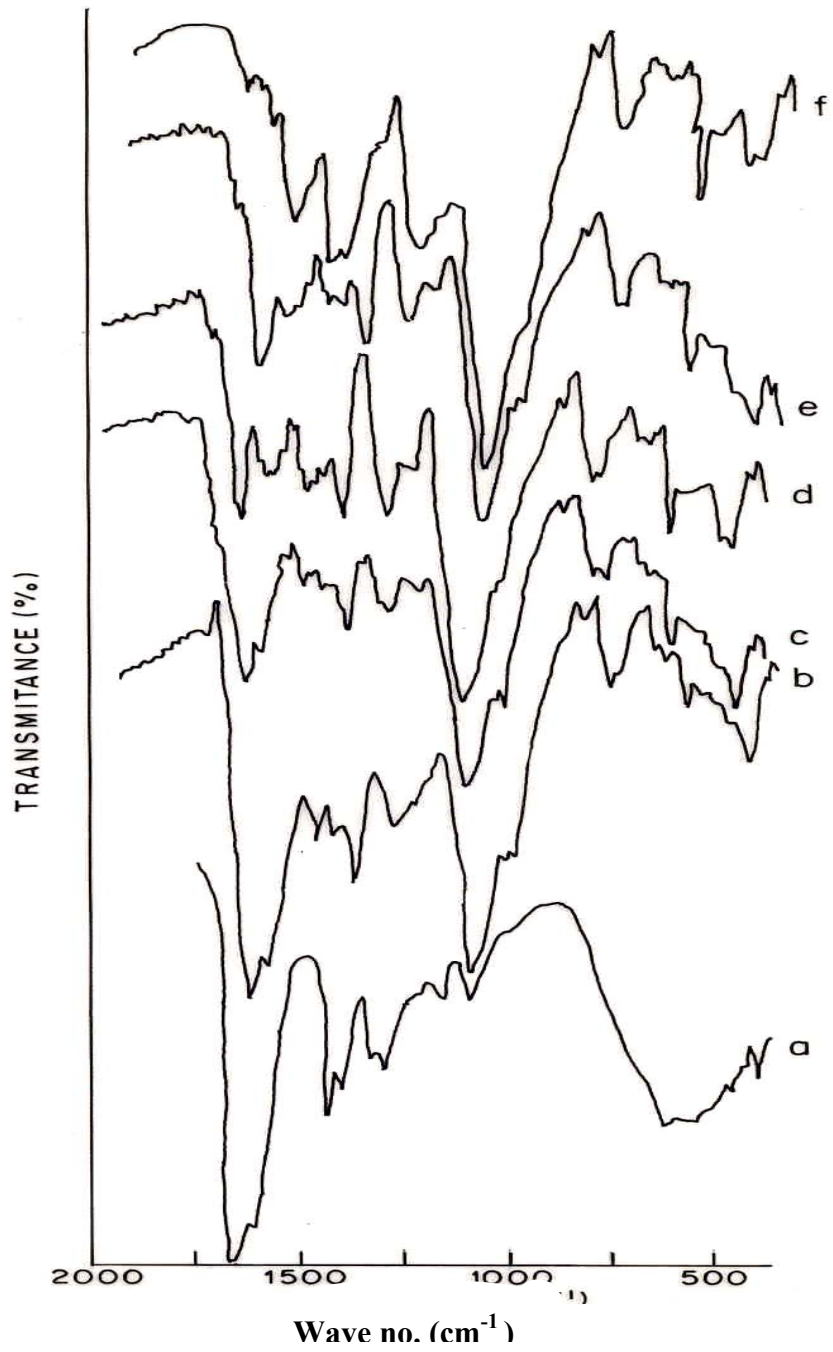


**Fig.4.3: FTIR-absorption spectrum of Pani-Pam insitu blend compositions**

**a) Pam, b) 11% Pani, c) 20% Pani, d) 48% Pani, e) 59% Pani and f) Pani**

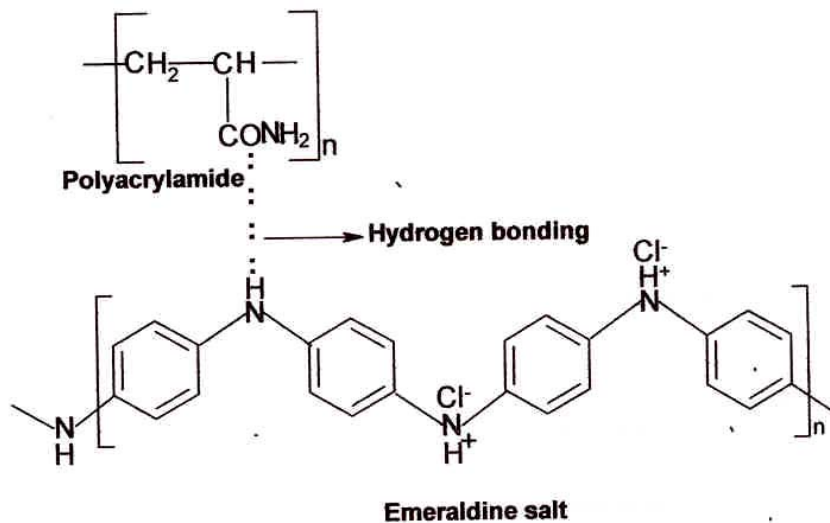


**Fig.4.4: Proposed scheme of the Hydrogen bonding between Pani and Pam**

(N-H...O=C).<sup>123</sup> The fig.4.4 shows hydrogen-bonding interaction between Pani-Pam as observed in Pani-PVAc blend.

The peaks at  $1600\text{cm}^{-1}$  and  $1500\text{cm}^{-1}$  were resulting from protonation and it is characteristic of the conversion of quinonoid ring to the benzenoid ring by the proton induced spin unpairing mechanism and stretching vibrations of nitrogen atoms in aromatic and diamine units respectively. These bands have equal strength in the emeraldine oxidation state of Pani.

The absorption band appears at  $1650\text{cm}^{-1}$ , have been associated with C=C stretching in quinonoid and benzenoid rings respectively. The absorption band observed at  $1300\text{cm}^{-1}$  region in the fig. was a halogen sensitive band that confirms the salt formation between chlorine anions and protonated nitrogen atoms next to the quinonoid rings. This absorption band is consistent with the higher conductivity of the protonated blend compositions than that of the unprotonated sample. The peak observed at  $1116\text{cm}^{-1}$  has been associated with electron delocalization and electrical conductivity in Pani.



**Table: 4.5, F.T.IR data of insitu blends**

<b>Polyacryl amide</b>	<b>Pani 11. %</b>	<b>Pani 20. %</b>	<b>Pani 48. %</b>	<b>Pani 59. %</b>	<b>Pani 100%</b>	<b>Assignment</b>
1665 s	1660 s	1657s	1655	1653	—	-CO group
—	—	—	—	—	1650 s	C=C, C=N
—	—	1604 w	1600 w	1600 w	1589 w	str.of N=Q=N
—	1500 w	1500 w	1500 w	1500 w	1500 w	str.of N-B-N
—	—	—	—	—	1469	str.of benzene ring
1452 m	1445 w	1441 w	1442 w	1440 w	—	alicyclicCH <sub>2</sub> CH (op)
1425 vw	1425 vw	1423 vw	1423vw	—	—	CH <sub>2</sub> in plane deformation
—	1402 m	1400 m	1400 m	1400 m	—	C-N Str.inQB <sub>t</sub> Q
—	—	1325 w	1300 w	1296 w	—	C-N str.inQB <sub>c</sub> Q QBB, BBQ;
1300 vw	1305 m	1305 m	1303 m	1305 vw	—	CH in-plane deformation
1275 m	1280 m	1280 m	1280 m	1275 m	—	aliphatic C-N linkage
—	—	—	—	—	1286 w	C-C, C-N
—	—	—	1240 w	1240 w	—	C-N str. in BBB
—	1116 s	1112 s	1114 s	1116vs.	1129 vs.	a mode of Q=N <sup>+</sup> H-B or B-NH-B;
1100 vw	—	—	—	—	—	Alkane groups
—	800 m	800 m	800 m	800 m	800 m	CHout-of-planebending of 1,4 ring
—	750 w	750 w	750 w	750 w	750 w	CHout-of-planebending of 1,2 ring
650 vw	650 vw	—	—	—	—	out-of-plane -NH <sub>2</sub>
—	625 w	617 w	617 w	617 w	617 w	aromatic ring deformation

Abbreviations: str: stretching; B: benzeniod unit; q: quinonoid unit; t: trans; c: cis.

Owing to a vibrational mode of a B-NH<sup>+</sup>=Q structure. However, the peak at 825 cm<sup>-1</sup> assigned to the out of plane deformation vibration of p-substituted benzene ring, which means formation of Pani starts. Pani is formed during protonation and its concentration increases. It indicates the positive charge in the chain and the distribution of the dihedral angle between the quinone and benzenoid ring. Peaks at 1452 cm<sup>-1</sup>, 1425 cm<sup>-1</sup>, 1300 cm<sup>-1</sup> and 1275 cm<sup>-1</sup> correspond to pristine Pam.

The peak observed at 617cm<sup>-1</sup>,<sup>124</sup>, which have direct correlation with conductivity also show pronounced intensity in Pani. This, suggest a greater  $\pi$ -electron delocalization in Pani materials and there by explains the enhanced conductivity. From the above results it was confirmed that 'insitu blend' formed successfully, the blend compositions were doped as such during 'in-situ' synthesis. H-bonding takes place and the blend was conductive electrically.

#### 4.5 UV-VIS Spectroscopy:

Given fig.4.6 shows UV-VIS spectra of the 'insitu blends'. 'c' corresponds to pristine Pani, 'a' and 'b' shows increasing Pani concentration in the blend. The samples were prepared in the HCOOH solution. Color of the solution was found to be green and scanned in the wavelength region 300nm-900nm.

In Pani-Pam blend, shows absorption band at 360nm; apparently, this results from overlapping of the amine excitation band and the imine-amine transformation band. This overlapping becomes effective particularly in the presence of the support polymer Pam. Solubilization of the effective dispersion of Pani formed in the presence of Pam, may arise as a consequences of coating Pani on the Pam molecule. 590 nm, shows  $\pi$ - $\pi^*$  transition and the excitation band of the quinonoid ring. From this band position, it is again clear that the blend doped during synthesis and was conductive. These peaks were found in blend compositions as shown in the spectra.

The main special feature of interest in the case of H<sup>+</sup> doped blend concentration is the band near 820 nm, which represents the strong absorption even for small concentration of Pani in the blend is the signature of protonated Pani.

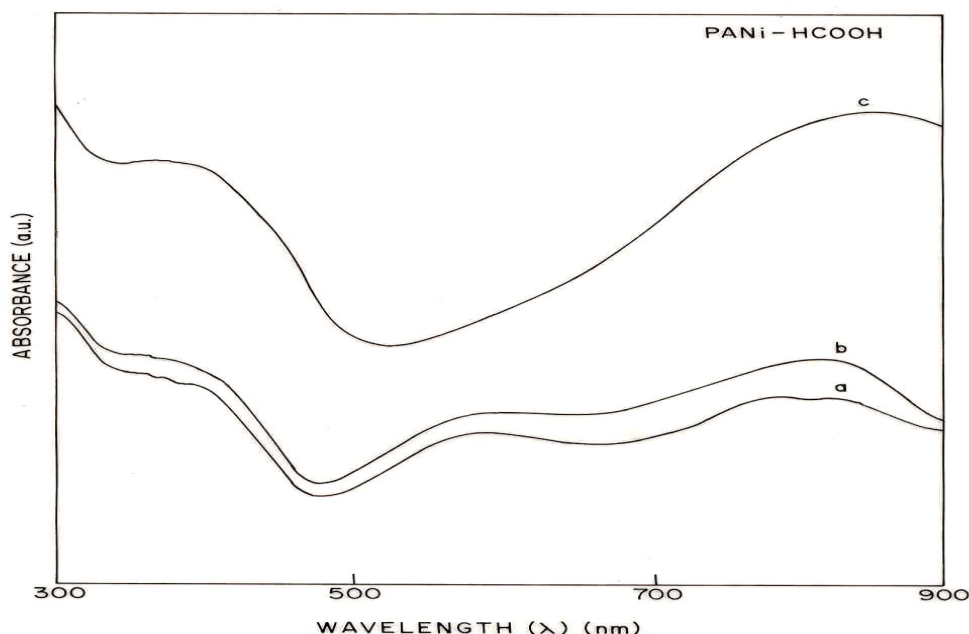


**Fig.4.6: UV-VIS spectrum of Pani-Pam insitu blend**

**a) Pani, b) 11% Pani, c) 20% Pani**

From the above results, it is confirmed that Pani as such gets doped during synthesis and the conductive blend is formed successfully.

#### **4.6 Electrical Conductivity Measurements**

##### **1) Compositional variation of Conductivity at ambient condition**

Compositional variation of conductivity at ambient condition was based on the conductivity model, which is given in the third chapter.

Fig.4.7 shows the graph of conductivity of insitu blends at room temperature with Pani content in the blend. The curve 'b' corresponds to blend compositions after additional doping while 'a' corresponds to blends as such obtained from reactor. It was observed that, initially 11% Pani in the blend gives conductivity  $0.505 \times 10^{-6}$  S/cm and as the concentration of Pani increases in the blend conductivity rises further,  $0.449 \times 10^{-3}$  S/cm. Conductivity remains constant after 59% Pani content in the blend.

It was noticed that the same blend composition after additional doping for 11% Pani gives, conductivity  $0.156 \times 10^{-6}$  S / cm.

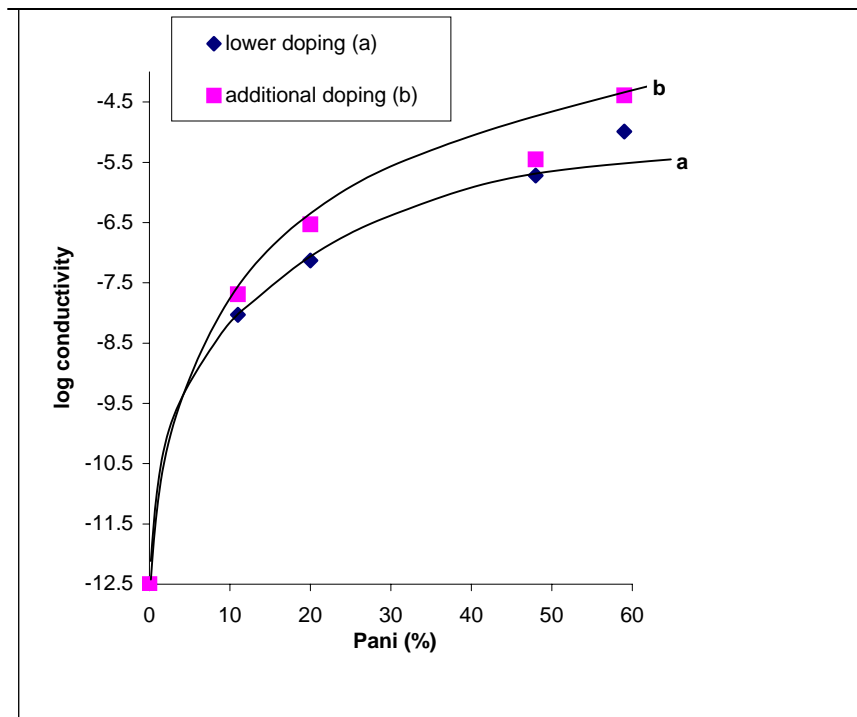
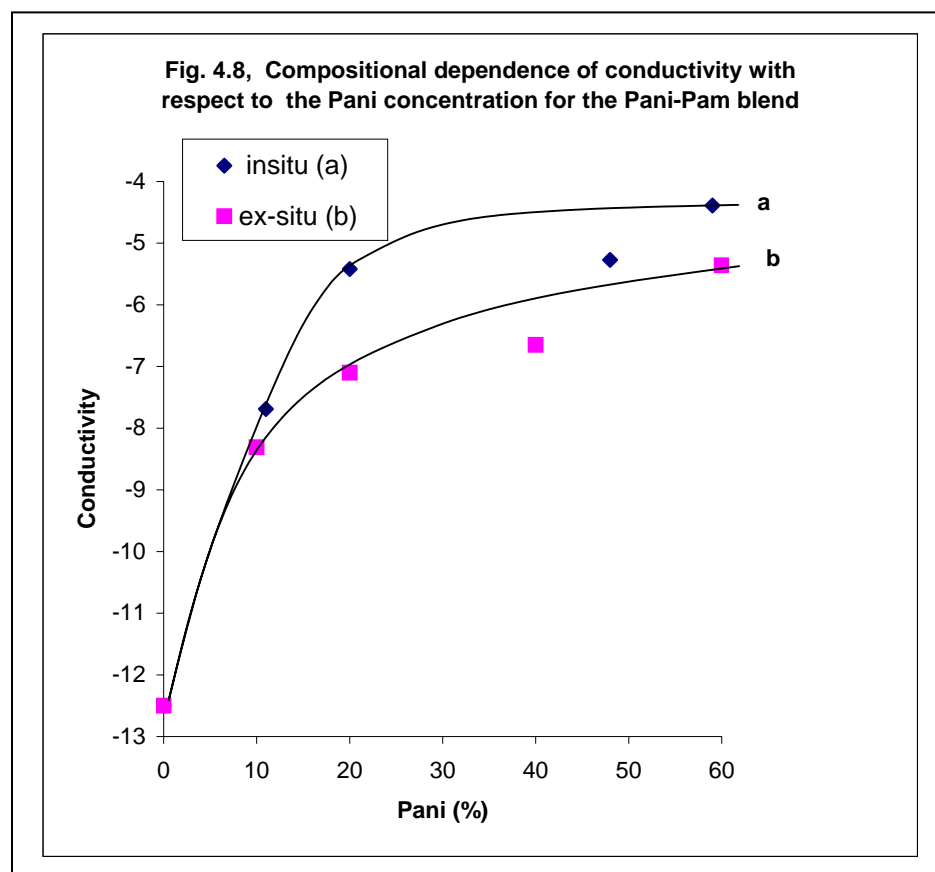


**Fig.4.7: Compositional dependence of conductivity with respect to the Pani concentration for the Pani-Pam insitu blends.**

As the concentration of Pani increases in the blend conductivity rises again and it gets saturated at 59% Pani content and conductivity was found to be  $0.719 \times 10^{-3}$  S/cm. Further increase in the Pani content was not found to have an appreciable effect on the conductivity. After redoping, the conductivity rises compare to the blend compositions obtained as such from the reactor (shown in the above fig.) and percolation threshold was found to be 11%.<sup>122</sup> Fig.4.8 shows that in the graph, 'a' corresponds to 'insitu' and 'b' corresponds to 'exsitu' blend. In the insitu blend, 11%Pani gives conductivity  $0.156 \times 10^{-6}$  S / cm. In the ex-situ blend, 10% Pani gives conductivity  $34.482 \times 10^{-9}$  S / cm. and as the concentration of Pani increases in the blend, conductivity rises further and reaches to saturation and there after it remains constant. As the loading density is increased the aggregates are more tightly packed and pressed against each other. Thus the net resistance decreases with increasing loading level. Once a high enough loading is reached so that contact resistance between aggregates is no longer significant,

Further increase in loading wouldn't be expected to cause any significant increase in



conductivity. It was found that in the insitu blend at 59 % Pani gives conductivity  $0.719 \times 10^{-3}$  S / cm. and ex-situ blend shows conductivity at 60% Pani,  $0.209 \times 10^{-3}$  S/cm. In the exsitu blend (Fig.4.8), the percolation threshold value was found to be 10%. Percolation threshold value depends on many factors, such as the size, shape and the special distribution (topology) of the filler particles with in the host polymer matrix, the adhesion and the possible interactions between two phases and finally the processing method. The percolation threshold varies considerably with the shape and agglomeration of the Pani and the type of Polymer used<sup>125</sup> also depends on the geometry of the filler particles. At this point (saturation point) conducting network is formed and the barrier of Pam gets reduced as the Pani concentration is increased in the blend. From the above results it was clear that conductivity rises after redoping the pellets. Thus insitu blend shows higher conductivity compare to ex-situ blends. The conducting elements of these

paths are either making physical contact between themselves or separated by very small distances across which electron can tunnel.

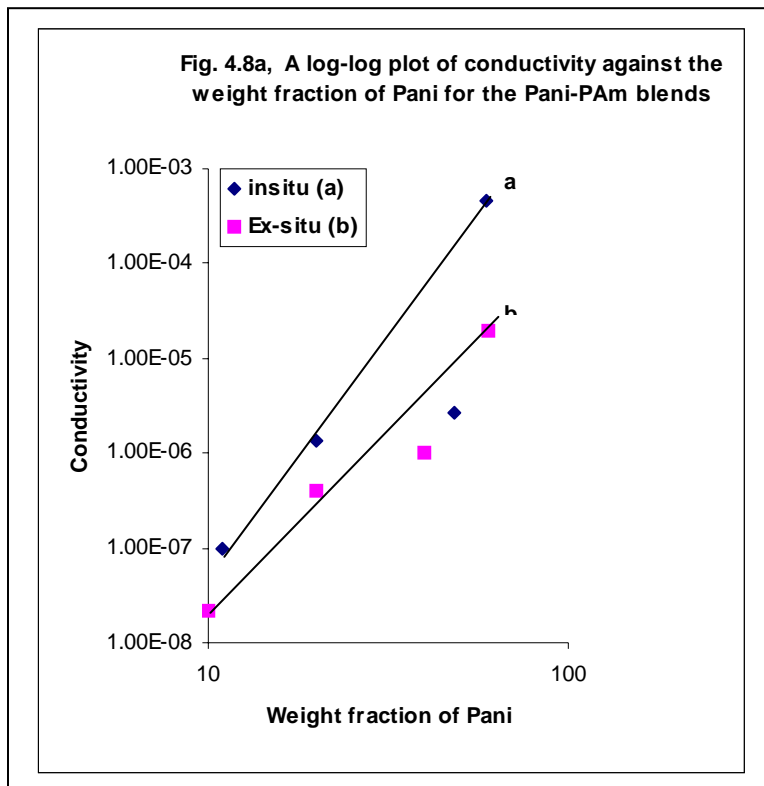
### **Percolation threshold**

The Fig.4.8a shows plot of log conductivity vs.  $\log(\phi - \phi_c)$ . In the graph, the curve 'a' corresponds to 'insitu' and 'b' corresponds to ex-situ blends respectively. The nature of the graph was found to be linear thus follows the percolation model of conduction. It is further seen that the percolation threshold for the in situ blend is much lower than that made by ex situ method. This can be explained with the help of conduction processes studied for the blends.

This may be arisen by the fact that, in the 'insitu blend', Pam molecule gets coated as the Pani concentration is increased in the blend ( $10^{-4}$  S/cm) and as the concentration of Pani increases in the blend, the number of Pani coated Pam molecules increases, which forms a conducting path; Pani particles contact each other forming a three-dimensional network and after that conductivity was observed to reach to saturation.

In the ex-situ blend, it was observed that graph shows straight line may be considered to form an M-I-M<sup>126</sup> structure, where the conducting regions are well separated from the insulating region (material) and it was found that as the concentration of Pani increases, barrier between the two conducting sites decreases. There is no such barrier formed between Pani particles at higher concentrations of Pani in the blend as observed in insitu blend i.e. network of conducting particles were observed in the insitu blend.

The lower  $\phi_c$  was obtained when the conditions favored the formation of cohesive contacts between the fillers rather than the adhesive contacts between the polymer and filler. If the percolation threshold value is high in the blend means poor dispersion and morphological features treated the case of a random 2-phase dispersion of conductor in an insulating matrix<sup>124</sup>. The exponent 'f' in the equation (1) was found to be 0.31 for in situ blend and ex-situ blend, 'f' was found to be 0.36.



## 2) Temperature Dependent of Conductivity:

The temperature dependent conductivity is predominantly of nonmetallic sign (i.e. conductivity increases with temperature) but often shows change to a metallic sign at higher temperature given in fig. 4.9, is depicted log conductivity vs. Temp. for insitu blends. In fig 4.9, a, b, c and d, for blend compositions obtained from the reactor and the A, B, C and D for additional doping of the blend compositions. It shows the rise in conductivity with temperature and further rise in conductivity is observed for the same blend composition after additional doping, this may be because of the charge carrier created. Excitation of mobile  $\pi$ -electrons from the valence band (HOMO) to the conduction band (LUMO) and the charge carrier hopping between the Pani coated Pam molecule.

To know the conduction phenomena better, it is proposed that when an electron is removed from the top of the valence band by doping of Pani a vacancy is observed (hole or radical cation). A radical cation i.e. partially delocalized over some polymer segment is called a polaron; a bipolaron i.e. cation has two charges associated with the localized polymer segment and their mobility is observed as the temperature varies.

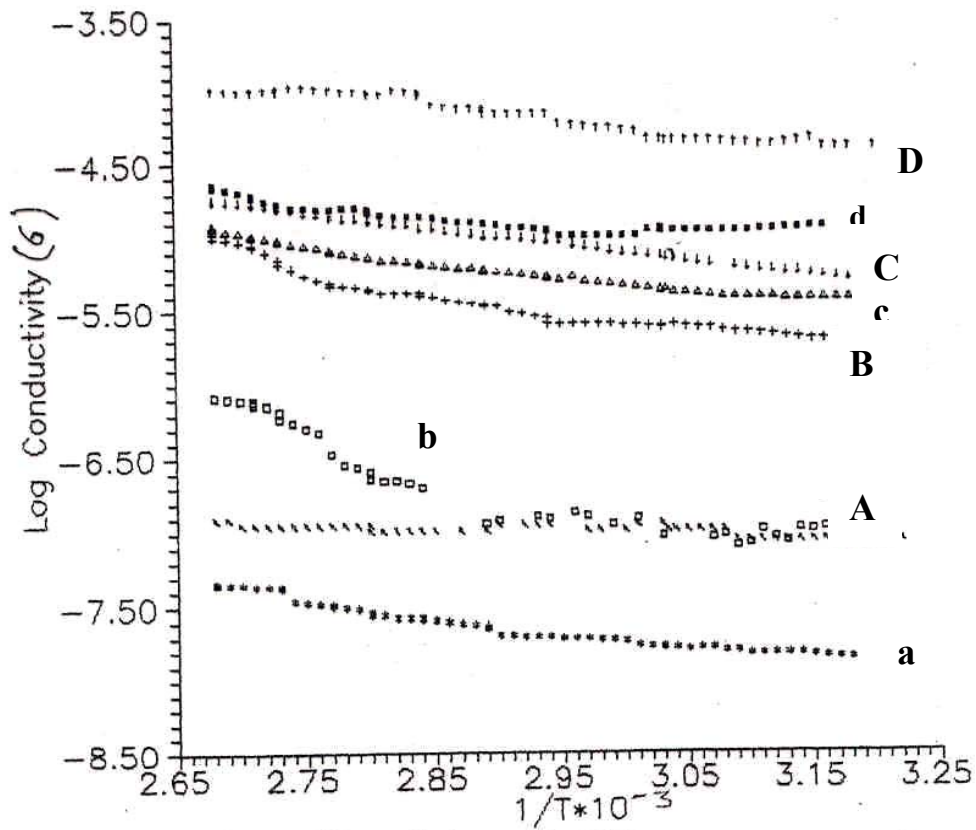


**Fig.4.9: Plots of log conductivity versus reciprocal of temperature for Pani-Pam in situ blends.**

**Blend compositions obtained as such from the reactor.**

a) 11% Pani, b) 20% Pani, c) 48% Pani, d) 59% Pani

**Blend compositions after additional doping.**

a) 11% Pani, B) 20% Pani, C) 48% Pani, D) 59% Pani



Their mobility is observed as the temperature varies. The electrical conductivity is observed in these blends are associated with thermal arrangement of double and single bonds in the conjugated system. Conduction by polarons and bipolarons is the mechanism of charge transport in polymers with degenerate ground states. The final magnitude of the conductivity depends both on the no. of charge carriers as well as their mobility. The no. of charge carriers are essentially dependent on the dopant level while the mobility is associated with the distance / barrier between the two defect sites in which the charge carrier hops, it was seen that the HCl dopant not only increases the dopant concentration but also creates the additional band gaps. In the insitu blend, (11%), Pani even after additional doping shows concave and nonlinear nature.

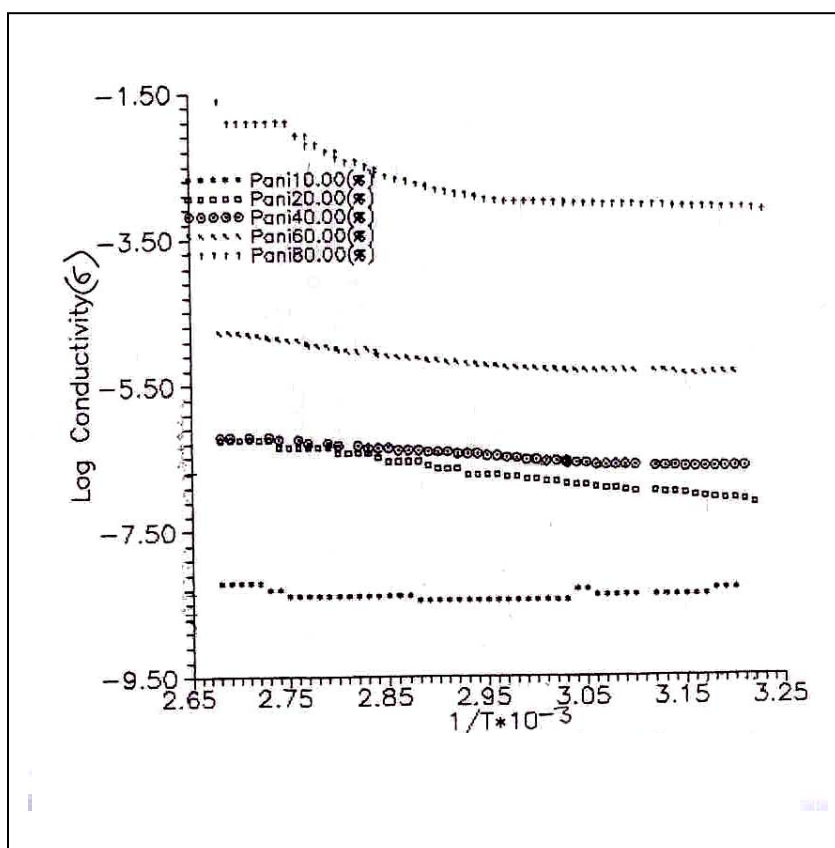


**Fig.4.10: Plots log conductivity versus reciprocal of temperature For Pani-Pam ex-situ blends.**

**A) 10%Pani, B) 20% Pani, C) 40% Pani, D) 60% Pani, E) 80% Pani**

Thus lower oxidation level yields polarons and at higher oxidation levels bipolarons are produced both polarons and bipolarons are mobile and can move along the polymer chain by the rearrangement of double and single bonds in the conjugated system.

This may be because of Pam barrier, hinders the carrier mobility of electron hopping from one conducting particle to another and the nature wasn't found to be straight, but as the Pani concentration increases in the blend, conductivity rises again and rises after additional doping. At this point, pani coated Pam particles forms a network and decreases the intergranular barriers. Hence, conduction occurs via interchain and intrachain hopping the Pam barrier get reduced and electrons hop from one conducting particle to another and the mobility of charge carriers is also increased as the temperature is increased and electrons requires very less activation energy to hop from one particle to another. As the conducting network is formed and the nature of the graph is found to be straight line, shows the electrical conduction in blends (insitu blend, Ex-situ blend) is thermally activated<sup>122</sup>. Physically the thermally activated process will correspond to electrons hopping from one molecule to another or to ions making their way through the blends. Increase in conductivity can be attributed to increase in polaron delocalization owing to thermal activation thus follows the ' Arrhenius law'.

In ex-situ blend, (fig.4.10) the temperature dependence of  $\sigma$  shows initially nonlinear nature for lower concentration of Pani and as the concentration of Pani increases, the conductivity rises. Barriers of Pam are reduced and linearity is observed. Nature of the graph follows the Arrhenius law. i.e. at this concentration the graph is more or less linear. The slope of the Arrhenius curve decreases suggesting that the activation energy for conduction decreases as the Pani content increases in the blend. i.e. at this concentration, electrons require very less activation energy to transport from one conducting particle to another.

### **3) Activation Energy: ( $\Delta E$ ) for the blends**

Given fig.4.11, shows the  $\Delta E$  vs. Pani (%) for the insitu blend. 'a' corresponds to blend compositions obtained from the reactor and 'b' corresponds to additional doping of the blend. Activation energy is calculated from the slope of graph of temperature dependent conductivity. It is observed that 11% Pani shows activation energy value 0.39

eV and as the concentration of Pani increases in the blend, activation energy decreases as the resistance decreases.

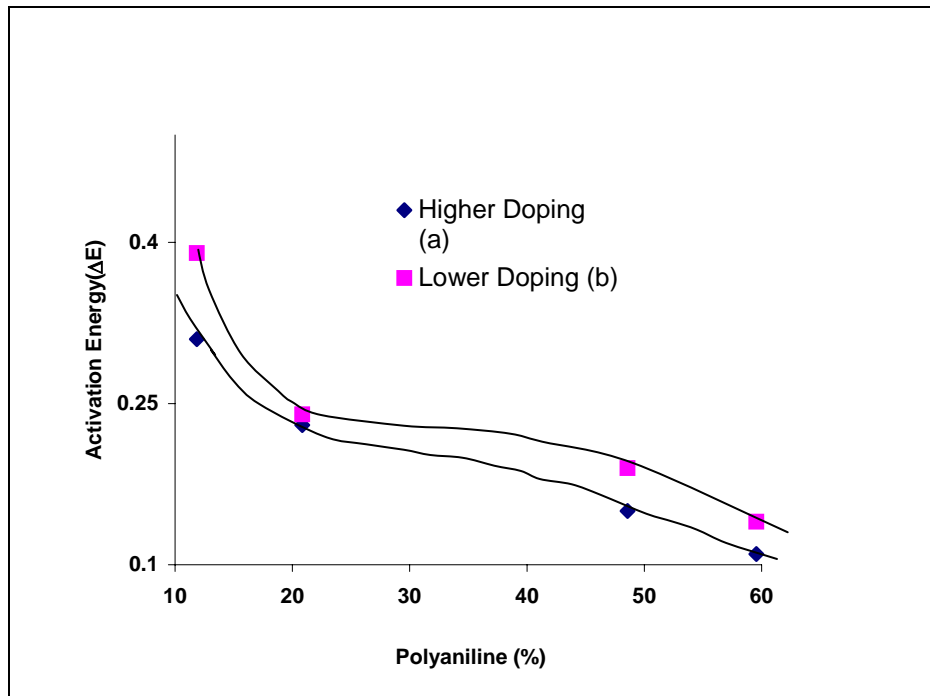


**Fig.4.11: Plot of activation energy versus Pani concentration For Pani-Pam insitu blends.**

**Table: 4.12, Activation energy value data for insitu blends**

Sr.No.	Pani (%)	blend compositions obtained from the reactor ΔE (eV)	Additional doping ΔE (eV)
1	11	0.39	0.31
2	20	0.24	0.23
3	48	0.19	0.15
4	59	0.14	0.11

Gradual decrease in activation energy value found to be 0.14 eV at 59% Pani in the insitu blend. The same trend found after additional doping also. The activation energy value for the 11% Pani in additional doping is 0.31eV and as the concentration of Pani increases to 59%, it is found to be 0.11eV.

In the ex-situ blend, 10% Pani shows activation energy value 0.46 eV and as the concentration of Pani increases in the blend, activation energy value is found to be decreases and at 60% it is observed to be 0.27eV From the comparative study of the blends, it is concluded that the insitu blending gives lower activation energy value compared to ex-situ blend and further decrease in activation energy value is found after additional doping. Additional energy levels are created, which reduces the barriers and gives lower  $\Delta E$  values. This may be arised by the fact that in the ‘insitu blend’, as the aniline polymerizes in the Pam solution, Pam get coated simultaneously and as the concentration of Pani coated Pam particles increases in the number of conducting three-dimensional network, barrier of the Pam is reduced. As the temperature increases, mobility of the charge

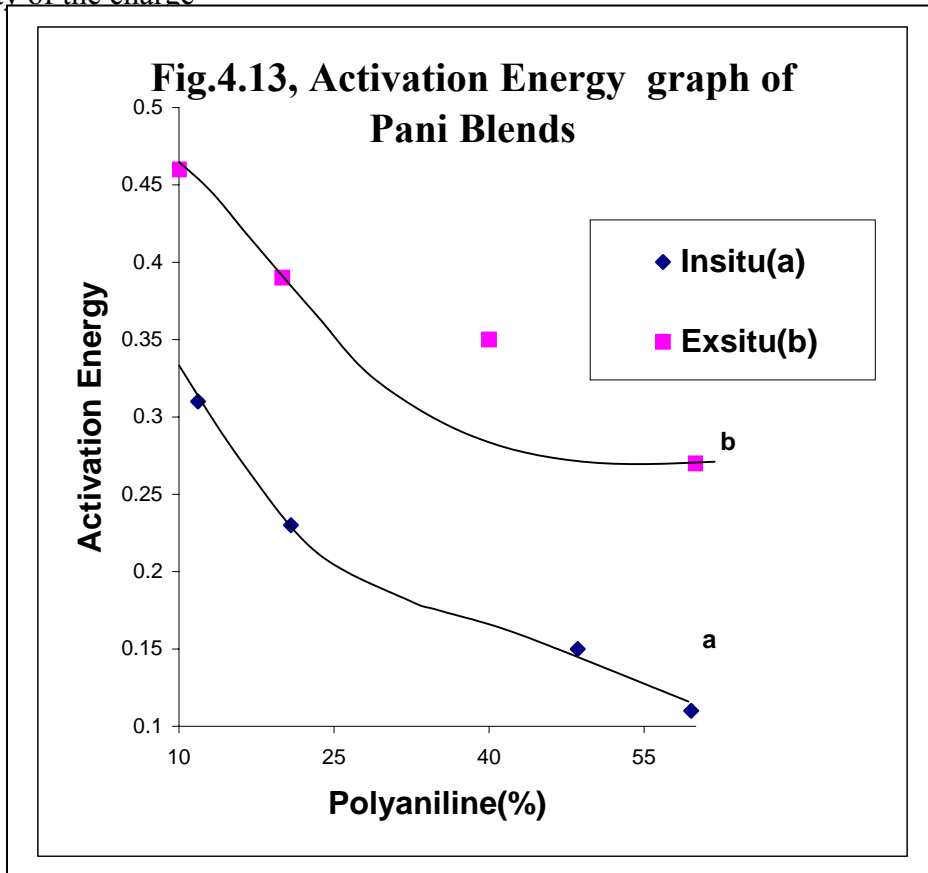


**Table-4.14: Activation energy data for Pani blends**

Sr.No.	Pani (%)	insitu blend	Pani (%)	ex-situ blend
1	11	0.31	10	0.46
2	20	0.23	20	0.39
3	48	0.15	40	0.35
4	59	0.11	60	0.27

carriers also increases, electrons get activated and it requires very less activation energy to cross the barrier compare to ex-situ blends. In this case, though the network is formed in the blend, Pam barrier inhibit electron hoping and subsequently resistance increases, which requires higher activation energy than insitu blend.

Varying in activation energy value data for the insitu blend and ex-situ blend is given in the table 4.12 and 4.14. From this results, it is again clear that insitu blend technique is more effective than exsitu blend. Since there are very few reports found on the activation energy for the blends.

#### **4) Current vs. Voltage (I-V) Characteristics:**

Charge transport process is based on the model, which is given in chapter-1. Fig.1.42 shows the hysteresis curve for insitu blends. In a fig.4.15, 11% Pani shows non ohmic (nonlinear) nature even after the same composition was doped additionally, which requires only low voltage to reach the 2000pA current. It was found that the graph shows ohmic nature as the concentration of Pani increases in the blend and current value was reached in  $\mu\text{A}$ . It requires very less voltage to reach 2000 $\mu\text{A}$ . This was observed at 59% Pani in the insitu blend composition obtained from the reactor. It was noticed that when

the compositions of the insitu blends were additionally doped, the nature of the graph shows ohmic (linear) and voltage was still reduced again to reach the 2000 $\mu$ A. Given fig. shows the IV-curves of the blend. The same charge transport process was observed in the 'ex-situ' blend as shown in the fig. 4.16. It was noticed that 10 % Pani in the ex-situ blend shows nonohmic nature and as the concentration of Pani increases in the blend, i.e. at 60% Pani shows ohmic nature and it requires low voltage to reach 2000  $\mu$ A.

In the ex-situ blend, the charge transport process was affected by the barrier of Pam particles and even at higher concentration of Pani, there was no close contact found, barrier still affects the charge transport process and the voltage value was found to be more in ex-situ blend comparing to insitu blend. It was observed that even at low concentration level of Pani in the insitu blend shows more ohmic nature compared to ex-situ blend. This was because the barrier of Pam gets reduced as the 'Pani' concentration increases in the blend and conducting network is formed, the conducting elements of these paths are either making physical contact between themselves or separated by very small distances across which electron can tunnel. The charge carriers are created and their mobility also increased at this point. The charge carriers overcome the barrier easily. Intramolecular as well as intermolecular charge transport takes place in the blend because of miscibility formed by the hydrogen bonding between the two polymers (Pani and Pam as observed in Pani-PVAc blend). The junction of Pam does not affect the charge transport because it acts as a good compatibiliser

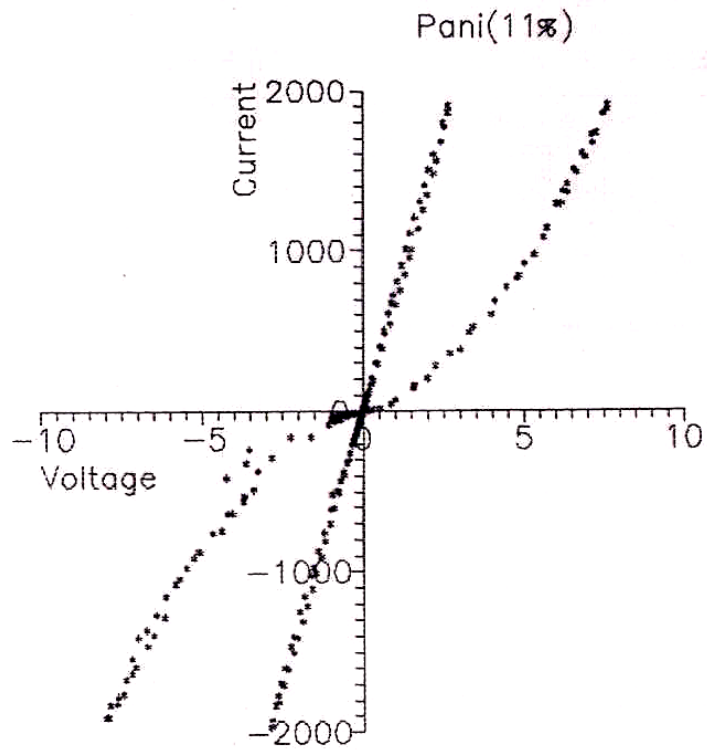
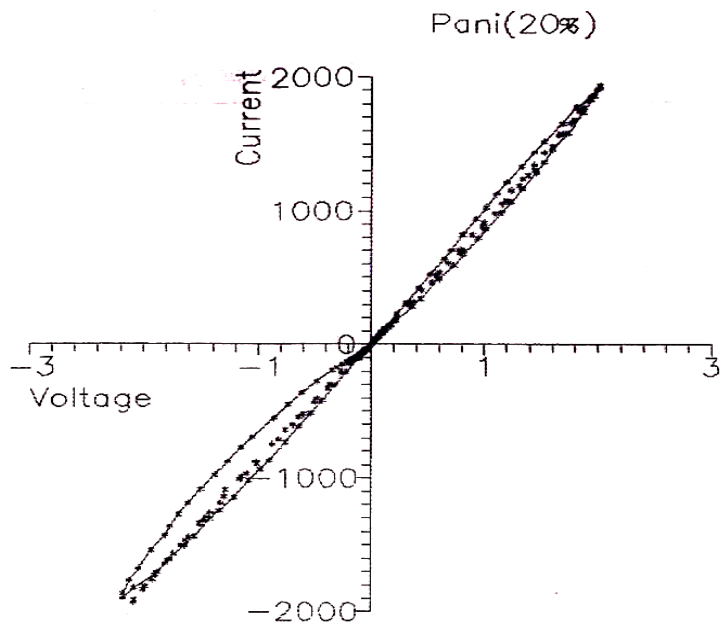
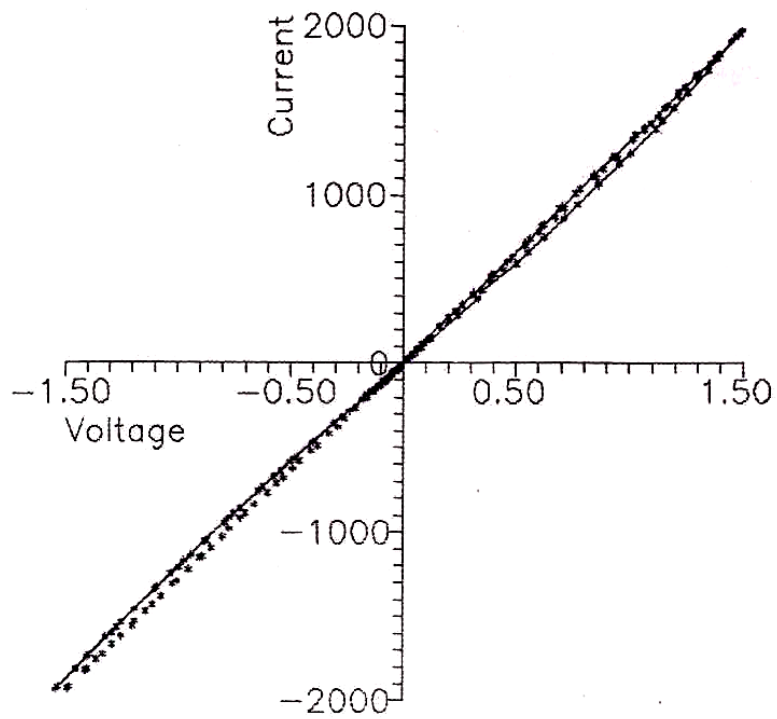


**Fig.4.15: insitu blend compositions**



Pani(48%)



Pani(59%)

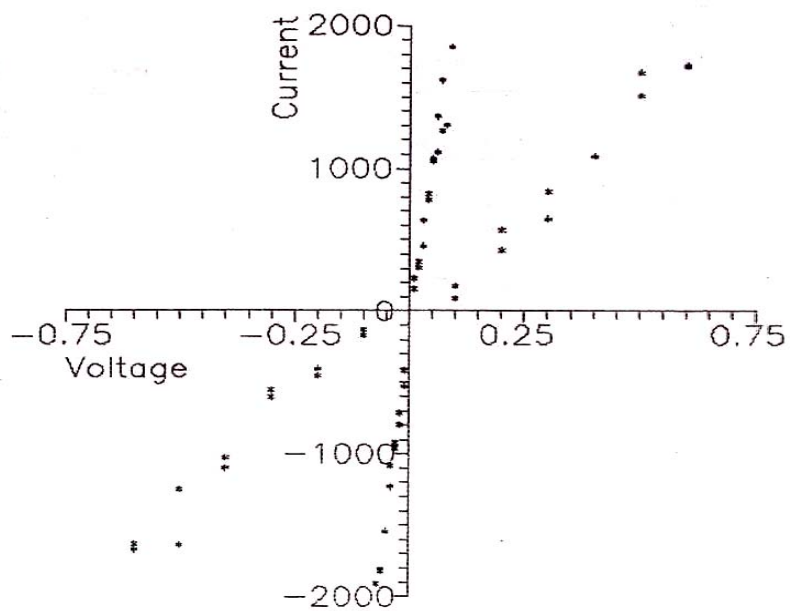
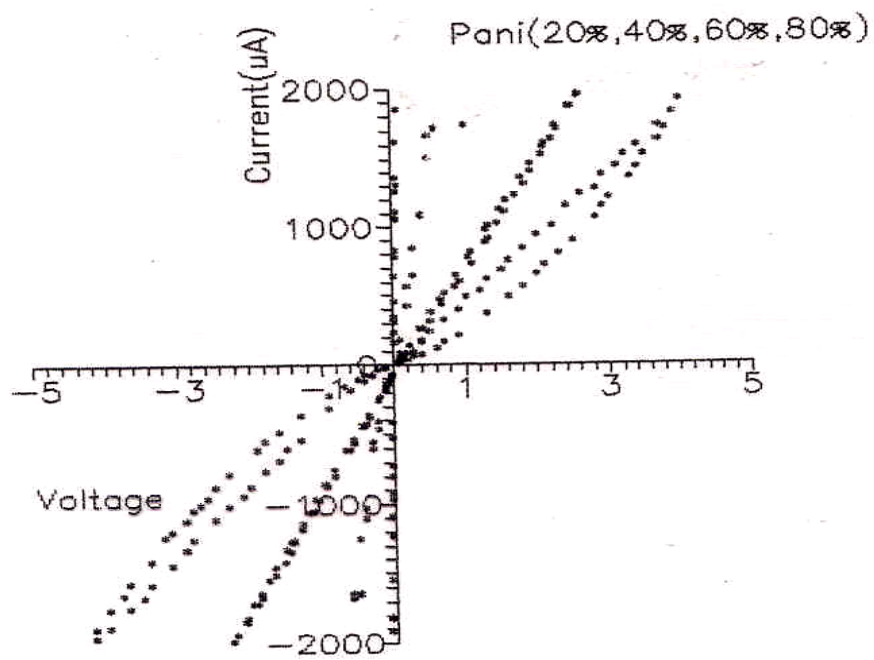
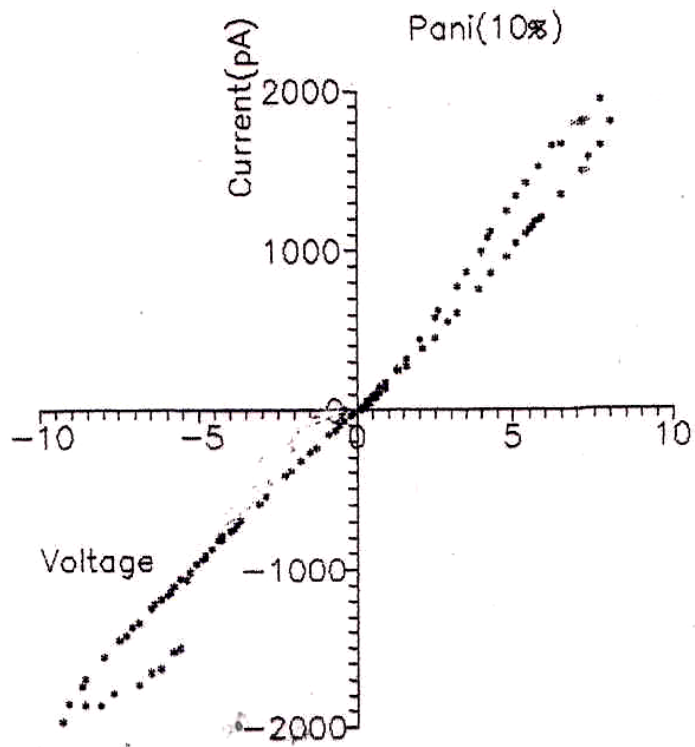




**Fig.4.16: Ex-situ blends**



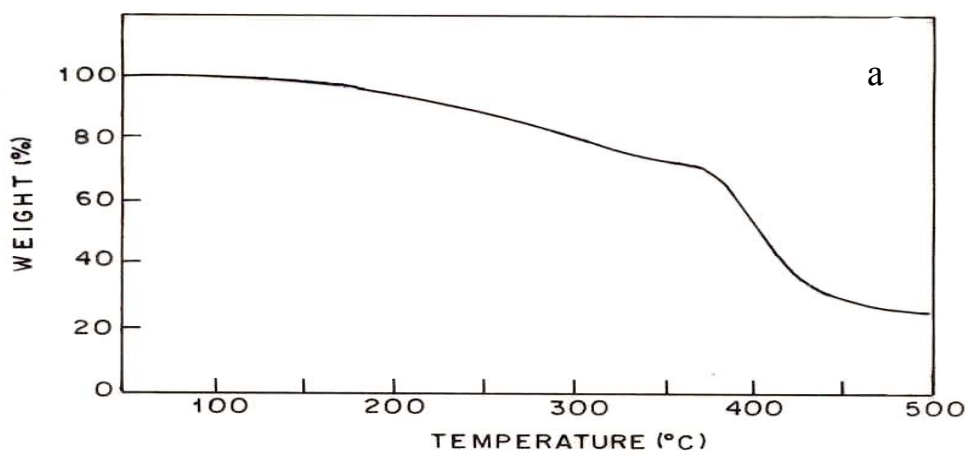
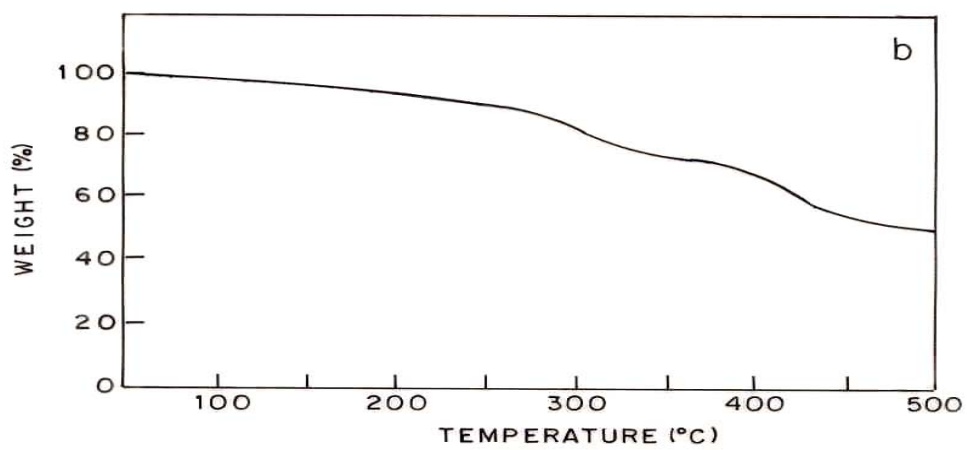
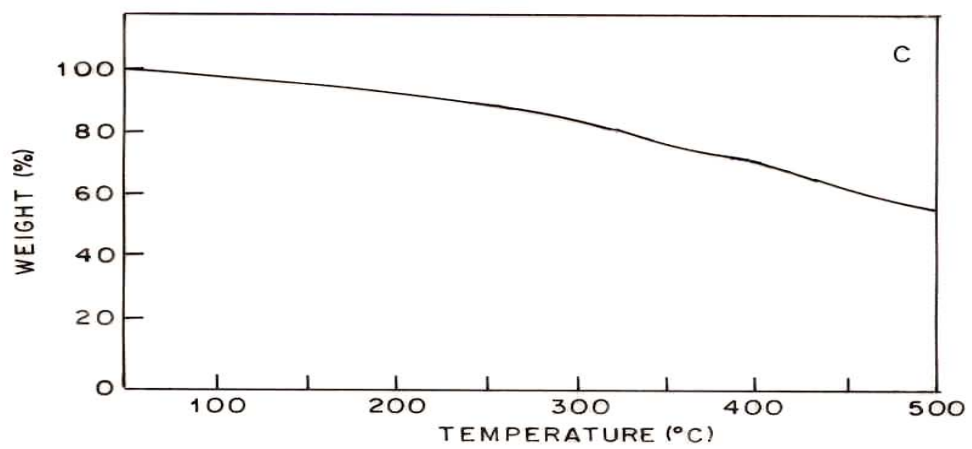
#### 4.7 TGA/DTA:

The interaction between the polymers can also be noted from the degradation curves through T.G.A. studies. Given fig.4.17 shows the wt.loss and thermal stability in the blend. Thermogram was scanned under the nitrogen atmosphere at the rate of  $10^{\circ}$  / min. (heating) and the temp.range were  $25^{\circ}$  c to  $500^{\circ}$  c. Thermal data is given in the table 4.18

In a given thermogram 'a' corresponds to pristine Pam and 'b', 'c', 'd' and 'e' is the increasing concentrations of Pani in the blend composition and 'f' is the pristine 'Pani'. TGA shows the three step wt.loss in both the pristine polymers.

First wt.loss in Pani was owing to the loss of absorbed moisture and solvent from room temperature to around  $175^{\circ}$ c, wasn't so sharp compare to pristine Pam. In Pam, it is found at room temperature to  $150^{\circ}$ c. Again a sharp mass loss beginning at nearly  $175^{\circ}$ c- $375^{\circ}$ c and continuing till about  $500^{\circ}$ c, presumably corresponds to large scale thermal degradation of Pani chains, nearly 74% residue is left for Pani at  $500^{\circ}$ c. For Pam, moisture release takes place at a slow rate over the temperature zone of  $150^{\circ}$ c- $300^{\circ}$ c, accounting for a successive release of a moisture and bound (H-bonded) water. A relatively high mass loss zone then follows  $310^{\circ}$ c- $500^{\circ}$ c, which corresponding to cyclization of Pam chains and associated to liberation of  $\text{NH}_3$ . A much sharper mass loss zone appears over the temperature zone of  $375^{\circ}$ c- $425^{\circ}$ c in the blend compositions accounting for large-scale thermal degradation (4 step wt.loss) with the liberation of  $\text{H}_2$ ,  $\text{CO}$  and  $\text{NH}_3$  leaving a residue of 28%.

It was noticed that as the concentration of Pani in the blend increases<sup>128</sup> the wt.loss decreases from  $98^{\circ}$ c to  $55^{\circ}$ c. From the thermogram, it was observed that the blend shows the improvement in thermal stability<sup>127</sup>. As the Pam concentration increases in the blend and blend concentration follows the same nature (trend) of degradation pattern as observed in Pani. The wt.loss found in the blend concentration is not observed in pristine polymers, suggesting the presence of interaction between the polymers alters the degradation pattern<sup>122</sup>.



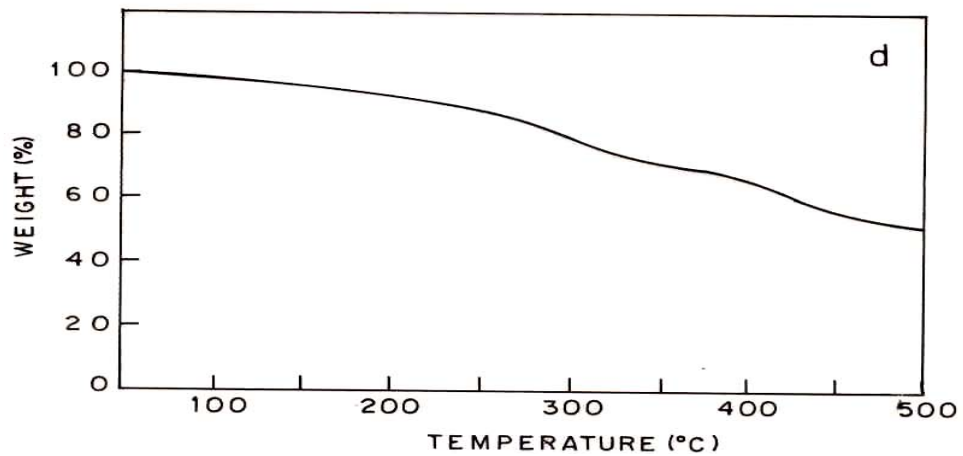
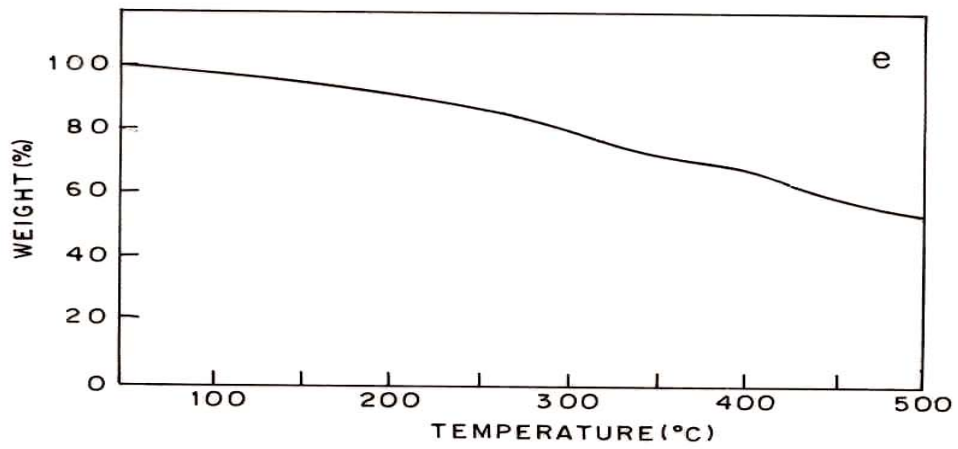
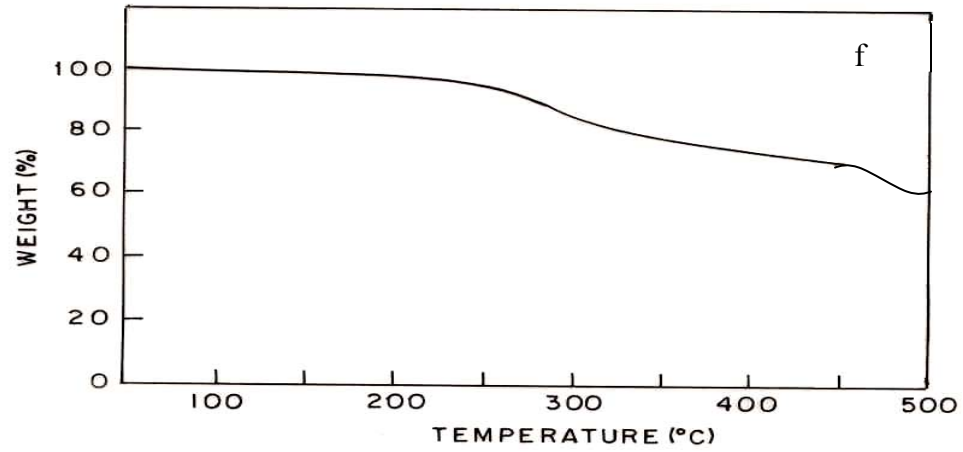


**Fig. 4.17 : TGA/DTA thermograms of Pani-Pam, insitu blends**

**Table4.18: Thermal Data Polyaniline (insitu) Blends**

<b>Temperature (°C)</b>	<b>Poly acryl amide wt.loss %</b>	<b>Pani (11%) wt.loss %</b>	<b>Pani (20%) wt.loss %</b>	<b>Pani (48%) wt.loss %</b>	<b>Pani (59%) wt.loss %</b>	<b>Pani (100%) wt.loss %</b>
100	0	2	2	1	5	2
200	5	6	4	6	8	4
300	18	16	11	15	18	10
400	44	31	23	30	30	12
500	72	49	49	45	45	26

#### **4.8 Moisture sensitivity:**

##### **Experimental:**

The sensor substrate with a dimension of (2x2) inches is made up of Epoxy polymer as a base. An interdigitated array of copper electrodes was deposited on one side of the Epoxy polymer chip. The two ends of this chip were soldered to thin copper wire, which is rubbed already to remove dust adsorbed on the Cu wire surfaces. The sensor chip electrode was cleaned with acetone.

**Polymer Film:** Pam-Pani blend (insitu) was dissolved in distilled water. The solution was stirred finely. A thin film of blend from solution was casted on the substrate. The fine thin film is observed when it is dried. The sensor assembly cell was then connected to Keithley Electrometer through the two terminals of the cell. The film exposed to moisture vapors. (By keeping the blend film coated electrode to the known

height from the water-containing cell). Sensitivity of this film was noted. A glass sheet packed the moisture cell by pasting grease to both the surfaces (Sensor cell and glass sheet) to prevent from external leaks.

### **Results and Discussions:**

Moisture sensitivity of the blend films was noted by varying pani concentrations in the films. In Pani-Pam blends, at lower concentration of pani (11%); charge transport takes place ionically. Intergranular distance between Pam molecules is found to be more and it is difficult to transport the charge, which affects the 'R' value as observed initially. As the pani concentration increases in the blend, two phenomena will be observed, the barrier in Pam molecules get reduced i.e. intergranular distance is reduced and charge transport takes place by ions very easily. Moisture absorption also depends upon the pores of the conventional polymers.

At 20% Pani in the blend, it is observed that the 'R' value shoots up to 25.42. At this point, the barrier is still reduced and intergranular distance decreases further and charge transport takes place very easily. It is noticed that at higher concentrations of pani there was no gap in between Pani molecules i.e. intergranular distance between two Pani molecules is very less and Pani is hydrophobic, which affect the charge carrier mobility and acts as a barrier in between least number of Pam molecules and here the 'R' value is found to be very low i.e. 1.6.

Response time, for Pani-Pam blend film, was found to be, 25.42. at 20% Pani in the blend film. It is observed that the 25% Pani dispersion is suitable to transport the charge in between the conventional polymer molecules

Sensitivity factor is calculated by the following formula

$$S = R_0 / R$$

Where,

S = Sensitivity

$R_0$  = Resistance before moisture absorption

R = Resistance after moisture absorption.

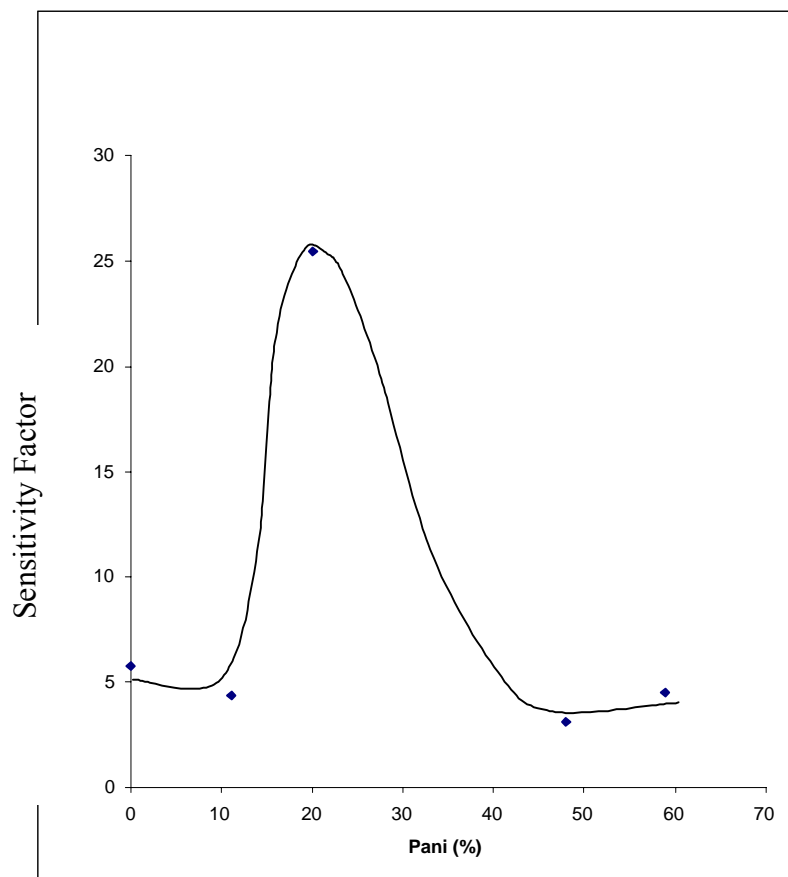


**Fig.4.18: Plots of sensitivity factor versus Pani concentration For water vapors with Pani-Pam interdigitated electrode.**

**Table: 4.20,Moisture Sensitivity of Pani-Pam Blends**

Sr.No.	Pani (%)	Sensitivity
		(Water) Moisture Vapors
1	0	5.77
2	11	4.36
3	20	25.42
4	48	3.1
5	59	4.5

Data of moisture sensitivity is given in the table4.20 and fig.4.19, shows the graph of moisture sensitivity effect, when plotted Pani content (%) vs. Sensitivity.

#### **4.9 Conclusions:**

The blend was studied with the help of characterization techniques; electrical conductivity measurements and comparative study of insitu blend and exsitu blends, following conclusions can be drawn, with the help of results obtained. Polymerization of aniline is carried out in Pam solution willn't be affected by Pam solution as observed in the (Pani-PVAc) systems, on the contrary it acts as a compatibiliser. This insitu blend system required approximately same induction period compare to Pani-PVAc blend.

FTIR studies of the insitu blend of Pani-Pam shows the peak at  $1664\text{ cm}^{-1}$ , shifts slightly to lower frequency as the Pani concentration increases in the blend, for the amide stretching and indicates the hydrogen bonding interaction between amine group of Pani and carbonyl group of Pam, which improves miscibility i.e. intermolecular interaction between the polymers .The peaks observed at  $1600\text{cm}^{-1}$  and  $1500\text{cm}^{-1}$ were the characteristics of the benzoid to quinoid transition and indication of blend compositions



doped as such during synthesis. Peaks observed at  $1116\text{ cm}^{-1}$ ,  $825\text{ cm}^{-1}$  and  $616\text{ cm}^{-1}$  confirms the formation of conductive Pani blend.

UV-VIS spectra shows the peak position at 360nm, 580nm and 820nm, it is the indication of conducting emeraldine salt formation and polaron-bipolaron transition, shows given blend is electrically conductive.

TGA/DTA data shows that, interaction between the polymers altered the rate of degradation and wt.loss decreases as the Pam concentration increases in the blend i.e. thermal stability increases and the decrease in wt.loss was observed from 72% to 45% , as observed in the Pani-PVAc blend.

Conductivity at ambient temperature for the insitu blends, shows that conductivity rises, after additional doping than the blend compositions obtained as such during synthesis. Percolation threshold is found at 11%, and 59% Pani shows conductivity in the range of  $10^{-3}$  to  $10^{-2}$  S/cm. The conductivity at ambient temperature was observed, it gave higher conductivity in the range of 40% to 60% Pani and percolation threshold observed at 10% Pani in the Ex-situ blend.

Temperature dependent conductivity showed that, insitu blend as well as ex-situ blend follows Arrhenius law. It was noticed that the higher concentration of Pani in the blend showed more linearity compare to ex-situ blend. The linear nature was observed because of charge carriers were created and the mobility was increased, the barrier of Pam was found to be decreased and it required very less Activation energy (excitation energy) compare to ex-situ blends i.e. in other words, electrons hop from one conducting particle to another without inhibition of Pam barrier.

Activation energy ( $\Delta E$ ), calculated from Temp.dependent conductivity for both the blends, was found to be decreased, as the Pani concentration was increased in both the blends (insitu blend and e-situ blend). The  $\Delta E$  value of the insitu blend was decreased from 0.31eV to 0.11eV and in the ex-situ blend the value was found to be in the range of 0.46 eV to 0.27 eV.

The percolation threshold temperature, corresponds to volume fraction of Pani of about 0.33 in the insitu blend and that in the ex-situ blend it was 0.36

The charge transport process was found to be ohmic (linear) as the concentration of Pani increases in both the blends i.e. the intermolecular and intermolecular charge transport process was not affected by Pam barrier.

Characterization studies and Electrical measurements show that insitu blending technique was effective than ex-situ blending technique. This can arise from the fact that, as the concentration of Pani increases in the blend, the contact points between the Pani coated Pam particles increase in the number and form close contact i.e. conducting network, is observed thus decreasing the inter chain separation while expanded molecular conformations reduce  $\pi$ -conjugation defects; both are able to increase the delocalization of electrons and finally the conductivity compares to physical mixtures (ex-situ blend). One of the important applications of Pam is that it is used in adhesives and its sticky property is also observed during bulk polymerization of Pam, as the Pani coats Pam molecule. It sticks to Pani very firmly thus effective insitu blend is formed and Pam acts as a good compatibiliser for formation of insitu blend.

But the viscosity of the Pam solution was found to be 0.530 poise, and the chances of trapping monomer inside the viscous solution were found to be more, which may affect the yield as well as on electrical conductivity. It is found that Pani-PVAc > Pani -Pam; this is because conductivity data shows that in Pani-PVAc system, 27% Pani reaches to  $10^{-2}$  S/cm conductivity and percolation threshold is observed at 7 %: and in Pani-Pam blend it is at 11%. The difference in the percolation threshold value is owing to the morphology of the conventional polymer, and the barrier of these polymers affects the formation of Pani network in the blend.

From the moisture sensitivity graph, it is noticed that, Pani-Pam insitu blend film responses to moisture, sensitivity is found to be 25.42. The low value observed because Pani may be dispersed thoroughly inside the film, and the slow response time is owing to the slow breakthrough of the moisture in the blend system.

The insitu blending technique is more effective because as the concentration of Pani in the blend increases the Pani coated Pam particles increase in the no. and form close contact i.e. conducting network, is observed thus decreasing the inter chain separation while expanded molecular conformations reduce  $\pi$ -conjugation defects; both are able to increase the delocalization of electrons and finally the conductivity compares to physical

mixtures (ex-situ blend). But the viscosity of the Pam solution was found to be 0.530 poise, and the chances of trapping monomer inside the viscous solution was found to be more, which may affect on the yield as well as on electrical conductivity. It is found that Pani- PVAc > Pani -Pam; this is because of conductivity data shows that in Pani-PVAc system, 27% Pani reaches to  $10^{-2}$  S/cm conductivity and percolation threshold is observed at 7 %: and in Pani- Pam blend it is at 10%. The difference in the percolation threshold value is owing to the morphology of the conventional polymer, and the barrier of these polymers affect the formation of Pani network in the blend.

From the moisture sensitivity graph, it is noticed that, Pani-Pam insitu blend film responses the moisture the sensitivity is found to be 25.42. The low value observed because Pani may dispersed thoroughly inside the film, and the slow response time is owing to the slow breakthrough of the moisture in the blend system.



## Chapter V: Polyaniline-Nylon-6 Blends

<b>5</b>	<b>INTRODUCTION-----</b>
5.1	Experimental-----
	1) Preparation of insitu blend-----
	2) Preparation of Ex-situ Blend-----
5.2	Results and Discussions-----
5.2	Characterization
5.3	FTIR Spectroscopy-----
5.4	UV-VIS Spectroscopy-----
5.5	X-ray Diffraction Technique-----
5.6	Optical Microscopy-----
5.7	Electrical Conductivity Measurement-----
	1) R.T. Electrical Conductivity Measurement-----
	2) Temperature Dependent Conductivity-----
	3) Activation Energy ( $\Delta E$ )-----
	4) I-V Characteristics-----
5.8	TGA/DTA-----
5.9	Moisture sensitivity-----
6	Conclusions-----

## **5 Introduction**

Amongst the various polymers blended with polyaniline, polyamides appear to be the closest in chemical nature to Pani. Due to the presence of the amide groups one can expect hydrogen bonding between the two polymers which may lead to better miscibility, crystalline order etc. Further nylon has been used extensively in special textiles/fabrics etc. By blending nylon with Pani it may be possible to obtain antistatic fibers and cloth. Hence Pani-nylon-6 blends were studied and this chapter describes the same.

The first chapter has given the literature survey of conducting polymer blends, and the general method for the synthesis of conducting polymers has been described in chapter two.

This chapter describes the blend formation of Pani with nylon-6. Which includes insitu blend formation by polymerisation of aniline in nylon-6 solution; miscibility, morphology, electrical conductivity and charge transport processes in these blends.

### **5.1 Experimental**

#### **1) Preparation of in-situ Blend**

Pani-nylon-6 blend was synthesized by insitu technique and exsitu technique. In the insitu synthesis, 1 gram nylon-6 was taken in 100ml distilled water in a four separate beakers. To that, 0.51 grams of monomer aniline (0.005 M) and 5 ml of 1N HCl solution were added. About 25 ml of 0.1M initiator ammonium per sulfate was added slowly to the above reaction mixture under constant stirring. Similar reactions were carried out with aniline concentration of 0.01M, 0.02 M and 0.05 M and 10 ml of 1N HCl, 20 ml of 1N HCl, 50ml of 1N HCl solution. The aniline to ammonium per sulfate molar ratio in all the above reactions was 1:1, so as to reproduce same conditions in all cases. The reaction was carried out at ambient temperature for 10 hr. The blend was precipitated in distilled water, filtered, washed with distilled water several times to remove impurities and traces of oligomers, and dried in a vacuum till moisture was removed. The green mass of, each composition of the blend was crushed in mortar and pestle to a fine powder. Samples for characterization and measurement of conductivity were made as described in the chapter II.

## **2. Preparation of Ex-situ Blend**

In the ex-situ technique commercial nylon-6 was purified and converted to powder form by dissolving in formic acid followed by precipitation in distilled water filtering and then drying thoroughly till moisture was removed. Aniline was polymerized separately in a clean and dry conical flask containing 150 ml distilled water, 9 ml aniline; 10ml HCl .The initiator ammonium per sulfate was taken 11 gm in separate beaker containing 100 ml distilled water and this solution was then added drop wise with stirring. Pani was formed after 8 hrs. and this was precipitated in the distilled water, filtered, washed, dried and crushed to fine powder.

The desired quantity of Pani powder was dry mixed with nylon-6 powder to form the ex-situ blend. The blend composition was varied from 0 to 100 % of Pani.The samples were formed by high-pressure compression moulding. These were made in the same manner as described in chapter II

## **5.2 RESULTS AND DISCUSSION:**

### **(a) Chemically synthesized Pani in nylon-6 solution**

Polymerization of aniline in the nylon-6 solutions, it was observed that as soon as ammonium per sulfate was added to the reaction mixture, the color change was almost instantaneous. Observation denotes that there is a decrease in the induction period owing to the addition of more quantity of aniline in it, resulting in faster reaction rate. After addition of initiator (APS) solution. The reaction became exothermic. The increase of temperature again accelerates the rate of reaction. The appearance of the reaction mixture was green to dark green in color. It was observed that as the aniline to initiator ratio increases in the reaction, the shade of color becomes darker. The yields obtained were in the range of 60-80% based on the aniline to initiator ratio. The various data of chemical synthesis obtained from different experiments are tabulated in table-5 the reaction scheme by which chemical synthesis proceeds for Pani-nylon-6 blend is presented in the Fig.5.1.

**TABLE 5**

**Chemical Synthesis data of Pani-nylon-6 insitu blends**

<b>Serial No.</b>	<b>Aniline Grams</b>	<b>Ammonium Per sulfate Grams</b>	<b>Hydrochloric Acid ml</b>	<b>NYLON 6 Grams</b>	<b>%Yield</b>
1	0.204	0.5	0.2	1	50.25
2	0.51	1.2	0.5	1	46.04
3	1.02	2.3	1	1	66.26
4	2.04	4.6	2.5	1	82.73
5	5.1	11.4	6	1	90

**Solvent: Distilled water 50 ml for each experiment**

**Reaction temperature: Room temperature (25°C)**

**Reaction time: 10 hours**

**(b) Effect of solvent:**

To improve (promote) specific interactions that lead to improvement in conductivity of the blend. Such as H-bonding, as shown in the fig.5.3, since the solubility parameter value of the aniline is  $10.3 \text{ (cal/cm}^3)^{1/2}$  and nylon-6 is  $13.5 \text{ (cal/cm}^3)^{1/2}$ .

As the polymerization of polyaniline and protonation of polyaniline at and with in the solution of nylon-6 proceeded, it was turned gradually dark green. Polyaniline has good adhering properties. The main goal of this research was to verify the conductivity with respect to doping the blends and find a way to improve its conductivity.



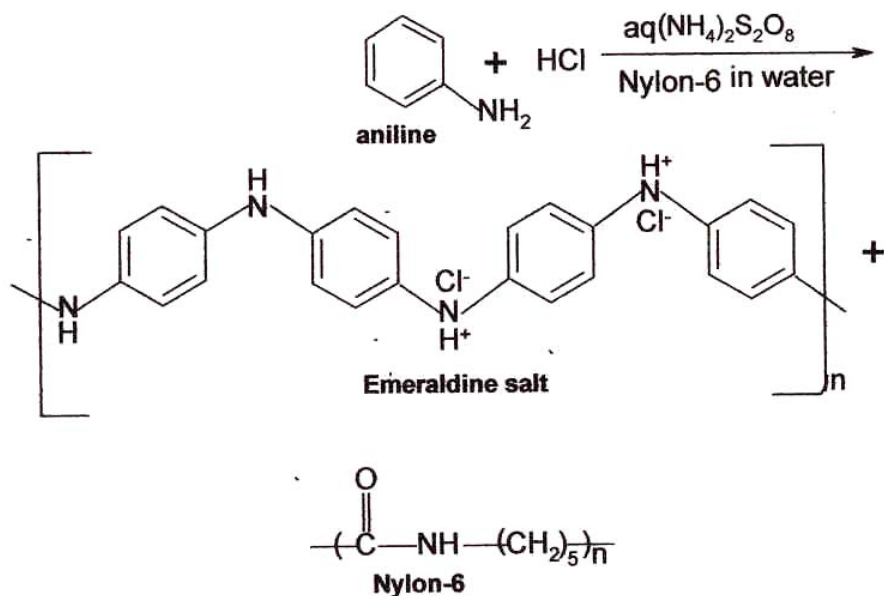


**Fig. 5.1: Insitu polymerization of Pani-Nylon-6 blend**

Though blends prepared by insitu method, phase separation takes place (since there was no entropy of mixing for macromolecules) polyaniline can be processed from formic acid, this was known since 1988. Formic acid is good solvent for nylon-6. The blends of polyaniline with nylon-6 can be prepared by solution processing.<sup>129</sup>

The blend was doped by HCl, various authors<sup>(129-130,136-137)</sup> studied the same blend using different protonic acids, mostly, it was found that the films were casted by solution processing technique or evaporated the films with dopants or monomer aniline in HCl. Our idea was to find miscibility, conductivity, a more efficient doping with HCl, if added to the polyaniline-distilled water solution.

## 5.2 Characterization:

### 5.3 FT-IR Spectroscopy of the insitu Blends

The polymerization of aniline in the solution of nylon 6 was confirmed by the IR studies. Fig. 5.2 shows the IR absorption spectrum for Pani-nylon-6 insitu blend compositions.

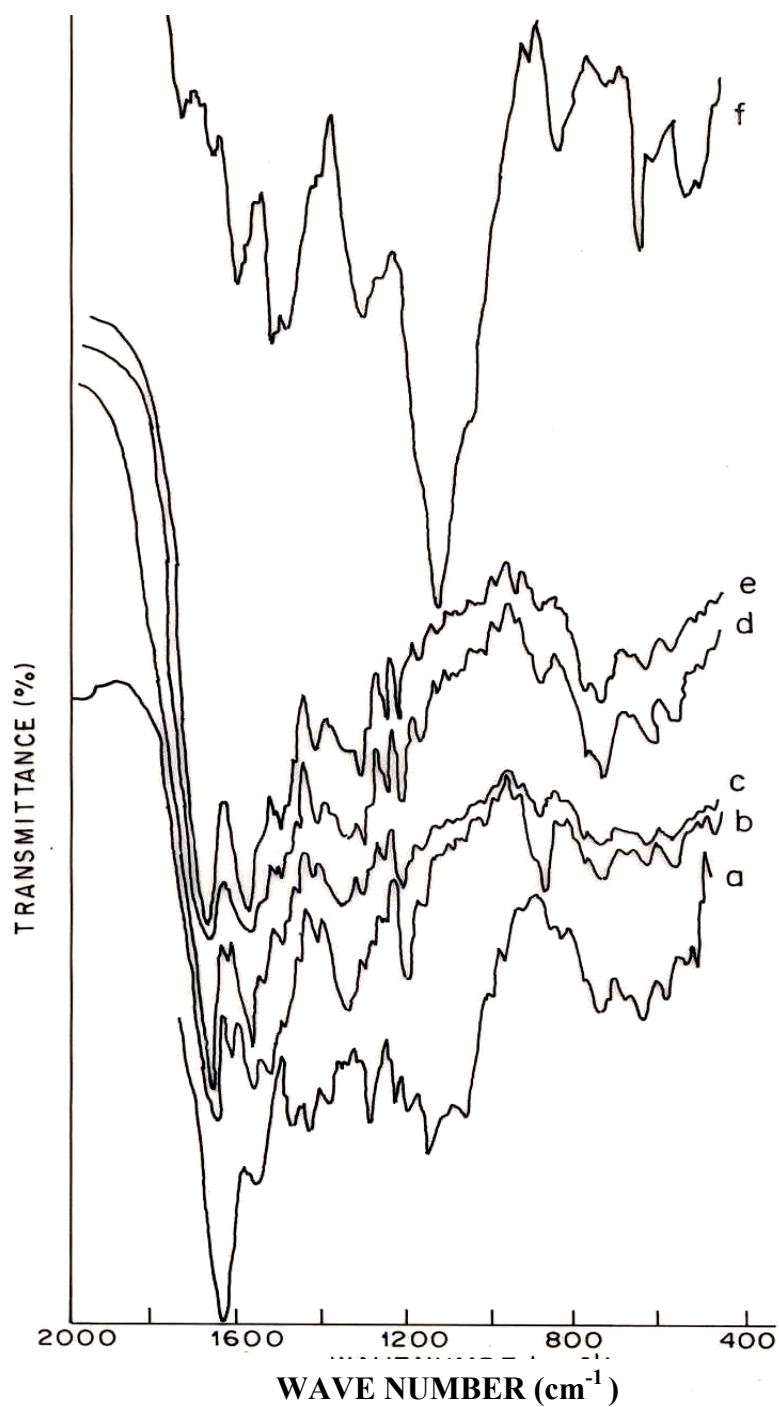


**Fig. 5.2: FTIR absorption spectrum of Pani-Nylon-6 insitu blend compositions. ; a) Nylon-6, b) 9 % Pani, c) 18% Pani, d) 39% Pani, e) 63% Pani, f) Pani.**

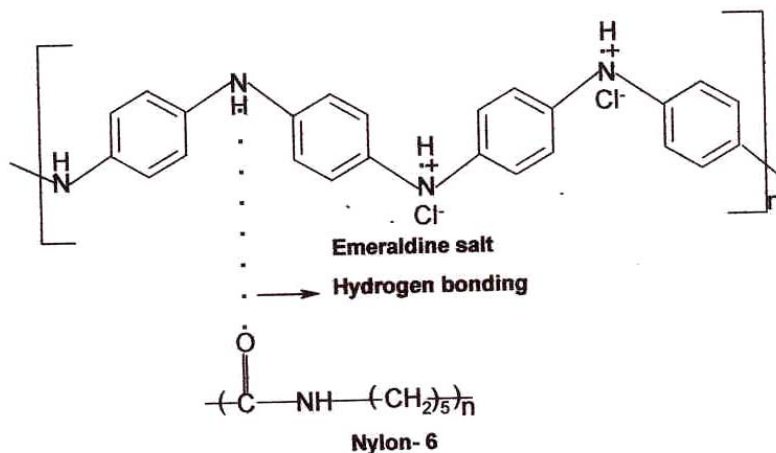


**Fig.5.3: Proposed scheme of hydrogen bonding between Pani and Nylon-6**

In the spectra 'a' corresponds to nylon-6 and 'b', 'c', 'd', 'e' is the increasing concentration of Pani in the blend and 'f' is pristine Pani.

Spectra of blends are compared with the spectra of nylon-6 and polyaniline by themselves. It was noted that there are few new peaks as well as shifts in certain absorption peaks belonging to the vibrational modes of original polymer<sup>140-141</sup>. The frequency data obtained and their possible assignments are presented in table.5.4

The vibrational band characteristics of polyaniline at  $1590 \text{ cm}^{-1}$ , (C-N stretching). The blend was doped as such during synthesis. This was further confirmed by the peaks arised at  $1590 \text{ cm}^{-1}$  and  $1600 \text{ cm}^{-1}$ . These changes resulting from protonation were the signatures of the conversion of the quinoid rings to benzenoid rings by the proton induced spin unpairing mechanism and the characteristic of the stretching vibration of Nitrogen atoms in aromatic and diamine units respectively and have been associated with C=C

**Table: 5.4, F.T.I.R. data of insitu blend**

<b>Nylon-6</b>	<b>Pani (9%)</b>	<b>Pani (18%)</b>	<b>Pani (39%)</b>	<b>Pani (63%)</b>	<b>Pani (100%)</b>	<b>Assignment</b>
1637 s	1637 s	1637 s	1637 s	1637 s	—	-CO group
					1650 vw	C=C, C=N
—	1590 w	1590 w	—	—	1589 w	Str. of N=Q=N
—	1540 w	1540 m	1540 m	1540 m	1500 w	Str. of N-B-N
1475	—	—	—	—	—	Alicyclic CH <sub>2</sub> (scissor)
					1469 s	Str. of benzene ring
—	1371 w	1371 w	1371 w	1371 w	—	C-N Str. in Q B <sub>t</sub> Q
—	1305 m	1305 w	1305 m	1305 w	—	C-N Str. In QB <sub>c</sub> Q, QBB, BBQ
1263 s	—	—	—	—	—	C-C
—	—	—	—	—	1286 w	C-N
—	1258 vw	1258 w	1258 w	1258 w	—	C-N Str. in BBB
1175	1164 m	1164 m	1164 m	—	—	Alkane groups
—	1111w	1111 w	1111w	1111w	1129 vs	A mode of Q=N <sup>+</sup> H-B or B-NH-B
—	829 m	829 vw	829 vw	829 m	806 w	C-H out-of-plane bending of 1,4,ring and C- C Stretching
—	691 w	691 w	691 w	691 w	617 w	Softening of the ring deformation

**Abbreviations: str, stretching; B, benzenoid unit; q, quinonoid unit; t, trans; c, cis.**

stretching in quinoas ring and C=C stretching in benzene ring respectively<sup>138-139</sup>1458cm<sup>-1</sup>, 1305cm<sup>-1</sup> is shifted after blending as shown in the spectra. 1637 cm<sup>-1</sup>, 1475 cm<sup>-1</sup> corresponds to nylon-6.

The absorption band at 1305 cm<sup>-1</sup> in fig.5.3 is a halogen sensitive band, which confirms the salt formation between the chlorine anions and protonated nitrogen atoms next to the quinoid rings. This absorption band is consistent with the higher conductivity of the protonated composite pellets than that of the unprotonated sample. The data represented for these polymers is well matched with the reported data on these blends<sup>130</sup> Thus the IR studies on insitu blend clearly give an evidence of blend formation where Pani is in the doped state as such during polymerization and nylon-6 solution doesn't inhibit formation of emeraldine salt.

#### 5.4. UV-VIS SPECTROSCOPY

The UV-VIS spectrum depends strongly on its oxidation states. Fig.5.5 shows the optical absorption spectra of 0.1gm pani, and pani doped HCl samples in 10ml HCOOH solution. In the wavelength range 300-900 nm. Curve 'a' corresponds to pure pani and b, c, d, e are the given compositions of pani blends. The three well-defined peaks at 344, 580-600 and 860 nm are characteristics of protonated pani with localized charge carriers (polarons)<sup>142</sup>, the peak is slightly shifted owing to blending.

580 nm represent the  $\pi-\pi^*$  and the excitation band of the quinoid ring respectively<sup>143</sup>. From the fig, it is observed that peak shifted near 700nm at 63% Pani in the blend. Where as pristine Pani does not show any change at that position. This is because blend composition is miscible in formic acid i.e. the indication of solubility of Pani and nylon-6 in formic acid and thus shows that the miscible blend is formed. The peak at 840 nm is owing to the polaron band transition. The data is closely matches to reported polyaniline-blend data<sup>129, 135</sup>

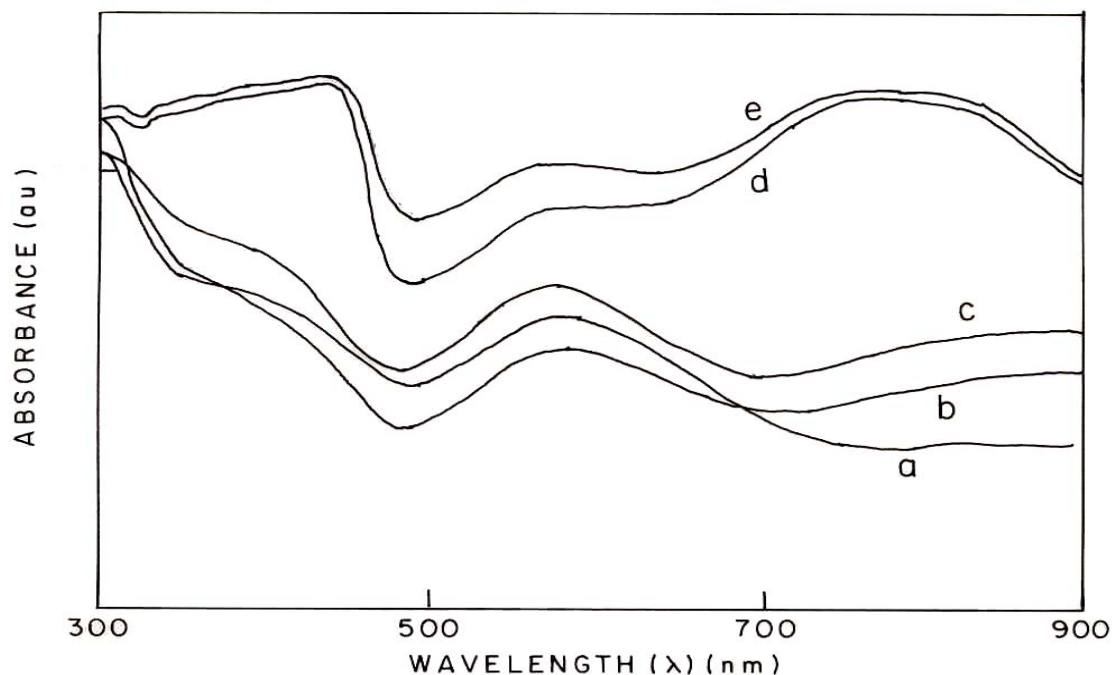


**Fig. 5.5: UV-VIS absorption spectrum of Pani – Nylon-6 insitu blend compositions in Formic acid.**

**a) 9% Pani, b) 18 % Pani, c) 39% Pani, d) 63% Pani, e) Pani**

### 5.5 X-Ray Diffraction Technique

X-ray diffraction patterns of polyaniline-nylon-6 insitu blend compositions are presented in the figure 5.6 in the fig. 'a' corresponds to pristine nylon-6 and 'b', 'c', 'd', 'e' and 'f' correspond to Pani concentrations of 9, 18, 39, 63, and 100 % in the blend respectively. Fig. 5.7 corresponds to ex-situ blends in which the scans designated by 'a' to 'f' correspond to concentration of 0, 10, 40, 60, 80, and 100 % Pani respectively. The effect on crystallinity with rising Pani concentration (in both the blends) is given in the tables 5.9 and 6.1

In the fig., 5.6 the two prominent peaks at diffraction angle of  $20^\circ$  and  $25^\circ$  are observed in the nylon-6 and the same peaks are observed in the blend compositions.

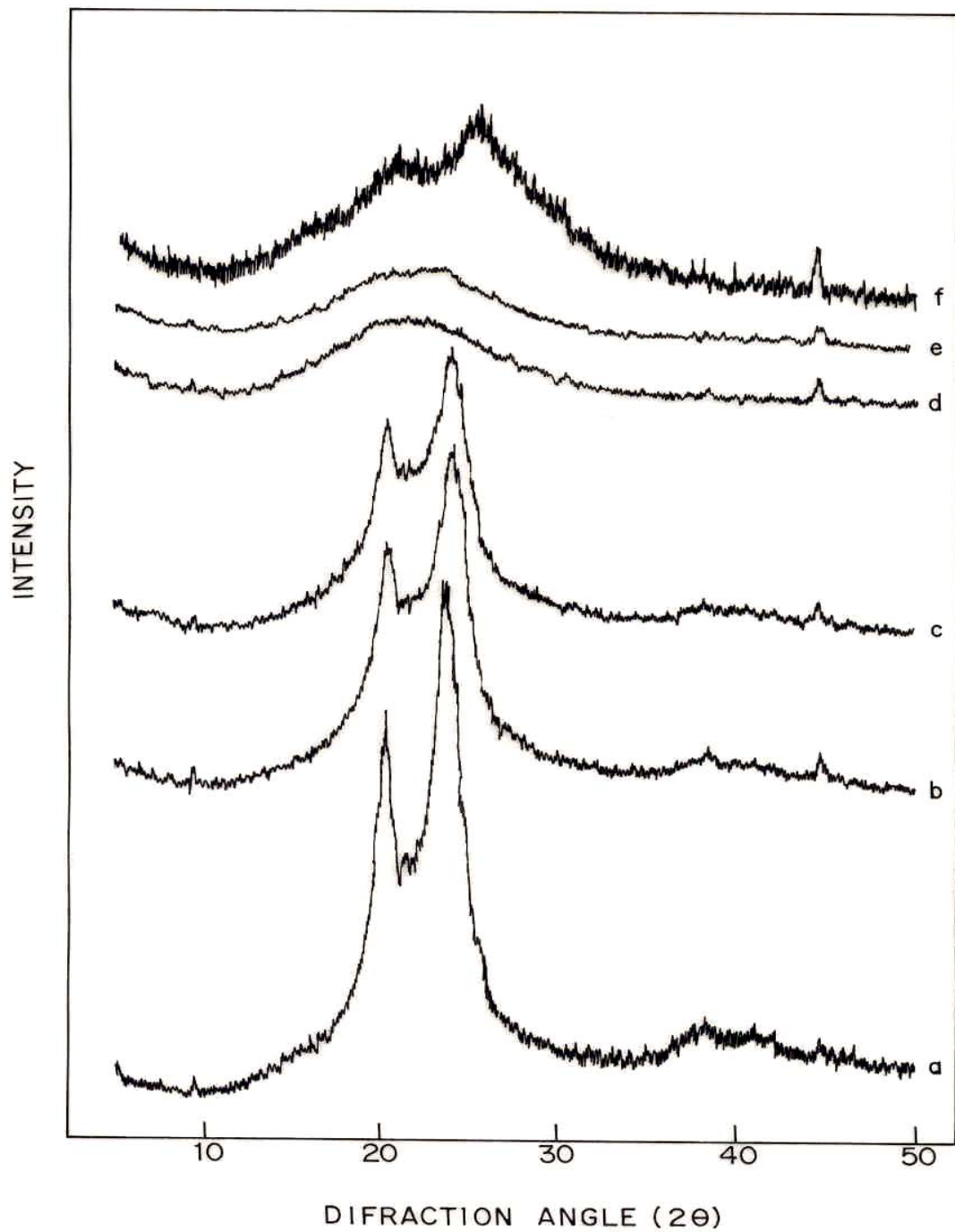


**Fig.5.6: X-ray diffraction patterns of Pani-Nylon-6 insitu blend Compositions. a) Nylon-6, b) 9% Pani, c) 18% Pani, d) 39% Pani, e) 63% Pani , f) Pani**

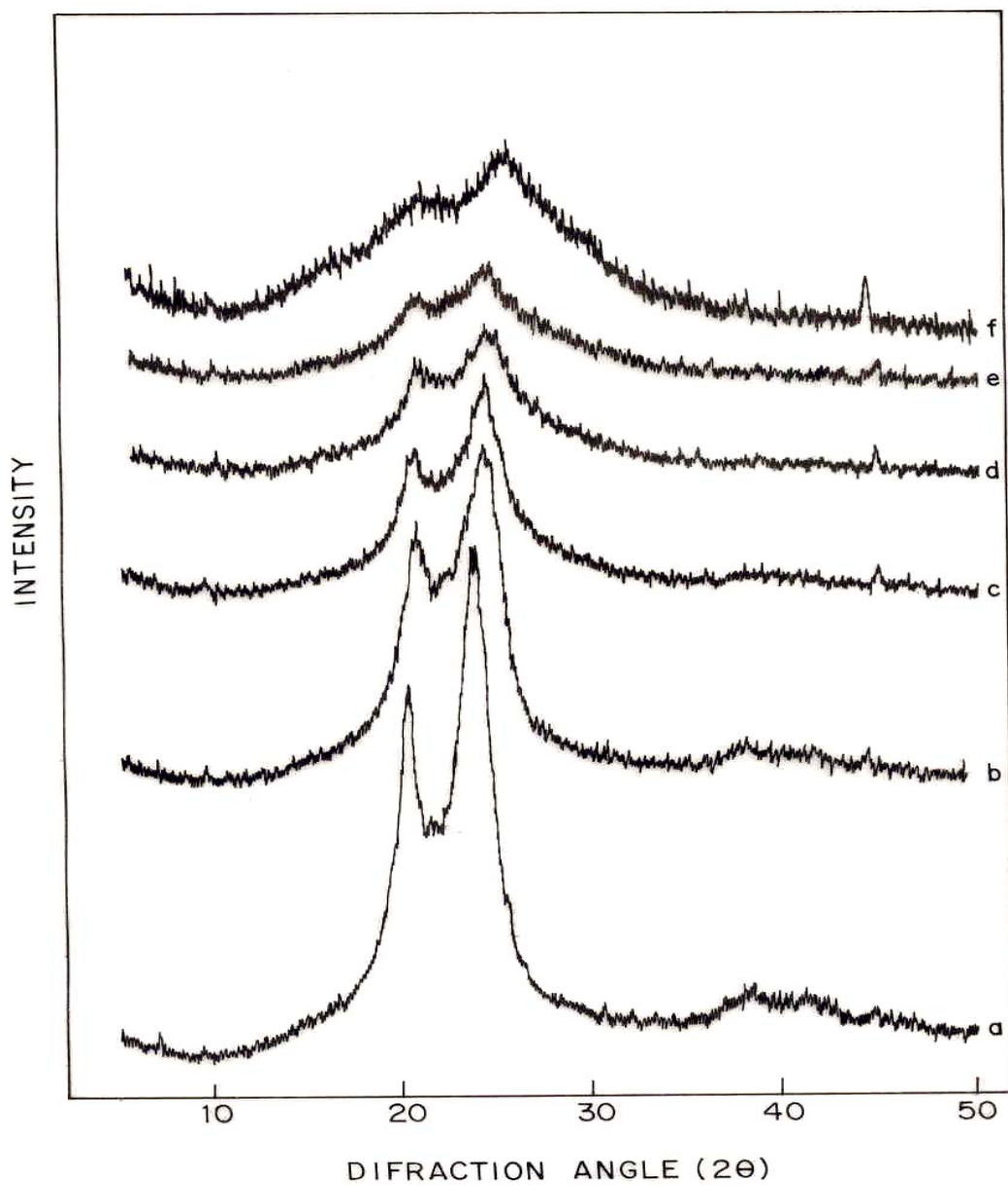
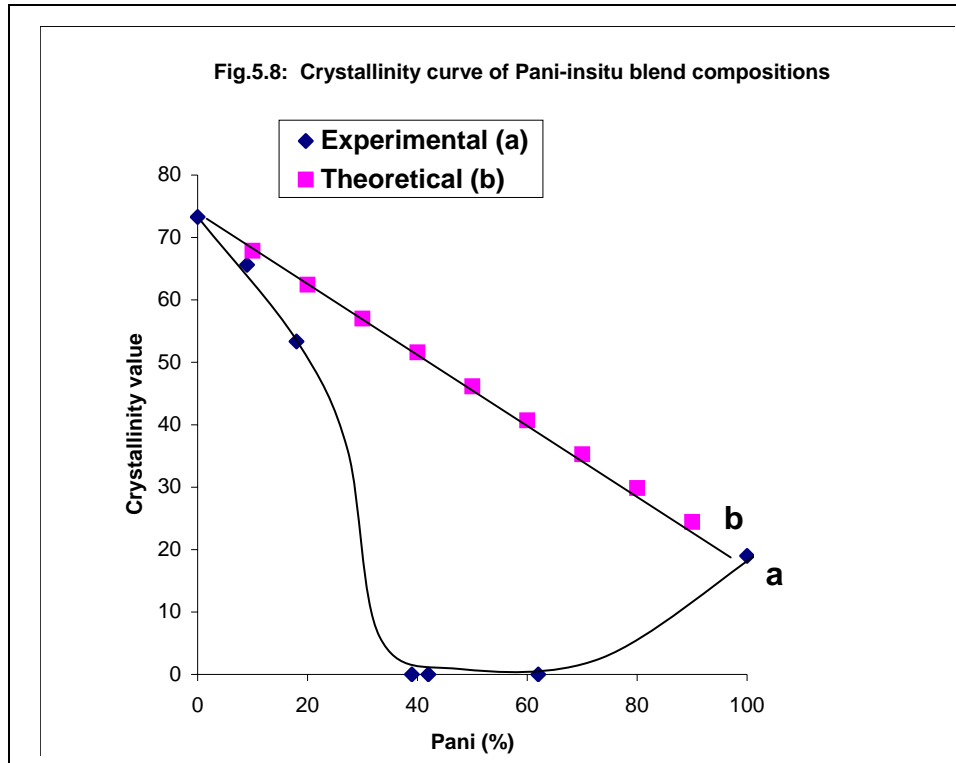


**Fig.5.7: X-ray diffraction patterns of Pani-Nylon-6 exsitu**  
**Blends: a) Nylon-6, b) 10% Pani, c) 20% Pani, d) 60%Pani, e) 80 % Pani,**  
**f) Pani**





**Pani (%)**

**Table: 5.9: Crystallinity data of insitu blends**

<b>Sr.no</b>	<b>Polyaniline (%)</b>	<b>Experimental (%)</b>	<b>Theoretical (%)</b>
<b>1</b>	0	73.27	—
<b>2</b>	9	65.62	—
<b>3</b>	10	—	67.87
<b>4</b>	18	53.33	—
<b>5</b>	20	—	62.44
<b>6</b>	30	—	57.01
<b>7</b>	39	0	—
<b>8</b>	40	—	51.58
<b>9</b>	50	—	46.15
<b>10</b>	60	—	40.72
<b>11</b>	62	0	—
<b>12</b>	70	—	35.29
<b>13</b>	80	—	29.86
<b>14</b>	90	—	24.43
<b>15</b>	100	19	—

However, the intensities of these peaks depend on Pani concentration in the blend as well as how the blend is formed. Pristine Pani XRD scans show very little crystallinity. From these XRD scans it may be concluded that the nylon-6 has the ‘ $\gamma$ ’ phase formed in it. At higher compositions of Pani the nylon-6 peaks practically disappear i.e. its crystalline nature is very much reduced.

The pristine polyaniline gives crystallinity 19%, where as nylon-6 gives crystallinity 73.27%; it is observed that as the concentration of the polyaniline increases in the insitu blend i.e. from 9% to 63% crystallinity decreases from 65.62% to 53.33% as shown above in the fig.5.8 and table 5.9. Interpenetrating network formation takes place (IPN) there is very little phase separation at low % polyaniline.

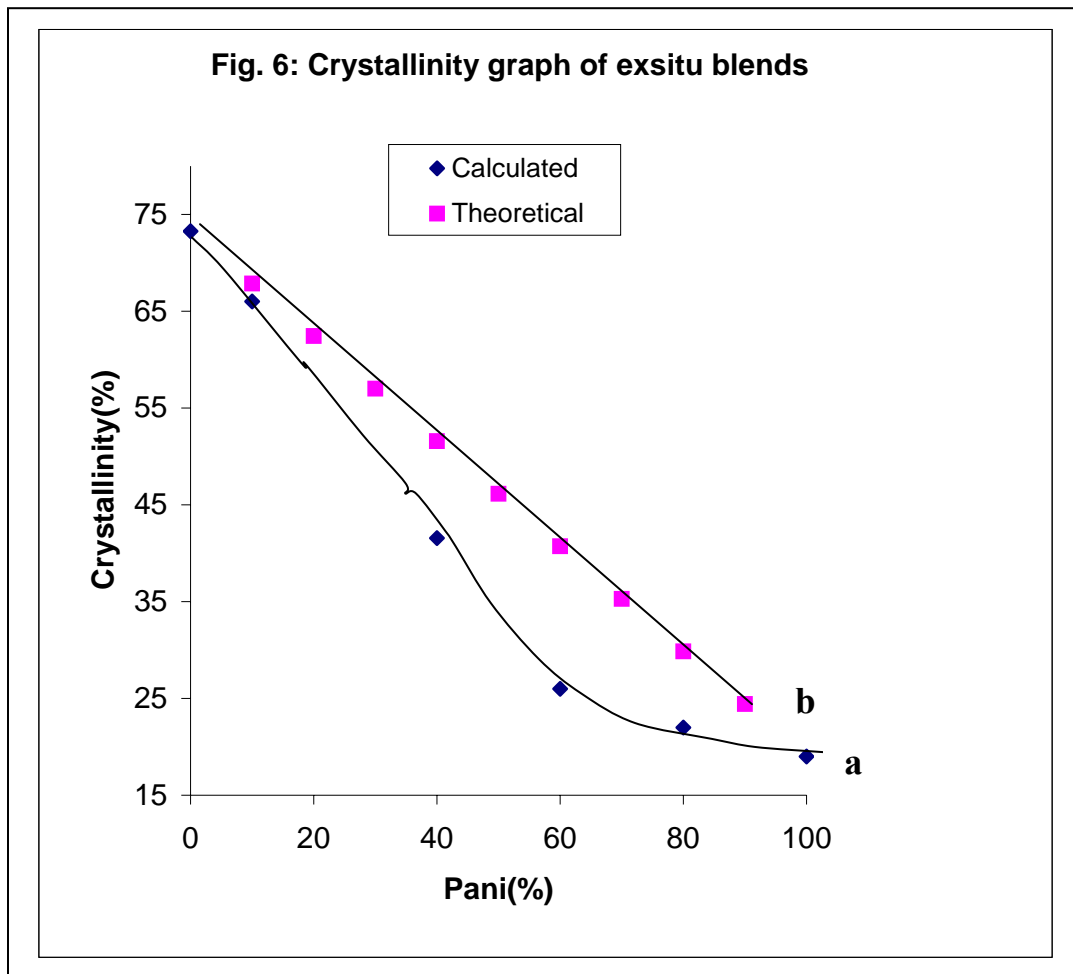


**Table: 6.1: X-Ray data of ex situ blends**

<b>Sr.No.</b>	<b>Pani (%)</b>	<b>Crystallinity (%)</b>	<b>Theoretical values</b>
<b>1</b>	0	73.27	73.27
<b>2</b>	10	66.01	67.87
<b>3</b>	20	—	62.44
<b>4</b>	30	—	57.01
<b>5</b>	40	—	51.58
<b>6</b>	50	—	46.15
<b>7</b>	60	26	40.72
<b>8</b>	70	—	35.29
<b>9</b>	80	—	29.86
<b>10</b>	90	—	24.43
<b>11</b>	98	22	—
<b>12</b>	100	19	—

On the contrary even at 98% of polyaniline in the ex-situ blends, nylon-6 domains are observed and crystallinity decreases slightly from the fig.6, and table6.1. It is observed that at 10% polyaniline gives 66.01% crystallinity and as the concentration increases i.e. at 98% of polyaniline crystallinity is found to be decreased i.e. 22%. It is the indication of miscibility of the blend. Graph is plotted for both the blends. The nature of the graph shows decrease in crystallinity with rising Pani concentration, graph compares theoretical values with calculated values.

Daniel Abraham et.al. Has got results in nylon-6-polyaniline films<sup>129</sup>. He observed the same reflections at the same angles.

The degree of crystallinity of these polyaniline is relatively low. The crystalline regions of nylon-6 in the blends were found to be affected by the formation of polyaniline. The  $C_i$  value decreased slightly with increase of Polyaniline. Maximum crystallinity has been obtained with the use of small molecular dopants, such as HCl in the doping of polyaniline as these dopants have been shown to improve the packing of the chain due to low interchain distance as compared with nylon-6<sup>145-146</sup> and this close packing of polymer chains decreases the barrier.

Yun Heum Park et al.<sup>137</sup> had studied nylon-6-polyaniline composition in his work insertion of cupric chloride and the formation of polyaniline in nylon-6 induced disorder in it; however in the composite retained the crystallinity by showing sharp peaks at  $2\theta = 7.8^\circ$  and  $16.4^\circ$ .

B.K. Amis et al.<sup>132</sup> had studied SAXS and WAXS of the nylon-6–fully doped polyaniline (emeraldine salt) using dopants MSA, DBSA and CSA. The changes in the crystallinity and crystalline disorder in nylon-6 is observed.

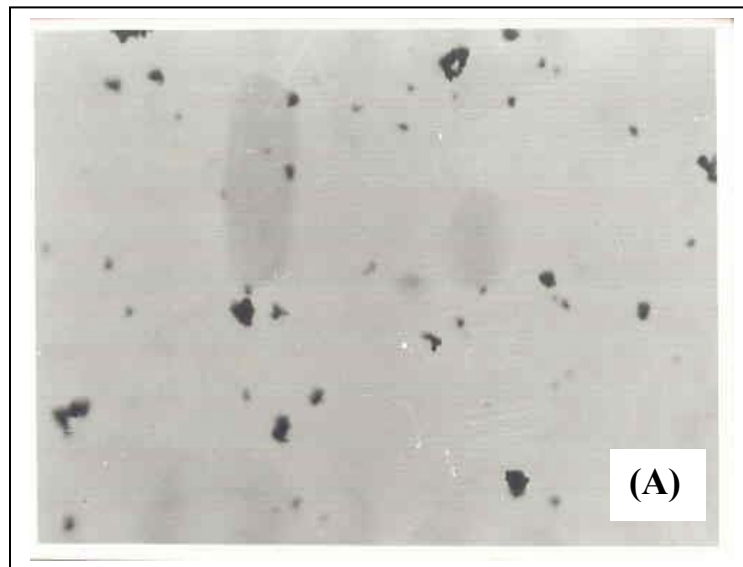
## 5.6, Morphological Features

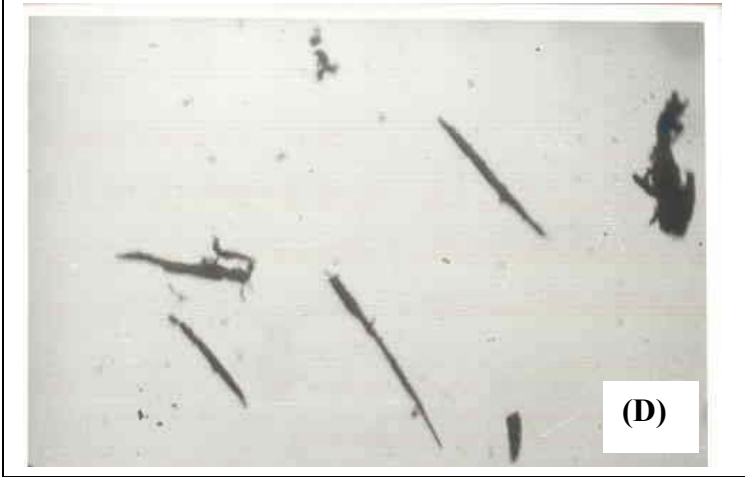
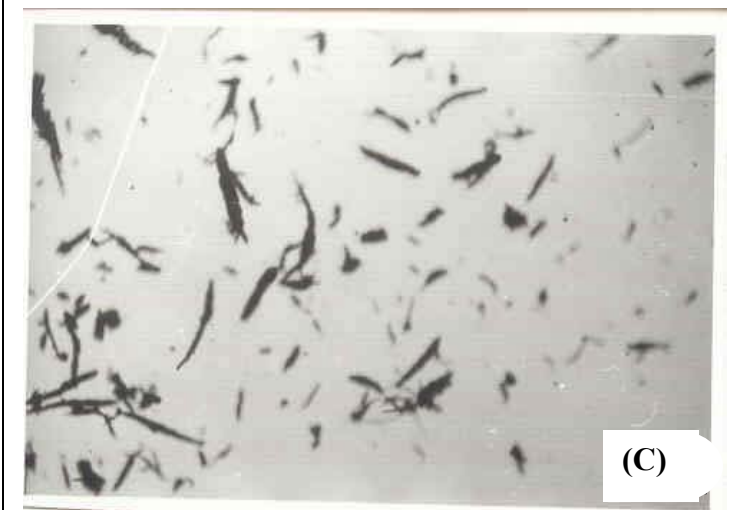
Detailed studies were carried out to know the morphology of the blend. Pristine Pani (2 mg.) powder and (2 mg.) powder of each blend composition was taken on a separate glass slide and these were heated for few min. on a hotplate and observed under optical polarizing microscope. These observations revealed very interesting morphological features and it was observed that these features were dependent upon increase in Pani content in the insitu blend. Since the features show a variation.<sup>153-154</sup>

Fig. 6.3: shows the micrographs of five slides, the micrograph, (A) corresponds to pristine Pani and (B) to (E) correspond to increasing Pani concentrations in the blend compositions. A globular morphology was seen in the pristine Pani, it changes to fibrillar morphology as the concentration of nylon-6 increases and it totally forms fibrillar morphology. It is observed that the dimension of the fiber changes fine; finer the morphology. For Pani-nylon-6 composites, the changes in morphology occurring as a result of synthetic conditions have been studied<sup>137</sup>. Morphology of the composite film was dependent upon the polymerization time, conc. of HCl and the matrix used. This difference in morphologies might arise from differing thermodynamic interactions

between Pani-HCl and the matrix polymers. Nylon-6 have some affinity with Pani through hydrogen bond interaction. This affinity may result in finer dispersions in nylon-6 .The Pani complex forms interconnected network with fibrillar morphology, <sup>155-156</sup> consistent with the existence of connected conducting pathways at volume fractions as low as 1% of the conducting Pani. At higher fractions of Pani, the density of the connected paths increases.

The organization of conducting Pani as a network of interconnected pathways was observed at all concentrations. This unusual morphology is the origin of the high electrical conductivities and excellent properties of these blends.<sup>157, 159-160</sup> Percolation threshold shift in lower concentration of fiber morphology than in the form of globular morphology, with further increase in loading (Pani-33%) above the percolation threshold to 0.5%, a thick network with wide nets develops. The morphology of the Pani-HCL-PVA<sup>158</sup> blend was similar to that reported by Yang et.al. For the Pani-CSA-PMMA blend system.







**Fig.6.3: Optical micrographs showing fibrillar morphology in Pani-Nylon-6 insitu blends, A) Pristine Pani, B) 11% Pani, C) 14% Pani, D) 25% Pani and E) 33% Pani**

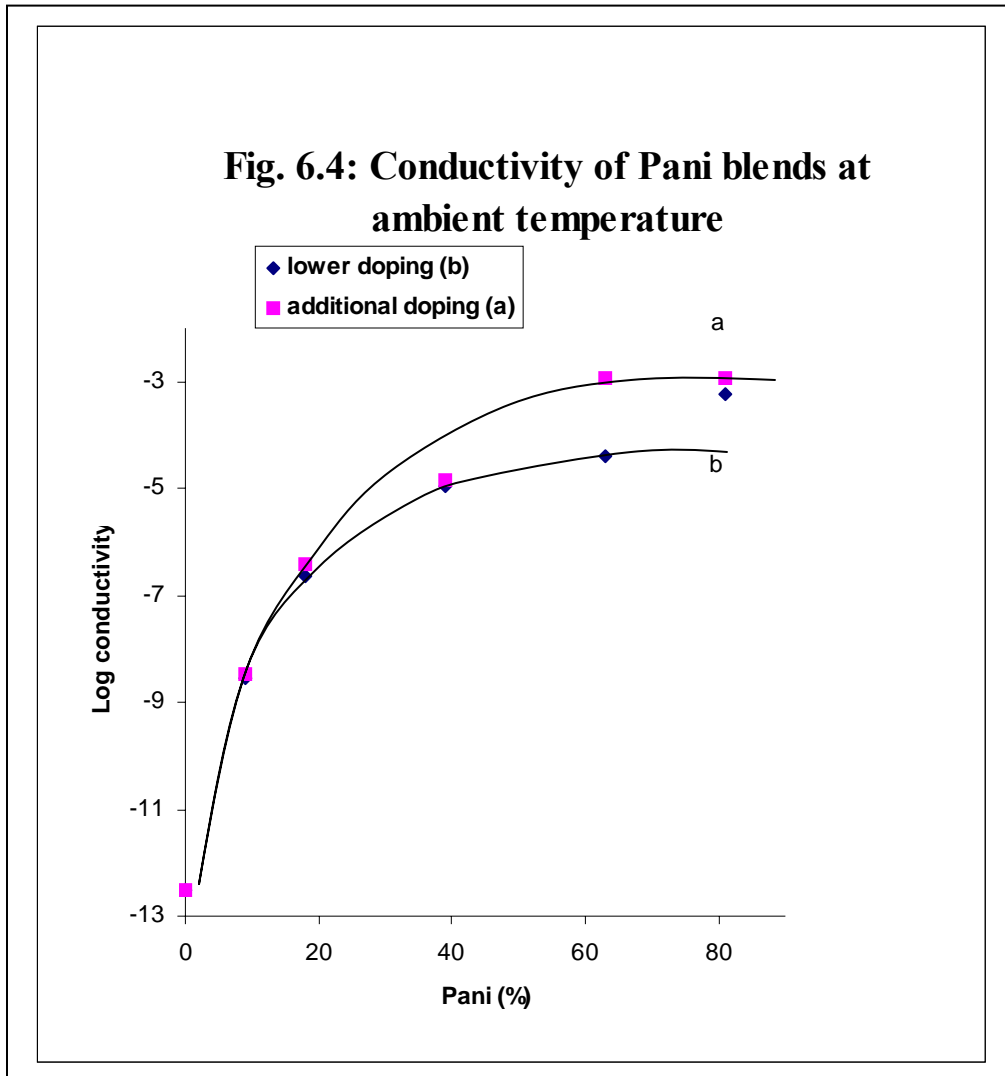
## **5.7 Electrical Conductivity Measurement**

### **1) R.T. Electrical Conductivity Measurement**

The room temperature conductivity for the insitu blends is shown in the fig.6.4, where 'a' represents log conductivity for synthesized blend while curve 'b' is for additionally doped samples. It is evident that as the concentration of Pani increases in the blend the conductivity rises sharply. The blend with 9% Pani has conductivity of  $2.73 \times 10^{-9}$  S/cm and as the concentration of Pani increases it attains higher resistivity value. 81% of Pani has conductivity  $5.64 \times 10^{-4}$  S/cm i.e. it rises by 5 orders of magnitude. After additional doping conductivity was found to be  $1.11 \times 10^{-3}$  S/cm for the same composition, as shown in the curve 'b'. This behavior is typical to many conducting polymer composites, which exhibit percolation threshold phenomena. Conductivity rises and reaches to saturation and thereafter it remains stable, this is because of the loading density is increased; the aggregates are more tightly packed and pressed against each other. This results in the reduction of resistance; thus the net resistance decreases with

increasing loading level. Further increase in loading would not be expected to cause any significant increase in conductivity.

Composition shows the typical ‘S’-shaped dependency with three regions (insulating, transition and conductive)<sup>(129-130,133-134,136)</sup> and fig.6.5, shows the log conductivity of the in-situ blends and ex-situ blends. Curve ‘a’ shows log conductivity for the ‘insitu additionally doped blends, and curve ‘b’ shows log conductivity for the ex-situ blends. R.T. log conductivity was explained on the basis of model, it is shown in the fig.1.2.a.

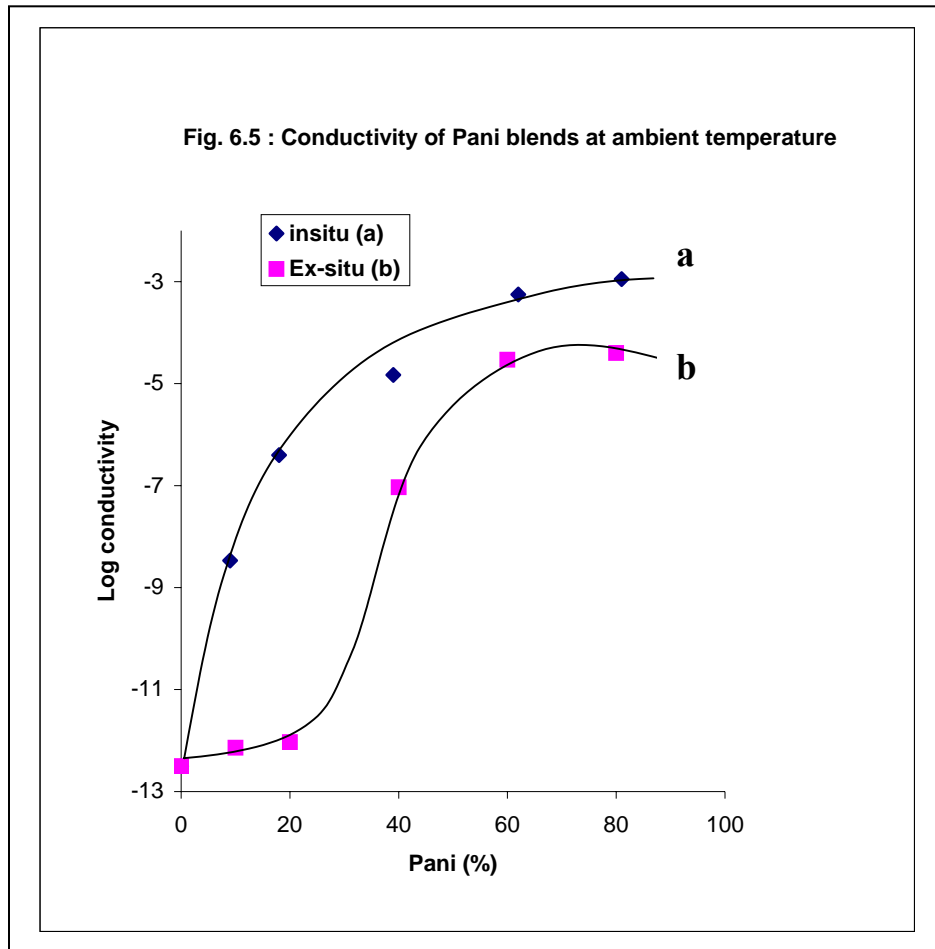


From the Fig.6.5, it is observed that, 9% Pani in the insitu blend gives conductivity  $3.35 \times 10^{-9}$  S/cm; conductivity rises further as the Pani concentration increases in the blend. In the ex-situ blend at 10% Pani has conductivity  $5.031 \times 10^{-12}$  S/cm



as concentration of the Pani increases in the blend i.e. at the 98% conductivity is found to be  $0.171 \times 10^{-3}$  S/cm. Thus it is clear that insitu blend is more conducting than ex-situ blend. Samples with low filler (pani powder) content were almost nonconductive. With the help of four mechanisms nonconductivity is explained, these are Schottky mechanism, Poole-Frenkel Mechanism, Space charge limited conduction Mechanism and Tunneling mechanism.

As the loading is increased a percolation of critical loading is reached where the conductivity starts to increase rapidly (or the resistivity decreases rapidly), as a function of loading the entire region of conductivity increase is called percolation region. In this region, conductivity is limited by barriers to passage of the charge carriers (electrons) from one pani aggregate to another which close but not touching. The gap distance 'w' may be of the order of  $15-100 \text{ \AA}$ , the electron must surmount a potential barrier  $V_0$ , to get out of the pani aggregate across the gap.;



In our work, in the insitu blend, the percolation threshold value is found to be 9% and in ex-situ Blend, the value is found to be 40%. according to Flandin et.al<sup>147</sup> values of 20-40% (v/v) are typical for spherical particles of filler. Percolation threshold depends upon the geometry of the filler particles, size and shape and the special distribution (topology) of the filler (pani) particles within the nylon-6 matrix Percolation threshold depends upon the geometry of the filler particles, size and shape and the special distribution (topology) of the filler (pani) particles within the nylon-6 matrix. Conductivity of the blends increases by as much as 5 orders of magnitude. From the above data, it is found that insitu technique is more effective than ex-situ technique. Gabriel Pinto et,al<sup>134</sup> has found the percolation threshold value at 18% in zinc filled nylon-6 composites.

M.Zagorskaa<sup>135</sup> shown that the stability of Pani-nylon-6 blends processed from formic acid can be significantly improved after adding protonating agents of the type of phosphoric acid, sulfonic acid, or phosphoric acid ester, it is observed that after addition of these protonating agents he has got very low percolation threshold (2-3%) and rise in electrical conductivity.

Yun Heum Park,<sup>137</sup> prepared Pani-nylon-6 films by vapor deposition process, nylon-6 chips are dissolved in formic acid and oxidizing agent cupric chloride dissolved in formic acid and added in nylon-6 solution. The nylon-6 solution containing cupric chloride is casted in the form of film, later the film is suspended over aniline and HCl aq.solution.The vapors of aniline and HCl diffuse in to the matrix polymer film and the simultaneous oxidative polymerization of aniline and the protonation of Pani occur.

Result shows that the unprotonated Pani-nylon-6 composite exhibits a threshold at around 12 wt % Pani content, but the protonated composite at around 21 wt.% Pani content. Higher percolation threshold of protonated Pani is owing to the differences of the dimensionality, arrangement, degree of dispersion and other morphological details. It is presumed that the conductivity difference between protonated and unprotonated composites results from the effects of protonation and morphology difference.

Sung Weon Byun<sup>130</sup> has got very low percolation threshold value, he prepared conducting Pani-nylon-6 composite, by immersing nylon-6 films containing aniline monomer in an oxidant. This oxidant was aq. APS solution containing one of various

protonic acids such as hydrochloric acid, benzene sulfonic acid, and sulfosalicylic acid and p-toluene sulfonic acid. The rise in conductivity is found to be  $\sim 3.5 \times 10^{-2}$  S/cm at 4.4 wt.% and percolation threshold is found to be 2.5. This means that the conductive paths of Pani in the Pani-nylon-6 can be generated uniformly over the molecular chain gaps of the nylon-6 matrix films with a small amount of Pani.

From the X-ray data, it was observed that IPN formation takes place, i.e. formation of continuous network morphology. This continuous network structure provides the composites electrically conducting paths. If we add pani particles such as, it aggregates one at a time; the particles will at first be isolated, and then isolated clusters will be formed, and finally a through paths will arise (the term ‘through going path’ is used here to refer to a continuous network of conductive particles in close enough contact) to permit flow of current from one end of the specimen to the opposite end, but not necessarily with negligible interparticle resistance, as in the ‘through going chains’ of the previous section.

**Percolation threshold:**

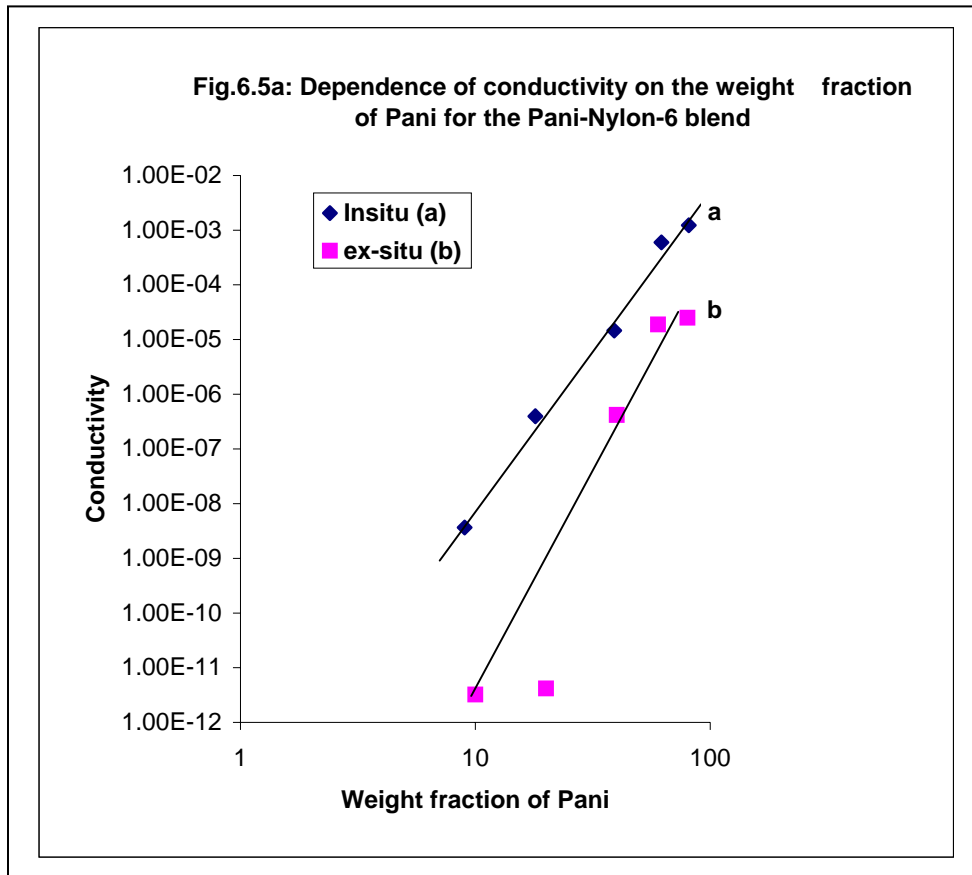
In order to identify the percolation threshold more precisely, we have applied to fit the data to the scaling law of percolation theory. The conductivity,  $\sigma$  depends on the volume fraction of the conductive material; the equation can be given as  $\phi - \phi_c$ ,

$$\sigma \propto A (\phi - \phi_c)^f \dots\dots\dots I$$

Hence  $\log \sigma = \log A + f \log (\phi - \phi_c)$ . II

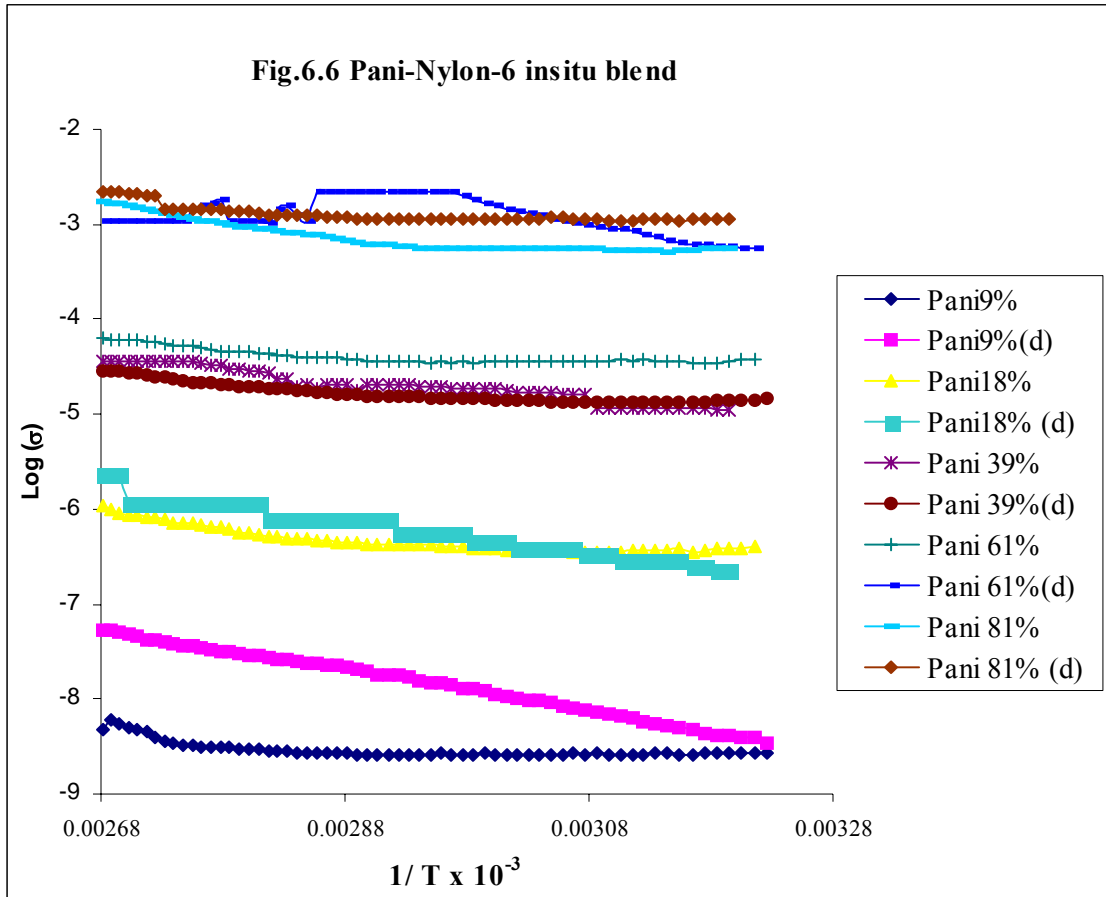
Where ‘ $\phi$ ’ is the volume fraction, ‘ $\phi_c$ ’ is the volume fraction at the critical concentration and ‘f’, an exponent. A plot of conductivity vs weight fraction of Pani is shown in **fig.6.5a**. Graph represents that ‘a’ corresponds to insitu blend and ‘b’ corresponds to ex-situ blend. The straight line thus following the percolation model of conduction. This behavior can be exhibited by the system, can be understood as follows. The insitu blends consisting of nylon-6 coated Pani particles ( $10^{-3}$  S/cm); the nylon we have used is pristine nylon-6 ( $10^{-12}$  S/cm). As the concentration of Pani increases, it forms a conducting path and definitely the system contains more nylon coated pani

particles. At a particular concentration, the Pani particles contact each other and forming three-dimensional network, there after the conductivity reaches to saturation. In ex-situ blends, it is observed that, the plot shows a straight line, it may be considered to form an M-I-M structure. Where the conducting regions are well separated from insulating (material) region<sup>148-149</sup> and it is found that as the concentration of Pani increases, the gap between the two conducting sites decreases. Volume fraction in insitu blend was found to be 0.29 and 0.32 in ex-situ blend.



## 2) Temperature dependent Conductivity

Resistance of the blend compositions for insitu blends and ex-situ blends



were measured at varying temperatures using Keithley 614 model electrometer and the conductivity is plotted against the inverse temperature, the plot is linear, indicating that the charge transport follows the polaron hopping model (i.e. conductivity variation with temperature follows Arrhenius law). The conductivity was recorded as a function of temperature.

The equation is given below:

$$\sigma = \sigma_0 \exp (A.1/T^{1/n}) \dots \dots \dots \text{I}$$

$$\text{Log } \sigma = \text{Log } \sigma_0 + A (1/T)^{1/n} \dots \dots \dots \text{II}$$

Graph is plotted with log conductivity vs.  $1/T$  for the insitu blends and ex-situ blends. Curves correspond to insitu blends, showing increasing concentration of polyaniline and shows the same blend composition after additional doping (d). Graph depicts concave nature is low concentration of Pani in the blend and as the concentration

of polyaniline increases, the conductivity rises and then the nature of the graph is found to be linear. The graph corresponds to additionally doped compositions shows more linearity and rises in conductivity and thus follows Arrhenius law.

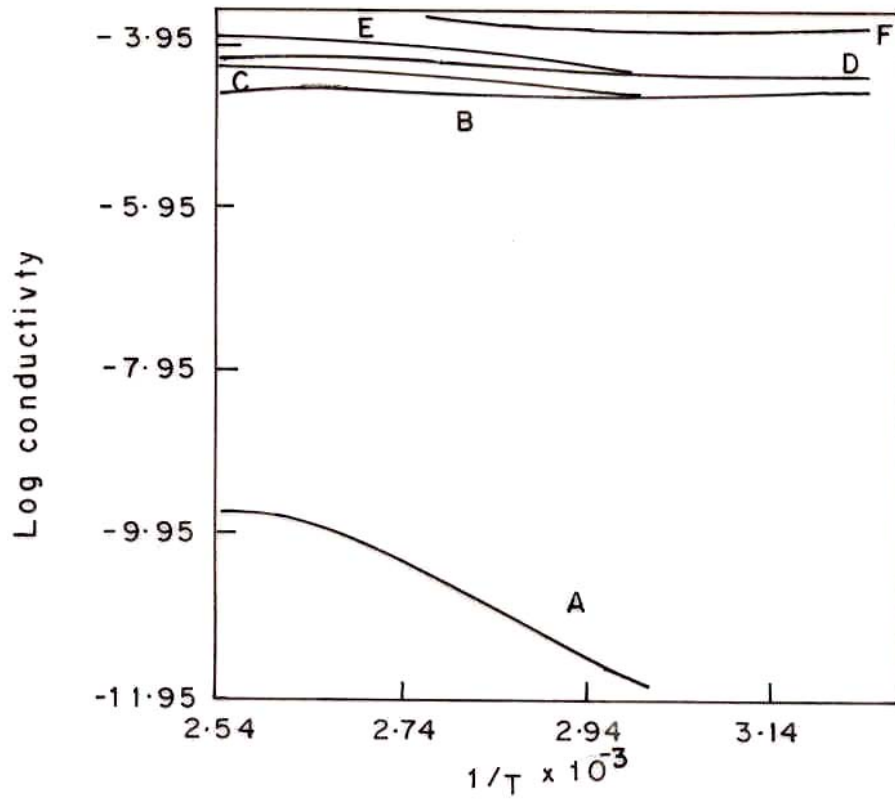


**Fig.6.7: Plots of log conductivity versus reciprocal of temperature for Pani-Nylon-6 exsitu blends, A) 10% Pani, B) 20% Pani, C) 40% Pani, D) 60% Pani, E) 80%Pani, F) 98% Pani**

The increase in conductivity with temperature is owing to thermal activation (the charge carriers absorb phonons and are thereby activated over the barriers. Charge carriers grow exponentially as the temperature rises, rising temperature gives more and more valence electrons with enough energy to jump in to the conduction band, freeing them and the corresponding holes to conduct an electric current). Physically the thermally activated process will correspond to electrons hopping from molecule to molecule or to

ions making their way through the blends. It shows that electrical conduction in blends is thermally activated and as the temperature increases further; the conductivity also increases but slightly departs from linear relationship.

Thermally activated transport of electrons takes place over the potential barrier (hopping), it is observed that nylon-6 barriers affect in the hopping process, the nature of the graph shows no linearity. We have calculated the activation energy to know the required  $E_a$  to hop the electrons in the blend. Very few reports were seen on this work<sup>137</sup>

The increase in conductivity with temperature can be attributed to the increase in polaron delocalization owing to thermal activation and increase in polyaniline concentration. Initially the log conductivity of the blend composition containing low concentration of polyaniline (9% Pani) is found to be  $10^{-12}$  S/cm, after additional doping of the same composition conductivity is found to be rises slightly. In the ex-situ blend, (**Fig6.7.**), 10% Pani gives log conductivity  $10^{-12}$  S/cm, and conductivity rises nine orders of magnitude at higher concentration of Pani i.e. at 98% polyaniline, the linear nature is observed at higher concentration of Pani.

### 3. Activation Energy ( $\Delta E$ ) For the Blends

Activation energy is calculated from the temperature dependent conductivity graph for insitu blends and ex-situ blends. **Fig.6.8** shows that line 'a' corresponds to insitu blend compositions obtained from the reactor, and line 'b' corresponds to additional doping of the same blend composition. From the given fig., it is observed that initially 9% Pani shows activation energy 0.21eV and as the concentration of Pani increases in the blend, activation energy found to be decreased and shows 0.03 eV when 81% Pani is added. After additional doping, activation energy of the blend is decreased from 0.19 eV to 0.02 eV. for the same blend compositions. **Fig.7** shows line 'a' corresponds to insitu blend composition and line 'b' corresponds to ex-situ blend. It is found that initiatally activation energy for the low concentration of polyaniline is more compare to insitu blend; it decreases further as the polyaniline concentration in the blend increases. In the ex-situ blend, 10% Pani shows activation energy 0.49 eV and as the concentration of Pani increases to 80 % it gives activation energy 0.09eV. From the activation energy data.

(Table-6.9 and Table7.1), it is observed that ex-situ blends require higher activation energy than insitu blends.

Hopping mobility is usually characterized by activation energy and filled dependence<sup>137, 150</sup>. The activation energy is generally made up of intramolecular and intermolecular contributions. The former represents the difference in the energy of the hopping sites. In this case, conjugated chain segments owing to difference in length, presence of defects and local polarization energy in addition to the potential drop due to the electric field. The intermolecular contribution arises from the change in conformation of the chain segments owing to the addition or removal of an electron in the polaronic effect.

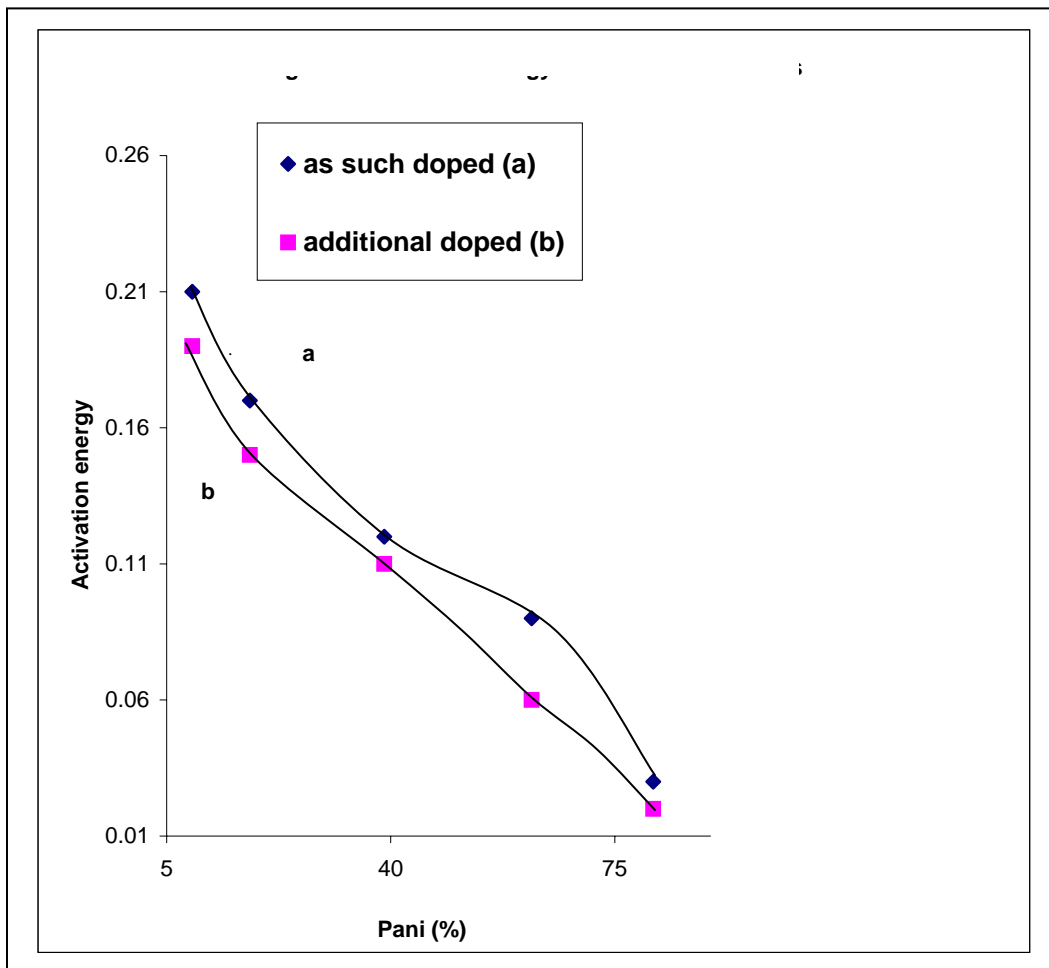


**Fig.6.8: Graph of Activation energy versus Pani concentration for Pani-Nylon-6 insitu blend.**



In the insitu blend, as the Pani concentration increases, resistance decreases, conductivity rises and activation energy decreases, barrier of nylon-6 decreases (reduced) and Pani coated nylon particles comes close to each other and forms a close contact thus created ‘conducting path’ in the nylon-6 solution. It requires very less activation energy to transport the charge, thus resistance decreases and conductivity increases.

In the ex-situ blends, the nylon-6 particle acts as a barrier in between Pani particles and electron requires higher energy to hop from one particle to other, thus it is showing high, low conductivity and so, activation energy required is high. This means that the conductive paths of Pani can be generated uniformly over the molecular chain gaps of nylon-6 matrix with small amount of Pani and nylon-6 has got linear structure.

The result of this conformational change is a reduction of structural defects along the Pani chain (eg. Twisting, buckling), which increases the  $\pi$ -orbital overlap between the phenyl  $\pi$ -electrons and nitrogen lone pair. This in turn increases both conjugation of the chains backbone and polarons delocalizations length and close packing of conducting Pani takes place. This close packing decreases the interchain separation. While expanded the molecular conformations,  $\pi$ -conjugation defects reduces and both are able to increase the delocalization of electrons and finally the conductivity.

**Table 6.9: Activation energy data for the Pani insitu blends**

<b>Sr.No.</b>	<b>Lower Doping</b>	<b>Activation energy (<math>\Delta E</math>) eV</b>	<b>Additional Doping</b>	<b>Activation energy (<math>\Delta E</math>)</b>
	<b>Pani (%)</b>	<b>(<math>\Delta E</math>)</b>	<b>Pani (%)</b>	<b>(<math>\Delta E</math>)</b>
1	9	0.21	9	0.19
2	18	0.17	18	0.15
3	39	0.12	39	0.11
5	63	0.09	63	0.06

**Fig.7: Graph of activation energy versus Pani concentration for Pani-nylon-6 blend**

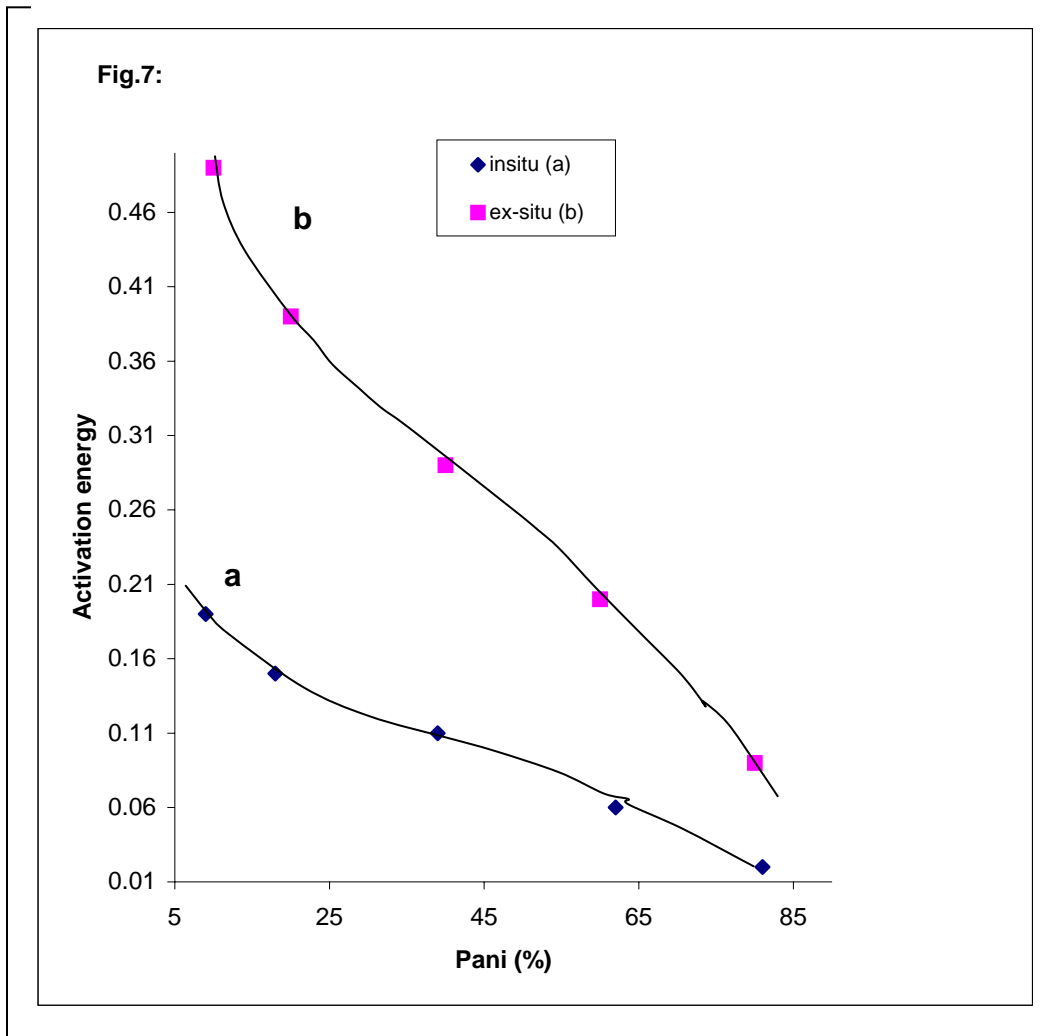


**Table: 7.1, Activation energy data of pani-nylon-6 blend**

Sr.No.	Insitu-blend composition	Activation Energy ( $\Delta E$ ) eV	Ex-situ-blend composition	Activation Energy ( $\Delta E$ ) eV
	Pani (%)		Pani (%)	
1	9	0.19	10	0.49
2	18	0.15	20	0.39
3	39	0.11	40	0.29
4	63	0.06	60	0.21
5	81	0.02	80	0.09

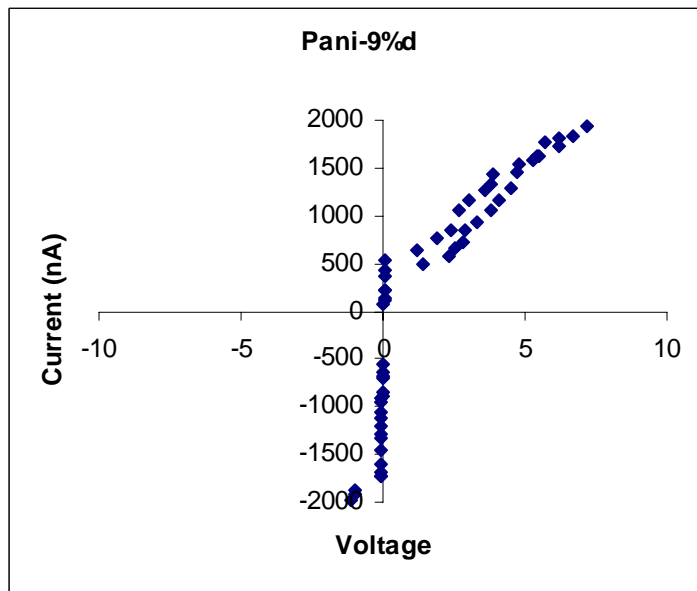
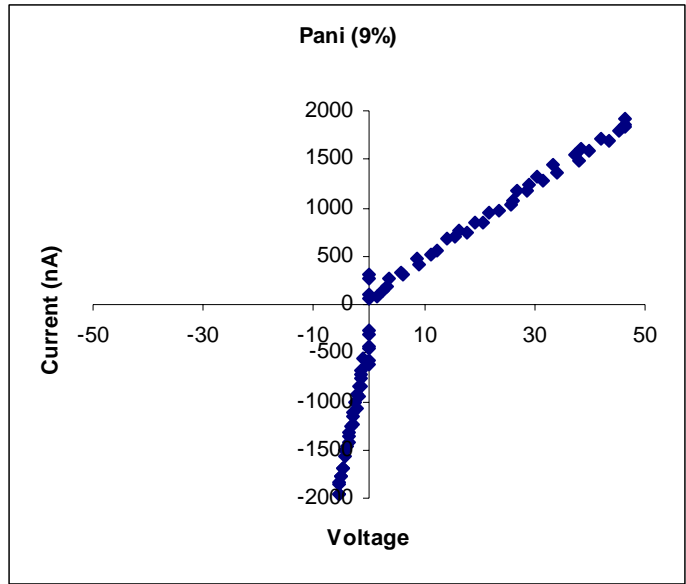
#### 4) Current vs. Voltage (I-V) Characteristics

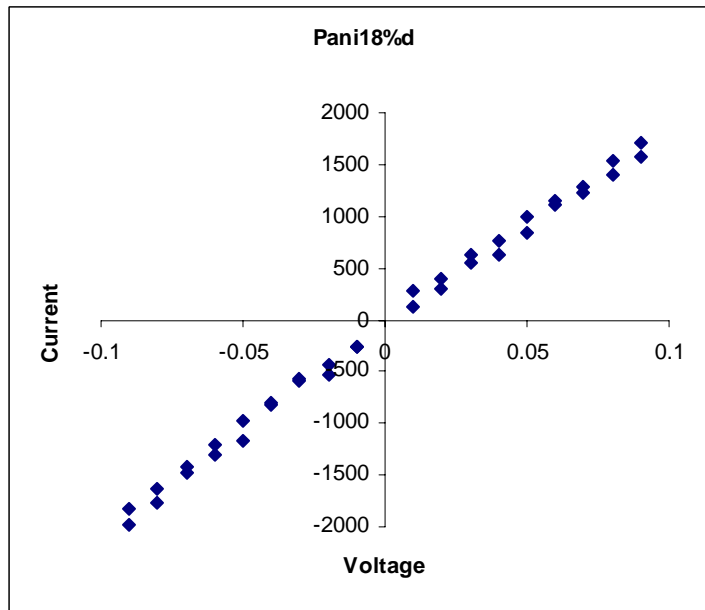
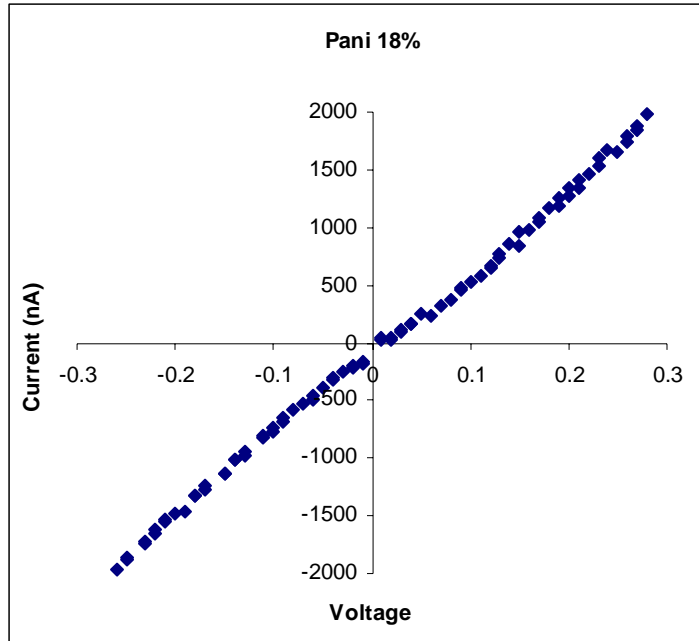
**Fig.7.2.** shows the dependence of current on applied potential for Pani-Ny-6 insitu blend and ex-situ blend respectively.

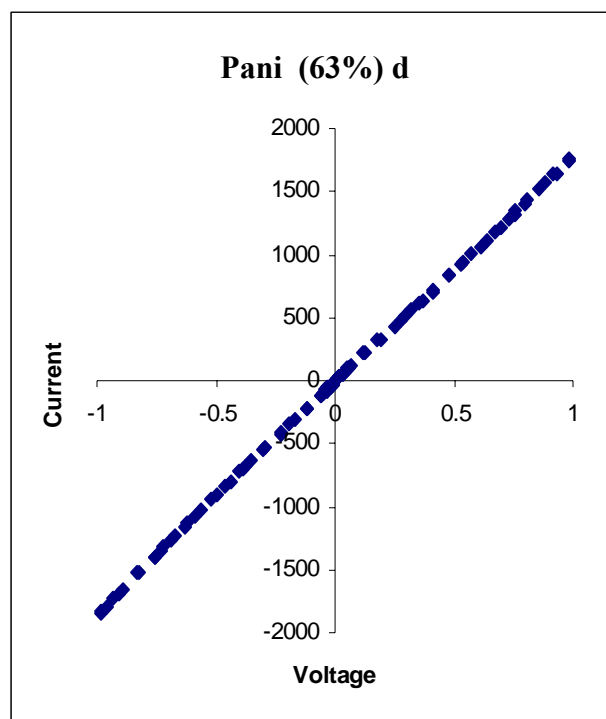
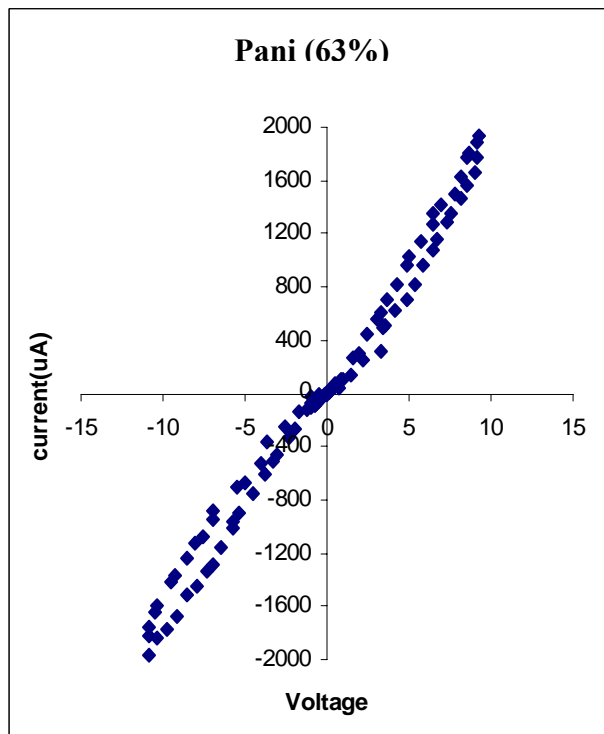
Graph shows non-ohmic and ohmic nature for the blend compositions obtained from the reactor and additional doped blend compositions. Current increases linearly with the applied potential. Initially it is observed that low Pani concentration (9%) shows non-ohmic charge transport and nature of the curve was nonlinear. As the Pani concentration increases in the blend, the nature of the curve found to be linear and required lower voltage to reach the higher current value (81%) Pani shows more linear nature, which

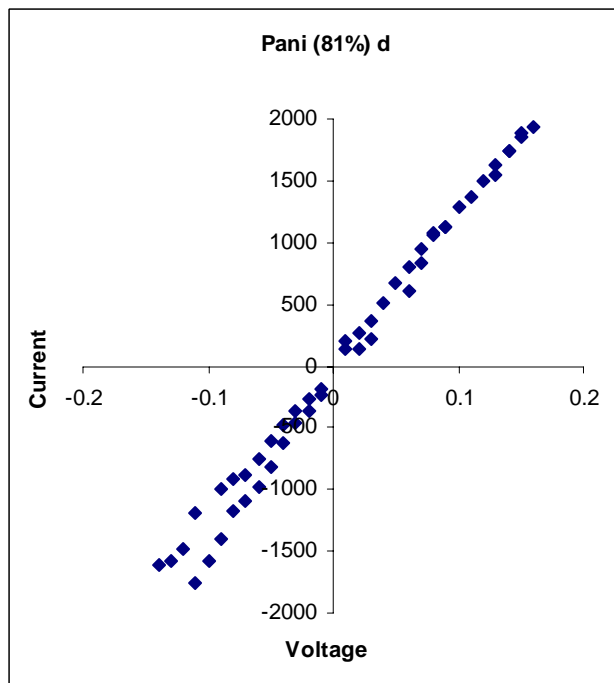
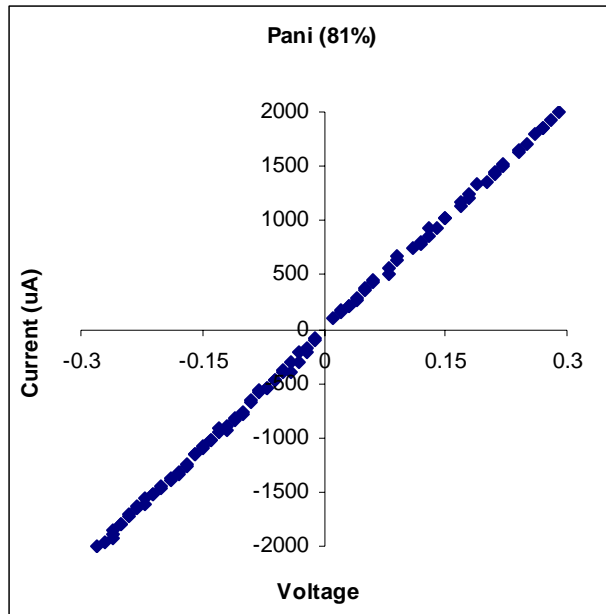
means that ohmic conduction occurs predominantly in it. Same blend compositions shows linear nature after additional doping and requires very less voltage compare to blend compositions obtained from the reactor.

**Fig.7.2: Charge transport process in insitu blends**









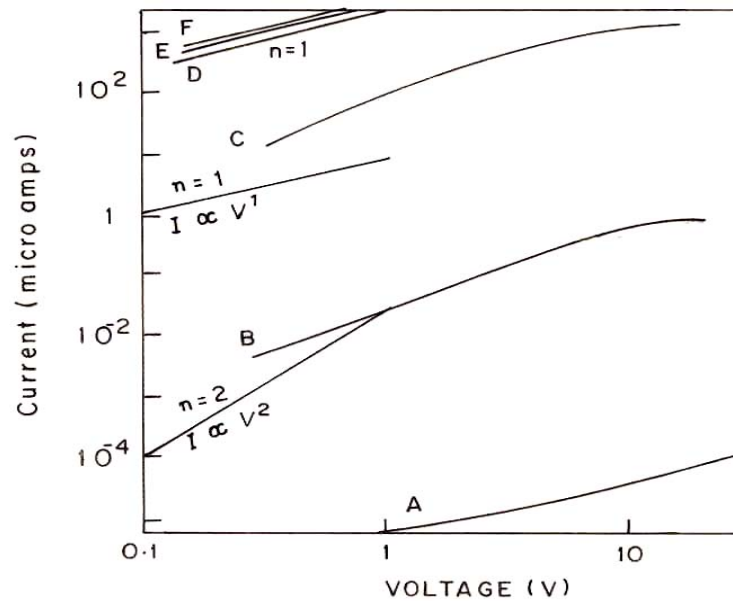


**Fig. 7.3: Charge transport process in ex-situ blends**

The junction of nylon-6 do not affect the charge transport because the work function value of nylon-6 was found to be 3.1 eV and that of Pani was found to be 5.1 eV, which doesn't match closely with one another.

Fig.7.3 shows the graph of ex-situ blend, curve 'A', 'B', 'C', 'D', 'E' and 'F' was the increase in Pani concentration in the blend. It was observed that lower concentration of Pani in the blend shows nonohmic nature; this is because barrier of nylon-6 affects the charge transport process, and as the concentration of Pani increases, conducting network is formed and barrier of nylon-6 get reduces showing linear nature i.e. charge transport process was ohmic. There was no close contact found even at higher concentration of pani, barrier still affects the charge transport process and the voltage value was found to be more in ex-situ blend compared to insitu blend. It was observed that low concentration of Pani in the insitu blend shows ohmic nature compared to ex-situ Blend. This was because the barrier of nylon-6 gets reduced as the 'Pani' concentration increases in the blend and conducting network is formed. The charge carriers are created and their



mobility also increased at this point. The charge carriers overcome the barrier easily and intramolecular as well as intermolecular charge transport takes place in the blend because of miscibility formed by the hydrogen-bonding between the two polymers (Pani and nylon-6).

## 5.8 TGA/DTA

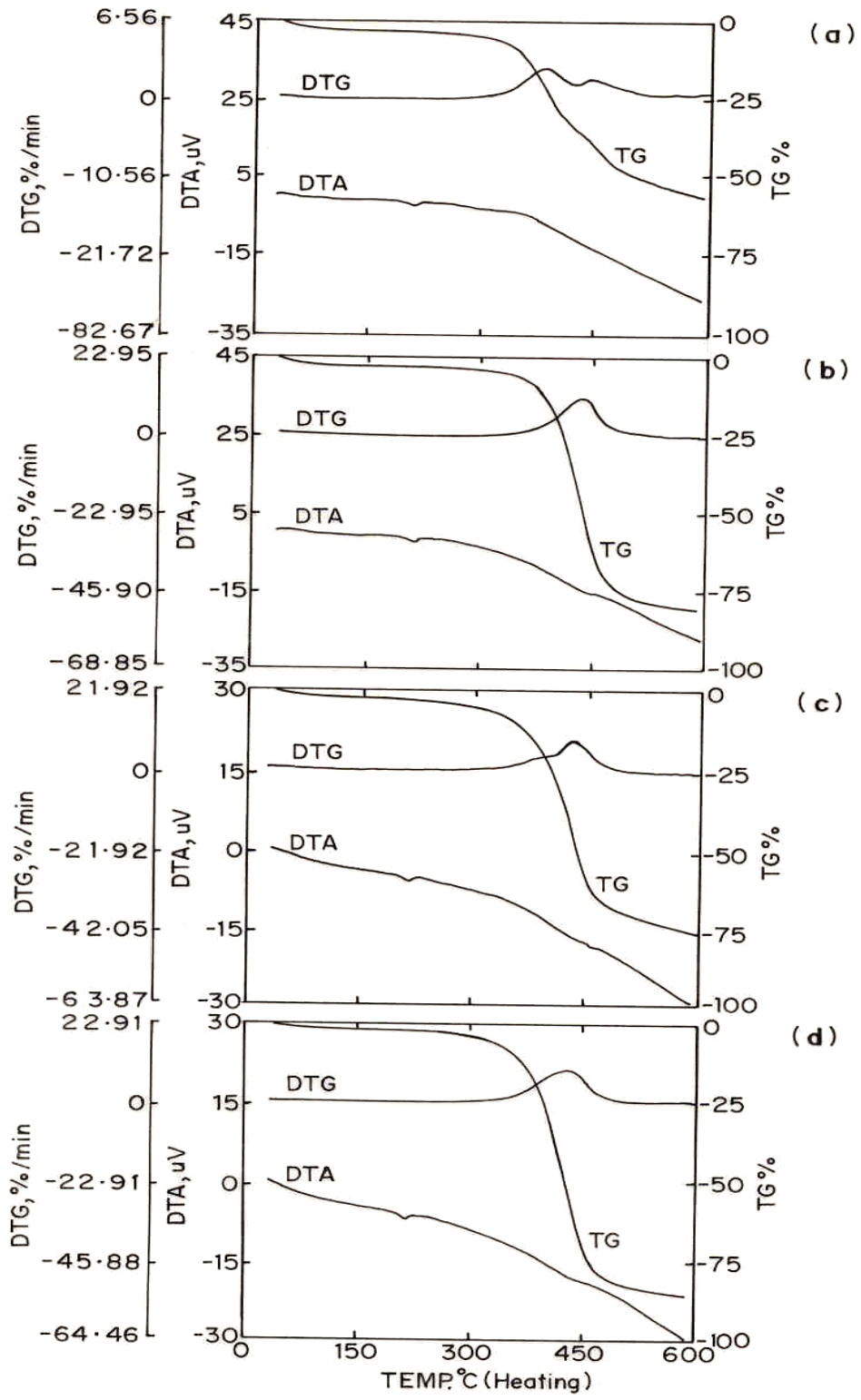
Pure polyaniline and the compositions of polyaniline-nylon-6 blends were subjected for thermal analysis in nitrogen atmosphere. The results obtained from these studies are given in the table 7.5 and thermogram (Fig 7.4) is shown below.

The table shows the percent weight loss with respect to temperature for various polymeric compositions.

The thermal degradation was actually carried out from room temperature to 500°C, at the rate of 10°/min. The nature of the degradation curve is shown in the thermogram. Thermogram 'f' corresponds to pristine pani, and 'a', 'b', 'c', and 'd' is the increasing concentrations of pani in the blend and 'e' corresponds to pure nylon-6.

It is noticed that pristine nylon-6 decomposes completely below 500°C and shows weight loss 80% where as pristine polyaniline shows 60% weight loss at 500°C and as the concentration of polyaniline increases i.e. from 9% to 63% in the blend, its weight loss decreases from 80% to 55%. The blend compositions follow two stage wt.loss, the same trend as observed in nylon-6<sup>151</sup>. The HCl-doped polyaniline shows two-step decomposition. The second step starting at 443°C corresponds to the decomposition of the backbone structures. A broad DTA peak of pristine nylon-6 also indicates that the melting temperature of nylon-6 is reduced on modification.

Nylon-6 shows, two stages wt.loss. Major weight loss observed at 350°C attributed to a structural decomposition. The polyaniline-nylon-6 blend exhibits a lower decomposition temperature than that of the nylon-6, but the slope of the decomposition curve is gentler.



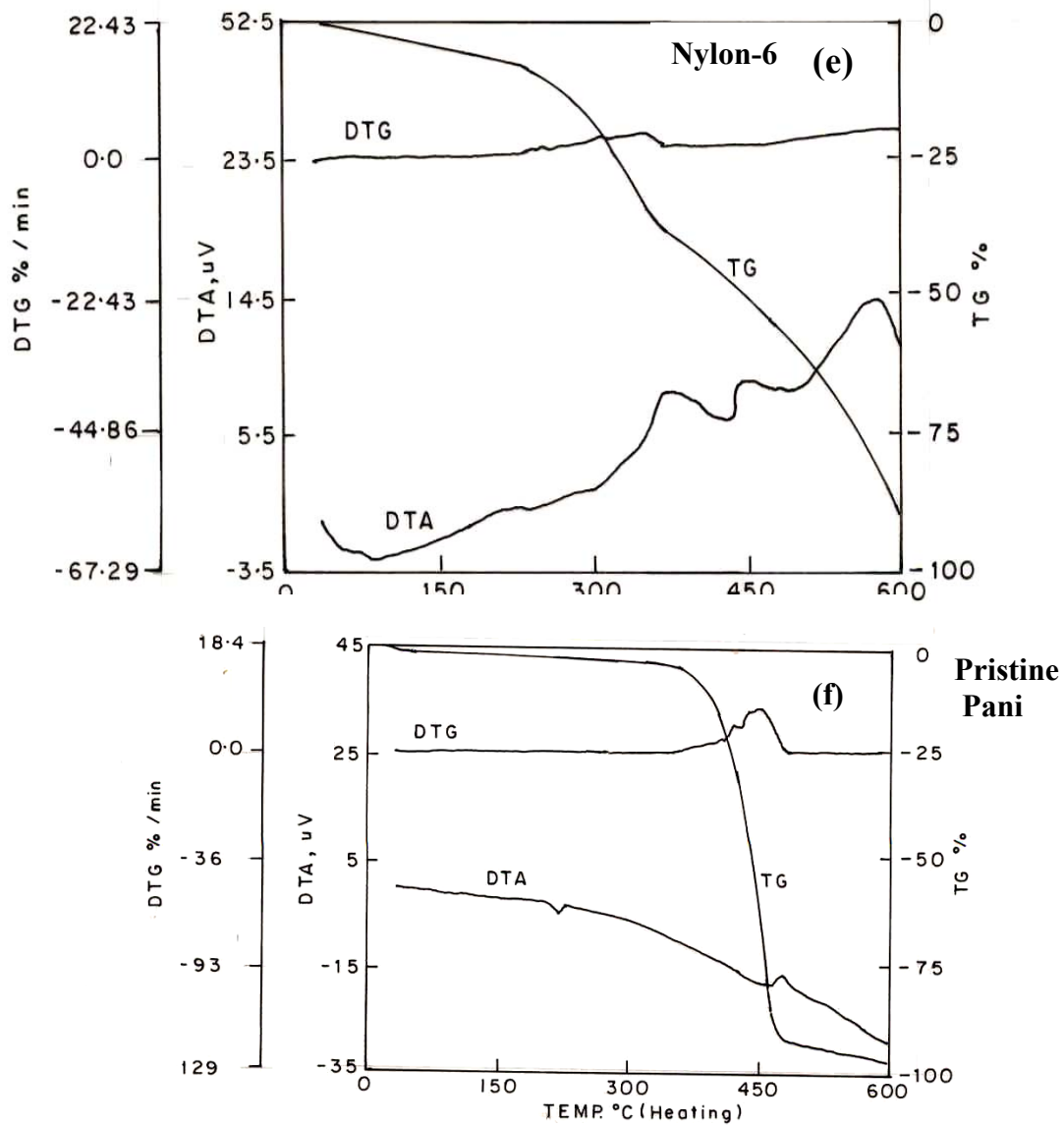


**Fig .7.4: TGA/DTA, thermograms of Pani-Nylon-6 insitu blends. a) 9% Pani, b) 18% Pani, c) 39% Pani, d) 63% Pani, e) Nylon-6, f) Pani**

**Table: 7.5: Thermal data of insitu blends (in nitrogen)**

Temp (°c)	Nylon -6	Pani (9%)	Pani (18%)	Pani (39%)	Pani (63%)	Pani (100%)
	Wt.loss in %					
100	1	1	1	1	1	3
200	2	2.5	1.5	1.5	1.5	6
300	3	6	4.3	5	3	18
400	12	31.25	10	18.75	13	40
500	95	51	78	74.75	85	60

From the thermogram, it is observed that the blend shows the significant improvement in thermal stability<sup>152</sup> as the concentration of pani increases in the blend. The weight loss observed in the pristine polymers, such as nylon-6 and polyaniline however are not observed in the t.g.a. curves of the blend, suggesting the presence of interaction between the polymers, which alters the degradation pattern. The wt.loss data of blend matches closely to the reported data of pani-nylon-6 blends.<sup>129</sup>

## 5.9 Moisture sensitivity

### Experimental:

The sensor substrate with a dimension of (2x2) inches is made up of Epoxy polymer as a base. An interdigitated array of copper electrodes was deposited on one side of the Epoxy polymer chip. The sensor chip electrode was cleaned well and nicely polished thin Cu wires were soldered at the two ends of this chip.

**Polymer Film:** Pani-nylon-6, blend (insitu) was dissolved in formic acid. The solution was stirred thoroughly. A thin film of blend from solution was casted on the substrate and dried it well. The sensor assembly cell was then connected to Keithley Electrometer through the two terminals of the cell. The film exposed to moisture vapors. (By keeping the blend film coated electrode to the known height from the water-containing cell). Sensitivity of this film is noted. A glass sheet was used to pack the moisture cell at the top opened portion to prevent from external leaks.

### Results and Discussions:

Moisture sensitivity of the blend films was noted by varying pani concentrations in the films. In Pani-nylon-6, blends, at lower concentration of Pani (9%); charge transport takes place ionically, intergranular distance between nylon-6 molecules is found to be more and it is difficult to transport the charge, that affects the 'R' value as observed initially. As the pani concentration increases in the blend, two phenomena will be observed, the barrier in nylon-6 molecules get reduced i.e. intergranular distance is reduced and charge transport takes place by ions very easily. Moisture absorption also depends upon the pores of the conventional polymers.

It is noticed that at higher concentrations of pani, there was no gap in between Pani molecules i.e. intergranular distance between two Pani molecules is very less and Pani is hydrophobic, which affect the charge carrier mobility. Data of moisture sensitivity is given in the table 7.7

**Table: 7.7: Sensitivity of Pani-Nylon-6 insitu Blends with Moisture Vapors**

Sr.No	Pani (%)	Sensitivity Factor
		Moisture vapor
1	0	11.71
2	14	2.33
3	25	86.95
4	33	25
5	87	1.6

Response time for Pani-nylon-6 blend film was found to be 86.95 at 25% pani in the blend film. It is observed that the 25% Pani dispersion is suitable to transport the charge in between the conventional polymer molecules. Sensitivity factor is calculated by the following formula and plotted against Pani conc. (Fig.7.6)

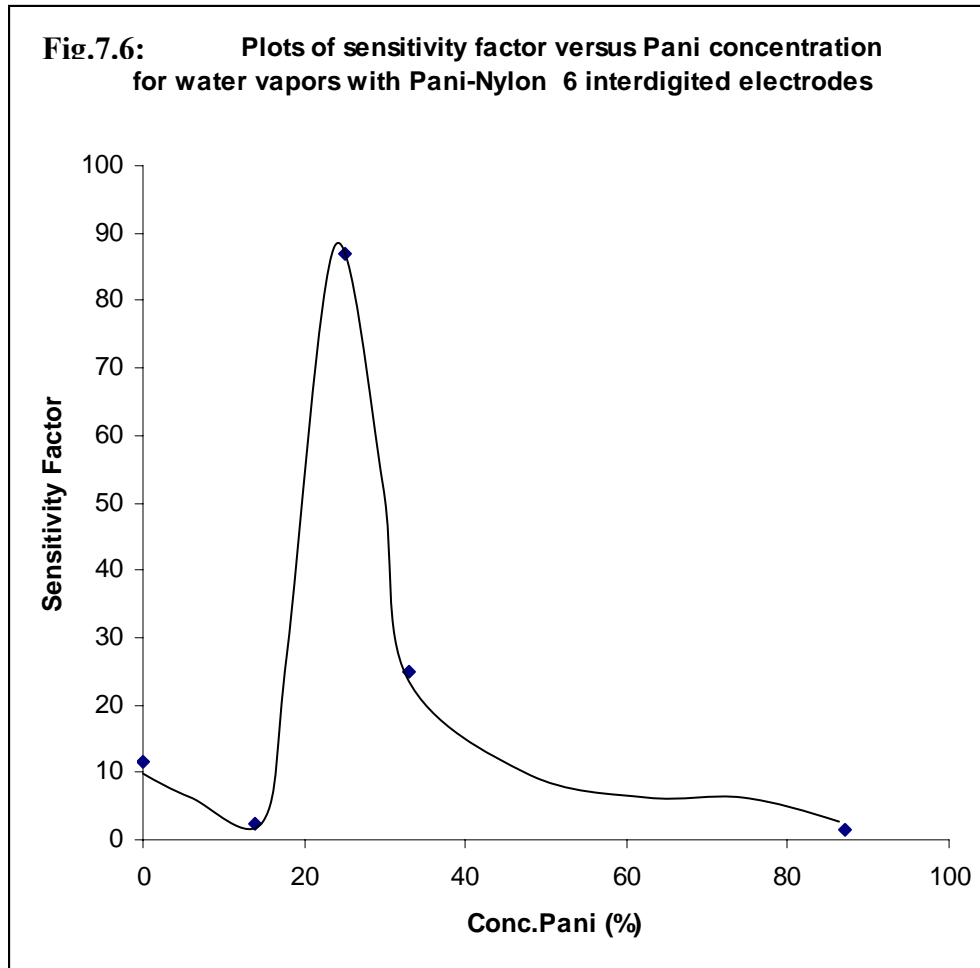
$$S = R_0 / R$$

Where,

S = Sensitivity

$R_0$  = Resistance before moisture absorption

R = Resistance after moisture absorption.



## 6. Conclusions

The blend was studied with the help of characterization, electrical conductivity and comparative study of insitu blend and ex-situ blend. It was found that in the 'insitu' synthesis, the polymerization of aniline didn't affect by the Nylon-6 solution, but it required approximately same induction period, like other blends (Pani-PVAc and Pani-Pam). Following conclusions were observed with the help of results obtained.

From the IR spectroscopy, it was noticed that, conductive insitu blend was formed, aniline polymerization in nylon-6 solution wasn't affected and Pani was doped as such during synthesis. The peaks observed confirmed this  $1590\text{ cm}^{-1}$ ,  $1540\text{ cm}^{-1}$  and  $1111\text{ cm}^{-1}$ . The peak found at  $1637\text{ cm}^{-1}$ , slightly shifted to lower frequencies when the concentration of Pani was increased in the blend composition, it was the indication of H-

bonding interaction between amine group of Pani and Carbonyl group of nylon-6, this confirmed the blend miscibility i.e. intermolecular interaction between the polymers.

The UV-VIS spectroscopy shows the peaks at 860nm, 580nm, and 344nm. From this peaks, it was again clear that conducting Pani (i.e. emeraldine salt) was formed and polarons-bipolarons were created in the blend.

X-ray diffraction spectra of the blends (insitu blends and ex-situ blend) shows that the Pani concentration increases in the blend compositions, crystallinity decreases. Decrease in crystallinity is found to be at lower concentration of Pani in the insitu blend than ex-situ blend. IPN formation takes place in the insitu blend.  $\gamma$  phase is formed in the nylon-6.

Optical microscopy shows the morphology of the insitu blends. It is found that Pani shows granular morphology and as the nylon concentration increases in the blend fibre morphology of the blend is observed.

TGA/DTA data shows that, interaction between the polymers, altered the rate of degradation and wt.loss decreases as the nylon-6 concentration increases in the blend i.e. thermal stability increases and the decrease in wt.loss. was observed from 95% to 85%.

Conductivity at ambient temperature of the insitu blends shows that, the blend after additional doping shows rise in conductivity than the blends doped as such during synthesis (i.e. lowers doping). Here percolation threshold value was observed at 9% Pani. And 63% Pani after additional doping log conductivity was found in the range of  $10^3$  to  $10^{-2}$  S/cm. The conductivity at ambient temperature was observed, it gave higher conductivity in the range of 40% to 60% Pani and percolation threshold observed at 40% Pani in the Ex-situ blend.

Temperature dependent conductivity showed that, insitu blend as well as ex-situ blend follows Arrhenius law. It was noticed that the higher concentration of Pani in the blend showed more linearity compare to ex-situ blend. The linear nature was observed because of charge carriers were created and the mobility was increased, the barrier of Pam was found to be decreased and it required very less Activation energy (excitation energy) compare to ex-situ blends i.e. in other words, electrons hop from one conducting particle to another without inhibition of nylon-6 barrier.



Activation energy ( $\Delta E$ ), calculated from Temp.dependent conductivity for both the blends, was found to be decreased, as the Pani concentration was increased in the blends (insitu blend and ex-situ blend). The  $\Delta E$  value of the insitu blend was decreased from 0.19 eV to 0.02eV and in the ex-situ blend the value was found to be in the range of 0.49 eV to 0.09 eV.

The percolation threshold temperature, corresponds to volume fraction of Pani of about 0.29 in the insitu blend and that in the ex-situ blend it was 0.32

The charge transport process was found to ohmic (linear) as the concentration of Pani increases in both the blends i.e. the intramolecular and intermolecular charge transport process was not affected by nylon-6 barrier.

Characterization studies and Electrical measurements show that insitu blending technique was effective than ex-situ blending technique. This can arise from the fact that, as the concentration of Pani increases in the blend, the contact points between the Pani coated nylon-6 particles increases in the number giving higher conductivity than the physical mixtures.

## Summary and Conclusions:

In the present work, blend was prepared by insitu technique and ex-situ technique and their electrical conductivity is compared. It was noticed that electrical conductivity was higher in insitu blend than exsitu blend. In the insitu technique, aniline was polymerized in a conventional polymer solution. More intimate mixing of the two components is possible than is obtained by mechanical blending (exsitu technique) because of the incompatibility of most polymers. Polyaniline forms blends with PVAc, Pam and Nylon-6.

This is a novel technique, very few reports observed on the 'insitu blending technique' electrical conductivity was enhanced using this technique. The polymerization kinetics for the conductive polymer will depend on the diffusion coefficient of the monomer in to the insulating polymer host. Properties of the resulting blends depend on the phase behavior of the solution. The polymerization of aniline to 'Pani' in the insitu blend was carried out using APS as an initiator and HCl as an oxidizing agent. The color observed changes from yellow-grey-green with coppery tint on the blend surface. It is the indication of emeraldine salt formation and is further confirmed by characterization techniques, such as F.T.I.R.spectroscopy; UV-VIS spectroscopy, Optical spectroscopy, X-ray, and TGA-DTA.

Miscibility also enhanced by H-bonding interaction between amino group of Pani and carbonyl group of the given polymers. Compatibility was formed i.e.intramolecular and intermolecular charge transport takes place, conducting path formed in the matrix solution, decreases the interchain separation while expanded molecular conformations reduce  $\pi$ -conjugation defects; both are able to increase the delocalization of electrons and finally the conductivity than physical mixtures (exsitu blends).  $\pi$ -electron delocalization takes place through the conjugated nature extended over the long portion of the polymer (Pani) chain. The enhanced conductivity was further observed after redoping the pellets of insitu blends. It was observed that percolation threshold value is lower than ex-situ blends.

In the ex-situ blend, it was found that conductivity was enhanced only when the particle size of the conducting filler (Pani powder) should be small. As the filler concentration increased, the conducting particles forms aggregates, illustrating a given

weight of Pani powder dispersed in a fixed volume with conventional polymer powder, the finer the aggregates of the Pani powder composing the given weight the more aggregates will be distributed throughout the fixed volume of conventional polymer powder and consequently the smaller will be the inter aggregate distances or gaps. This translates to increasing ease of electron transfer from aggregate to aggregate on its path through the conventional polymer powder.

In short, the finer the prime particles, and consequently the smaller the aggregates, the lower will be the level of electrical resistivity when dispersed (mixed) with the conventional polymer powder, other properties will remain constant.

The structure of the physical blending was a complex property that refers to the morphology of the primary aggregates. It not only expresses the number of prime particles composing the primary aggregate but it indicates the manner in which they were fused together, lower concentration of the Pani powder may form 'branching and chaining'. It was noticed that, the effect of the structure on the resistivity of mixed Pani powder with conventional polymer powder was two fold. It contributes to aggregate size as discussed above, and it determines the relative anisometry, or shape, irregularity of the aggregate. The latter effect was by far, the more important with the regard to electrical conductivity.

This illustrates how higher structure Pani powder creates more electron path. This translates to decreasing resistivity with increasing structure when mixed with conventional polymer powder in physical blending.

Pani powder particles will have finer particle/aggregate size, higher structure higher porosity and lower volatile content. It was the combined effect of these four properties that result in optimal conductivity. However it was important for the formulator to know the desired level of conductivity before choosing a conductive grade, For.eg. too high a structure level tends to limit loading capacity, too fine a particle increases cost and makes dispersion more difficult and so on. Therefore choosing a grade of conductive polymer powder usually involves a compromise that best fits the situation.

The systems have been successfully modeled to predict their threshold, conductive filler concentrations, converting them from insulative to conductive materials. Percolation threshold depends upon many factors such as the size, the shape and the

spatial distribution (topology) of the filler particles with the host polymer matrix, the adhesions and the possible interactions between the two phases and finally the processing method. The percolation also depends on the geometry of the filler particles. At the percolation concentration infinitely long chains of contacts are formed, characterized by an average number of contacts per particle, which can be computed through the probability or percolative theory.

Chapter III describes Pani-PVAc blend, with the help of characterization techniques and conductivity measurement. From the IR spectroscopy, it was noticed that, conductive insitu blend was formed, aniline polymerization in PVAc solution wasn't affected and Pani was doped as such during synthesis. The peaks observed confirmed this  $1600\text{ cm}^{-1}$ ,  $1500\text{ cm}^{-1}$  and  $1120\text{ cm}^{-1}$ . The peak found at  $1714\text{ cm}^{-1}$ , was the indication of H-bonding interaction between amine group of Pani and carbonyl group of PVAc, this confirmed the blend miscibility i.e. intramolecular interaction between the polymers.

The UV-VIS spectroscopy shows the peaks at 820nm, 420nm, 320nm and 590nm. shows  $\pi$ - $\pi^*$  transition, benzenoid-quinoid transition and polaron-bipolaron formation from this peaks, it was again clear that conducting Pani (i.e. emeraldine salt) was formed. TGA/DTA data shows that wt.loss decreases as the PVAc concentration increases in the blend i.e. thermal stability increases and the decrease in wt.loss. was observed from 68.75% to 52%.

Conductivity at ambient temperature of the insitu blends shows that, the blend after additional doping shows rise in conductivity. 68% Pani after additional doping log conductivity was found in the range of  $10^{-2}$  to  $10^{-1}$  S/cm. Here percolation threshold value was observed at 7% Pani. In the Ex-situ blend, the conductivity at ambient temperature was observed, it gave higher conductivity in the range of 40% to 60% Pani and percolation threshold observed at 20% Pani.

The percolation threshold temperature, corresponds to volume fraction of Pani of about 0.26 in the insitu blend and that in the ex-situ blend it was 0.28

Temperature dependent conductivity showed that, insitu blend as well as ex-situ blend follows Arrhenius law. It was noticed that the higher concentration of Pani in the blend showed more linearity compare to ex-situ blend.

Activation energy ( $\Delta E$ ), calculated from Temp.dependent conductivity for both the blends, was found to be decreased, as the Pani concentration was increased in both the blends (insitu blend and e-situ blend). The  $\Delta E$  value of the insitu blend was decreased from 0.43eV to 0.09eV and in the ex-situ blend the value was found to be in the range of 0.49 eV to 0.15eV.

The charge transport process was found to ohmic (linear) as the concentration of Pani increases in both the blends i.e. the intramolecular and intermolecular charge transport process was not affected by PVAc barrier.

From the moisture sensitivity graph, it is noticed that, Pani-PVAc insitu blend film responses the moisture and sensitivity is found to be 156.71. The higher value observed because PVAc has low moisture affinity i.e. difference between resistance before moisture absorption ( $R_o$ ) and resistance after moisture absorption ( $R_f$ ) was higher.

Chapter IV investigates the results of Pani-Pam blend system. Pam solution didn't affect insitu blend formation; this was confirmed by FTIR spectroscopy and UV-VIS spectroscopy.

The peak at  $1664\text{ cm}^{-1}$ , shifts slightly to lower frequency as the Pani concentration increases in the blend, for the amide stretching and indicates the hydrogen bonding interaction between amine group of Pani and carbonyl group of Pam. The peaks observed at  $1600\text{ cm}^{-1}$  and  $1500\text{ cm}^{-1}$  were the characteristics of the benzoid to quinoid transition and indication of blend compositions doped as such during synthesis. Peaks observed at  $1116\text{ cm}^{-1}$ ,  $825\text{ cm}^{-1}$  and  $616\text{ cm}^{-1}$  confirms the formation of conductive Pani blend.

UV-VIS spectra shows the peak position at 360nm, 580nm and 820nm, it is the indication of conducting emeraldine salt formation

TGA/DTA data shows that, the rate of degradation and wt.loss decreases as the Pam concentration increases in the blend i.e. thermal stability increases and the decrease in wt.loss was observed from 72% to 45%. , as observed in the Pani-PVAc blend.

Conductivity at ambient temperature for the insitu blends shows that conductivity rises, after additional doping Percolation threshold is found at 11%, and 59% Pani shows conductivity in the range of  $10^{-3}$  to  $10^{-2}$  S/cm. The conductivity at ambient temperature was observed, it gave higher conductivity in the range of 40% to 60% Pani and percolation threshold observed at 10% Pani in the Ex-situ blend.

Temperature dependent conductivity showed that, insitu blend as well as ex-situ blend follows Arrhenius law. It was noticed that the higher concentration of Pani in the blend showed more linearity compare to ex-situ blend.

Activation energy ( $\Delta E$ ) was found to be decreased, as the Pani concentration was increased in both the blends (insitu blend and e-situ blend). The  $\Delta E$  value of the insitu blend was decreased from 0.31eV to 0.11eV and in the ex-situ blend the value was found to be in the range of 0.46 eV to 0.27 eV.

The percolation threshold temperature, corresponds to volume fraction of Pani of about 0.33 in the insitu blend and that in the ex-situ blend it was 0.36

The charge transport process was found to ohmic (linear) as the concentration of Pani increases in both the blends i.e. the intramolecular and intermolecular charge transport process was not affected by Pam barrier.

From the moisture sensitivity graph, it is noticed that, Pani-Pam insitu blend film responses moisture and sensitivity is found to be 25.42. The low value observed because difference in ( $R_o$ ) and ( $R_f$ ) is very low.

Chapter-V describes, result of Pani-Nylon-6 blends. Nylon-6 solution also didn't affect aniline Polymerization investigated by FTIR spectroscopy and UV-VIS spectroscopy. However, an IR spectrum shows that, Pani was doped as such during synthesis. The peaks observed confirmed this  $1590\text{ cm}^{-1}$ ,  $1540\text{ cm}^{-1}$  and  $1111\text{ cm}^{-1}$ . The peak found at  $1637\text{ cm}^{-1}$ , was the indication of H-bonding interaction between amine group of Pani and carbonyl group of nylon-6, this confirmed the blend miscibility i.e. intramolecular interaction between the polymers.

The UV-VIS spectroscopy shows the peaks at 860nm, 580nm, and 344nm. From this peaks, it was again clear that conducting Pani (i.e. emeraldine salt) was formed

X-ray diffraction spectra of the blends (insitu blends and ex-situ blend) shows that the Pani concentration increases in the blend compositions, crystallinity decreases. Decrease in crystallinity is found to be at lower concentration of Pani in the insitu blend than ex-situ blend i.e. the indication of IPN formation takes place in the insitu blend.  $\gamma$  phase is formed in the nylon-6.

Optical microscopy shows the morphology of the insitu blends. It is found that Pani shows granular morphology and as the nylon concentration increases in the blend fibre morphology of the blend is observed.

TGA/DTA data shows that, interaction between the polymers, altered the rate of degradation and wt.loss decreases as the nylon-6 concentration increases in the blend i.e. thermal stability increases and the decrease in wt.loss. was observed from 95% to 85%.

Conductivity at ambient temperature of the insitu blends shows that, the blend after additional doping shows rise in conductivity than the blends doped as such during synthesis (i.e. lowers doping). Here percolation threshold value was observed at 9% Pani. And 63% Pani after additional doping log conductivity was found in the range of  $10^{-3}$  to  $10^{-2}$  S/cm. The conductivity at ambient temperature was observed, it gave higher conductivity in the range of 40% to 60% Pani and percolation threshold observed at 40% Pani in the Ex-situ blend.

Temperature dependent conductivity showed that, insitu blend as well as ex-situ blend follows Arrhenius law. It was noticed that the higher concentration of Pani in the blend showed more linearity compare to ex-situ blend.

Activation energy ( $\Delta E$ ), was found to be decreased, as the Pani concentration was increased in the blends (insitu blend and ex-situ blend). The  $\Delta E$  value of the insitu blend was decreased from 0.19 eV to 0.06eV and in the ex-situ blend the value was found to be in the range of 0.49 eV to 0.21 eV.

The percolation threshold temperature, corresponds to volume fraction of Pani of about 0.29 in the insitu blend and that in the ex-situ blend it was 0.32

The charge transport process was found to ohmic (linear) as the concentration of Pani increases in both the blends i.e. the intramolecular and intermolecular charge transport process was not affected by nylon-6 barrier.

Sensitivity of Pani-nylon-6 blend film, was found to be, i.e.86.95 at 14% Pani in the blend film. Difference in ( $R_o$ ) and ( $R_f$ ) is low.

Moisture absorption characteristics for the blend was found to be,

Pam > Nylon-6 > PVAc.

Hence, prior to sensitivity measurements ( $R_o$ ) will change as

$$(R_o) (\text{Pam}) < (R_o) (\text{Nylon-6}) < (R_o) (\text{PVAc})$$

$(R_f)$  will change according to moisture also. Difference in  $(R_o)$  and  $(R_f)$  is least for Pam and low for Nylon-6 because  $-\text{CO-NH}-$  group in it shows affinity towards moisture and PVAc shows less affinity than Nylon-6, so the difference in  $(R_o)$  and  $(R_f)$  was found more in it.

It is found that, the enhanced electrical conductivity follows the trend, Pani-PVAc /Pani-ny-6/Pani-Pam. This is because conductivity data shows that in Pani-PVAc system after redoping the 68% blend concentration reaches to  $10^{-2}$  S/cm conductivity, and percolation threshold value observed at 7% in nylon-6 system, it is found to be 9% and in Pam blend it is 11%. In Pani-ny-6, conductivity reaches to  $10^{-3}$  S/cm. The same is observed in Pam system.

From this comparative data, it is noticed that PVAc blend is more conductive among the other blends. This is further supported by the physical properties obtained. It is found that the solubility parameter value, work function data matches closely in PVAc-blend system, further it is supported by the percolation threshold value, also found to be less compare to other blends which studied in this work.

This is further supported by the viscosity data. PVAc solution is found to be less viscous than nylon-6 solution than Pam solution, so the chances of trapping aniline monomer inside the PVAc solution in insitu blend, is very less compare to rest of the two systems. It is observed that Pam-blend shows less conductivity than the rest of the two systems because viscosity value found to be more here.

Nature of conducting states of conducting polymer in insulating matrix depends upon morphology, crystallinity defect, concentration and chain length. This is arised from the fact that, in the insitu blend, Pani coats the conventional polymer and as the concentration of Pani increases in the blend the conventional polymer coated Pani molecules comes close to each other and forms a close contact when Pani is increased in the solution and the conducting network is observed thus decreases the interchain separation while expanded molecular conformations reduce  $\pi$ -conjugation defects; both are able to increase the delocalization of electrons and finally the conductivity than physical mixtures (exsitu blends).







## References

1. Burroughes, J.H., Jones, C.A., Friend, R.H., **Nature** 335 (1988) 137
2. Frank Lux, **Polymer**, 35, 2915 (1994)
3. Shirakawa H, Louis E J, Macdiarmid, A.G, Chiang, C.K, Heeger, A.J, 578 (1977) **J.Chem.Soc.Chem.Comm.**
4. Bredas J.L., Silbey R, **Conjugated Polymers** (Kluwer Dodrecht, 1991)
5. Salaneck W.R., Conjugated Polymer Surfaces and Interfaces, Chapter 4 Stafstrom S and Bredas, J.L. Cambridge University Press, (1996)
6. Heeger, A.J., Kivelson S, Scrieffer and Su W, P, **Rev.Mod.Phys**, 60 (1988) 781
7. Salaneck W.R. and Bredas, J.L, **Solid State Communications**, special issue on Highlights in Condensed Matter Physics and Material Science 92 (1994) 31
8. Letheby, H., **J.Am.Chem.Soc.**15, 161(1862)
9. Willstatter and Moore, **Ber.** 40, 2665 (1907)
10. Willstatter and Dorogi, **Ber.**42, 2147 and 4118 (1909)
11. Green, A.G. and Woodhead, A.E., **J.Chem.Soc.**97, 2388 (1910)
12. MacDiarmid, A.G., Chiang, J.C., Halpern, M., Huang, W.S., Mu, S.L., Somasiri, N.L., Wu, M., and Yaniger, S.I. **Mol.cryst.Liq.cryst.** 121,173 (1985)
13. Chiang, J.C.and MacDiarmid, A.G. **Synth.Metals** 13,193 (1986)
14. Pron, A., Genoud, F., Menardo, C. and Nechtschein, M. **Synth.Metals** 24, 193 (1988)
15. Armes, S.P. and Miller, J.F. **Synth.Metals** 22,385 (1988)
16. Asturias, G.E., MacDiarmid, A.G., and Epstein, A.J. **Synth.Metals** 29,E157 (1989)
17. Cao, Y., Andretta, A., Heeger, A.J. and Smith, P. **Polymer**, 30, 2305 (1989)
18. Mohilner, D.M., Adams, R.N. and Argersinger, W.J. **J.Am.Soc.**84, 3618 (1962)
19. Diaz, A.F., Castillo, J.I., Logan, J.A., and Lee, W.Y. **J.Electro.anal.Chem.** 129,115 (1981)
20. Delamer, G. Lacaze, P.C., Dumousseu, J.Y. and Dubois, **J. Electrochem.**

**Acta**, 27,61 (1982)

21. Diaz, A.F. and Logan, J.A., **J.Electro.Anal.Chem.**111 (1980), 111
22. Genies, E.M., Syed, A.A. and Tsintavis, C. **Mol.cryst.Liq.cryst** 121,181 (1985)
23. Naufi, R., Nozik, A.J., White, J. and Watten, L. **J. Electrochem.Soc.** 129, 2261 (1982).
24. Toshima, N., Yan, H., Gotoh, Y. and Ishiwatari, M. **Chem.Lett.**2229 (1994)
25. Kang, E.T., Neoh, K.G., Woo, Y.L., Tan, K.L., Huan, C.H.A. and Wee, A.T.S. **Synth.Metals** 53,333, (1993)
26. Shaolin, Mu. and Jinqing, Kan. **Synth.Metals** 92 (2), 149 (1998)
27. Chen, Show.An.and Lee, Hsun-Tsing, **Macromolecules** 26,3254 (1993)
28. Yasuda, A and Shimadzu, T. **Synth.Metals** 61,239 (1993)
29. Genies, E.M. and Lapkowski, M. **J.Electro.anal.Chem.** 236,189 (1987)
30. Trivedi, D.C. and Dhawan, S.K., **Bull.Electrochem.**5, 208 (1989)
31. Trivedi, D.C. and Dhawan, S.K., **J.Appl.Electrochem.**22, 563 (1992)
32. Trivedi, D.C. and Dhawan, S.K., **Polymer International** 25,55 (1991)
33. Trivedi, D.C. and Dhawan, S.K., **Synth.Metals** 58,309 (1993)
34. Trivedi, D.C.**Bull.Electrochem** 8,94 (1993).
35. Trivedi, D.C. Indo french Symposium on new trends in Tailored Polymer Science and Technology, 79 (1993), Ed.S.Shivram, NCL, Pune India
36. Bughman, R.H., Wolf, J.F., Eckhardt, H and Shacklette, L.W. **Synth.Metals** 25,121 (1988)
37. Pouget, J.P.Jozefowicz, M.E., Epstein, A.J., Tang, X, MacDiarmid, A.G. **Macromolecules** 24,779 (1991)
38. D.Kumar and R.C.Sharma, **Eur.Polym.J**, 34,8,1053 (1998)
39. Chen, S.A. and Tsai, C.C. **Macromolecules** 1991,26 2234
40. Wei, Y., Tian, J., MacDiarmid, A.G., Masters, J.G., Smith, A.L. and Li, D., **J.Chem.Soc.Chem.Comm.**1994, 7, 552
41. Beadle, P., Armes, S.P., Gottesfeld, Mombourquette, C., Houlton.R. , Andrew, W.D. and Agnew, S.F. **Macromolecules** 1992,25,2526
42. Somnathan, N. and Wehner, G. **Ind.J.Chem.** 1994,33A, 572

43. Skotheim, T.A., In **Handbook of Conducting Polymers**, Volm. 1 and2  
MarcelDekker, New York 1986
44. Malhotra, B.D., Ghosh, S and Chandra, R., **J.Appl.Polym.Sci.** 1990,40,1049
45. Neglur, B.R., Laxmeshwar, N.B. and Santanan, K.S.V., **Ind.J.Chem.**1994,  
33A, 547
46. Curran, D., Grimshaw, J and Perera, S.D., **Chem.Soc.Rev.** 1991,20,1
47. Malli, S., **Ind.J.Chem.**1994, 33A, 524
48. Annapoorni, S., Sundaresan, N.S., Pandey, S.S. and Malhotra, B.D. (1993)  
**J.Appl.Phys.** 74, 2109
49. MacDiarmid, A.G., Mammone, R.J., Krawczyk, J.R. and Porter, S. **J. Mol.**  
**Cryst. Liq.Cryst.**105, 89 (1984)
50. Roth, S.S., **Mater.Sci.Forum**, 21,10 (1987)
51. Thakur, M., **Macromolecules**, 1988,21,661
52. Donald, A. Seanor (Ed.),'**Electrical Properties of Polymers**' (1982) 15,  
Chapter-1, Academic Press, New York.
53. Hari Singh Nalwa (Ed.),'**Handbook of Organic Conductive Molecules and**  
**Polymers**', vol.2, Chapter-18, (1997) 773,John Wiley &Sons
54. H.Naarmann, in ' Science and Applications of Conducting Polymers' (Ed).  
W.R.Salaneck, D.T.Clark and E.J.Samuelsen, Adam Hilger, Bristol (1990)
55. Z.Berdjane, D.R. Rueda, and F.J.Balta, Calleja and JM. Palacios, **Synth.**  
**Metals**, 52,101 (1992)
56. A.Yassar, J.Roncali and F.Garnier, **Polym.Commun.**28, 103 (1987)
57. S.P.Armes and M. Aldissi, **Polymer** 31,569 (1990)
58. T.Iyoda, A.Ohtani, K.Honda and T.Shimadzu, **Macromolecules**, 23,1971  
(1990)
59. M.Morita, I.Hashida and M.Nishimura, **J.Appl.Polym.Sci.** 36,1639 (1988)
60. V.Bocchi, G.P. Gardini and S.Rapi. , **J.Mater.Sci.Lett.** 6,1283 (1987)
61. C.Li and Z.Song, **Synth.Metal.**41, 1013 (1991)
62. Y.Chen, R, Qian, G.Li and Y.Li. **Polym.Commun.** 32,189 (1991)
63. R.A.Zoppi, M.I.Felisberti and M. -A. DePaoli, **J.Polym.Sci.Polym.Chem.**  
32,1001 (1994)

64. T.Ueno, H.D.Arntz, S.Flesh and J.Bargon, **J.Macromol.Sci.Chem.** A 25, 1557 (1988)
65. V.Mano, M.I.Felisberti and M. -A. De Paoli, **Polymer** (to be published)
66. F.Jouseem and L.Olmedo, **Synth.Metal.** 41,385 (1991)
67. Geoffrey Pritchard (Ed.), '**Plastic Additives**', Chapman &Hall, P-183 (1998)
68. A.T. Ponomarenko, V.G.Shevchenko, N.S.Enikolopyan,'**Advances in Polymer Science**' (1996), 126 Springer-Verlag.
69. Sichel.EK (1982) **Carbon black-Polymer Composites**, MarcelDekker, New York
70. Sheng P (1980) **Phys.Rev.** 21B: 2180
71. Malliaris, A., Turner, D.T. (1971), **J.Appl.Phys.**42: 614
72. Gurland, JC, Tanner, DB (eds) (1978) **Electrical Transport and Optical Properties of Inhomogeneous Media** AIP, New York
73. Broadbent SR, Hammersley JM, (1957) **Proc. Cambr. Soc.** 53:629
74. Shante, VKS, Kirkpatrick, S, (1971) **Adv.Phys**, 20:325
75. Kirkpatrick, S, (1973) **Rev. Mod. Phys.** 45:574
76. Crossman, RA (1985) **Polym.Eng.Sci.**25: 507
77. Bigg DM, Stutz DE (1983) **Polym.Comp.**4: 40
78. Klason, C., Kubat, J., (1975), **J.Appl.Polym.Sci.** 24:831
79. Scutnik Bolesh, J. (1984), **Rubber Chem.Tech.** 57:403
80. Enikolopor, N.S. (1980), **Nature**, USSR 8: 62
81. Dyachkovsky FS, Novokshonova LA (1984), **Advances in Chemistry**, USSR, 53:200
82. Baulin, A.A, Krasnoshchekov A, M. Deyanova, AS, Vasilenok, YI (1982) **Applied Chemistry J.**, USSR, 55:2534
83. Galashina, NM, Nedorezova, PM, Tsvetkova, VN, Dyachkovsky, FS, Enikolopyan, NS (1984) **USSR Academy of SciencesProceedings**278: 620
84. S.Roth, W.Graupner, **Synth.Metal.** , (1993), 57,3623
85. O.T.Ikkala, J.Laakso, Vakiparta, E.Virtanen, H.Ruohonen, H.Jarvinen, T.Taka,P.Passiniemi,J.E.Osterholm,Y.Cao,A.Andretta, P.Smith, A.J.Heeger, **Synth.Metal**, 69,97 (1995)

86. B.Wessling, **Synth.Metal**, (1997), 85,1313
87. F.Jonas, J.T.Morrison, **Synth.Metal** (1997), 85,1397
88. S.Panero, P.Prosperi, F.Bonino, B.Scrosati, M.Mastragostino, **Electrochim.Acta**, 32,1007 (1987)
89. C.Arbizzani, M.C.Gallazzi, M.Mastragostino, M, Rossi, F.Soavi, **Electrochem.Comm.** (2001), 3,16
90. C.Arbizzani, M.Mastragostino, L.Meneghello, M.Morselli, A. Zanelli, **J.Appl. Electrochem.** 26,121(1995)
91. W.A.Gtazotti, G.Casalbore-Miceli, A. Geri, M. –A.De Paoli, **Adv.Mater.** 10,60(1998)
92. W.A.Gtazotti, M. –A.De Paoli, G.Casalbore-Miceli, A. Geri, G.Zotti, (1999) 29,753 **J.Appl. Electrochem.**
93. C.T.Kuo, W.H.Chiou, **Synth.Metal**, (1997), 88, 23
94. H.Sirringhaus, N.Tessler, R.H.Friend, (1999), 857,102 **Synth.Metal**
95. J.H.Burroughes, D.D.C.Bradley, A. brown, R.N.Marks, K.Mackay, R.H Friend, P.L.Burns, A.B. Holmes, **Nature** (1990), 347,539
96. N.Camaioni, G.Casalbore-Miceli, A. Geri, G.Zotti, **J.Phys.D: Appl.Phys** (1998) 31,1245
97. T.Yohannes, O.Inganas, **Sol. Energy Mater.Sol.Cells** (2001) 69,315
98. A.Pron, J.Laska, J.E.Osterholm, P.Smith, **Polymer** (1993) 34,4235
99. A.Pron, J.E.Osterholm, P.Smith, A.J.Heeger, J.Laska, M. Zagorska (1993) 55,3520 **Synth.Metal**
- 100 T.Taka, **Synth.Metal** (1991), 41,1177
101. Coleman, M.M., and Moskala, E. J. **Polymer**, (1983) 24,251
102. J.Tang, X.Jing, B.Wang and F.Wang **Synth.Metal** 24(1988) 231
103. Y.H.Kim, C.Foster, J.Chiang and A.J.Heeger **Synth.Metal**, 25 (1988) 49
104. A.J.Epstein, J.M.Ginder, F.Zuo, R.W.Bigelow, H.S.Woo, D.B.Tanner, A.F. Richter, W.S.Huang and A.G.Macdiarmid, **Synth.Metal**, 18 (1987) 303
105. J.G.Masters, Y., Sun, A.G.Macdiarmid, A.J.Epstein, **Synth.Metal**, 41,715 (1991)
106. Y.Cao, Smith, P and Heeger, A.J., **Synth.Metal**, 32,263 (1989)

107. Pallab Banerjee and Broja, M.Mandal, **Macromolecules** (1995) 28, 3940
108. Goh, S.H., Chan, H.S.O. and Ong, C.H., **Polymer** 2675,37 (1996)
109. E.Segal, Y.Haba, M.Narkis, A.Siegman, **J.Appl.Polym.Sci.** 760,4 (2001)
110. Junqing, M.A., HuihongSong, Harry, L., Frisch, Shahin Maaref, Sam.S. Sun, **J.Appl.Polym.Sci.** , 2287,85,11 (2002)
111. Avrom, I., Medalia, **Rubber Chem. and Tech.** 59 (1986), 433
112. Dr.S.Radhakrishnan, **Polym Commun.** (1985) 26,153
113. Fizazi, Moulton, J, Pakbaz, K, Rughooputh, S.D.D.V., Smith, P, Heeger, A. J. **Phys.Rev.Lett.** 64,2180 (1990)
114. Mott.N.F.and Davis, E.A., *Electronic Processes in Non-Crystalline Materials*, Clarendon Press (1979) Oxford.
115. Chutia, J and Barua, K, (1980), **J.Phys.D.Appl.Phys.**13, L9
116. Gabor Harsanyi, '**Polymer Films in Sensor Applications**' (1995), P-318 (Chapter-4, 4.5.2) TECHNOMIC
117. Kirkothmer, **ENC.POLYM.SCI.TECH.** Vol.1, P-177, (1994) John Wiley & Sons, Inc.
118. A.Tager, '**PHYSICAL CHEMISTRY OF POLYMERS**' (1978), Mir Publishers P-499
119. V.R.Gowarikar, '**Polymer Science**', (2003), P-355, New Age International (P) Ltd.
120. P.Ghosh, et.al, **Euro.Polym.J**, 35 (1999), 803
121. Kenji Yamada, Hirokazu Yamane, TerukiHaishi, Katsuhiko and Yamamoto ToshihideHaraguchi, Tisatokajiyama, **J.Appl.Polym.Sci.**86, 5,1113 (2002)
122. R.Murugesan and E.Subramanian. 25,7,613 (2002) **Bull.Mater.Sci.**
123. Miyasaka, K. et.al, **J.Mater.Sci.**1982, 17,1610
124. Stephen.H.Foulger, **J. Appl.Polym.Sci.** (1999), 72,1573
125. Armes, S.P., Gottesfeld, S., Beery, J.G., Garzon, F. and Agnew, S.F., 32, 2325 (1991) **Polymer**
126. Beadle, P., Armes, S.P., Gottesfeld, S., Mombourquette, C, Houlton, R, , Andrews, W.D. and Agnew, S.F., **Macromolecules**, (1992), 25,2526



- 127 Abraham, D., Bharathi, A., Subramaniam, S.V., **Polymer**, 37,5295,120 (1996)
- 128 Byun, S.W., Im, S.S., **Polymer**, 39,485 (1998)
- 129 Kyung Wha Oh, Seong Hun Kim, Eun Ae Kim, 684,81,3 (2001)  
**J.Appl.Polym.Sci.**
130. Annis, B.K., Wignall, G.D., Hopkins, Alan, R, Rasmussen, Paul G, Basheer, Rafil, A, **J.Polym.Sci, Part B: Polym.Phys.** , 35(17), 2765 (1997)
- 131 Rafil, A, Basheer, Alan, R, Hopkins and Paul G, Rasmussen, 32,128,4706  
**Macromolecules**, (1999)
132. Gabriel Pinto, Monica, B., Maidana, 1449,82,6 (2001) **J.Appl.Polym.Sci.**
133. M.Zagroska, E.Taler, I., Kulszewicz-Bajer, A., Pron, J.Niziol, 258,73,8, 1423 (1999), **J.Appl.Polym.Sci**,
- 134 Im, S.S., Byan, S.W., **J.Appl.Polym.Sci**, 51,178,1221 (1994)
- 135 YunHeumPark, Sang.Hoon Choi, Suk Kyu Song and Seijo Miyata, 45, 843  
**J. Appl.Polym.Sci.** (1992)
- 136 Tang, J, Jing, X., Wang, B and Wang, F., **Synth.Metal**, (1988), 24,231
- 137 Kim.Y.H, Foster, C, Chiang, J and Heeger, A.J., **Synth.Metal**, 25,49 (1988)
- 138 Chen, S.A. and Fang, W.G., **Macromolecules**, 24,1242, (1991)
- 139 Wang, H.L.and Fernandez, J.E., **Macromolecules**, 1993,26,3336
- 140 Xia, Y., Weiesinger, J.M., MacDiarmid, A.G., **Chem.Mater.** , 7,443 (1995)
- 141 Wan, M., **Synth.Metal**, (1989), 31,51
- 142 Min, Y. and MacDiarmid, A.G., **Polym.Preprints**, (1994), 35,231
- 143 G.W. Heffner, S.J.Dahman, D.S.Pearson, C.L.Gettinger, **Polymer**,334, 315 3155 (1993)
- 144 J.P.Pouget, M.E.Jozefowiz, A.J.Epstein, X.Tang, A.G.MacDiarmid, 24,779 (1991) **Macromolecules**
- 145 Flandin, L, Chang, A, Nazarenko, S, Hiltner, A., Baer, E. **J. Appl.Polym.Sci** (2000), 76,894
- 146 K.Cheah, G.P.Simon, and M.Forsyth, **Polymer.Int**, 50,27(2001)
- 147 Reghu, M.et.al. **Macromolecules**, (1993), 26,7245
- 148 S.H.Khor, K.G.Neoh and E.T.Kang, **J. Appl.Polym.Sci**, 40,2015 (1990)

149. Gill, M., Mykytiuk, J., Armes, S.P., Edwards, J.L., Yeates, T., Moreland, P., J and Mollett, C., **J.Chem.Soc.Chem.Comm.** (1992) 108
150. Thangarathinavelu, M., Tripathi, A.K., Goel, T.C. and Varma, I.K., 51,1347  
**J. Appl.Polym.Sci** (1994)
151. Gill, M., Mykytiuk, J., Armes, S.P., Edwards, J.L., Yeates, T., Moreland, P., J and Mollett, C., **J.Chem.Soc.Chem.Comm.** (1992) 108
152. Thangarathinavelu, M., Tripathi, A.K., Goel, T.C. and Varma, I.K., 51,1347  
**J. Appl.Polym.Sci** (1994)
153. Beadle, P., Armes, S.P., Gottesfeld, S., Mombourquette, C., Houlton, R., Andrews, W.D. and Agnew, S.F., **Macromolecules**, 1992,25,2526
154. Armes, S.P., Gottesfeld, S., Berry, J.G., Garzon, F and Agnew, S.F., 2325  
**Polymer**, 1991,32,
155. Yang, C.Y., Cao, Y., Smith, P and Heeger, A.J., **Synth.Met**, 1993,53,293
156. Reghu, M., Yoon, C.O., Yang, C.Y., Moses, D, Heeger, A.J. and Cao.Y,  
1993,26,7245,**Macromolecule**
157. Ruckenstein, E., and Yang, S, **Synth.Met**, 1993,53,223
158. Yang, S and Ruckenstein, E, **Synth.Met**, 1993,59,1
159. Copper, E.C., and Vincent. B, **J.Phys. D: Appl.Phys**, 1989,22,1580
160. Shacklette, L.W., Han, C.C. and Luly, M.H. **Synth.Met**, 1993,57,3532

